

What Is the Optimal Ranking Score Between Precision and Recall? We Can Always Find It and It Is Rarely F_1

Sébastien Piérard, Adrien Delière, and Marc Van Droogenbroeck

Montefiore Institute, University of Liège, Liège, Belgium

{S.Pierard,Adrien.Deliege,M.VanDroogenbroeck}@uliege.be

Abstract

Ranking methods or models based on their performance is of prime importance but is tricky because performance is fundamentally multidimensional. In the case of classification, precision and recall are scores with probabilistic interpretations that are both important to consider and complementary. The rankings induced by these two scores are often in partial contradiction. In practice, therefore, it is extremely useful to establish a compromise between the two views to obtain a single, global ranking. Over the last fifty years or so, it has been proposed to take a weighted harmonic mean, known as the F -score, F -measure, or F_β . Generally speaking, by averaging basic scores, we obtain a score that is intermediate in terms of values. However, there is no guarantee that these scores lead to meaningful rankings and no guarantee that the rankings are good tradeoffs between these base scores. Given the ubiquity of F_β scores in the literature, some clarification is in order. Concretely: (1) We establish that F_β -induced rankings are meaningful and define a shortest path between precision- and recall-induced rankings. (2) We frame the problem of finding a tradeoff between two scores as an optimization problem expressed with Kendall rank correlations. We show that F_1 and its skew-insensitive version are far from being optimal in that regard. (3) We provide theoretical tools and a closed-form expression to find the optimal value for β for any distribution or set of performances, and we illustrate their use on six case studies. Code is available at <https://github.com/pierard/cvpr-2026-optimal-tradeoff-precision-recall>.

1. Introduction

The precision Pr (also called *positive predictive value*) and recall Re (also called *true positive rate*) are of first importance in classification and other related problems. These scores have a straightforward interpretation, as they give the probabilities of taking the correct decision when the pre-

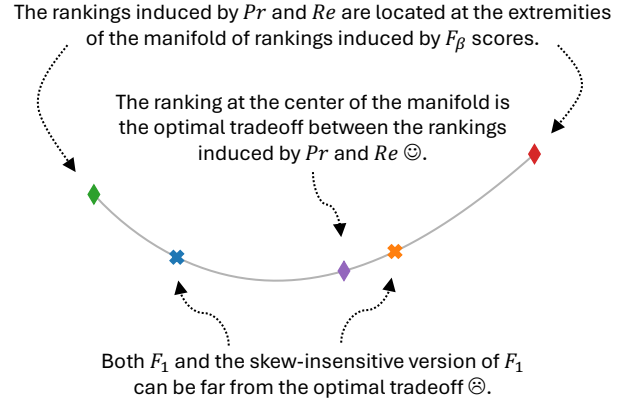


Figure 1. The manifold of rankings inducible with the F_β scores is a curve (drawn as \smile) that depends on the set or distribution of performances that is considered. The distance along the curve is proportional to the number of swaps of neighboring classifiers needed to transform a ranking into another. The rankings induced by precision \blacklozenge and recall \blacklozenge are at the extremities of the manifold. The rankings induced by the traditional (balanced) F_1 \blackstar and by the skew-insensitive version of F_1 \blackstar [10] can be anywhere, depending on the set or distribution of performances that are compared, and cannot be considered as the optimal tradeoff between precision and recall. We consider that the ranking located at equal distance, along the curve, from precision and recall is the optimal tradeoff \blacklozenge .

dicted or ground-truth class is positive, respectively [13].

Unfortunately, working with several scores is often impractical. For this reason, it is common to average the values of Pr and Re . Most often, this is done with a harmonic mean, leading to the family of F -scores F_β , with $\beta \geq 0$:

$$F_\beta^{-1} = (1 - b) Pr^{-1} + b Re^{-1} \quad \text{with } b = \beta^2 / (1 + \beta^2). \quad (1)$$

These last decades, this family of scores has become very popular in the literature¹. It forms a continuum between pre-

¹With the requests “F-measure + classification”, “F-score + classification”, and “F-beta + classification”, Google Scholar reported on July 23th 2025 that there was about 315,000, 205,000, and 9,080 matching documents, respectively. Moreover, we estimated that about 10% of the papers accepted at CVPR 2025 refer to or use F_1 .

cision $Pr = F_0$ and recall $Re = F_\infty$. The traditional (balanced) F-score, F_1 , gives equal weights to Pr and Re . But is F_1 really the optimal tradeoff between precision and recall? The answer to this question depends on the point of view.

The point of view of values. The F-scores are obviously between Pr and Re in the sense that, for any given performance P (i.e., a confusion matrix), the value $F_\beta(P)$ varies monotonically with β , between $Pr(P)$ and $Re(P)$.

The point of view of ranks. This is the point of view that we develop. Although many authors use the F_1 or F_β scores to rank and compare methods, the claim that they are an appropriate compromise for ranking deserves to be studied. Several questions arise. How are the rankings induced by the F_β scores spatially organized? Are the F_β scores suitable to induce performance-based rankings? Do the F_β scores induce rankings that form a shortest path between those induced by Pr and Re ? For which $\beta(s)$ do we obtain the optimal tradeoff between the rankings induced by Pr and Re ?

The objective of this paper is to provide answers, teased in Fig. 1, to all these questions. For that purpose, we develop the theory, and we provide experimental results for various distributions and sets of two-class classification performances. We summarize our contributions as follows:

1. We establish that the F_β -family is the right set of scores to consider when looking for an optimal tradeoff between Pr and Re for ranking, as, on the one hand, all F_β lead to meaningful rankings according to the theory of performance-based ranking [31] and, on the other hand, the rankings induced by F_β always form a shortest path between the rankings induced by Pr and Re .
2. We show that neither F_1 , traditionally considered as a balanced compromise between Pr and Re , nor its skew-insensitive version (denoted by $SIVF$) introduced in [10] are acceptable tradeoffs for ranking, in general. These scores can lead to rankings far from optimal.
3. We provide the theory and methods for defining and finding (with a closed-form expression) the optimal tradeoffs between the rankings induced by Pr and Re . These methods are then successfully applied to numerous sets and distributions of performances.

2. Related Work

2.1. Useful References

The meaning of F-scores is discussed in countless papers; see, for example, the work by Christen et al. [6] for a recent review about the F-scores. A plethora of other scores have been defined for classification. They can be found in several reviews [1, 4, 5, 7, 8, 16, 19, 32, 33], to cite only a few.

Regarding the ranking of methods or models based on their performances, theoretical foundations have been provided in [31] and the theory has been particularized to the case of two-class crisp classification in [15, 29]. When com-

paring performances with the same class priors, the isometrics depicted in the ROC (Receiver Operating Characteristic) space is a graphical representation of the performance ordering induced by a given score. The isometrics of Pr and F_1 have been depicted in [10] for different class priors.

There are only a few studies of the correlations between the rankings induced by scores in classification. Both Ferri et al. [8] and Liu et al. [25] used Pearson linear correlations and Spearman rank correlations. To the best of our knowledge, there is no study comparing classification scores based on Kendall rank correlations.

2.2. Building Upon the Related Work

2.2.1. Sometimes, F_1 Mimics the Rankings Induced by Pr or Re and Ignores the Other One

Let us consider the particular case in which the class priors are fixed and denote them by π_- and π_+ for the negative and positive classes, respectively. Extending the work of [10], we depict, in Fig. 2, the isometrics of Pr , F_β for different values of β , Re , and $SIVF$ in the ROC space. For all these scores, we found that the isometrics form pencils of lines with vertices located at $(FPR, TPR) = (-\ell, 0)$ with some $\ell \geq 0$. The performance orderings, and the resulting rankings, depend only on the location of the vertex, and thus on ℓ . For Pr , $\ell = 0$. For Re , $\ell = \infty$. For $SIVF$, $\ell = 1$. And for F_β ,

$$\ell = \beta^2 \frac{\pi_+}{\pi_-} = \beta^2 \frac{\pi_+}{1 - \pi_+}. \quad (2)$$

When $\pi_+ \rightarrow 0$, we see that $\ell \rightarrow 0$ and that all F_β mimic the ranking of $Pr = F_0$ and ignore Re . Similarly, when $\pi_+ \rightarrow 1$, we see that $\ell \rightarrow \infty$ and that all F_β mimic the ranking of $Re = F_\infty$, ignoring Pr . So, *a single value of β cannot provide the optimal ranking for all priors.*

2.2.2. All F_β Scores Lead to Meaningful Rankings, Without Any Constraint on the Performances

There are some conditions that a performance ordering must fulfill to be meaningful. They have been given in the form of axioms in [31] (reminded in suppl. mat.). We found that all these axioms are satisfied by the performance orderings induced by F_β , $\forall \beta \geq 0$. In other words, *all F_β lead to meaningful performance orderings.* It was not a foregone conclusion, because the scores that are, from the point of view of values, between two scores suitable for ranking are not guaranteed to be themselves suitable for ranking. For example, the performance orderings induced by the arithmetic and geometric means of Pr and Re do not satisfy the axioms of performance-based ranking. As the ranking induced by $SIVF$ is the same as the ranking induced by F_β when β^2 is equal to the skew ratio [10] π_-/π_+ , $SIVF$ leads to a meaningful performance ordering when the priors are fixed. However, we found that it does not satisfy the axioms of [31] without this constraint.

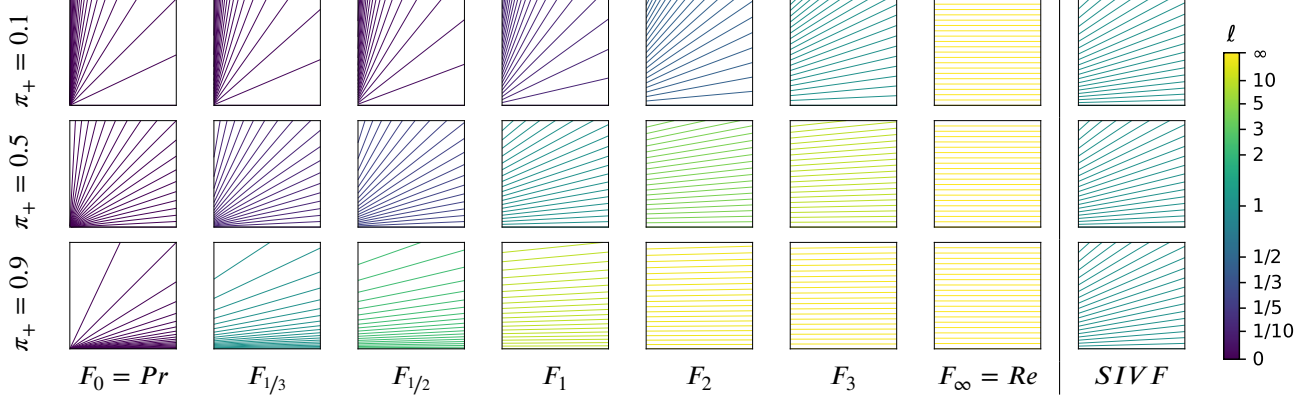


Figure 2. Isometrics of F_β and $SIVF$ in the ROC space $(FPR, TPR) \in [0, 1]^2$, for three class priors. An isometric is a locus of equivalent performances, according to the score value. We plotted here those corresponding to the values 0.05, 0.10, 0.15, ..., 0.95. The isometrics of F_β form a pencil of lines intersecting at $(FPR, TPR) = (-\ell, 0)$ with $\ell = \beta^2 \pi_+ / \pi_-$. The isometrics of $SIVF$ intersect at $(FPR, TPR) = (-1, 0)$, no matter what the class priors are. The score $SIVF$ induces the same performance ordering as F_β with $\beta^2 = \pi_- / \pi_+$.

3. Theory

3.1. Preliminaries

We use the notations of [31]. $\mathbb{P}_{(\Omega, \Sigma)}$ is the set of all possible performances P in two-class crisp classification, *i.e.* the set of all probability measures with a sample space Ω containing the four cases that can arise: tn (true negative), fp (false positive), fn (false negative), and tp (true positive). The negative and positive class priors are $\pi_- = P(\{tn, fp\})$ and $\pi_+ = P(\{fn, tp\})$, respectively.

We are interested in the rankings induced by scores. Scores are functions $X : \mathbb{P}_{(\Omega, \Sigma)} \rightarrow \mathbb{R} : P \mapsto X(P)$. The unconditional probabilities of a false positive, false negative, and true positive are given by the scores PFN , PFP , and PTP , respectively. The precision (Pr), also called positive predictive value (PPV), is defined as $Pr = PPV = F_0 : P \mapsto P(\{tp\} | \{fp, tp\})$. The recall (Re) or true positive rate (TPR), is $Re = TPR = F_\infty : P \mapsto P(\{tp\} | \{fn, tp\})$. The skew-insensitive version of F_1 [10] is $SIVF = \frac{2TPR}{TPR + FPR + 1}$, where FPR is the false positive rate.

3.2. The Rankings and Their Manifold

Without loss of generality, let us consider a finite set $\Pi = \{P_1, \dots, P_n\} \subset \mathbb{P}_{(\Omega, \Sigma)}$ of performances (for infinitely many performances, consider a distribution² \mathcal{P} instead of a set Π). The rankings of Π are its permutations, in finite number.

Let us consider a score X that induces meaningful rankings. Assuming that the value of X is defined for all $P \in \Pi$,

²Technically, we need to consider a measurable space whose sample space is $\mathbb{P}_{(\Omega, \Sigma)}$. A performance distribution \mathcal{P} then corresponds to a probability measure. Scores, defined as real functions on $\mathbb{P}_{(\Omega, \Sigma)}$, become random variables, and we can rigorously speak of correlation between scores.

and that X does not assign the same value to two performances of Π (absence of ties), X induces the ranking:

$$\mathbf{x} = (\text{rank}_X(P_1), \dots, \text{rank}_X(P_n)), \quad (3)$$

where $\text{rank}_X(P)$ denotes the number of performances in Π for which X takes a value greater or equal to $X(P)$.

A set of scores (*e.g.* all F_β) corresponds to a set of points as written in Eq. (3). The Euclidean distance (*i.e.* along a straight line) between two rankings is their Spearman distance d_ρ , related to Spearman's ρ [34]. *The distance measured along the manifold of rankings is Kendall's distance d_τ (a.k.a. bubble-sort distance), related to Kendall's τ [23].* We can explain it as follows. Let us create the path graph that connects the rankings that are neighbors. Two rankings \mathbf{x}_a and \mathbf{x}_b are neighbors if and only if they differ only by one swap of two classifiers at consecutive ranks. The geodesic distance, *i.e.* the length of the shortest path, between \mathbf{x}_a and \mathbf{x}_b , is the minimum number of swaps needed to transform \mathbf{x}_a into \mathbf{x}_b , and it is proportional to the Kendall distance d_τ . For this reason, we consider this distance to be adequate for specifying the optimal tradeoff between two rankings.

As we observed in all our case studies that the manifold is curved, as depicted in Fig. 1, we will define the optimal tradeoff in terms of Kendall's distance d_τ or in terms of Kendall's rank correlation τ .

3.3. The Shortest Paths and the Means of Scores

The score F_β is the weighted harmonic mean between precision Pr and recall Re . The harmonic mean is the generalized f -mean, also called the regular mean [24], with $f : x \mapsto x^{-1}$. This has an important implication for the performance orderings induced by Pr , Re , and F_β .

Consider an interval $\xi \subseteq \mathbb{R}$, m scores X_1, \dots, X_m whose images are included in ξ , and a continuous strictly mono-

tonic real function f defined on ξ . If a performance P_A is better than, equivalent to, or worse than a performance P_B according to all the scores X_1, \dots, X_m , then so is it according to all their generalized f -means \bar{X} . This extends to weighted f -means. So, *if a performance P_A is better than, equivalent to, or worse than a performance P_B according to Pr and to Re , then so is it according to all the F_β scores.*

Let us introduce the indicator $\Delta_{X_1, X_2}^{P_A, P_B} \in \{0, 1\}$ that specifies if the scores X_1 and X_2 disagree on the relative order between the performances P_A and P_B . Given the implication that a mean of scores has on the rankings, we have

$$\Delta_{Pr, Re}^{P_A, P_B} = \Delta_{Pr, F_\beta}^{P_A, P_B} + \Delta_{F_\beta, Re}^{P_A, P_B} \quad \forall \beta \geq 0. \quad (4)$$

And, as [23]

$$d_\tau(X_1; X_2) = \frac{2}{n(n-1)} \sum_{i < j} \Delta_{X_1, X_2}^{P_i, P_j} \in [0, 1], \quad (5)$$

$$d_\tau(Pr; Re) = d_\tau(Pr; F_\beta) + d_\tau(F_\beta; Re) \quad \forall \beta \geq 0. \quad (6)$$

This means that *the rankings induced by the F_β scores form one shortest path (i.e. a geodesic) between the rankings induced by Pr and Re .* This is a key result for this paper, as it proves meaningful the search for the optimal tradeoff between Pr and Re in the family of F_β scores. An example is provided in Fig. 3. As $\tau = 1 - 2d_\tau$, Eq. (6) can be rewritten in terms of correlations as

$$1 + \tau(Pr; Re) = \tau(Pr; F_\beta) + \tau(F_\beta; Re) \quad \forall \beta \geq 0. \quad (7)$$

3.4. The Optimal Tradeoff Between Pr and Re

3.4.1. Optimal Tradeoffs as Karcher Means

The optimal tradeoffs are the F_β scores that minimize the Fréchet variance [11] (see Fig. 3c):

$$\sigma^2(\beta) = d_\tau^2(Pr; F_\beta) + d_\tau^2(F_\beta; Re). \quad (8)$$

The solutions $F_\beta = F_*$ of Eq. (8), known as the Karcher means [21] are those that are equidistant of Pr and Re (this is detailed in supplementary material), i.e. such that

$$d_\tau(Pr; F_*) = d_\tau(F_*; Re) = \frac{d_\tau(Pr; Re)}{2} \quad (9)$$

$$\Leftrightarrow \tau(Pr; F_*) = \tau(F_*; Re) = \frac{1 + \tau(Pr; Re)}{2}. \quad (10)$$

Note that, putting aside the perspective of performances and scores, the idea of minimizing either the sum of distances between rankings or the sum of squared distances has been proposed by Kemeny [22]. However, Eqs. (6) and (7) show that, in our case, the minimization of the sum of distances is undefined. But the minimization of the sum of squared distances (Eq. (8)) is well defined.

3.4.2. A Closed-Form Expression for the Optimal β

Let us, by thought, place ourselves at the ranking induced by $Pr = F_0$ and then continuously increase β , following the path of rankings induced by the F_β scores, towards the one induced by $Re = F_\infty$. With a finite number of performances, we stay at a given ranking during a range of values for β and then, suddenly, move to the next ranking. The value of β at which such a transition occurs is a value for which two performances are put on an equal footing by F_β . Let us consider any two performances P_1 and P_2 . We have $F_\beta(P_1) = F_\beta(P_2)$ if and only if $\beta^2 = \vartheta(P_1, P_2)$ with

$$\vartheta(P_1, P_2) = -\frac{PTP(P_1)PFP(P_2) - PTP(P_2)PFP(P_1)}{PTP(P_1)PFN(P_2) - PTP(P_2)PFN(P_1)}, \quad (11)$$

when this value is positive. Otherwise, there is no score F_β that puts the performances P_1 and P_2 in equivalence. Kendall's distance between Pr and F_β increases linearly with the number of swaps. This leads us to the conclusion that *the optimal tradeoff is $F_* = F_\beta$ with*

$$\beta^2 = \text{median}(\{\vartheta(P_i, P_j) \mid i \neq j \wedge \vartheta(P_i, P_j) \geq 0\}). \quad (12)$$

3.4.3. Assessing the Degree of Optimality of Some F_β

The choice of β comes down to choosing a permutation of the classifiers. Looking at the level of pairwise comparisons, we can identify three mutually exclusive cases: \boxtimes , \boxtimes , and \checkmark .

\boxtimes : the pairs of classifiers that are ordered in the same way by Pr and Re . As it is also the case for all β , there is no choice to make. The proportion of such pairs is given by

$$P(\boxtimes) = 1 - d_\tau(Pr; Re) \quad (13)$$

$$= 1/2 [1 + \tau(Pr; Re)] = 1/2 [\tau(Pr; F_\beta) + \tau(F_\beta; Re)].$$

\boxtimes : the pairs of classifiers for which a choice has to be made because Pr and Re contradict each other, and for which the choice is not optimal (F_β disagrees with F_*). The proportion of such pairs is given by

$$P(\boxtimes) = d_\tau(F_\beta; F_*) = 1/4 |\tau(Pr; F_\beta) - \tau(F_\beta; Re)|. \quad (14)$$

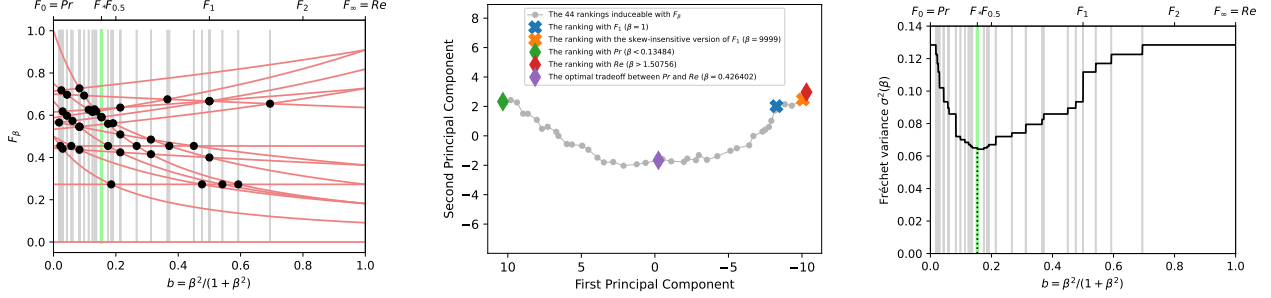
\checkmark : the pairs of classifiers for which a choice has to be made and for which the choice is optimal. The proportion of such pairs is given by

$$P(\checkmark) = d_\tau(Pr; Re) - d_\tau(F_\beta; F_*) = 1 - P(\boxtimes) - P(\boxtimes). \quad (15)$$

It appears from Eqs. (13) and (14) that *if one uses some F_β to rank and reports the values for both $\tau(Pr; F_\beta)$ and $\tau(F_\beta; Re)$, then we can determine the degree of optimality for the chosen β .* We define it as follows:

$$\mathcal{O} = P(\checkmark | \boxtimes) = \frac{P(\checkmark)}{P(\checkmark) + P(\boxtimes)} = 1 - \frac{P(\boxtimes)}{1 - P(\boxtimes)}. \quad (16)$$

Note that $\mathcal{O} = 1$ if and only if $\tau(Pr; F_*) = \tau(F_*; Re)$, which is what is targeted by minimizing the Fréchet variance.



(a) The curves F_β w.r.t. β for the 16 performances to rank. The swaps in the ranking are shown by the black dots and the gray vertical lines, which delimit the 44 different rankings. The ranking with $F_\beta \geq 1.508$ perfectly mimics Re , ignoring Pr . There is the same amount of black dots on both sides of the optimal compromise (green vertical bar, $\beta = 0.426$ by Eq. (12)).

(b) Visualization of the manifold of rankings inducible by the F_β scores with two-components PCA (93.57% variance explained). Each point corresponds to a different ranking and to a range of β s. A line segment between consecutive points represents a value of β for which there is a swap between classifiers. See Fig. 1 for a detailed description of such a plot.

(c) Fréchet variance $\sigma^2(\beta)$ (Eq. (8)) w.r.t. β . It is a piecewise constant function, the discontinuities occurring at the values for which there is a swap between two classifiers in the ranking. The optimal trade-off(s) between Pr and Re is (are) obtained with the values of β for which the Fréchet variance is minimized. The value computed by Eq. (15) belongs to them (green vertical bar).

Figure 3. The leaderboard for the medical imaging challenge CADA-RRE [17], with $|\Pi| = 16$ performances to rank (details provided in supplementary material). Thanks to Eq. (6), we know that the optimal tradeoff between the rankings induced by the precision Pr (on the left hand side of each plot) and the recall Re (on the right hand side) is induced by some F_β score. This figure shows how the rankings change with β . There are $44 \leq |\Pi|^2 + 1$ different rankings inducible by the F_β scores. The optimal trade-off is given by Eqs. (8) and (12).

Case study	$\tau(Pr; Re)$	F_1 ($\beta^2 = 1$)	$SIVF$ ($\equiv \beta^2 = \frac{\pi_-}{\pi_+}$)	Heuristic $\beta^2 = \frac{E[FPF]}{E[PFN]}$	Optimal tradeoff, $\mathcal{O} = 100\%$
uniform distribution over all performances	$1/3$	$\mathcal{O} = 100\%$ (optimal)	NA (meaningless ranking)	$\mathcal{O} = 100\%$ (optimal) (it selects F_1)	our analytical result cf. Eq. (17)
uniform distributions with fixed probability of true negatives	$1/3$	$\mathcal{O} = 100\%$ (optimal)	NA (meaningless ranking)	$\mathcal{O} = 100\%$ (optimal) (it selects F_1)	our analytical result cf. Eq. (18)
uniform distributions with fixed class priors	$1/2$	$\mathcal{O} \in [50\%, 100\%]$ optimal only for $\pi_+ \simeq 0.381$	$\mathcal{O} = \log(4) - 1/2 \simeq 88.63\%$	$\mathcal{O} = \log(4) - 1/2 \simeq 88.63\%$ (it selects $SIVF$)	our analytical result cf. Eq. (20) and Fig. 5c
uniform distributions with fixed class priors, above no-skill	0	$\mathcal{O} \in [50\%, 100\%]$ optimal only for $\pi_+ \simeq 0.325$	$\mathcal{O} = 5/6 \simeq 83.33\%$	$\mathcal{O} = 5/6 \simeq 83.33\%$ (it selects $SIVF$)	our analytical result cf. Eq. (21)
uniform distributions with fixed class priors, close to oracle	$\in (0, 1/2)$	$\mathcal{O} \in [87.85\%, 100\%]$ optimal only for $\pi_+ \rightarrow 1$	$\mathcal{O} \in [50\%, 100\%]$ optimal only for $\pi_+ \simeq 0.561$	$\mathcal{O} \in [87.85\%, 100\%]$ (it selects F_1)	our numerical result cf. Fig. 5f
53 real sets of about 60 performances	$\in [-0.31, 0.65]$	$\mathcal{O} \in [52.23\%, 100.00\%]$ (mean: 78.44%)	$\mathcal{O} \in [50.00\%, 99.13\%]$ (mean: 56.71%)	$\mathcal{O} \in [69.69\%, 100.00\%]$ (mean: 89.53%)	our closed-form expression for the optimal β , Eq. (12)

Table 1. Summary of our results emphasizing the degree of optimality \mathcal{O} introduced in Eq. (16). As shown by the last column, we can always find the optimal ranking score (in green) between Pr and Re . Relying on a fixed and arbitrarily chosen score like F_1 or $SIVF$ can lead to catastrophic cases (in red). In our case studies, the simple heuristic introduced in Sec. 4.6 never led to such catastrophic cases, but nevertheless appeared to be suboptimal in some cases (in orange).

4. Case Studies

We now perform case studies for several distributions (see Fig. 4) and many sets of performances. The results have been obtained either analytically (all details in supplementary material) or numerically based on Monte Carlo simulations. A summary of the results, emphasizing the degree of optimality and providing the links to results that can be used to determine the optimal tradeoff, is provided in Tab. 1.

4.1. Uniform Distribution Over All Performances

Let us start by considering the uniform distribution over the set Π_1 of all performances: $\Pi_1 = \mathbb{P}_{(\Omega, \Sigma)}$. It is the Dirichlet distribution with all concentration parameters set to 1, and corresponds to a uniform distribution in a tetrahedron (see Fig. 4a). With this distribution, precision and

recall are uniformly distributed and positively correlated: $\tau(Pr; Re) = 1/3$. The F_1 score has not uniformly distributed values, but is the optimal tradeoff between Pr and Re :

$$\tau(Pr; F_1) = \tau(F_1; Re) = 2/3. \quad (17)$$

The skew-insensitive version of F_1 , $SIVF$, does not lead to meaningful rankings as it does not satisfy the 3rd axiom of the theory of performance-based ranking [31] on Π_1 . Moreover, we computed $\tau(Pr; SIVF) \simeq 0.43$ and $\tau(SIVF; Re) \simeq 0.81$, which implies that $SIVF$ it is not located on a shortest path between Pr and Re and is not at equidistance from them.

4.2. With Fixed Probability of True Negatives

Motivated by the fact that Pr , Re , and F_β give no importance to true negatives, we now consider a second

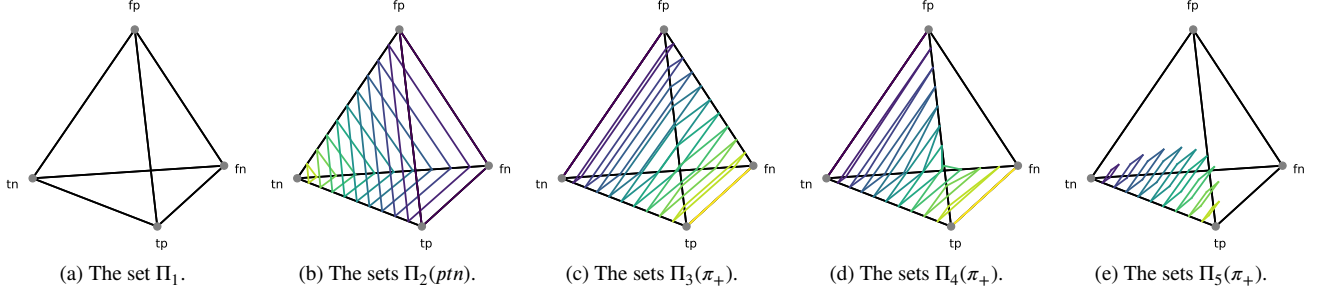


Figure 4. Graphical representation of some sets of two-class crisp classification performances considered in this paper. (a) All possible performances correspond to points in a regular tetrahedron. (b) The performances corresponding to fixed probabilities of true negatives are points in parallel equilateral triangles. (c) The performances corresponding to fixed class priors are points in parallel rectangles [27]. (d) The performances corresponding to fixed class priors and “above” no-skills are points in parallel right triangles. (e) The performances for given class priors, and “close to the oracle” are points in parallel squares. The color represents the value of the fixed parameter (ptn or π_+).

type of distributions, the uniform distribution over the sets $\Pi_2(pn) = \{P \in \mathbb{P}_{(\Omega, \Sigma)} : P(\{tn\}) = ptn\} \subset \Pi_1$. Note that $\Pi_2(0)$ is the set of performances considered in detection problems. As shown in Fig. 4b, these distributions correspond to uniform distributions over equilateral triangles. Pr and Re have uniformly distributed values and are positively correlated: $\tau(Pr; Re) = 1/3$.

For F_1 , our observations remain the same as what we had without any constraint, *i.e.* it is the optimal tradeoff:

$$\tau(Pr; F_1) = \tau(F_1; Re) = 2/3. \quad (18)$$

For *SIVF*, we found that it does not satisfy the 3rd axiom of the theory of performance-based ranking [31] on $\Pi_2(pn)$, unless $ptn = 0$. But, to the contrary of what we had without any constraint, *SIVF* is now located on a shortest path between Pr and Re . However, it is still far from being at equidistance from them. For $ptn = 0$, we found $\tau(Pr; SIVF) = 1/3$ and $\tau(SIVF; Re) = 1$.

4.3. With Fixed Class Priors

We now move to more realistic distributions for classification, and consider that one needs to rank only performances corresponding to some given class priors (π_-, π_+). For this reason, we consider the uniform distributions over the sets $\Pi_3(\pi_+) = \{P \in \mathbb{P}_{(\Omega, \Sigma)} : P(\{fn, tp\}) = \pi_+\} \subset \Pi_1$. As shown in Fig. 4c, these distributions correspond to uniform distributions over rectangles. This classical reference distribution is used, *e.g.*, in [36, 37]. It turns out that their axes correspond to $FPR \in [0, 1]$ and to $TPR \in [0, 1]$. The uniform distributions over $\Pi_3(\pi_+)$ correspond thus to uniform distributions of points in ROC. We found, no matter what the class priors are, that $\tau(Pr; Re) = 1/2$.

If we apply a two-components PCA to the rankings obtained with $\Pi_3(\pi_+)$ for $\pi_+ = 0.1$, we obtain the curve depicted in Fig. 1 (98.77% of total variance explained).

We stress that, to the contrary of what we concluded for the two previous distributions, when the class priors are

fixed, F_1 is far from the optimal tradeoff, as shown in Fig. 5a: unless $\pi_+ \simeq 0.381$, $\tau(Pr; F_1) \neq \tau(F_1; Re)$. In the extreme cases for which the prior of the negative (positive) class tends towards 1.0, the ranking induced by F_1 perfectly mimics the ranking induced by Pr (Re), thus totally ignoring the ranking induced by Re (Pr).

To find the optimal threshold, we need first to compute either $\tau(Pr; F_\beta)$ or $\tau(F_\beta; Re)$. The other can be found using Eq. (7). Analytically, we found

$$\tau(F_\beta; Re) = \frac{1}{2} + \ell - \ell^2 \log \frac{1 + \ell}{\ell}, \quad (19)$$

with ℓ defined as in Eq. (2). Then, we minimized the Fréchet variance, given in Eq. (8). If one considers some given class priors, then it is a function of β (see Fig. 5b) and the minimization leads to the optimal value of β for $F_* = F_\beta$. However, it is also possible to see the Fréchet variance as a function of ℓ . Its minimization leads to the solution $\ell \simeq 0.61585$. Injecting this value into Eq. (2), we obtained the link between the optimal β and the class priors:

$$\beta^2 = \ell \frac{\pi_-}{\pi_+} \Rightarrow b \simeq \frac{0.61585(1 - \pi_+)}{\pi_+ + 0.61585(1 - \pi_+)} \quad (20)$$

It is depicted in Fig. 5c. We see that the optimal relationship is quite close to that of *SIVF* (*i.e.*, $b = 1 - \pi_+$), but very different from that of F_1 (*i.e.*, $b = 1/2$).

4.4. With Fixed Class Priors, Above No-Skill

Performances below the rising diagonal of ROC, where the no-skill performances lie, are usually of little interest. For this reason, we study the case of the uniform distributions over the sets $\Pi_4(\pi_+) = \{P \in \mathbb{P}_{(\Omega, \Sigma)} : P(\{fn, tp\}) = \pi_+ \wedge TPR(P) \geq FPR(P)\} \subset \Pi_3(\pi_+)$. These sets are depicted in Fig. 4d. No matter what the class priors are, we obtain $\tau(Pr; Re) = 0$. All detailed results are in supplementary material. In a nutshell, the observations are very close to those reported for the uniform distributions with fixed class

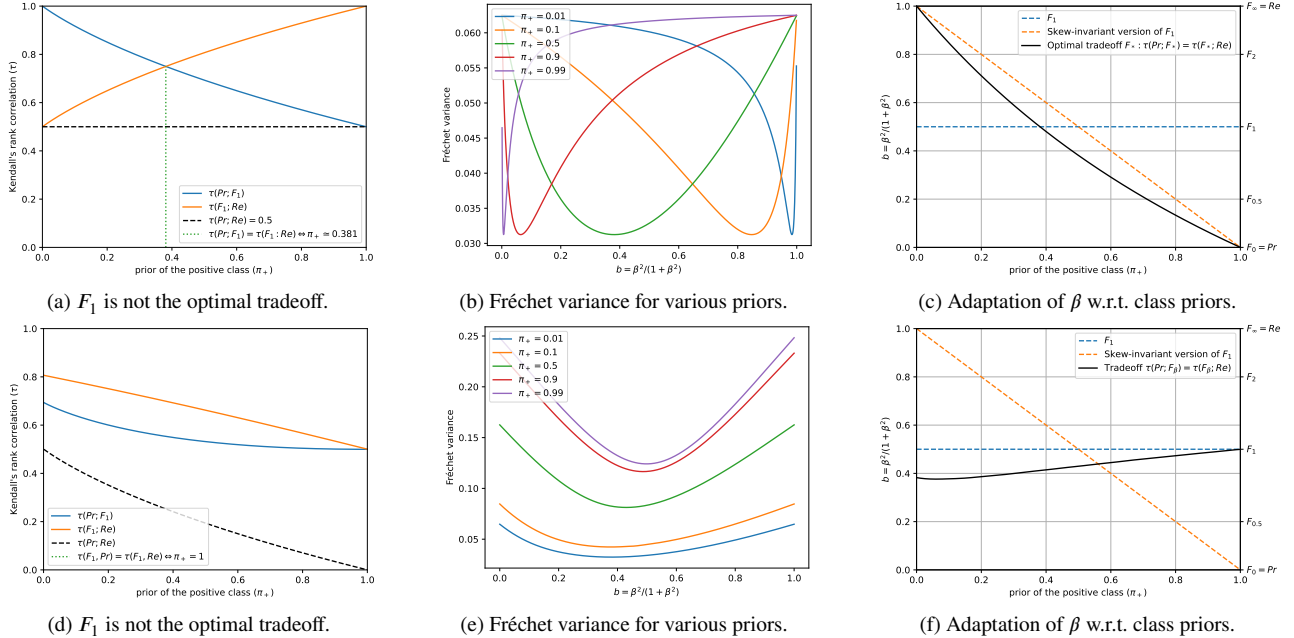


Figure 5. Results for uniform distributions with fixed class priors (top), *i.e.* $\Pi_3(\pi_+)$, and close to the oracle (bottom), *i.e.* $\Pi_5(\pi_+)$.

priors. The overall shape of the manifold, as observed by PCA, is very similar. $\tau(Pr; F_1)$ monotonically increases from 0 to 1 (instead of 0.5 to 1) and $\tau(F_1; Re)$ monotonically decreases from 1 to 0 (instead of 1 to 0.5) when π_+ sweeps the $[0, 1]$ interval. The F_1 score is the optimal tradeoff only for $\pi_+ \simeq 0.325$. Regarding the adaptation, the curve is slightly more curved and lower than the one we depicted in Fig. 5c, with the optimal value $\ell \simeq 0.48$:

$$\beta^2 = \ell \frac{\pi_-}{\pi_+} \Rightarrow b \simeq \frac{0.48(1 - \pi_+)}{\pi_+ + 0.48(1 - \pi_+)}. \quad (21)$$

4.5. With Fixed Class Priors, Close to Oracle

In competitions, a setting in which ranking is omnipresent, contenders usually refrain from choosing decision thresholds that would lead either to a high TPR at the cost of a high FPR or to a low FPR at the cost of a low TPR . In our opinion, this means that $FPR < \pi_+$ and $TPR > \pi_+$. In ROC, these performances are above and on the left-hand side of the no-skill performance that results from randomly choosing the negative or positive class with respective probabilities equal to π_- and π_+ . So, we now discuss the case of uniform distributions over the sets $\Pi_5(\pi_+) = \{P \in \mathbb{P}(\Omega, \Sigma) : P(\{fn, tp\}) = \pi_+ \wedge FPR(P) < \pi_+ \wedge TPR(P) > \pi_+\} \subset \Pi_4(\pi_+)$. As shown in Fig. 4e, these distributions correspond to uniform distributions over squares. Drawing a performance at random can be achieved by drawing independent values uniformly in $[0, \pi_+]$ for FPR and in $[\pi_+, 1]$ for TPR .

The results, shown in Figs. 5d to 5f, are remarkably different from the previous ones. In comparison to Fig. 5c,

Fig. 5f shows that the optimal β now increases from about 0.8 to 1, when π_+ increases from 0 to 1, while it was previously decreasing from ∞ to 0.

4.6. Some Real Sets of Performances

We now report results for performances encountered in existing rankings. They are either performances of some baseline methods or performances that people considered good enough for a competition. We consider a computer vision task known as *background subtraction*, similar to a pixelwise classification between background and foreground [12, 20]. The results of about 60 methods (classifiers), on 53 videos—a dataset known as *CDnet 2014* [35]—are publicly available on changedetection.net. According to [14], the multi-criteria ranking proposed by this platform is well correlated with F_1 . On any given video, all performances belong to $\Pi_3(\pi_+)$. Moreover, 99.9% and 99.4% of them belong to $\Pi_4(\pi_+)$ and $\Pi_5(\pi_+)$, respectively. Depending on the video, $\tau(Pr; Re) \in [-0.31, 0.65]$. Figure 6 shows the results for the set of performances reported for one video; more results are in the supplementary material. The optimal β is between 0.29 and 22.79 depending on the video. It is in the $[0.5, 2]$ range for only 35 videos among the 53.

An interesting observation, shown in Fig. 7, is that the class priors (π_-, π_+) are poor predictors for the optimal value of β . However, it also suggests that

$$\beta^2 = \frac{\mathbf{E}[PFP]}{\mathbf{E}[PFN]} = \frac{\sum_{P \in \Pi} P(\{fp\})}{\sum_{P \in \Pi} P(\{fn\})} \quad (22)$$

is a simple heuristic that is worth trying as an alternative to

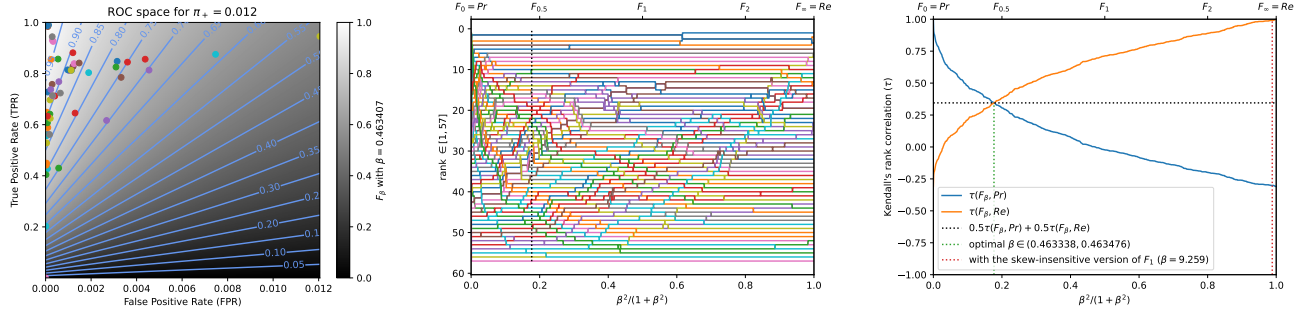


Figure 6. What is the optimal tradeoff for the performances of 57 background subtraction methods (pixelwise classifiers) on the *blizzard* video of *CDnet 2014*? Left: the 57 performances to be ranked, depicted in the ROC space, with the isometrics of the optimal tradeoff. Center: the ranks of each classifier, w.r.t. β . Right: $\tau(Pr; F_\beta)$ and $\tau(F_\beta; Re)$ w.r.t. β . The ranking with F_1 , at the center, is too far from Pr and too close to Re . The optimal tradeoff, for which $\tau(Pr; F_\beta) = \tau(F_\beta; Re)$ is at $\beta \simeq 0.463$.

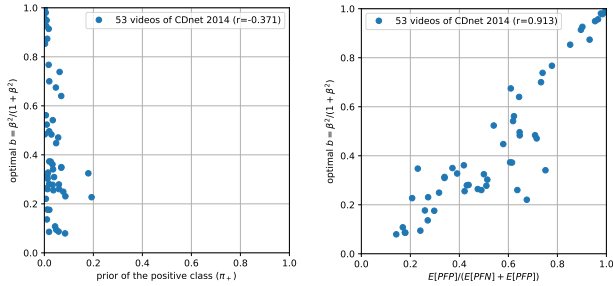


Figure 7. Which statistic about the sets of performances can be used to predict the optimal value of β ? These results are based on 53 sets of performances (those of about 60 methods on each video of *CDnet 2014*). Left: the class priors are not suitable. Right: the ratio of the average probability of false positives ($\mathbf{E}[PFP]$) to the average probability of errors ($\mathbf{E}[PFN] + \mathbf{E}[PFP]$) seems to be a good predictor for β , as Pearson's linear correlation between $\frac{\mathbf{E}[PFP]}{\mathbf{E}[PFN] + \mathbf{E}[PFP]}$ and $\frac{\beta^2}{1 + \beta^2}$ is $r \simeq 0.913$.

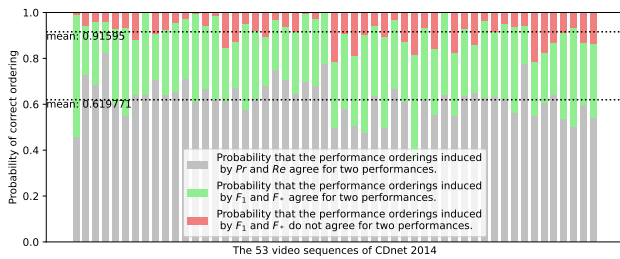


Figure 8. How far is F_1 from the optimal tradeoff F_* ? Each vertical bar is for a specific set of performances. \blacksquare : $P(\times)$, \blacksquare : $P(\checkmark)$, \blacksquare : $P(\times)$.

the closed-form and optimal solution provided in Eq. (12). The degree of optimality \mathcal{O} achieved by this heuristic is provided in Tab. 1 for all our case studies.

Figure 8 shows the consequences of using F_1 for ranking instead of the optimal tradeoff F_* . On average, there is

61.98% (\blacksquare) of chance that a randomly chosen pair of methods is ranked the same by Pr and Re . In this case, which tradeoff is chosen among all F_β is not relevant. But when Pr and Re disagree, the value of β matters. The degree of optimality for F_1 is only about $\mathcal{O} \simeq 78\%$ (\blacksquare) on average.

5. Conclusion

Nobody would ever choose a classifier solely based on the precision Pr or the recall Re . The traditional approach of calculating the harmonic mean F_1 of these two scores and then ranking the classifiers based on it is, unfortunately, nothing but a red herring. The colossal problem, ignored in the literature until now, is that the ranking built upon the balanced average of two scores is generally not a good tradeoff between the rankings obtained with the two base scores. In extreme cases, the ranking obtained with F_1 copies the ranking based on Pr or Re and totally ignores the other.

To solve these issues, we defined and described the manifold of rankings induced by scores (see Fig. 1) and found that the distance along it is linearly related to Kendall's rank correlation τ . Besides, we showed that all F_β scores induce meaningful rankings, even without any constraint on the performances. We further proved that the F_β scores induce rankings that form a shortest path between the rankings of Pr and Re . Also, we provided the theory and methods (including a closed-form expression) for defining and identifying the optimal tradeoffs between the rankings induced by Pr and Re . Lastly, we exemplified six case studies, covering numerous distributions and sets of performances. A summary of our results is provided in Tab. 1.

Acknowledgments. S. Piérard is funded by grants 8573 (ReconnAissance project) and 2010235 (ARIAC by DIGITALWALLONIA4.AI) of the SPW EER, Wallonia, Belgium; A. Deliège is a F.R.S.-FNRS postdoc researcher.

References

- [1] Davide Ballabio, Francesca Grisoni, and Roberto Todeschini. Multivariate comparison of classification performance measures. *Chemometrics and Intelligent Laboratory Systems*, 174:33–44, 2018. [2](#)
- [2] Thierry Bouwmans, Antonio Greco, Sébastien Piérard, Andrea Vincenzo Ricciardi, Carlo Sansone, Marc Van Droogenbroeck, and Bruno Vento. Illegal waste dumping detection. In *IEEE/CVF Winter Conference on Applications of Computer Vision Workshops (WACVW)*, pages 539–548, Tucson, Arizona, USA, 2026. [12](#)
- [3] Ted Byrt, Janet Bishop, and John B. Carlin. Bias, prevalence and kappa. *Journal of Clinical Epidemiology*, 46(5):423–429, 1993. [87](#)
- [4] Gürol Canbek, Seref Sagiroglu, Tugba Taskaya Temizel, and Nazife Baykal. Binary classification performance measures/metrics: A comprehensive visualized roadmap to gain new insights. In *International Conference on Computer Science and Engineering (UBMK)*, pages 821–826, Antalya, Turkey, 2017. IEEE. [2](#)
- [5] Seung-Seok Choi, Sung-Hyuk Cha, and Charles C. and Tapert. A survey of binary similarity and distance measures. *Journal of Systemics, Cybernetics and Informatics*, 8(1):43–48, 2010. [2](#)
- [6] Peter Christen, David J. Hand, and Nishadi Kirielle. A review of the F-measure: Its history, properties, criticism, and alternatives. *ACM Computing Surveys*, 56(3):1–24, 2023. [2](#)
- [7] Luciana Ferrer. Analysis and comparison of classification metrics. *arXiv*, abs/2209.05355, 2022. [2](#)
- [8] Cèsar Ferri, José Hernández-Orallo, and Ramona Modroiu. An experimental comparison of performance measures for classification. *Pattern Recognition Letters*, 30(1):27–38, 2009. [2](#)
- [9] Peter Flach and Meelis Kull. Precision-recall-gain curves: PR analysis done right. In *Advances in Neural Information Processing Systems (NeurIPS)*, pages 838–846, Montréal, Canada, 2015. Curran Associates, Inc. [14](#)
- [10] Peter A. Flach. The geometry of ROC space: Understanding machine learning metrics through ROC isometrics. In *International Conference on Machine Learning (ICML)*, pages 194–201, Washington, District of Columbia, USA, 2003. ML Research Press. [1](#), [2](#), [3](#), [13](#), [24](#), [27](#), [30](#), [87](#)
- [11] Maurice Fréchet. Les éléments aléatoires de nature quelconque dans un espace distancié. *Annales de l’institut Henri Poincaré*, 10(4):215–310, 1948. [4](#), [14](#)
- [12] Belmar Garcia-Garcia, Thierry Bouwmans, and Alberto Jorge Rosales Silva. Background subtraction in real applications: Challenges, current models and future directions. *Computer Science Review*, 35:1–42, 2020. [7](#)
- [13] Cyril Goutte and Eric Gaussier. A probabilistic interpretation of precision, recall and F-score, with implication for evaluation. In *Advances in Information Retrieval (Proceedings of ECIR)*, pages 345–359. Springer, 2005. [1](#)
- [14] Nil Goyette, Pierre-Marc Jodoin, Fatih Porikli, Janusz Konrad, and Prakash Ishwar. Changedetection.net: A new change detection benchmark dataset. In *IEEE International Conference on Computer Vision and Pattern Recognition Work-*
- shops (CVPRW)*, pages 1–8, Providence, RI, USA, 2012. Institute of Electrical and Electronics Engineers (IEEE). [7](#)
- [15] Anaïs Halin, Sébastien Piérard, Anthony Cioppa, and Marc Van Droogenbroeck. A hitchhiker’s guide to understanding performances of two-class classifiers. *arXiv*, abs/2412.04377, 2024. [2](#)
- [16] Mohammad Hossin and M. N. Sulaiman. A review on evaluation metrics for data classification evaluations. *International Journal of Data Mining & Knowledge Management Process*, 5(2):1–11, 2015. [2](#)
- [17] Matthias Ivantsits, Leonid Goubergrits, Jan-Martin Kuhnigk, Markus Huellebrand, Jan Brüning, Tabea Kossen, Boris Pfahringer, Jens Schaller, Andreas Spuler, Titus Kuehne, and Anja Hennemuth. Cerebral aneurysm detection and analysis challenge 2020 (CADA). In *International workshop on Cerebral Aneurysm Detection (CADA)*, pages 3–17, Lima, Peru, 2021. Springer International Publishing. [5](#), [12](#), [16](#), [17](#)
- [18] Matthias Ivantsits, Markus Huellebrand, Sebastian Kelle, Titus Kuehne, and Anja Hennemuth. Intracranial aneurysm rupture risk estimation utilizing vessel-graphs and machine learning. In *International workshop on Cerebral Aneurysm Detection (CADA)*, pages 93–103, Lima, Peru, 2021. Springer International Publishing. [17](#)
- [19] Nathalie Japkowicz and Mohak Shah. *Evaluating Learning Algorithms: A Classification Perspective*. Cambridge University Press, 2011. [2](#)
- [20] Pierre-Marc Jodoin, Sébastien Piérard, Yi Wang, and Marc Van Droogenbroeck. Overview and benchmarking of motion detection methods. In *Background Modeling and Foreground Detection for Video Surveillance*, chapter 24. Chapman and Hall/CRC, 2014. [7](#)
- [21] Hermann Karcher. Riemannian center of mass and mollifier smoothing. *Communications on Pure and Applied Mathematics*, 30(5):509–541, 1977. [4](#), [14](#)
- [22] John G. Kemeny. Mathematics without numbers. *Daedalus*, 88(4):577–591, 1959. [4](#)
- [23] Maurice George Kendall. A new measure of rank correlation. *Biometrika*, 30(1/2):81, 1938. [3](#), [4](#)
- [24] Andrey Nikolaevich Kolmogorov. Sur la notion de la moyenne. *Atti della Accademia Nazionale dei Lincei*, 12(9):388–391, 1930. [3](#)
- [25] Yanguang Liu, Yangming Zhou, Shiting Wen, and Chao-gang Tang. A strategy on selecting performance metrics for classifier evaluation. *International Journal of Mobile Computing and Multimedia Communications*, 6(4):20–35, 2014. [2](#)
- [26] Yanfei Liu, Yunqiao Yang, Yi Lin, Yuexiang Li, Dong Wei, Kai Ma, and Yefeng Zheng. Cerebral aneurysm rupture risk estimation using XGBoost and fully connected neural network. In *International workshop on Cerebral Aneurysm Detection (CADA)*, pages 87–92, Lima, Peru, 2021. Springer International Publishing. [17](#)
- [27] David Lovell, Dimity Miller, Jaiden Capra, and Andrew P. Bradley. Never mind the metrics – what about the uncertainty? visualising binary confusion matrix metric distributions to put performance in perspective. In *International Conference on Machine Learning (ICML)*, pages 22702–22757, 2023. [6](#)

- [28] Sébastien Piérard and Marc Van Droogenbroeck. Summarizing the performances of a background subtraction algorithm measured on several videos. In *IEEE International Conference on Image Processing (ICIP)*, pages 3234–3238, Abu Dhabi, United Arab Emirates, 2020. 86, 88
- [29] Sébastien Piérard, Anaïs Halin, Anthony Cioppa, Adrien Delière, and Marc Van Droogenbroeck. The Tile: A 2D map of ranking scores for two-class classification. *arXiv*, abs/2412.04309, 2024. 2
- [30] Sébastien Piérard, Adrien Delière, and Marc Van Droogenbroeck. Multi-domain performance analysis with scores tailored to user preferences. *arXiv*, abs/2512.08715, 2025. 86
- [31] Sébastien Piérard, Anaïs Halin, Anthony Cioppa, Adrien Delière, and Marc Van Droogenbroeck. Foundations of the theory of performance-based ranking. In *IEEE/CVF Conference on Computer Vision and Pattern Recognition (CVPR)*, pages 14293–14302, Nashville, Tennessee, USA, 2025. IEEE. 2, 3, 5, 6, 12, 13, 16
- [32] David M. W. Powers. Evaluation: from precision, recall and F-measure to ROC, informedness, markedness & correlation. *Journal of Machine Learning Technologies*, 2(1): 37–63, 2011. 2
- [33] Marina Sokolova and Guy Lapalme. A systematic analysis of performance measures for classification tasks. *Information Processing & Management*, 45(4):427–437, 2009. 2
- [34] Charles Spearman. The proof and measurement of association between two things. *The American Journal of Psychology*, 15(1):72–101, 1904. 3
- [35] Yi Wang, Pierre-Marc Jodoin, Fatih Porikli, Janusz Konrad, Yannick Benezeth, and Prakash Ishwar. CDnet 2014: An expanded change detection benchmark dataset. In *IEEE/CVF Conference on Computer Vision and Pattern Recognition Workshops (CVPRW)*, pages 393–400, Columbus, Ohio, USA, 2014. Institute of Electrical and Electronics Engineers (IEEE). 7
- [36] Ningsheng Zhao, Jia Yuan Yu, and Krzysztof Dzieciolowski. Classifier rank – a new classification assessment method. In *International Conference Big Data Analytics, Data Mining and Computational Intelligence*, pages 233–237, Lisbon, Portugal, 2022. iadis. 6
- [37] Ningsheng Zhao, Trang Bui, Jia Yuan Yu, and Krzysztof Dzieciolowski. Outperformance score: A universal standardization method for confusion-matrix-based classification performance metrics. *arXiv*, abs/2505.07033, 2025. 6

A. Supplementary Material

This is the supplementary material for paper *What Is the Optimal Ranking Score Between Precision and Recall? We Can Always Find It and It Is Rarely F_1 .*

Contents

A.1. Supplementary Material About Sec. 2.2.(Building Upon the Related Work)	12
A.1.1. Wide Use of F_1	12
A.1.2. Reminder of the Three Axioms of Performance-Based Ranking	12
A.1.3. All F_β Lead to Meaningful Performance Orderings	12
A.1.4. <i>SIVF</i> Leads to a Meaningful Performance Ordering When the Class Priors Are Fixed	13
A.1.5. <i>SIVF</i> Leads to the Same Ranking as F_β with $\beta^2 = \frac{\pi_-}{\pi_+}$	13
A.2. Supplementary Material About Sec. 3.(Theory)	14
A.2.1. On the Minimization of Fréchet Variance (Eq. (8))	14
A.2.2. On the Close-Form Expression for the Optimal β (Eqs. (11) and (12))	14
A.2.3. On the Formulas for Degree of Optimality of Some F_β	14
A.2.4. On the CADA-RRE Example Used to Illustrate the Theory	16
A.3. Supplementary Material About Sec. 4.(Case Studies)	18
A.3.1. Principle of Analytical Computations for Kendall's rank correlations τ with Distributions of Performances	18
A.3.2. Detailed Results for the Uniform Distribution Over All Performances	19
A.3.3. Detailed Results for the Uniform Distributions With Fixed Probability of True Negatives	20
A.3.4. Detailed Results for the Uniform Distributions With Fixed Class Priors	22
A.3.5. Detailed Results for the Uniform Distributions With Fixed Class Priors, Above No-Skill	25
A.3.6. Detailed Results for the Uniform Distributions With Fixed Class Priors, Close to Oracle	28
A.3.7. All Results for Some Real Sets of Performances	31
A.3.8. More information on our simple heuristic for ROC users	86

A.1. Supplementary Material About Sec. 2.2.(Building Upon the Related Work)

A.1.1. Wide Use of F_1

The F_1 score (*a.k.a.* Dice) is definitely standard in computer vision, serving as ranking criteria in benchmarks and challenges on tasks such as image/video classification in medical imaging (COVID-CT, PAIP, ECDP, TN-SCUI), and behavior analysis (ABAW), segmentation in video surveillance (IWDD [2]), medical imaging (3D-TEETH-SEG, DRAC, UNICORN), and visual quality control (VAND), detection in medical imaging (MIDOG, UNICORN). Also, CADA-RRE [17] uses F_2 ; we discuss it in Sec. A.2.4. Notably, some are from CVPR'25 (VAND, ABAW). More exist in computer vision and beyond.

A.1.2. Reminder of the Three Axioms of Performance-Based Ranking

These axioms are from last year CVPR paper [31].

The first axiom states that a ranking must be established based on a preorder \lesssim on the performances. Following Theorem 1 of [31], in this paper, we consider only preorders \lesssim_X induced by a score X in the following manner. Regardless of whether the performances P_1 and P_2 to be compared belong to the domain of definition of X , we decide that $P_1 \lesssim_X P_2$ when $P_1 = P_2$. If P_1 and P_2 are both in the domain of definition of X , then we decide that $P_1 \lesssim_X P_2$ if and only if $X(P_1) \leq X(P_2)$. In all other cases, $P_1 \not\lesssim_X P_2$. Such a preorder is called *performance ordering induced by X* . As an immediate consequence of this first axiom, the rankings are stable: it is impossible to swap two previously compared methods by inserting or deleting methods in the ranking.

The two other axioms ensure that one can interpret the binary relation \lesssim_X as *worse or equivalent*. For the sake of consistency, all the other binary relations of interest (*worse than, better than, equivalent to, incomparable with, etc.*) are derived from \lesssim_X . When the two following axioms are satisfied, we say that the performance ordering induced by X satisfy the axioms of performance-based ranking, or more simply that X satisfy the axioms.

The second axiom specifies a condition that must be satisfied for the preorder \lesssim_X on performances to be compatible with the task. In the case of the two-class crisp classification task studied in this paper, the satisfaction S is binary: we are not at all satisfied with a false positive or a false negative, and we are fully satisfied with a true negative and a true positive. Denoting the accuracy by A , the second axiom, given in a generic form in [31], is in this case equivalent to three conditions: (1) there is no performance worse than a performance P such that $A(P) = 0$; (2) if a performance P_1 is such that $A(P_1) = 0$ and a performance P_2 is such that $A(P_2) = 1$, then P_1 can never be better than P_2 ; (3) there exists no performance better than a performance P such that $A(P) = 1$. The second axiom thus focuses on the extreme cases of the worst and best performances, but says nothing about intermediate performances. It should be noted that it is very permissive. A score may put performances for which $A(P) > 0$ on the same footing the worst performances, or performances for which $A(P) < 0$ on the same footing the best performances. This is for example the case of F_1 : $A = 0 \Rightarrow F_1 = 0$ but $F_1 = 0 \not\Rightarrow A = 0$.

The third axiom specifies a condition that must be satisfied for the preorder \lesssim_X on performances to be compatible with evaluation (*i.e.*, the mapping from methods to performances). It is this third axiom that constrains the ordering of performances that are neither among the best nor among the worst ones. Consider a *blind* and non-deterministic combination of some base methods to form a hybrid method: each time the hybrid method is used, it begins by randomly selecting one of the base methods, *independently of its input*, and then executes that method. As the combination is *blind*, it would not make sense for the hybrid method to be better or worse than the best or the worst of the combined methods, respectively. Note that this axiom is not satisfied by *SIVF* in general, but is satisfied by it when the priors are fixed.

A.1.3. All F_β Lead to Meaningful Performance Orderings

It has been shown in [31] that all performance orderings derived from some score of the form

$$R_I(P) = \frac{I(tn)P(\{tn\}) + I(tp)P(\{tp\})}{I(tn)P(\{tn\}) + I(fp)P(\{fp\}) + I(fn)P(\{fn\}) + I(tp)P(\{tp\})}, \quad (23)$$

where I denotes a positive random variable called *Importance*, satisfy all the axioms of the theory of performance-based ranking. These scores are known as *ranking scores*.

In order to prove that all F_β lead to meaningful performance orderings, we show here that the F_β are particular cases of R_I . The proofs for $\beta = 1/2$, $\beta = 1$, and $\beta = 2$ were already given in [31], so here we give a generalization. Our proof is based on the well known fact that F_β has two nearly equivalent definitions. The first one, that we have used in the introduction (Eq. (1)), is as follows:

$$F_\beta : \{P \in \mathbb{P}_{(\Omega, \Sigma)} : P(\{tp\}) \neq 0\} \rightarrow [0, 1] : P \mapsto \left(\frac{1}{1 + \beta^2} Pr^{-1}(P) + \frac{\beta^2}{1 + \beta^2} Re^{-1}(P) \right)^{-1}. \quad (24)$$

The second one is

$$F_\beta : \{P \in \mathbb{P}_{(\Omega, \Sigma)} : P(\{tn\}) \neq 1\} \rightarrow [0, 1] : P \mapsto \frac{(1 + \beta^2) P(\{tp\})}{1 P(\{fp\}) + \beta^2 P(\{fn\}) + (1 + \beta^2) P(\{tp\})}. \quad (25)$$

It turns out that the first definition is a restriction of the second one: $P(\{tp\}) \neq 0 \Rightarrow P(\{tn\}) \neq 1$ and both F_β are equal on $\{P \in \mathbb{P}_{(\Omega, \Sigma)} : P(\{tp\}) \neq 0\}$. It is now possible to compare Eq. (25) with Eq. (23) and to see that, for any given β , F_β is a particular case of ranking score with

$$(I(tn), I(fp), I(fn), I(tp)) \propto (0, 1, \beta^2, 1 + \beta^2), \quad (26)$$

or equivalently

$$(I(tn), I(fp), I(fn), I(tp)) \propto (0, 1 - b, b, 1), \quad (27)$$

with $b = \beta^2 / (1 + \beta^2)$.

A.1.4. *SIVF* Leads to a Meaningful Performance Ordering When the Class Priors Are Fixed

The skew-insensitive version of F_1 as been defined in [10] as

$$SIVF = \frac{2TPR}{TPR + FPR + 1}. \quad (28)$$

When the class priors are fixed and such that $\pi_- \neq 0$ and $\pi_+ \neq 0$,

$$\begin{aligned} SIVF(P) &= \frac{2 \frac{P(\{tp\})}{\pi_+}}{\frac{P(\{tp\})}{\pi_+} + \frac{P(\{fp\})}{\pi_-} + 1} = \frac{2 \pi_- P(\{tp\})}{\pi_- P(\{tp\}) + \pi_+ P(\{fp\}) + \pi_- \pi_+} \\ &= \frac{2 \pi_- P(\{tp\})}{\pi_- P(\{tp\}) + \pi_+ P(\{fp\}) + \pi_- (P(\{fn\}) + P(\{tp\}))} = \frac{2 \pi_- P(\{tp\})}{\pi_+ P(\{fp\}) + \pi_- P(\{fn\}) + 2 \pi_- P(\{tp\})}. \end{aligned} \quad (29)$$

The comparison of Eq. (29) with Eq. (23) shows that *SIVF* is a particular case of ranking score with

$$(I(tn), I(fp), I(fn), I(tp)) \propto (0, \pi_+, \pi_-, 2 \pi_-). \quad (30)$$

A.1.5. *SIVF* Leads to the Same Ranking as F_β with $\beta^2 = \frac{\pi_-}{\pi_+}$

A first demonstration, based on the relationship between *SIVF* and F_β . From [10], it is already known that $SIVF = F_1$ when $\pi_- = \pi_+ = 1/2$. Here, we give a generalization for $\pi_- \neq 0$ and $\pi_+ \neq 0$. We noticed that

$$\beta^2 = \frac{\pi_-}{\pi_+} \Rightarrow F_\beta = \frac{SIVF}{(\pi_+ - \pi_-) SIVF + 2 \pi_-}. \quad (31)$$

When $\pi_- \neq 0$, we have

$$\beta^2 = \frac{\pi_-}{\pi_+} \Rightarrow \frac{\partial F_\beta}{\partial SIVF} > 0. \quad (32)$$

Therefore, when the priors are fixed, *SIVF* leads to the same performance ordering as F_β with $\beta^2 = \frac{\pi_-}{\pi_+}$.

A second demonstration, based on the importance values. Property 4 of [31], when particularized for two-class classification, states that the performance ordering induced by a ranking score is insensitive to the uniform scaling of the importance given to the unsatisfying samples (*fp* and *fn*) or to the satisfying (*tn* and *tp*) samples. The comparison between Eq. (26) and Eq. (30) shows that:

- for the unsatisfying samples, we have $(\bullet, 1, \beta^2, \bullet) \propto (\bullet, \pi_+, \pi_-, \bullet)$ when $\beta^2 = \frac{\pi_-}{\pi_+}$;
- for the satisfying samples, we have always $(0, \bullet, \bullet, 1 + \beta^2) \propto (0, \bullet, \bullet, 2 \pi_-)$.

Therefore, when the priors are fixed, *SIVF* leads to the same performance ordering as F_β with $\beta^2 = \frac{\pi_-}{\pi_+}$.

A.2. Supplementary Material About Sec. 3.(Theory)

A.2.1. On the Minimization of Fréchet Variance (Eq. (8))

In Sec. 3.4.1, we say that the optimal tradeoffs are the F_β scores that minimize the Fréchet variance [11]:

$$\sigma^2(\beta) = d_\tau^2(Pr; F_\beta) + d_\tau^2(F_\beta; Re).$$

We also say that the solutions, known as the Karcher means [21] are those that are equidistant of Pr and Re , *i.e.* such that

$$\begin{aligned} d_\tau(Pr; F_*) &= d_\tau(F_*; Re) = \frac{d_\tau(Pr; Re)}{2} \\ \Leftrightarrow \tau(Pr; F_*) &= \tau(F_*; Re) = \frac{1 + \tau(Pr; Re)}{2}. \end{aligned}$$

Hereafter, we discuss here the case of a continuum of rankings, as shown in Fig. A.2.1a. The case of a finite amount of rankings is depicted in Fig. A.2.1b and Fig. A.2.1c for, respectively, an odd and an even amount.

By restricting to the family of F_β scores, the solution is actually unique and is thus a Fréchet mean. Indeed, since Eq. (6) states that

$$d_\tau(Pr; Re) = d_\tau(Pr; F_\beta) + d_\tau(F_\beta; Re) \quad \forall \beta \geq 0$$

we have

$$\sigma^2(\beta) = d_\tau^2(Pr; F_\beta) + (d_\tau(Pr; Re) - d_\tau(Pr; F_\beta))^2 \quad (33)$$

$$= 2d_\tau^2(Pr; F_\beta) - 2d_\tau(Pr; Re)d_\tau(Pr; F_\beta) + d_\tau^2(Pr; Re) \quad (34)$$

which is quadratic in $d_\tau(Pr; F_\beta)$ and thus uniquely minimized for β such that

$$d_\tau(Pr; F_\beta) = \frac{d_\tau(Pr; Re)}{2}. \quad (35)$$

This incidentally yields the same equality for $d_\tau(F_\beta; Re)$. The result in terms of correlation stems from the relation $\tau = 1 - 2d_\tau$.

A.2.2. On the Close-Form Expression for the Optimal β (Eqs. (11) and (12))

Complexity/scalability. After evaluating n classifiers, a straightforward computation of the optimal β with our formulas requires indeed $O(n^2)$ uses of Eq. (11) (same as for Kendall's τ). Even for $n = 1000$ (hardly met in practice), this takes less than one second on a modern laptop.

An alternative to Eq. (11). We thank Peter Flach for pointing out that Eq. (11) can be rewritten in terms of only precision and recall values as follows:

$$\vartheta(P_1, P_2) = -\frac{Pr^{-1}(P_1) - Pr^{-1}(P_2)}{Re^{-1}(P_1) - Re^{-1}(P_2)}. \quad (36)$$

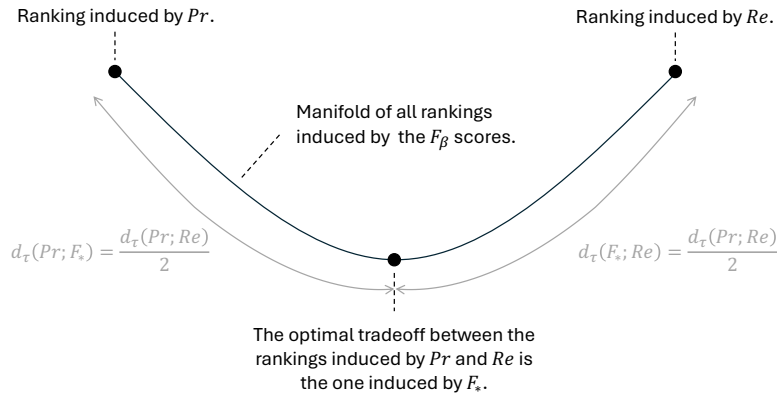
This formula is Eq. (6) in [9].

Downstream objective. We can generalize Eq. (8) by weighting d_τ^2 and Eq. (12) by replacing the median by a quantile. To ensure that the 0% quantile corresponds to Pr and that the 100% quantile corresponds to Re , the quantile is taken over $\{0, \infty\} \cup \{\vartheta(P_i, P_j) \mid i \neq j \wedge \vartheta(P_i, P_j) \geq 0\}$. For instance, to weight four times more Re than Pr , from the *point of view of values* one uses $b = 0.8$ in Eq. (1) (*i.e.*, $\beta = 2$, as in CADA-RRE). But from the *point of view of ranks*, we take the 80th percentile of ϑ values. This leads to $\beta = 0.914$ in the example of CADA-RRE (Sec. A.2.4). The relationship between the downstream objective (*i.e.*, the chosen quantile) and the optimal value for β is shown in Fig. A.2.2.

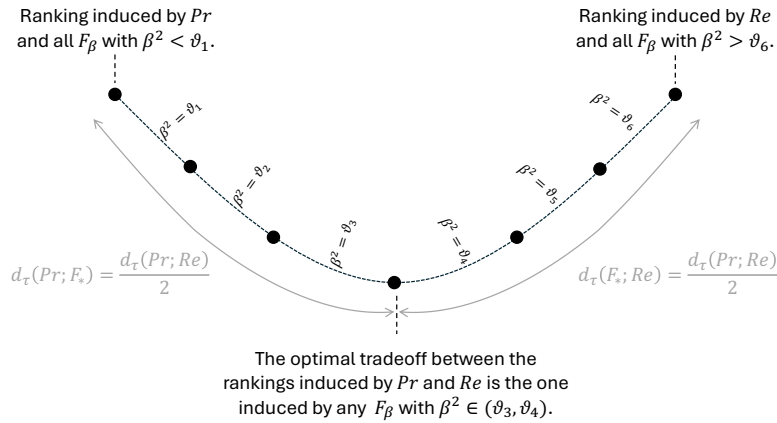
A.2.3. On the Formulas for Degree of Optimality of Some F_β

We provide here a few explanations about how Eqs. (13) to (15) can be derived. For that, let us remind three interpretations for Kendall's distance $d_\tau(X_1; X_2) \in [0, 1]$.

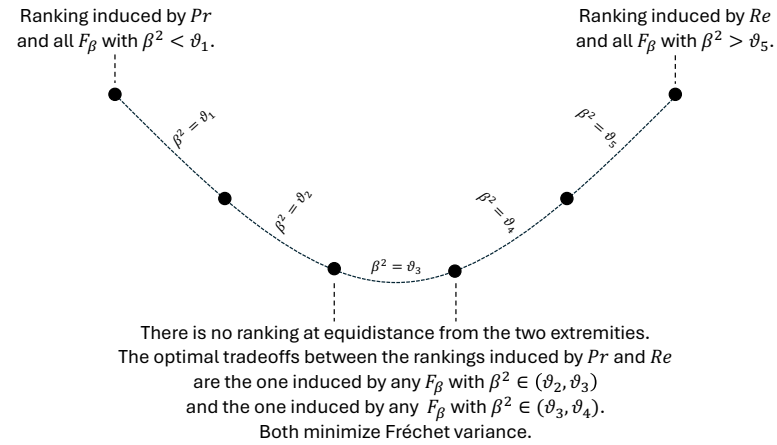
- First, Eq. (5) shows that $d_\tau(X_1; X_2)$ is equal to the proportion of pairs of elements for which X_1 and X_2 do not agree on the relative order. This interpretation is the cornerstone for probabilistic reasoning.



(a) Case in which there is a bijection between the values of β and the rankings induced by F_β . The rankings form a continuum (manifold) and the minimization of Fréchet variance leads to the midpoint where $d_\tau(Pr; F_*) = d_\tau(F_*; Re)$.



(b) Case in which the number of rankings induced by the F_β scores is odd. The rankings form a path graph. The nodes correspond to the rankings, each of them being induced by a range of values for β . The edges correspond to the swaps that occur between the consecutive rankings, at some given values ϑ for the β parameter. Assuming there is no group of at least three co-aligned performances, the median of all these ϑ values belongs to the range of β s for which the ranking is at the midpoint where $d_\tau(Pr; F_*) = d_\tau(F_*; Re)$.



(c) Case in which the number of rankings induced by the F_β scores is even. Assuming there is no group of at least three co-aligned performances, the median of all the ϑ values corresponds to the swap between the two rankings minimizing Fréchet variance.

Figure A.2.1. The optimal tradeoff as the solution of the minimization of Fréchet variance $\sigma^2(\beta)$.

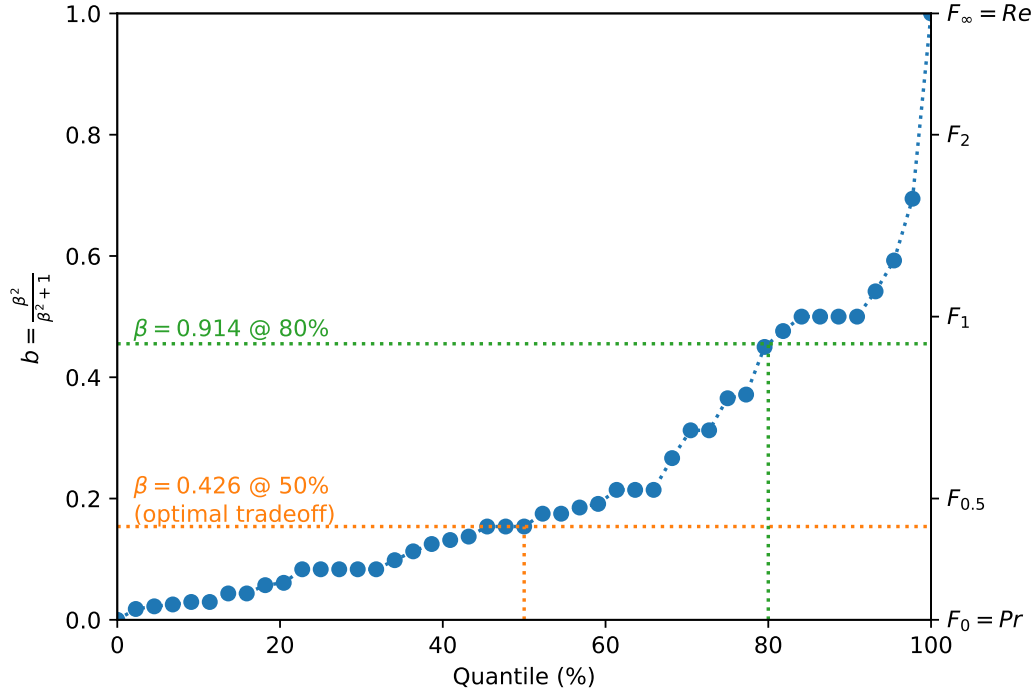


Figure A.2.2. The relationship between the downstream objective (*i.e.*, the chosen quantile) and the optimal value for β , for the CADA-RRE example described in Sec. A.2.4. The points correspond to the various values of β for which a swap between two consecutive classifiers occurs in the ranking. Taking the median (*i.e.*, the 50% quantile) leads to the optimal, balanced, tradeoff studied in this paper.

- Second, $d_\tau(X_1; X_2)$ is equal to the minimum number of swaps of consecutive elements that are needed to transform the ranking induced by X_1 into the ranking induced by X_2 and vice versa. This interpretation is the cornerstone for geometric reasoning, as it makes the connection with the distance along the manifold (or path graph) of rankings.
- Third, $d_\tau(X_1; X_2)$ is linearly related to the rank correlation $\tau(X_1; X_2)$ as $d_\tau = \frac{1-\tau}{2}$.

Keeping these three interpretations in mind is helpful to derive Eqs. (13) to (15).

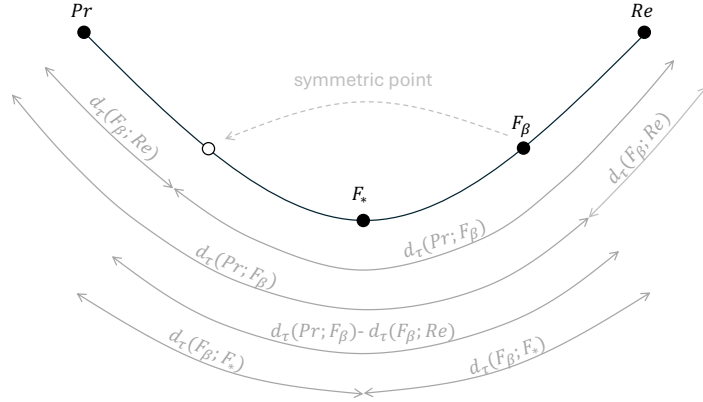
Let us consider Eq. (14), for example. We are interested in the probability $P(\mathcal{X})$. The first interpretation allows us to express it as $d_\tau(F_\beta; F_*)$. Then, it is possible to perform some geometric reasoning based on the second interpretation. As shown in Fig. A.2.3, $d_\tau(F_\beta; F_*) = 1/2 |d_\tau(F_\beta; Re) - d_\tau(Pr; F_\beta)|$. Finally, using the third interpretation, we find that $1/2 |d_\tau(F_\beta; Re) - d_\tau(Pr; F_\beta)| = 1/4 |\tau(Pr; F_\beta) - \tau(F_\beta; Re)|$.

A.2.4. On the CADA-RRE Example Used to Illustrate the Theory

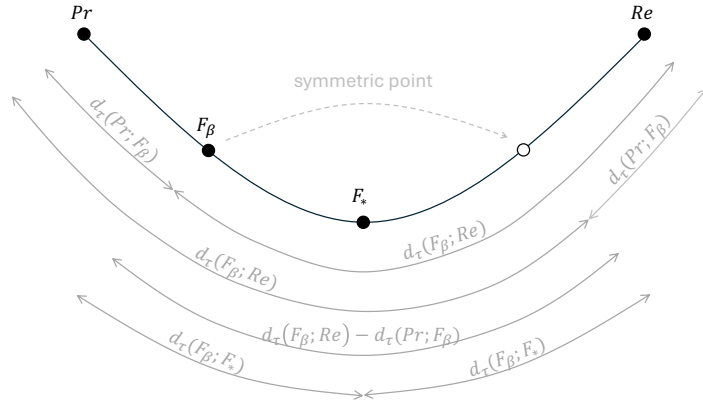
Among the various challenges hosted on *Grand Challenge*, we found that the third task of the *Cerebral Aneurysm Detection and Analysis* (CADA) challenge [17] is particularly interesting. This task is known as CADA-RRE for *Cerebral Aneurysm Rupture Risk Estimation* and is hosted at <https://cada-rre.grand-challenge.org/>. It consists in the automatic classification of known ruptured and unruptured aneurysms based on rotational X-ray angiographic images.

Even if the ranking chosen by the organizers is only based on F_2 , the logs contain for each entry the values of five ranking scores [31]: the precision Pr , recall Re , accuracy A , F_1 , and indeed F_2 . This information allows one to recover the complete (normalized) confusion matrix with the probabilities of a true negative (PTN), false positive (PFN), false negative (PFN), and true positive (PTP). From these confusion matrices, we observed that the class priors are fixed and given by $\pi_- = 19/30$ and $\pi_+ = 11/30$. The values of PFN , PFN , and PTP can be used in Eq. (11), which gives the values used in Eq. (12) to compute an optimal β . The values of PFN and PFN can be used to derive $\mathbf{E}[PFN]$ and $\mathbf{E}[PFN]$, which in turn can be used to recommend a value for β with our heuristic Eq. (22).

At the time of writing these lines, the [challenge leaderboard](#) contains 29 entries. However, there are only 16 unique pairs of precision and recall values. This can be explained by the low number of cases on which the methods are tested. In our example based on CADA-RRE, we decided to rank the classifiers corresponding to these 16 unique pairs. This stands in contrast with



(a) Case in which the ranking induced by F_β is closer to the ranking induced by Re than to the ranking induced by Pr . We see that $d_\tau(F_\beta; F_*) = \frac{d_\tau(Pr; F_\beta) - d_\tau(F_\beta; Re)}{2}$.



(b) Case in which the ranking induced by F_β is closer to the ranking induced by Pr than to the ranking induced by Re . We see that $d_\tau(F_\beta; F_*) = \frac{d_\tau(F_\beta; Re) - d_\tau(Pr; F_\beta)}{2}$.

Figure A.2.3. Kendall distances on the manifold of rankings induced by the F_β scores. We see that $d_\tau(F_\beta; F_*) = \frac{|d_\tau(F_\beta; Re) - d_\tau(Pr; F_\beta)|}{2}$.

the official ranking of CADA-RRE as, for each participant, the organizers only considered the first three submissions with $F_2 \geq 0.1$. On the one hand, according to [17], the official ranking only contains three methods as only three teams submitted their solution: the 1st place is for [18] with $F_2 = 0.702$, the 2nd place is for [26] with $F_2 = 0.678$, and the 3rd place is for an unpublished method with $F_2 = 0.377$. On the other hand, the F_2 score is between 0.0 and 0.862 in the 16 entries that we rank. The results that we have obtained with the 16 performances to rank are provided in Figs. A.2.2, 3 and A.3.64.

What is particularly interesting with this example is that the organizers chose to rank the participants according to the F_2 score, as “the identification of aneurysms at risk is considered more important than the avoidance of false-positive risk classification”. As shown in the plots of Fig. 3, the ranking induced by F_2 perfectly mimics the ranking induced by Re , totally ignoring the ranking induced by Pr . This is certainly not what is expected when one chooses to rank according to some F_β . As shown in Fig. A.2.2 and already discussed in Sec. A.2.2, $\beta = 2$ is the value to use if one wants to weight four times more Re than Pr from the *point of view of values*, but $\beta = 0.914$ is the value to use to weight four times more Re than Pr from the *point of view of ranks*.

A.3. Supplementary Material About Sec. 4.(Case Studies)

A.3.1. Principle of Analytical Computations for Kendall's rank correlations τ with Distributions of Performances

Let us consider two scores X_1, X_2 . We denote the probability for them to order differently two (different) performances P_A and P_B drawn at random, independently, by $d_\tau(X_1; X_2)$. Kendall's rank correlation is given by $\tau(X_1; X_2) = 1 - 2d_\tau(X_1; X_2)$. When we consider a distribution of performances \mathcal{P} , instead of a finite set Π , we cannot compute $d_\tau(X_1; X_2)$ with Eq. (5). Instead, we can compute analytically the following probabilities:

$$\text{Proba} [X_1(P_A) < X_1(P_B), X_2(P_A) < X_2(P_B)] = \int_{P_A \in \mathbb{P}(\Omega, \Sigma)} \int_{P_B \in \mathbb{P}(\Omega, \Sigma)} \mathbf{1}_{X_1(P_A) < X_1(P_B), X_2(P_A) < X_2(P_B)} f_{\mathcal{P}}(P_A) f_{\mathcal{P}}(P_B) dP_A dP_B, \quad (37)$$

$$\text{Proba} [X_1(P_A) < X_1(P_B), X_2(P_A) > X_2(P_B)] = \int_{P_A \in \mathbb{P}(\Omega, \Sigma)} \int_{P_B \in \mathbb{P}(\Omega, \Sigma)} \mathbf{1}_{X_1(P_A) < X_1(P_B), X_2(P_A) > X_2(P_B)} f_{\mathcal{P}}(P_A) f_{\mathcal{P}}(P_B) dP_A dP_B, \quad (38)$$

$$\text{Proba} [X_1(P_A) > X_1(P_B), X_2(P_A) < X_2(P_B)] = \int_{P_A \in \mathbb{P}(\Omega, \Sigma)} \int_{P_B \in \mathbb{P}(\Omega, \Sigma)} \mathbf{1}_{X_1(P_A) > X_1(P_B), X_2(P_A) < X_2(P_B)} f_{\mathcal{P}}(P_A) f_{\mathcal{P}}(P_B) dP_A dP_B, \quad (39)$$

$$\text{Proba} [X_1(P_A) > X_1(P_B), X_2(P_A) > X_2(P_B)] = \int_{P_A \in \mathbb{P}(\Omega, \Sigma)} \int_{P_B \in \mathbb{P}(\Omega, \Sigma)} \mathbf{1}_{X_1(P_A) > X_1(P_B), X_2(P_A) > X_2(P_B)} f_{\mathcal{P}}(P_A) f_{\mathcal{P}}(P_B) dP_A dP_B, \quad (40)$$

where the symbol $\mathbf{1}$ denotes the indicator and $f_{\mathcal{P}}$ the probability density function related to the distribution \mathcal{P} .

Kendall's rank correlation τ is then given by

$$\tau(X_1; X_2) = 1 - 2 \left(\text{Proba} [X_1(P_A) < X_1(P_B), X_2(P_A) > X_2(P_B)] + \text{Proba} [X_1(P_A) > X_1(P_B), X_2(P_A) < X_2(P_B)] \right). \quad (41)$$

Note that P_A and P_B are exchangeable in these equalities since they are drawn independently from the same distribution. Thus, by symmetry, we have

$$\text{Proba} [X_1(P_A) < X_1(P_B), X_2(P_A) < X_2(P_B)] = \text{Proba} [X_1(P_A) > X_1(P_B), X_2(P_A) > X_2(P_B)], \quad (42)$$

and

$$\text{Proba} [X_1(P_A) < X_1(P_B), X_2(P_A) > X_2(P_B)] = \text{Proba} [X_1(P_A) > X_1(P_B), X_2(P_A) < X_2(P_B)]. \quad (43)$$

Moreover, the four probabilities sum to one. Thus, computing one of these four probabilities suffices to be able to determine τ , and if we know τ , then we are able to recover the four probabilities:

$$\tau(X_1; X_2) = 4 \text{Proba} [X_1(P_A) < X_1(P_B), X_2(P_A) < X_2(P_B)] - 1, \quad (44)$$

$$\tau(X_1; X_2) = 1 - 4 \text{Proba} [X_1(P_A) < X_1(P_B), X_2(P_A) > X_2(P_B)], \quad (45)$$

$$\tau(X_1; X_2) = 1 - 4 \text{Proba} [X_1(P_A) > X_1(P_B), X_2(P_A) < X_2(P_B)], \quad (46)$$

$$\tau(X_1; X_2) = 4 \text{Proba} [X_1(P_A) > X_1(P_B), X_2(P_A) > X_2(P_B)] - 1. \quad (47)$$

The source codes for the analytical results provided hereafter are for *Wolfram 14.2 (a.k.a. Mathematica)*.

A.3.2. Detailed Results for the Uniform Distribution Over All Performances

To find the probabilities necessary to compute τ , we integrate over the tetrahedron. We start with a few initializations.

```

1 Tetra = Simplex[{{1, 0, 0, 0}, {0, 1, 0, 0}, {0, 0, 1, 0}, {0, 0, 0, 1}}]
2 Ppv[ptn_, pfp_, pfn_, ptp_] := ptp/(pfp + ptp)
3 Tpr[ptn_, pfp_, pfn_, ptp_] := ptp/(pfn + ptp)
4 Fone[ptn_, pfp_, pfn_, ptp_] := 2*ptp/(pfp + pfn + 2*ptp)
5
6 tot = Integrate[
7     1,
8     {ptn1, pfp1, pfn1, ptp1} \[Element] Tetra,
9     {ptn2, pfp2, pfn2, ptp2} \[Element] Tetra
10 ]

```

We have

$$\tau(Pr; Re) = \frac{1}{3}, \quad (48)$$

as shown with the code:

```

1 pLtLt = Integrate[
2     Boole[
3         Ppv[ptn1, pfp1, pfn1, ptp1] < Ppv[ptn2, pfp2, pfn2, ptp2] &&
4         Tpr[ptn1, pfp1, pfn1, ptp1] < Tpr[ptn2, pfp2, pfn2, ptp2]
5     ],
6     {ptn1, pfp1, pfn1, ptp1} \[Element] Tetra,
7     {ptn2, pfp2, pfn2, ptp2} \[Element] Tetra
8 ] / tot
9 tau = 4 * pLtLt - 1

```

We have

$$\tau(Pr; F_1) = \frac{2}{3}, \quad (49)$$

as shown with the code:

```

1 pLtGt = Integrate[
2     Boole[
3         Ppv[ptn1, pfp1, pfn1, ptp1] < Ppv[ptn2, pfp2, pfn2, ptp2] &&
4         Fone[ptn1, pfp1, pfn1, ptp1] > Fone[ptn2, pfp2, pfn2, ptp2]
5     ],
6     {ptn1, pfp1, pfn1, ptp1} \[Element] Tetra,
7     {ptn2, pfp2, pfn2, ptp2} \[Element] Tetra
8 ] / tot
9 tau = 1 - 4 * pLtGt

```

And we have

$$\tau(F_1; Re) = \frac{2}{3}, \quad (50)$$

as shown with the code:

```

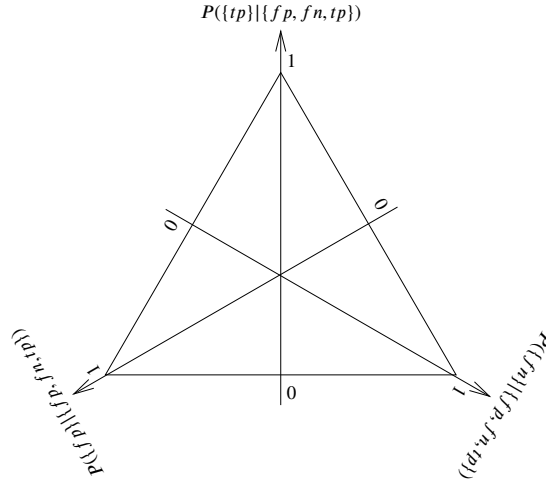
1 pLtGt = Integrate[
2     Boole[
3         Fone[ptn1, pfp1, pfn1, ptp1] < Fone[ptn2, pfp2, pfn2, ptp2] &&
4         Tpr[ptn1, pfp1, pfn1, ptp1] > Tpr[ptn2, pfp2, pfn2, ptp2]
5     ],
6     {ptn1, pfp1, pfn1, ptp1} \[Element] Tetra,
7     {ptn2, pfp2, pfn2, ptp2} \[Element] Tetra
8 ] / tot
9 tau = 1 - 4 * pLtGt

```

A.3.3. Detailed Results for the Uniform Distributions With Fixed Probability of True Negatives

The demonstration could be provided similarly as we did for the previous case study, taking a simplex in two dimensions instead of a simplex in three dimensions. However, we would like to show a geometrical reasoning instead.

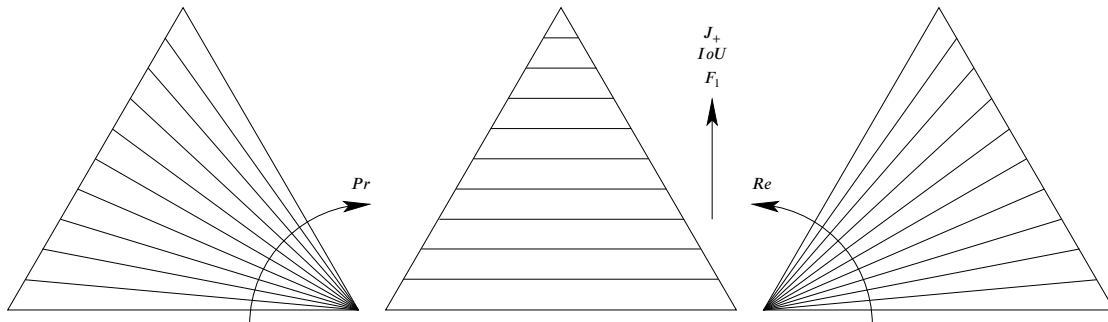
The equilateral triangles depicted in Fig. 4b form a "triangular space" in which the performances are assumed to be uniformly distributed. This "space" is parameterized as follows.



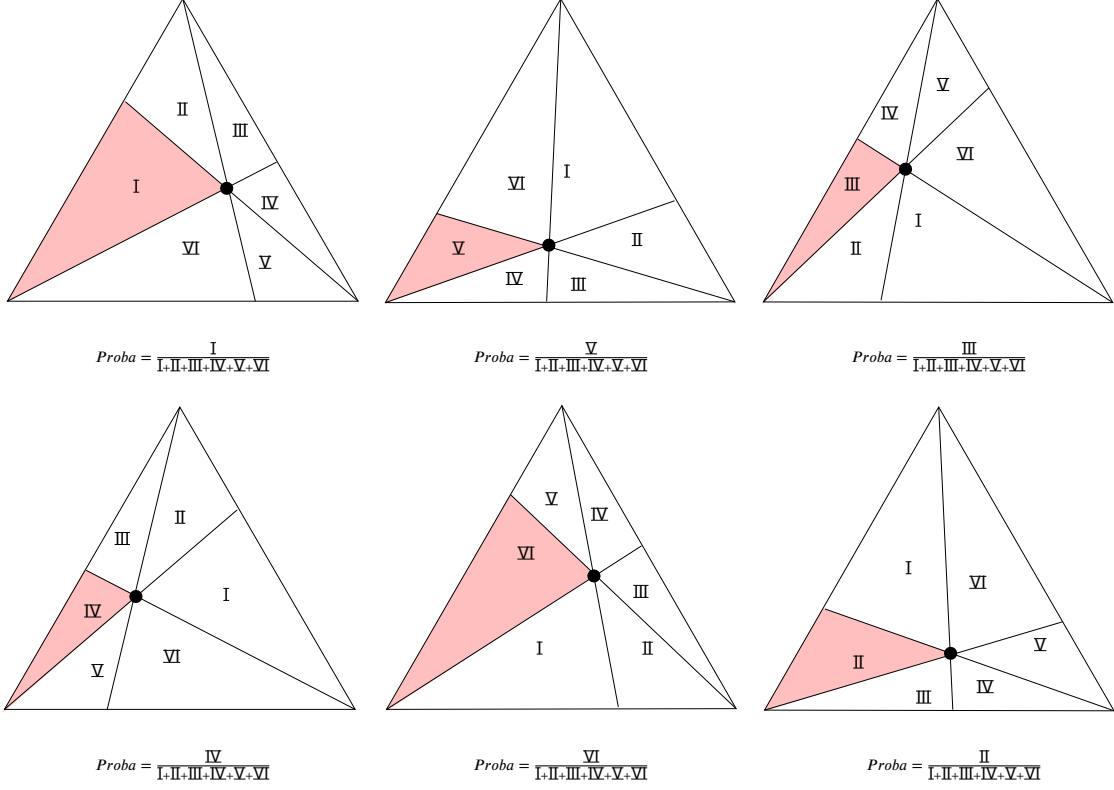
In fact, in the drawing shown here-above, the vertical axis corresponds to a score known as the *Intersection over Union IoU* or *Jaccard Coefficient J_+* . It is monotonically increasing with F_1 :

$$F_1 = \frac{2IoU}{1 + IoU} \Rightarrow \frac{\partial F_1}{\partial IoU} > 0 \quad (51)$$

The isometrics of Pr form a pencil of lines whose vertex is located at the bottom-right corner. The isometrics of F_1 are horizontal lines. The isometrics of Re form a pencil of lines whose vertex is located at the bottom-left corner.



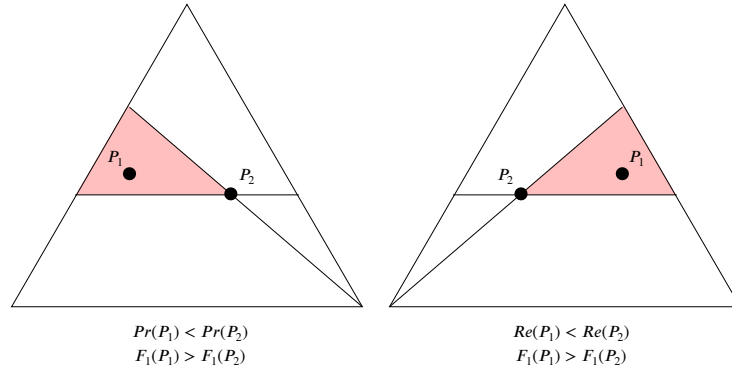
We now show that $\tau(Pr; Re) = 1/3$. In the following drawings, we consider a performance P_1 that can be anywhere in the "triangular space" and we choose one particular performance P_2 , shown as a black point. The pink area represents the probability that $Pr(P_1) < Pr(P_2)$ and $Re(P_1) > Re(P_2)$. The six cases are symmetrical: one can obtain them by mirroring or rotating.



We see that, in average (that is, if we let P_2 be anywhere in the "triangular space"), the probability that $Pr(P_1) < Pr(P_2)$ and $Re(P_1) > Re(P_2)$ is $1/6$. Using Eq. (45), we find the announced result:

$$\tau(Pr; Re) = 1/3 \quad (52)$$

We now show that $\tau(Pr; F_1) = \tau(Re; F_1)$. Using Eq. (45), we know that it is the case if and only if the probability that $Pr(P_1) < Pr(P_2)$ and $F_1(P_1) > F_1(P_2)$ is equal to the probability that $Re(P_1) < Re(P_2)$ and $F_1(P_1) > F_1(P_2)$. These two probabilities are shown as pink areas, for some arbitrarily fixed P_2 (the black dot), in the following drawings.



We see that, by symmetry, the two probabilities are equal. If, furthermore, we do not fix anymore the performance P_2 but let it be anywhere in the "triangular space", the two probabilities remain equal. Using Eq. (45), we find the announced result:

$$\tau(Pr; F_1) = \tau(Re; F_1) \quad (53)$$

A.3.4. Detailed Results for the Uniform Distributions With Fixed Class Priors

To find the probabilities necessary to compute τ , we integrate over the whole ROC space. Let us denote by $(FPR, TPR) = (x, y)$ the coordinates of a performance in this space. We have

$$Pr(P_1) < Pr(P_2) \Leftrightarrow \frac{y_1}{x_1} < \frac{y_2}{x_2} \quad (54)$$

$$Re(P_1) < Re(P_2) \Leftrightarrow y_1 < y_2 \quad (55)$$

$$F_\beta(P_1) < F_\beta(P_2) \Leftrightarrow \frac{y_1}{x_1 + \ell} < \frac{y_2}{x_2 + \ell} \quad (56)$$

We start with a few initializations.

```

1 tot = Integrate [
2   1,
3   {x1, 0, 1}, {y1, 0, 1},
4   {x2, 0, 1}, {y2, 0, 1}
5 ]

```

We have

$$\tau(Pr; Re) = \frac{1}{2}, \quad (57)$$

as shown with the code (see Fig. A.3.4a):

```

1 pLtGt = Integrate [
2   Boole [(y1 x2 < y2 x1) && (y1 > y2)],
3   {x1, 0, 1}, {y1, 0, 1},
4   {x2, 0, 1}, {y2, 0, 1}
5 ] / tot
6 tau = 1 - 4 * pLtGt

```

We have

$$\tau(Pr; F_\beta) = 1 - \ell \left(\ell \log \left(\frac{\ell}{\ell + 1} \right) + 1 \right), \quad (58)$$

as shown with the code (see Fig. A.3.4b):

```

1 pLtGt = Integrate [
2   Boole [(y1 x2 < y2 x1) && (y1 (x2 + 1) > y2 (x1 + 1))],
3   {x1, 0, 1}, {y1, 0, 1},
4   {x2, 0, 1}, {y2, 0, 1},
5   Assumptions -> 1 > 0
6 ] / tot
7 pLtGt = FullSimplify [pLtGt, Assumptions -> 1 > 0]
8 tau = 1 - 4 * pLtGt

```

And we have

$$\tau(F_\beta; Re) = \ell^2 \left(-\log \left(\frac{1}{\ell} + 1 \right) \right) + \ell + \frac{1}{2}, \quad (59)$$

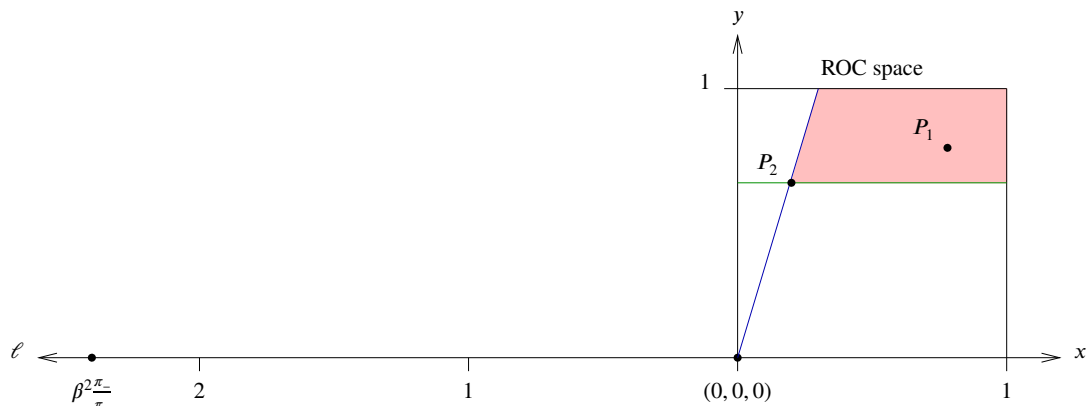
as shown with the code (see Fig. A.3.4c):

```

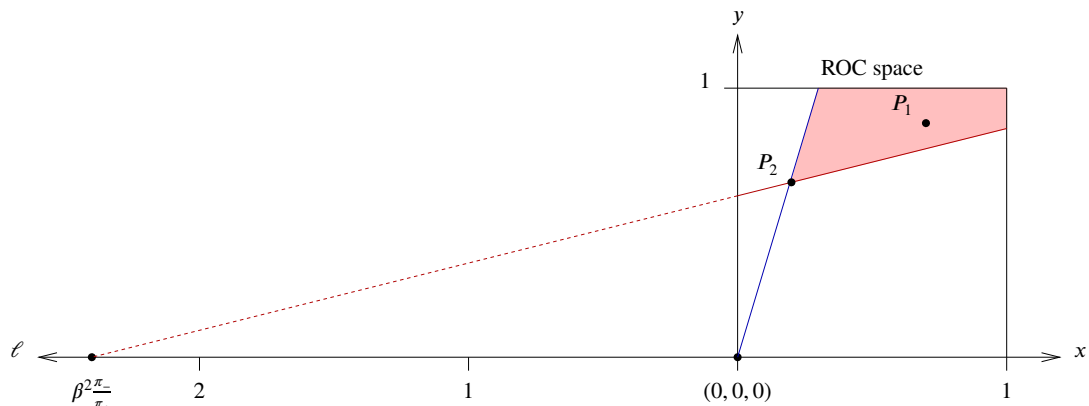
1 pLtGt = Integrate [
2   Boole [(y1 (x2 + 1) < y2 (x1 + 1)) && (y1 > y2)],
3   {x1, 0, 1}, {y1, 0, 1},
4   {x2, 0, 1}, {y2, 0, 1},
5   Assumptions -> 1 > 0
6 ] / tot
7 tau = 1 - 4 * pLtGt
8 tau = FullSimplify [tau, Assumptions -> 1 > 0]

```

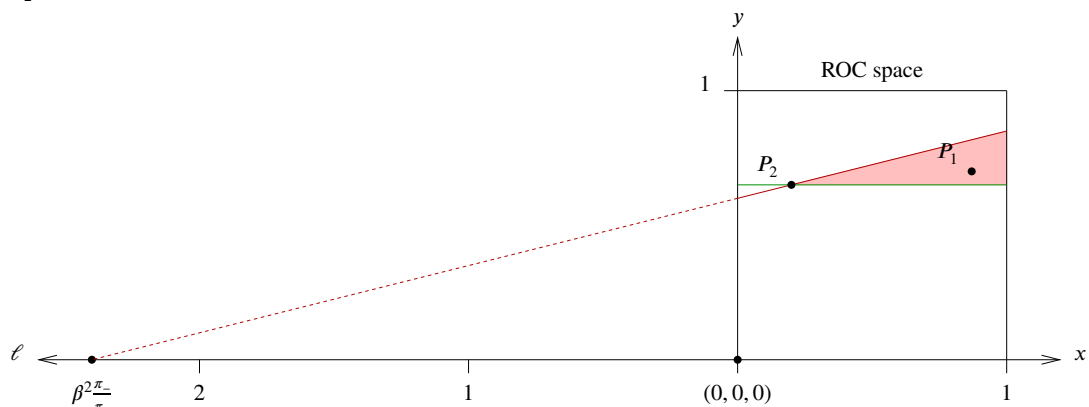
The plots are provided in Fig. A.3.5.



(a) To compute $\tau(Pr; Re)$ with Eq. (45), we determine the probability that $Pr(P_1) < Pr(P_2)$ (the performance P_1 is under the blue line) and $Re(P_1) > Re(P_2)$ (the performance P_1 is above the green line), which is the pink area averaged for all positions of P_2 .

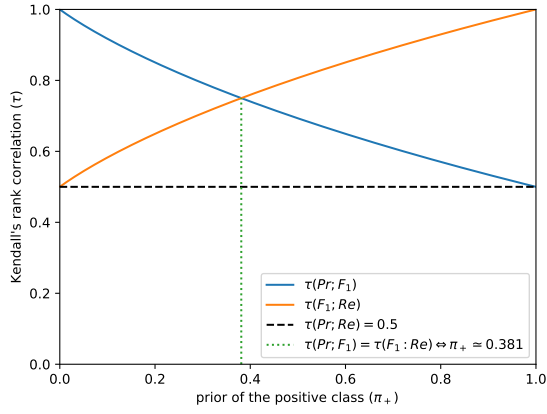


(b) To compute $\tau(Pr; F_\beta)$ with Eq. (45), we determine the probability that $Pr(P_1) < Pr(P_2)$ (the performance P_1 is under the blue line) and $F_\beta(P_1) > F_\beta(P_2)$ (the performance P_1 is above the red line), which is the pink area averaged for all positions of P_2 .

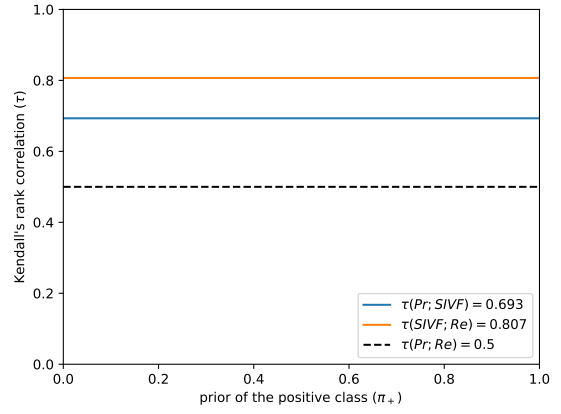


(c) To compute $\tau(F_\beta; Re)$ with Eq. (45), we determine the probability that $F_\beta(P_1) < F_\beta(P_2)$ (the performance P_1 is under the red line) and $Re(P_1) > Re(P_2)$ (the performance P_1 is above the green line), which is the pink area averaged for all positions of P_2 .

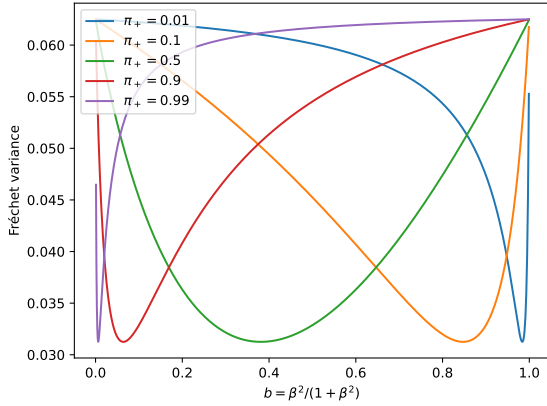
Figure A.3.4. Graphical representation, in and around the ROC space, of the principle that we use to derive the analytical expression for the optimal tradeoff between precision and recall for the purpose of ranking, in the case of uniform distributions with fixed class priors. Note that the ROC space is a linear mapping of the rectangles depicted in Fig. 4c.



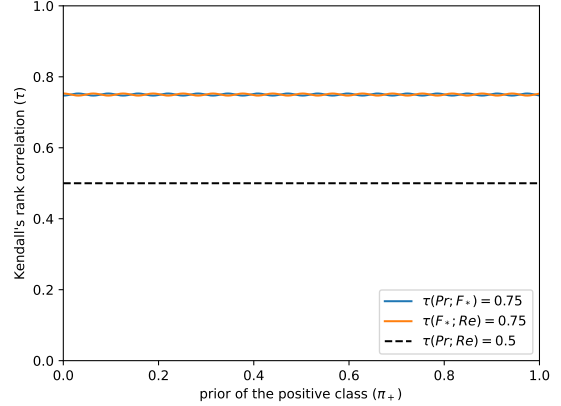
(a) F_1 , the traditional (balanced) F-score, is not the optimal tradeoff: $\tau(Pr; F_1) \neq \tau(F_1; Re)$.



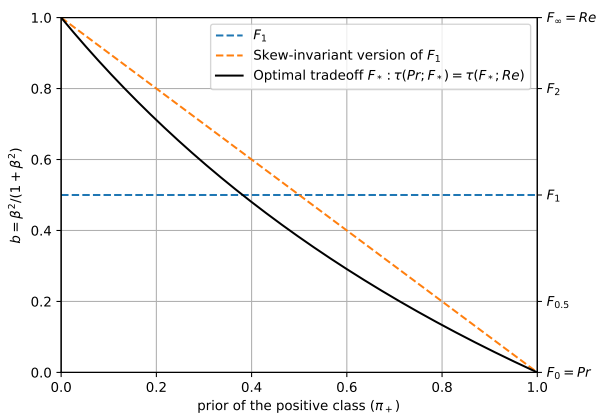
(b) $SIVF$, the skew-insensitive version of F_1 [10], is not the optimal tradeoff: $\tau(Pr; SIVF) \neq \tau(SIVF; Re)$.



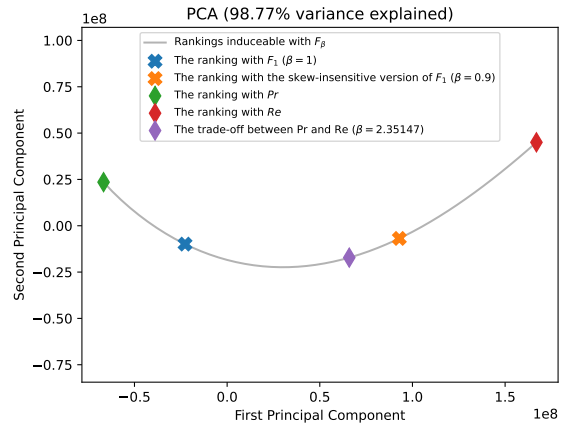
(c) Fréchet variance for various priors. It is defined at Eq. (8) and should be minimized to obtain the optimal tradeoff.



(d) F_* if the optimal tradeoff: $\tau(Pr; F_*) = \tau(F_*; Re)$.



(e) Adaptation of β w.r.t. class priors.



(f) PCA of the manifold (for $\pi_+ = 0.1$).

Figure A.3.5. Results for uniform distributions over the performances with fixed class priors, *i.e.* $\Pi_3(\pi_+)$.

A.3.5. Detailed Results for the Uniform Distributions With Fixed Class Priors, Above No-Skill

To find the probabilities necessary to compute τ , we integrate over half of the ROC space, the half above the raising diagonal. Let us denote by $(FPR, TPR) = (x, y)$ the coordinates of a performance in this space. We have

$$Pr(P_1) < Pr(P_2) \Leftrightarrow \frac{y_1}{x_1} < \frac{y_2}{x_2} \quad (60)$$

$$Re(P_1) < Re(P_2) \Leftrightarrow y_1 < y_2 \quad (61)$$

$$F_\beta(P_1) < F_\beta(P_2) \Leftrightarrow \frac{y_1}{x_1 + \ell} < \frac{y_2}{x_2 + \ell} \quad (62)$$

We start with a few initializations.

```

1 tot = Integrate [
2   1,
3   {x1, 0, 1}, {y1, x1, 1},
4   {x2, 0, 1}, {y2, x2, 1}
5 ]

```

We have

$$\tau(Pr; Re) = 0, \quad (63)$$

as shown with the code (see Fig. A.3.6a):

```

1 pLtGt = Integrate [
2   Boole [(y1 x2 < y2 x1) && (y1 > y2)],
3   {x1, 0, 1}, {y1, x1, 1},
4   {x2, 0, 1}, {y2, x2, 1}
5 ] / tot
6 tau = 1 - 4 * pLtGt

```

We have

$$\tau(Pr; F_\beta) = 1 - \frac{2}{3}\ell \left(-6\ell^2 - 6(\ell^2 - 1)\ell \log\left(\frac{\ell}{\ell + 1}\right) + 3\ell + 4 \right), \quad (64)$$

as shown with the code (see Fig. A.3.6b):

```

1 pLtGt = Integrate [
2   Boole [(y1 x2 < y2 x1) && (y1 (x2 + 1) > y2 (x1 + 1))],
3   {x1, 0, 1}, {y1, x1, 1},
4   {x2, 0, 1}, {y2, x2, 1},
5   Assumptions -> 1 > 0
6 ] / tot
7 pLtGt = FullSimplify [pLtGt, Assumptions -> 1 > 0]
8 tau = 1 - 4 * pLtGt

```

And we have

$$\tau(F_\beta; Re) = \frac{2}{3}\ell \left(-6\ell^2 + 6(\ell^2 - 1)\ell \log\left(\frac{1}{\ell} + 1\right) + 3\ell + 4 \right), \quad (65)$$

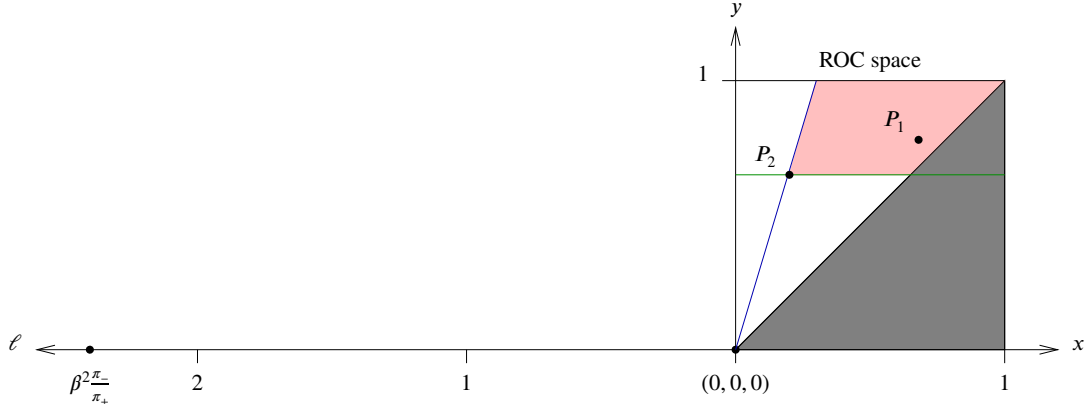
as shown with the code (see Fig. A.3.6c):

```

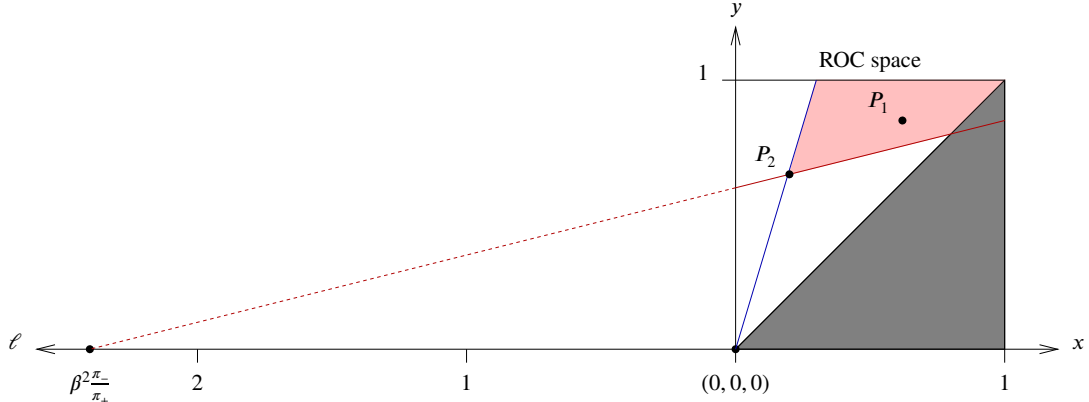
1 pLtGt = Integrate [
2   Boole [(y1 (x2 + 1) < y2 (x1 + 1)) && (y1 > y2)],
3   {x1, 0, 1}, {y1, x1, 1},
4   {x2, 0, 1}, {y2, x2, 1},
5   Assumptions -> 1 > 0
6 ] / tot
7 tau = 1 - 4 * pLtGt
8 tau = FullSimplify [tau, Assumptions -> 1 > 0]

```

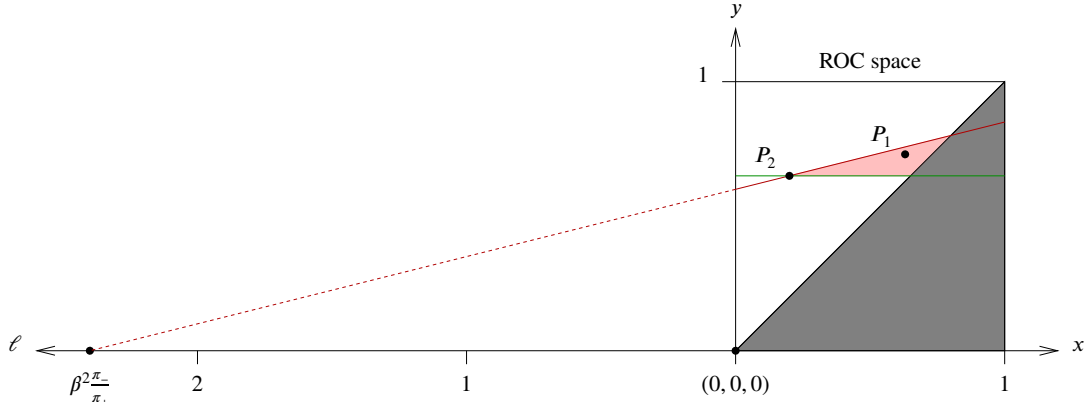
The plots are provided in Fig. A.3.7.



(a) To compute $\tau(Pr; Re)$ with Eq. (45), we determine the probability that $Pr(P_1) < Pr(P_2)$ (the performance P_1 is under the blue line) and $Re(P_1) > Re(P_2)$ (the performance P_1 is above the green line), which is the pink area averaged for all positions of P_2 .

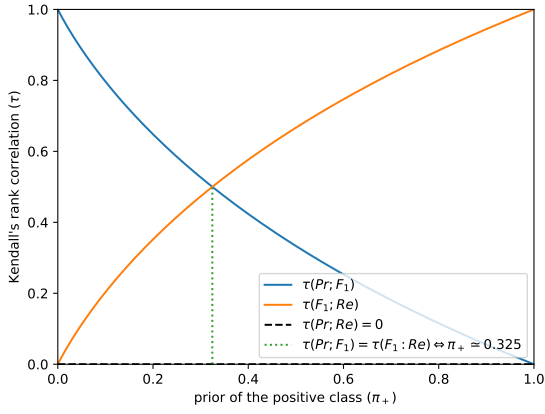


(b) To compute $\tau(Pr; F_\beta)$ with Eq. (45), we determine the probability that $Pr(P_1) < Pr(P_2)$ (the performance P_1 is under the blue line) and $F_\beta(P_1) > F_\beta(P_2)$ (the performance P_1 is above the red line), which is the pink area averaged for all positions of P_2 .

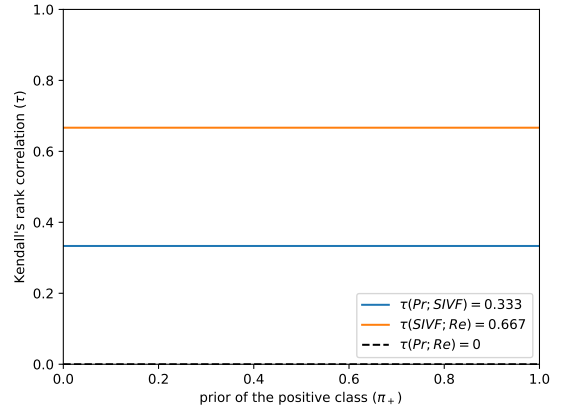


(c) To compute $\tau(F_\beta; Re)$ with Eq. (45), we determine the probability that $F_\beta(P_1) < F_\beta(P_2)$ (the performance P_1 is under the red line) and $Re(P_1) > Re(P_2)$ (the performance P_1 is above the green line), which is the pink area averaged for all positions of P_2 .

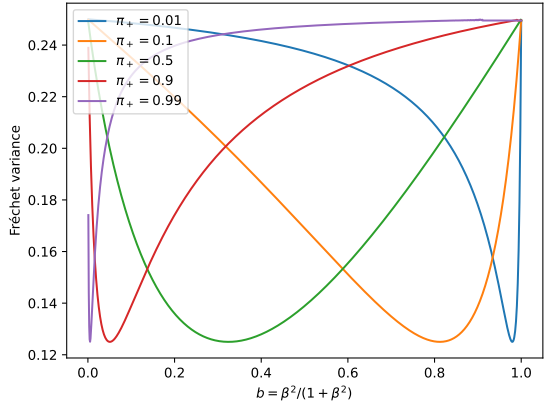
Figure A.3.6. Graphical representation, in and around the ROC space, of the principle that we use to derive the analytical expression for the optimal tradeoff between precision and recall for the purpose of ranking, in the case of uniform distributions with fixed class priors above no-skill. Note that the unshaded area of ROC space is a linear mapping of the triangles depicted in Fig. 4d.



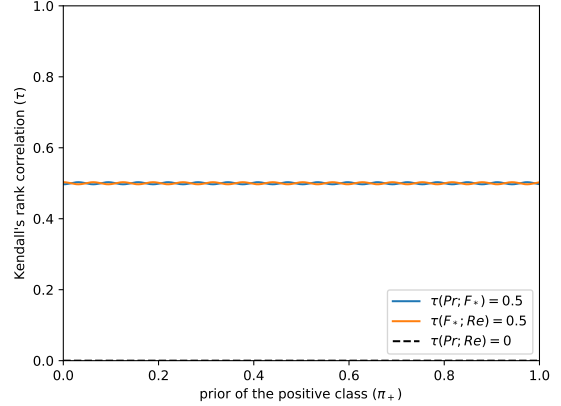
(a) F_1 , the traditional (balanced) F-score, is not the optimal tradeoff: $\tau(Pr; F_1) \neq \tau(F_1; Re)$.



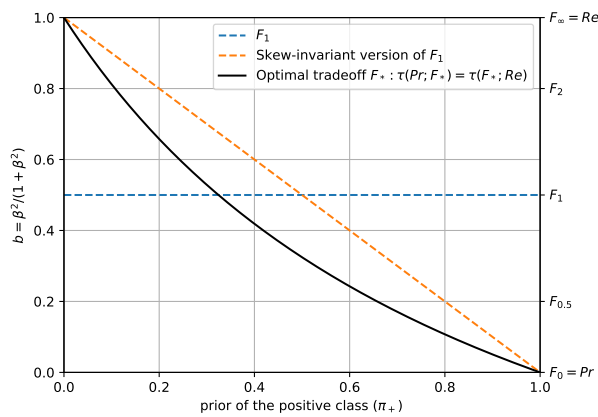
(b) $SIVF$, the skew-insensitive version of F_1 [10], is not the optimal tradeoff: $\tau(Pr; SIVF) \neq \tau(SIVF; Re)$.



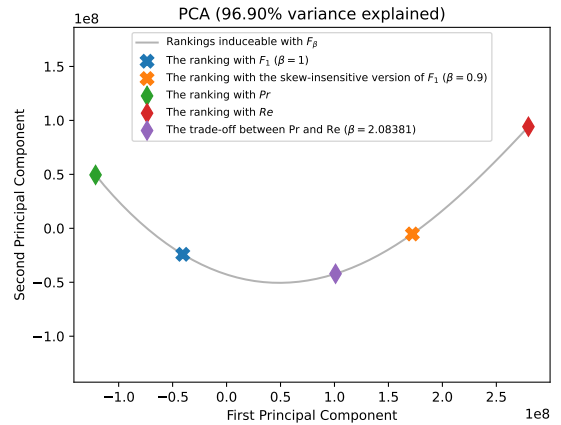
(c) Fréchet variance for various priors. It is defined at Eq. (8) and should be minimized to obtain the optimal tradeoff.



(d) F_* if the optimal tradeoff: $\tau(Pr; F_*) = \tau(F_*; Re)$.



(e) Adaptation of β w.r.t. class priors.



(f) PCA of the manifold (for $\pi_+ = 0.1$).

Figure A.3.7. Results for uniform distributions over the performances with fixed class priors, i.e. $\Pi_4(\pi_+)$.

A.3.6. Detailed Results for the Uniform Distributions With Fixed Class Priors, Close to Oracle

To find the probabilities necessary to compute τ , we integrate over a rectangle in the ROC space. Let us denote by $(FPR, TPR) = (x, y)$ the coordinates of a performance in this space. We have

$$Pr(P_1) < Pr(P_2) \Leftrightarrow \frac{y_1}{x_1} < \frac{y_2}{x_2} \quad (66)$$

$$Re(P_1) < Re(P_2) \Leftrightarrow y_1 < y_2 \quad (67)$$

$$F_\beta(P_1) < F_\beta(P_2) \Leftrightarrow \frac{y_1}{x_1 + \ell} < \frac{y_2}{x_2 + \ell} \quad \text{with} \quad \ell = \beta^2 \frac{\pi_+}{\pi_-} = \frac{b}{1-b} \frac{\pi_+}{1-\pi_+} \quad (68)$$

Unlike the previous cases, here we can no longer group π_+ and β together to form ℓ , as π_+ appears alone in the integration bounds of x and y . More precisely, we cannot anymore minimize Fréchet variance as a function of just ℓ . The optimal ℓ is not a constant anymore: it is now a function of π_+ . This explains why the look of the curve for the adaptation differs from what we had before.

We start with a few initializations.

```

1 tot = Integrate [
2   1,
3   {x1, 0, p}, {y1, p, 1},
4   {x2, 0, p}, {y2, p, 1},
5   Assumptions -> 0 < p < 1
6 ]

```

We have

$$\tau(Pr; Re) = 1 - \frac{-\pi_+^4 + 2\pi_+^4 \log(\pi_+) + \pi_+^2}{2(1-\pi_+)^2 \pi_+^2}, \quad (69)$$

as shown with the code (see Fig. A.3.8a):

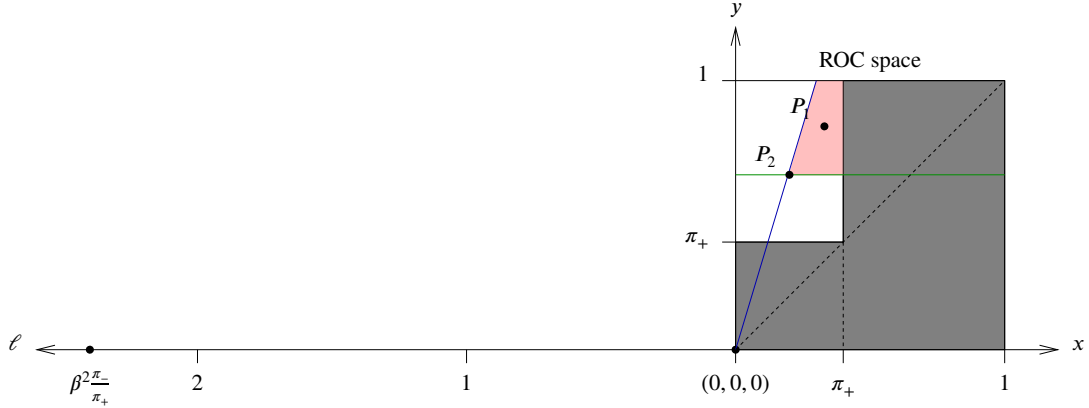
```

1 pLtGt = Integrate [
2   Boole[(y1 x2 < y2 x1) && (y1 > y2)],
3   {x1, 0, p}, {y1, p, 1},
4   {x2, 0, p}, {y2, p, 1},
5   Assumptions -> 0 < p < 1
6 ] / tot
7 tau = 1 - 4 * pLtGt

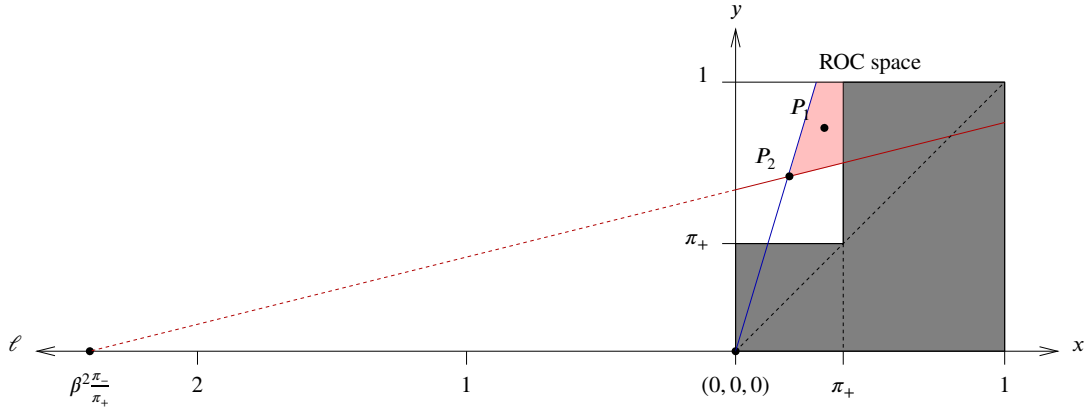
```

With Wolfram, we were unable to obtain the analytical expression of $\tau(Pr; F_\beta)$ and $\tau(F_\beta; Re)$ for this family of distributions. Wolfram was unable to provide you with the analytical expression in a reasonable time. We therefore report the results obtained using the Monte-Carlo technique.

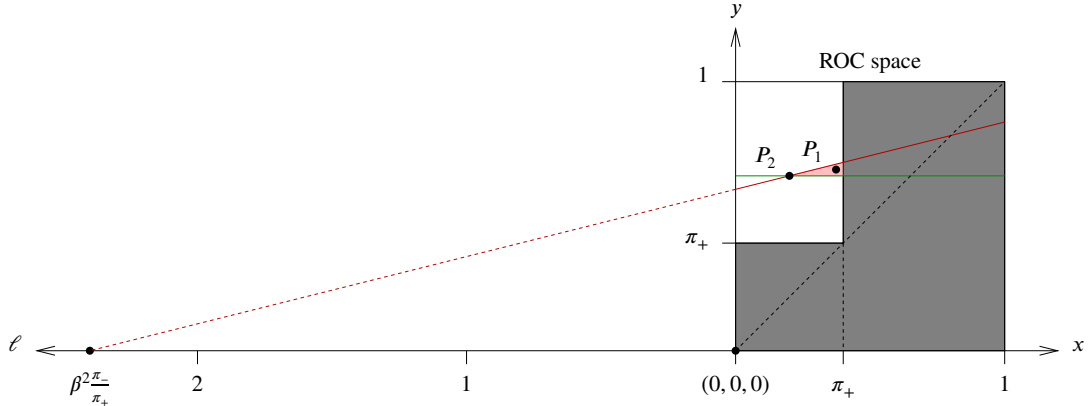
The plots are provided in Fig. A.3.9.



(a) To compute $\tau(Pr; Re)$ with Eq. (45), we determine the probability that $Pr(P_1) < Pr(P_2)$ (the performance P_1 is under the blue line) and $Re(P_1) > Re(P_2)$ (the performance P_1 is above the green line), which is the pink area averaged for all positions of P_2 .

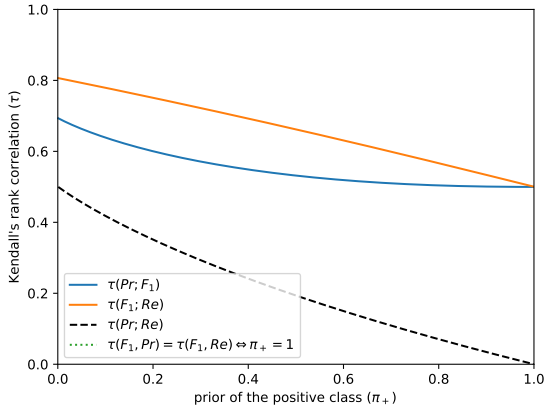


(b) To compute $\tau(Pr; F_\beta)$ with Eq. (45), we determine the probability that $Pr(P_1) < Pr(P_2)$ (the performance P_1 is under the blue line) and $F_\beta(P_1) > F_\beta(P_2)$ (the performance P_1 is above the red line), which is the pink area averaged for all positions of P_2 .

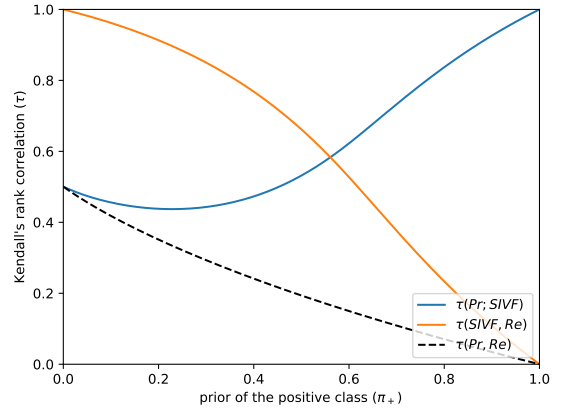


(c) To compute $\tau(F_\beta; Re)$ with Eq. (45), we determine the probability that $F_\beta(P_1) < F_\beta(P_2)$ (the performance P_1 is under the red line) and $Re(P_1) > Re(P_2)$ (the performance P_1 is above the green line), which is the pink area averaged for all positions of P_2 .

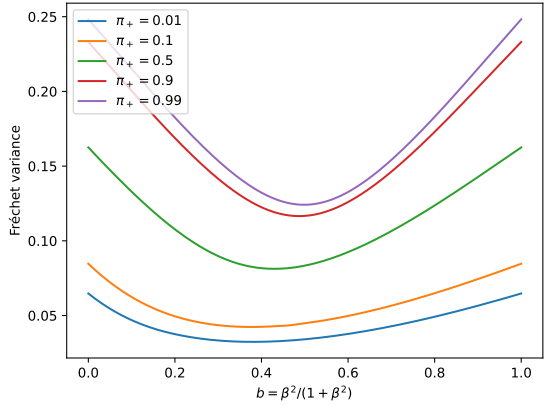
Figure A.3.8. Graphical representation, in and around the ROC space, of the principle that we use to derive the analytical expression for the optimal tradeoff between precision and recall for the purpose of ranking, in the case of uniform distributions with fixed class priors close to oracle. Note that the unshaded area of ROC space is a linear mapping of the squares depicted in Fig. 4e.



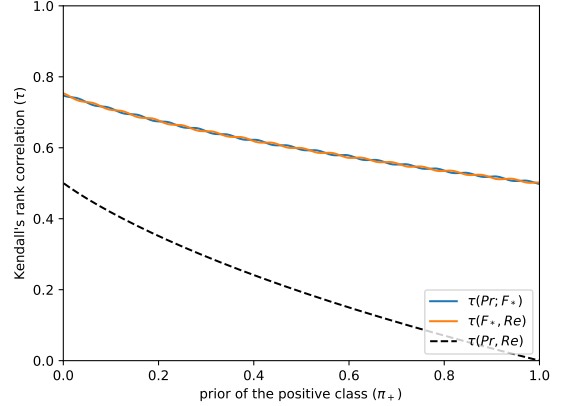
(a) F_1 , the traditional (balanced) F-score, is not the optimal tradeoff: $\tau(Pr; F_1) \neq \tau(F_1; Re)$.



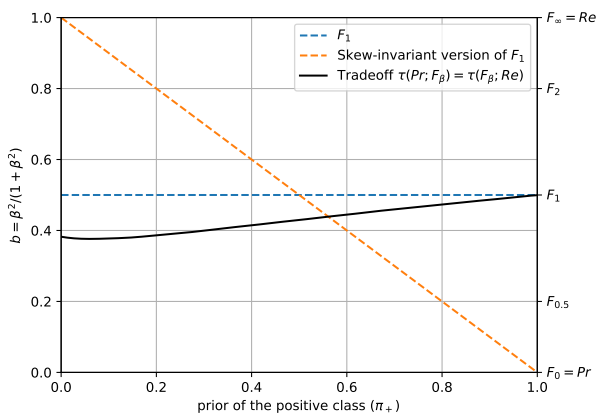
(b) $SIVF$, the skew-insensitive version of F_1 [10], is not the optimal tradeoff: $\tau(Pr; SIVF) \neq \tau(SIVF; Re)$.



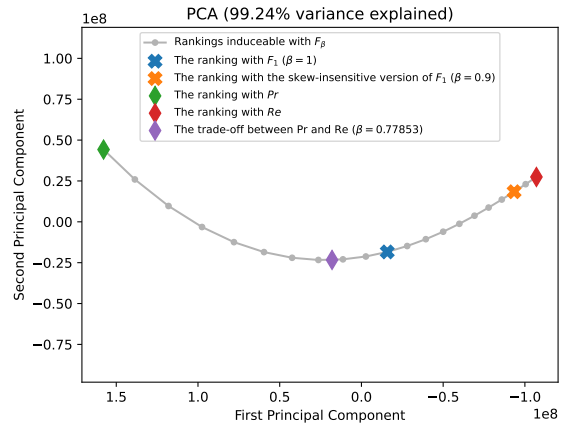
(c) Fréchet variance for various priors. It is defined at Eq. (8) and should be minimized to obtain the optimal tradeoff.



(d) F_* if the optimal tradeoff: $\tau(Pr; F_*) = \tau(F_*; Re)$.



(e) Adaptation of β w.r.t. class priors.



(f) PCA of the manifold (for $\pi_+ = 0.1$).

Figure A.3.9. Results for uniform distributions over the performances with fixed class priors, i.e. $\Pi_5(\pi_+)$.

A.3.7. All Results for Some Real Sets of Performances

We provide here the detailed results for each video of *CDnet 2014*.

Category "Baseline"

- The results for video "pedestrians" (ranking of 57 methods; $\pi_+ = 0.0098$) can be found at Fig. A.3.10.
- The results for video "PETS2006" (ranking of 57 methods; $\pi_+ = 0.0130$) can be found at Fig. A.3.11.
- The results for video "office" (ranking of 57 methods; $\pi_+ = 0.0690$) can be found at Fig. A.3.12.
- The results for video "highway" (ranking of 57 methods; $\pi_+ = 0.0593$) can be found at Fig. A.3.13.

Category "Dynamic Background"

- The results for video "overpass" (ranking of 57 methods; $\pi_+ = 0.0134$) can be found at Fig. A.3.14.
- The results for video "canoe" (ranking of 57 methods; $\pi_+ = 0.0354$) can be found at Fig. A.3.15.
- The results for video "fountain01" (ranking of 57 methods; $\pi_+ = 0.0008$) can be found at Fig. A.3.16.
- The results for video "fountain02" (ranking of 57 methods; $\pi_+ = 0.0022$) can be found at Fig. A.3.17.
- The results for video "fall" (ranking of 57 methods; $\pi_+ = 0.0177$) can be found at Fig. A.3.18.
- The results for video "boats" (ranking of 57 methods; $\pi_+ = 0.0063$) can be found at Fig. A.3.19.

Category "Camera Jitter"

- The results for video "boulevard" (ranking of 57 methods; $\pi_+ = 0.0469$) can be found at Fig. A.3.20.
- The results for video "sidewalk" (ranking of 57 methods; $\pi_+ = 0.0261$) can be found at Fig. A.3.21.
- The results for video "badminton" (ranking of 57 methods; $\pi_+ = 0.0343$) can be found at Fig. A.3.22.
- The results for video "traffic" (ranking of 57 methods; $\pi_+ = 0.0623$) can be found at Fig. A.3.23.

Category "Intermittent Object Motion"

- The results for video "abandonedBox" (ranking of 57 methods; $\pi_+ = 0.0481$) can be found at Fig. A.3.24.
- The results for video "winterDriveway" (ranking of 57 methods; $\pi_+ = 0.0075$) can be found at Fig. A.3.25.
- The results for video "sofa" (ranking of 57 methods; $\pi_+ = 0.0437$) can be found at Fig. A.3.26.
- The results for video "tramstop" (ranking of 57 methods; $\pi_+ = 0.1795$) can be found at Fig. A.3.27.
- The results for video "parking" (ranking of 57 methods; $\pi_+ = 0.0773$) can be found at Fig. A.3.28.
- The results for video "streetLight" (ranking of 57 methods; $\pi_+ = 0.0485$) can be found at Fig. A.3.29.

Category "Shadow"

- The results for video "copyMachine" (ranking of 57 methods; $\pi_+ = 0.0693$) can be found at Fig. A.3.30.
- The results for video "bungalows" (ranking of 57 methods; $\pi_+ = 0.0600$) can be found at Fig. A.3.31.
- The results for video "busStation" (ranking of 57 methods; $\pi_+ = 0.0369$) can be found at Fig. A.3.32.
- The results for video "peopleInShade" (ranking of 57 methods; $\pi_+ = 0.0564$) can be found at Fig. A.3.33.
- The results for video "backdoor" (ranking of 57 methods; $\pi_+ = 0.0199$) can be found at Fig. A.3.34.
- The results for video "cubicle" (ranking of 57 methods; $\pi_+ = 0.0196$) can be found at Fig. A.3.35.

Category "Thermal"

- The results for video "lakeSide" (ranking of 57 methods; $\pi_+ = 0.0192$) can be found at Fig. A.3.36.
- The results for video "diningRoom" (ranking of 57 methods; $\pi_+ = 0.0859$) can be found at Fig. A.3.37.
- The results for video "park" (ranking of 57 methods; $\pi_+ = 0.0203$) can be found at Fig. A.3.38.
- The results for video "corridor" (ranking of 57 methods; $\pi_+ = 0.0331$) can be found at Fig. A.3.39.
- The results for video "library" (ranking of 57 methods; $\pi_+ = 0.1928$) can be found at Fig. A.3.40.

Category "Bad Weather"

- The results for video "skating" (ranking of 57 methods; $\pi_+ = 0.0397$) can be found at Fig. A.3.41.
- The results for video "wetSnow" (ranking of 57 methods; $\pi_+ = 0.0150$) can be found at Fig. A.3.42.
- The results for video "snowFall" (ranking of 57 methods; $\pi_+ = 0.0105$) can be found at Fig. A.3.43.
- The results for video "blizzard" (ranking of 57 methods; $\pi_+ = 0.0115$) can be found at Fig. A.3.44.

Category "Low Framerate"

- The results for video "tunnelExit_0_35fps" (ranking of 57 methods; $\pi_+ = 0.0195$) can be found at Fig. A.3.45.
- The results for video "port_0_17fps" (ranking of 57 methods; $\pi_+ = 0.0002$) can be found at Fig. A.3.46.
- The results for video "tramCrossroad_1fps" (ranking of 57 methods; $\pi_+ = 0.0288$) can be found at Fig. A.3.47.
- The results for video "turnpike_0_5fps" (ranking of 57 methods; $\pi_+ = 0.0581$) can be found at Fig. A.3.48.

Category "Night Videos"

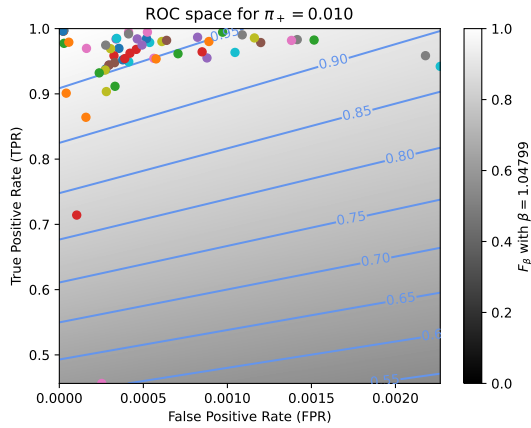
- The results for video "tramStation" (ranking of 58 methods; $\pi_+ = 0.0339$) can be found at Fig. A.3.49.
- The results for video "busyBoulevard" (ranking of 58 methods; $\pi_+ = 0.0847$) can be found at Fig. A.3.50.
- The results for video "streetCornerAtNight" (ranking of 58 methods; $\pi_+ = 0.0062$) can be found at Fig. A.3.51.
- The results for video "fluidHighway" (ranking of 58 methods; $\pi_+ = 0.0175$) can be found at Fig. A.3.52.
- The results for video "bridgeEntry" (ranking of 58 methods; $\pi_+ = 0.0200$) can be found at Fig. A.3.53.
- The results for video "winterStreet" (ranking of 58 methods; $\pi_+ = 0.0689$) can be found at Fig. A.3.54.

Category "PTZ"

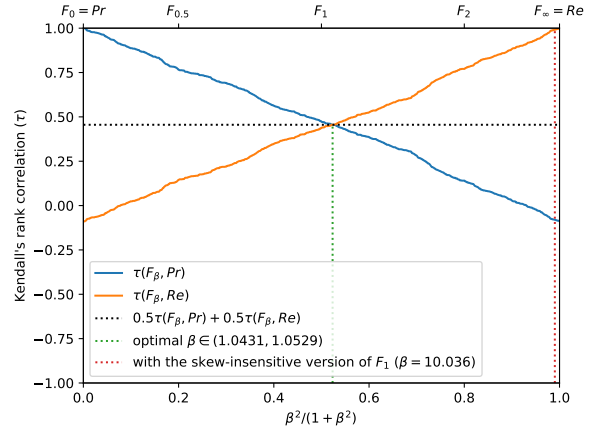
- The results for video "twoPositionPTZCam" (ranking of 56 methods; $\pi_+ = 0.0117$) can be found at Fig. A.3.55.
- The results for video "zoomInZoomOut" (ranking of 56 methods; $\pi_+ = 0.0019$) can be found at Fig. A.3.56.
- The results for video "continuousPan" (ranking of 56 methods; $\pi_+ = 0.0056$) can be found at Fig. A.3.57.
- The results for video "intermittentPan" (ranking of 56 methods; $\pi_+ = 0.0094$) can be found at Fig. A.3.58.

Category "Turbulence"

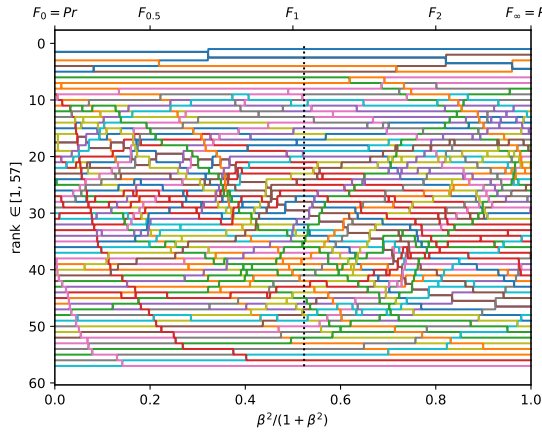
- The results for video "turbulence2" (ranking of 57 methods; $\pi_+ = 0.0008$) can be found at Fig. A.3.59.
- The results for video "turbulence3" (ranking of 57 methods; $\pi_+ = 0.0121$) can be found at Fig. A.3.60.
- The results for video "turbulence0" (ranking of 57 methods; $\pi_+ = 0.0015$) can be found at Fig. A.3.61.
- The results for video "turbulence1" (ranking of 57 methods; $\pi_+ = 0.0026$) can be found at Fig. A.3.62.



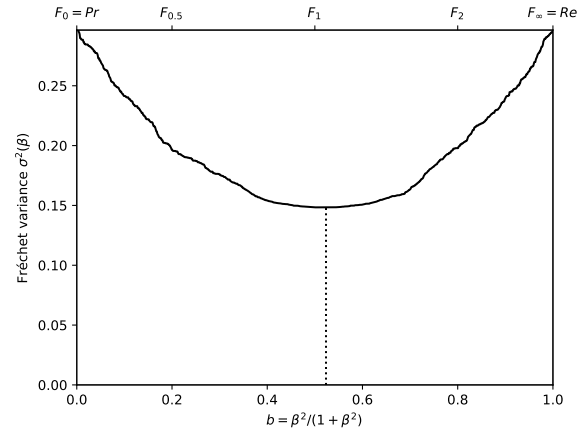
(a) The performances of 57 classifiers (BGS methods) depicted as points in the ROC space, with the isometrics of the optimal tradeoff score, from the ranking point of view, between precision and recall. See Eq. (12).



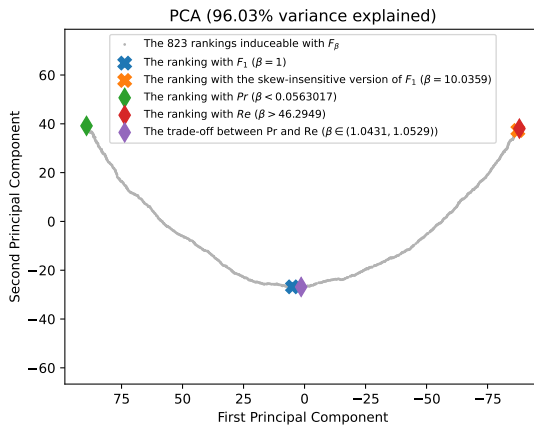
(b) The rank correlations $\tau(F_\beta; Pr)$ and $\tau(F_\beta; Re)$ w.r.t. β . The optimal value (or range of optimal values) for β is where the two curves intersect.



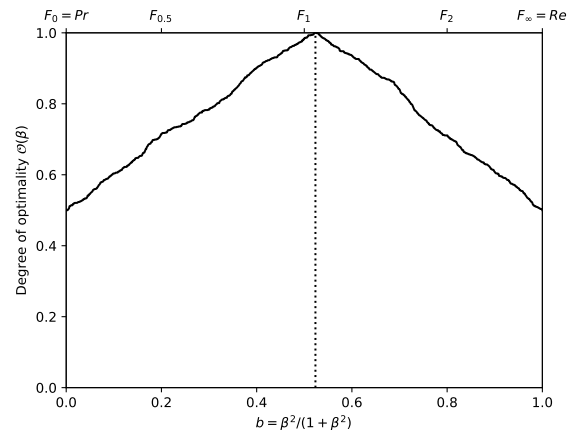
(c) The ranks of each classifier w.r.t. β . The optimal value (or range of optimal values) for β , shown here by the vertical line, is such that the number of swaps on its left is equal to the number of swaps on its right.



(d) The Fréchet variance $\sigma^2(\beta) = d_\tau^2(Pr; F_\beta) + d_\tau^2(F_\beta; Re)$ w.r.t. β . The optimal value (or range of optimal values) for β is where the curve has its minimum.

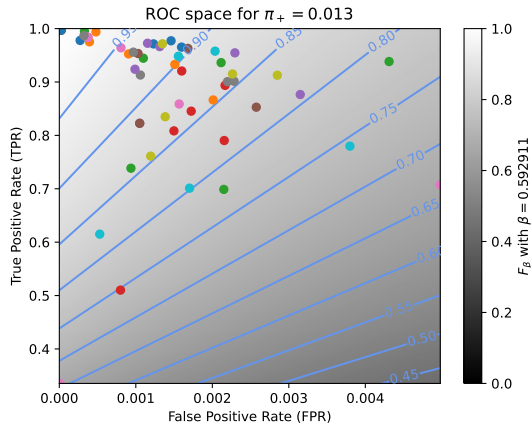


(e) Linear projection (PCA) of the manifold of the rankings induced by the F_β scores. The color points indicate the precision, the recall, F_1 , $SIVF$, as well as the optimal tradeoff. The optimal tradeoff is at the same distance of the two extremities when the distance is measured along the manifold, with Kendall's distance d_τ .

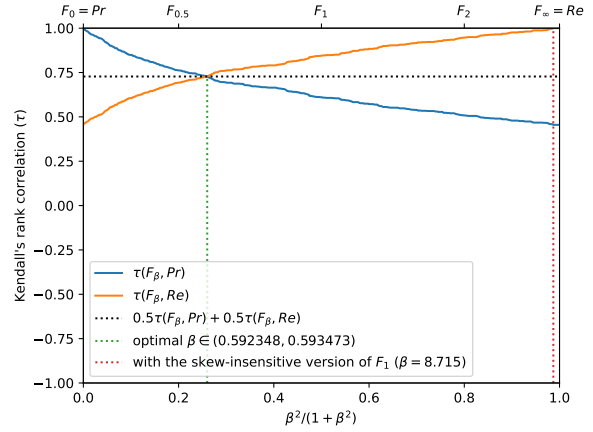


(f) The degree of optimality $\mathcal{O}(\beta)$ w.r.t. β . It is the probability to optimally ordering a pair of classifiers (BGS methods) given that it is not trivial (*i.e.*, that Pr and Re are in contradiction). The optimal value (or range of optimal values) for β is where the curve reaches 100%.

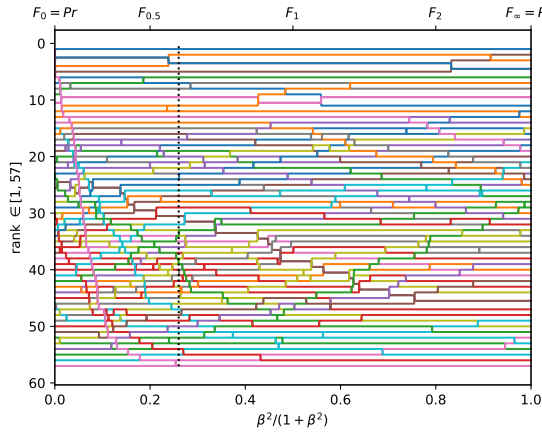
Figure A.3.10. Ranking of 57 BGS methods evaluated on the video "pedestrians" ($\pi_+ = 0.0098$).



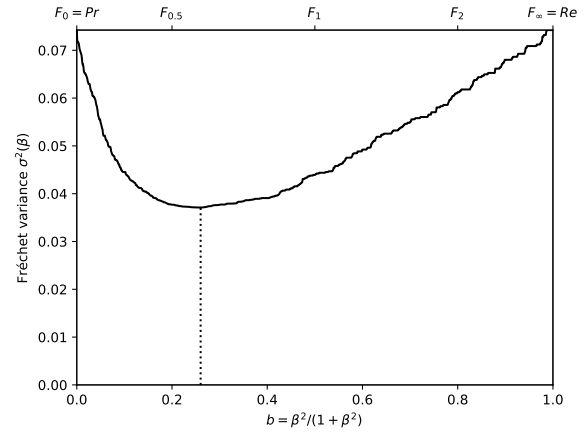
(a) The performances of 57 classifiers (BGS methods) depicted as points in the ROC space, with the isometrics of the optimal tradeoff score, from the ranking point of view, between precision and recall. See Eq. (12).



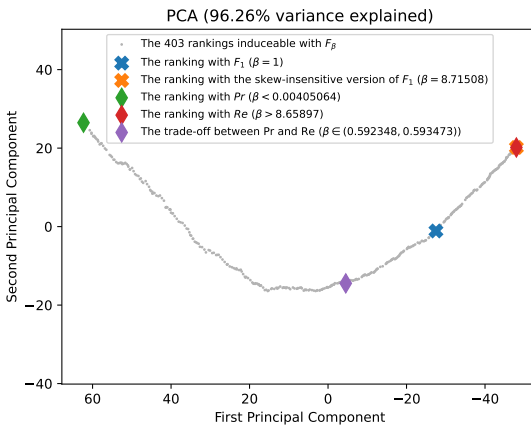
(b) The rank correlations $\tau(F_\beta; Pr)$ and $\tau(F_\beta; Re)$ w.r.t. β . The optimal value (or range of optimal values) for β is where the two curves intersect.



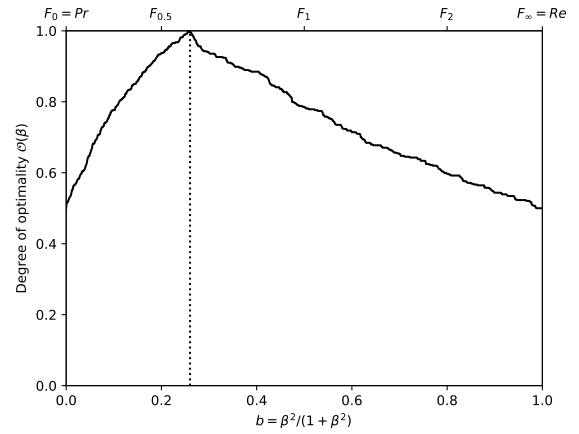
(c) The ranks of each classifier w.r.t. β . The optimal value (or range of optimal values) for β , shown here by the vertical line, is such that the number of swaps on its left is equal to the number of swaps on its right.



(d) The Fréchet variance $\sigma^2(\beta) = d_\tau^2(Pr; F_\beta) + d_\tau^2(F_\beta; Re)$ w.r.t. β . The optimal value (or range of optimal values) for β is where the curve has its minimum.

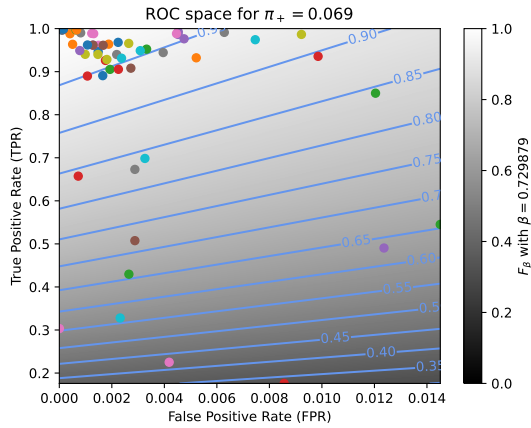


(e) Linear projection (PCA) of the manifold of the rankings induced by the F_β scores. The color points indicate the precision, the recall, F_1 , $SIVF$, as well as the optimal tradeoff. The optimal tradeoff is at the same distance of the two extremities when the distance is measured along the manifold, with Kendall's distance d_τ .

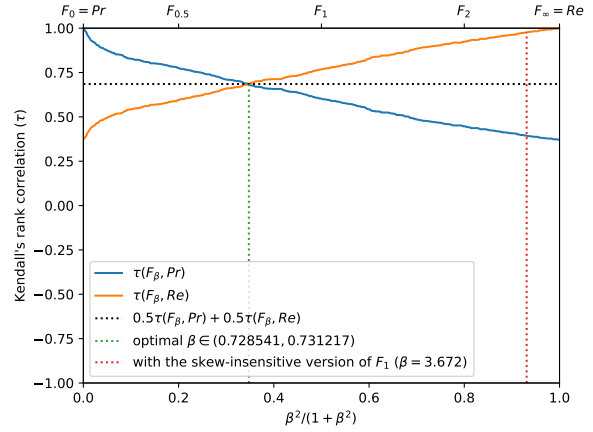


(f) The degree of optimality $\mathcal{O}(\beta)$ w.r.t. β . It is the probability to optimally ordering a pair of classifiers (BGS methods) given that it is not trivial (*i.e.*, that Pr and Re are in contradiction). The optimal value (or range of optimal values) for β is where the curve reaches 100%.

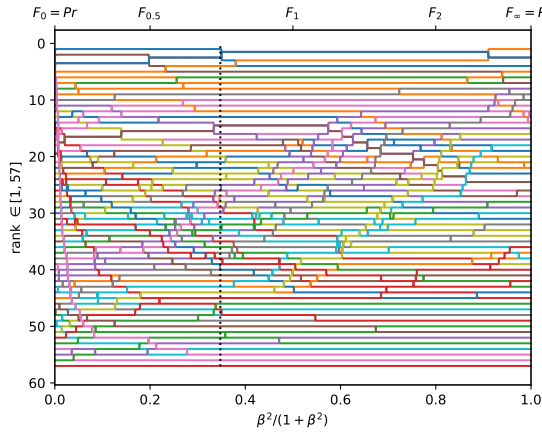
Figure A.3.11. Ranking of 57 BGS methods evaluated on the video "PETS2006" ($\pi_+ = 0.0130$).



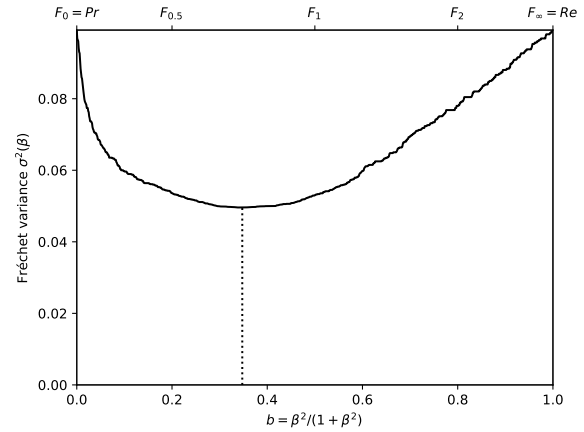
(a) The performances of 57 classifiers (BGS methods) depicted as points in the ROC space, with the isometrics of the optimal tradeoff score, from the ranking point of view, between precision and recall. See Eq. (12).



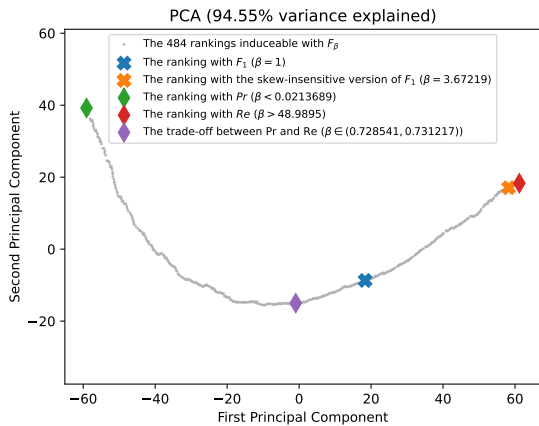
(b) The rank correlations $\tau(F_\beta; Pr)$ and $\tau(F_\beta; Re)$ w.r.t. β . The optimal value (or range of optimal values) for β is where the two curves intersect.



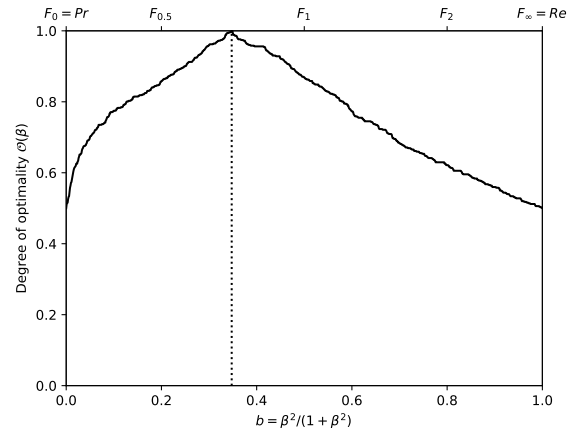
(c) The ranks of each classifier w.r.t. β . The optimal value (or range of optimal values) for β , shown here by the vertical line, is such that the number of swaps on its left is equal to the number of swaps on its right.



(d) The Fréchet variance $\sigma^2(\beta) = d_\tau^2(Pr; F_\beta) + d_\tau^2(F_\beta; Re)$ w.r.t. β . The optimal value (or range of optimal values) for β is where the curve has its minimum.

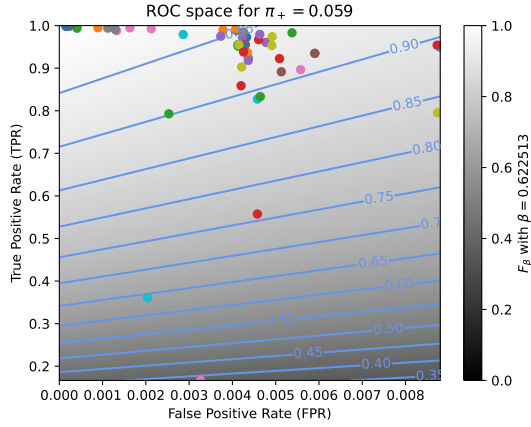


(e) Linear projection (PCA) of the manifold of the rankings induced by the F_β scores. The color points indicate the precision, the recall, F_1 , $SIVF$, as well as the optimal tradeoff. The optimal tradeoff is at the same distance of the two extremities when the distance is measured along the manifold, with Kendall's distance d_τ .

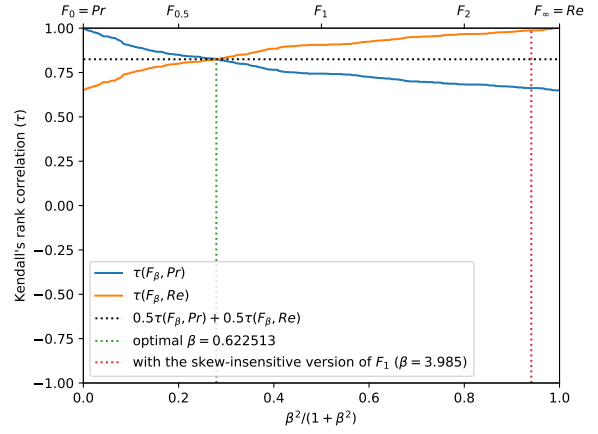


(f) The degree of optimality $\mathcal{O}(\beta)$ w.r.t. β . It is the probability to optimally ordering a pair of classifiers (BGS methods) given that it is not trivial (*i.e.*, that Pr and Re are in contradiction). The optimal value (or range of optimal values) for β is where the curve reaches 100%.

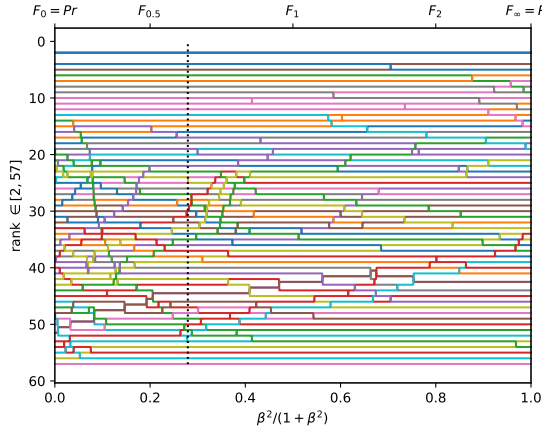
Figure A.3.12. Ranking of 57 BGS methods evaluated on the video "office" ($\pi_+ = 0.0690$).



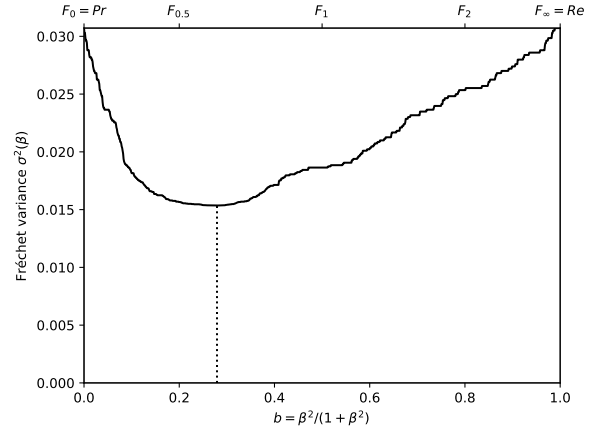
(a) The performances of 57 classifiers (BGS methods) depicted as points in the ROC space, with the isometrics of the optimal tradeoff score, from the ranking point of view, between precision and recall. See Eq. (12).



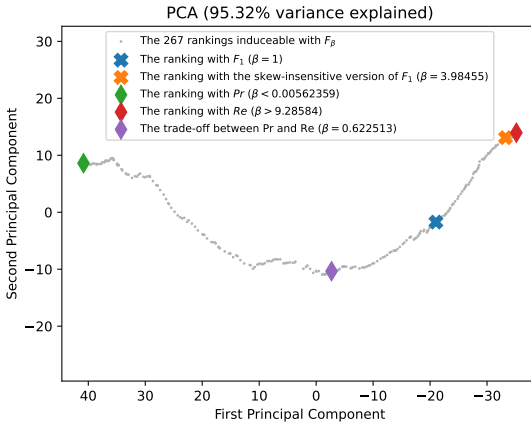
(b) The rank correlations $\tau(F_\beta; Pr)$ and $\tau(F_\beta; Re)$ w.r.t. β . The optimal value (or range of optimal values) for β is where the two curves intersect.



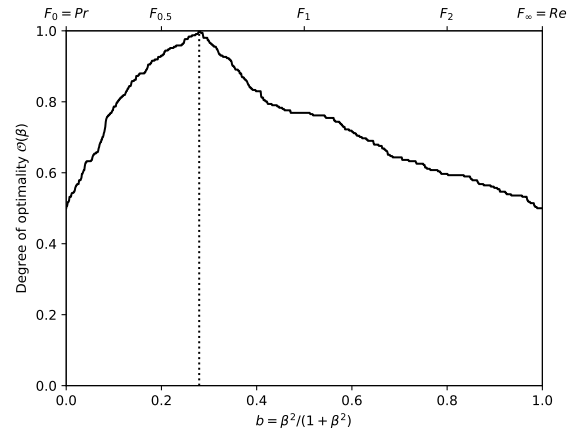
(c) The ranks of each classifier w.r.t. β . The optimal value (or range of optimal values) for β , shown here by the vertical line, is such that the number of swaps on its left is equal to the number of swaps on its right.



(d) The Fréchet variance $\sigma^2(\beta) = d_\tau^2(Pr; F_\beta) + d_\tau^2(F_\beta; Re)$ w.r.t. β . The optimal value (or range of optimal values) for β is where the curve has its minimum.

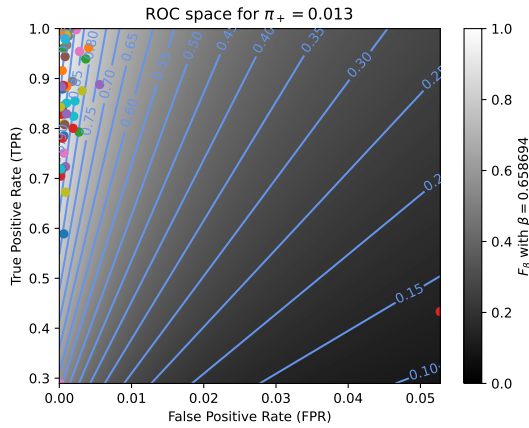


(e) Linear projection (PCA) of the manifold of the rankings induced by the F_β scores. The color points indicate the precision, the recall, F_1 , $SIVF$, as well as the optimal tradeoff. The optimal tradeoff is at the same distance of the two extremities when the distance is measured along the manifold, with Kendall's distance d_τ .

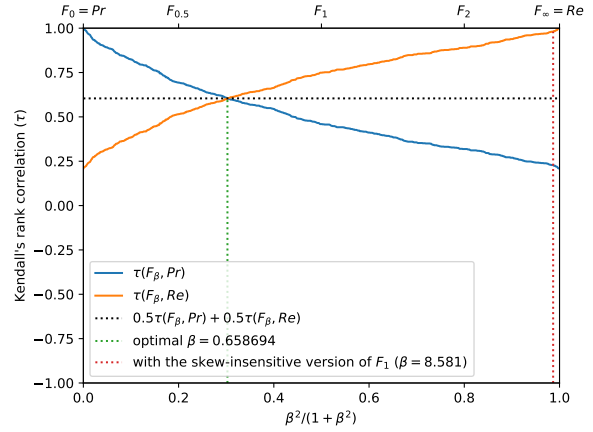


(f) The degree of optimality $\mathcal{O}(\beta)$ w.r.t. β . It is the probability to optimally ordering a pair of classifiers (BGS methods) given that it is not trivial (*i.e.*, that Pr and Re are in contradiction). The optimal value (or range of optimal values) for β is where the curve reaches 100%.

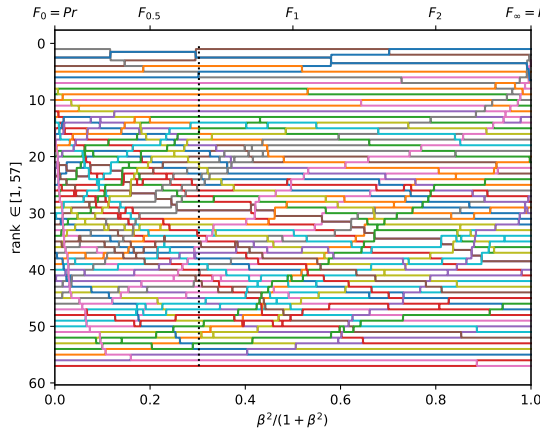
Figure A.3.13. Ranking of 57 BGS methods evaluated on the video "highway" ($\pi_+ = 0.0593$).



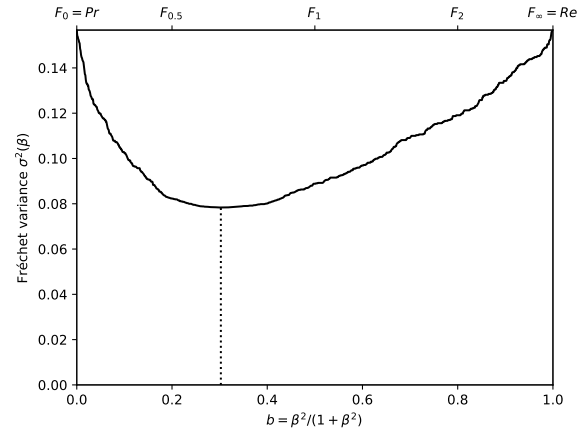
(a) The performances of 57 classifiers (BGS methods) depicted as points in the ROC space, with the isometrics of the optimal tradeoff score, from the ranking point of view, between precision and recall. See Eq. (12).



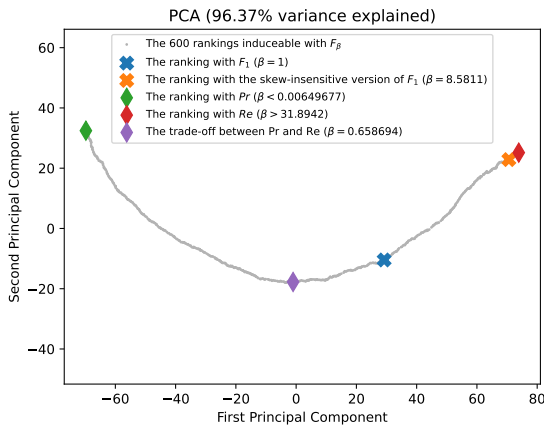
(b) The rank correlations $\tau(F_\beta; Pr)$ and $\tau(F_\beta; Re)$ w.r.t. β . The optimal value (or range of optimal values) for β is where the two curves intersect.



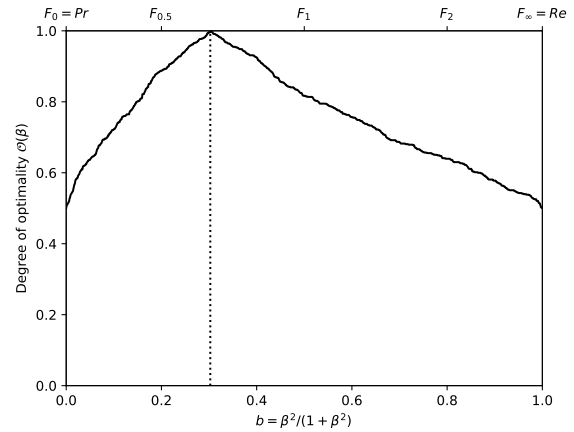
(c) The ranks of each classifier w.r.t. β . The optimal value (or range of optimal values) for β , shown here by the vertical line, is such that the number of swaps on its left is equal to the number of swaps on its right.



(d) The Fréchet variance $\sigma^2(\beta) = d_\tau^2(Pr; F_\beta) + d_\tau^2(F_\beta; Re)$ w.r.t. β . The optimal value (or range of optimal values) for β is where the curve has its minimum.

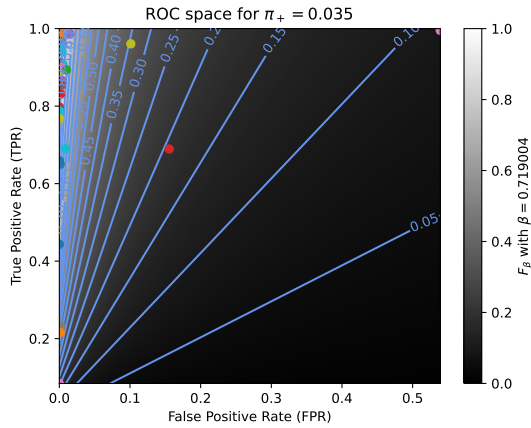


(e) Linear projection (PCA) of the manifold of the rankings induced by the F_β scores. The color points indicate the precision, the recall, F_1 , $SIVF$, as well as the optimal tradeoff. The optimal tradeoff is at the same distance of the two extremities when the distance is measured along the manifold, with Kendall's distance d_* .

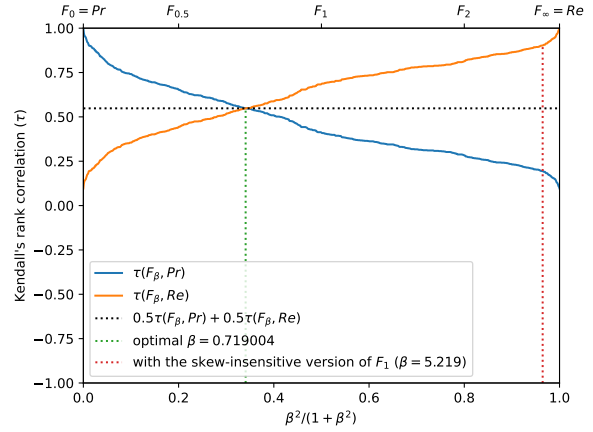


(f) The degree of optimality $\mathcal{O}(\beta)$ w.r.t. β . It is the probability to optimally ordering a pair of classifiers (BGS methods) given that it is not trivial (*i.e.*, that Pr and Re are in contradiction). The optimal value (or range of optimal values) for β is where the curve reaches 100%.

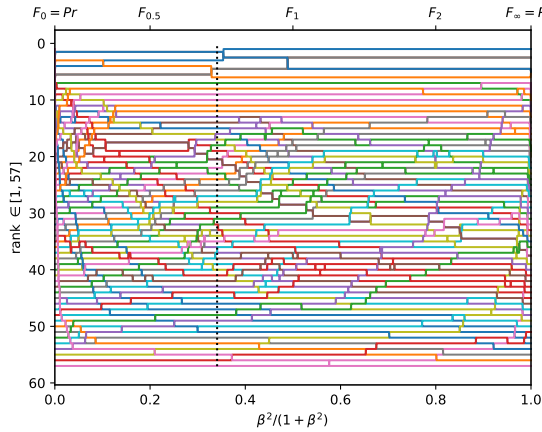
Figure A.3.14. Ranking of 57 BGS methods evaluated on the video "overpass" ($\pi_+ = 0.0134$).



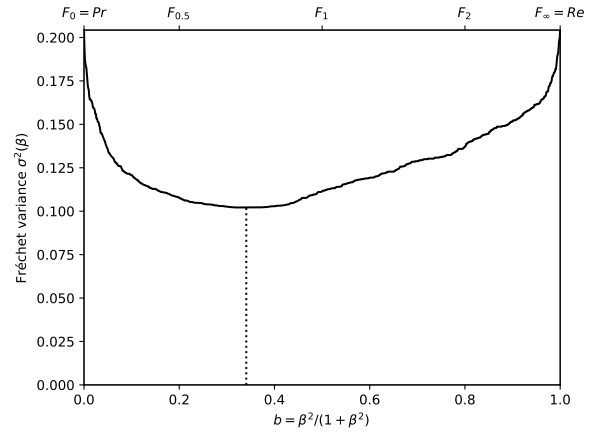
(a) The performances of 57 classifiers (BGS methods) depicted as points in the ROC space, with the isometrics of the optimal tradeoff score, from the ranking point of view, between precision and recall. See Eq. (12).



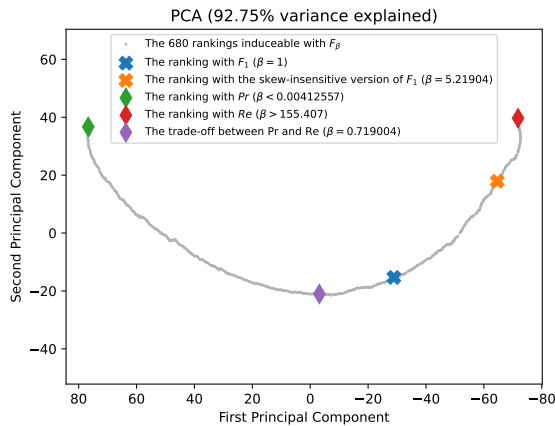
(b) The rank correlations $\tau(F_\beta; Pr)$ and $\tau(F_\beta; Re)$ w.r.t. β . The optimal value (or range of optimal values) for β is where the two curves intersect.



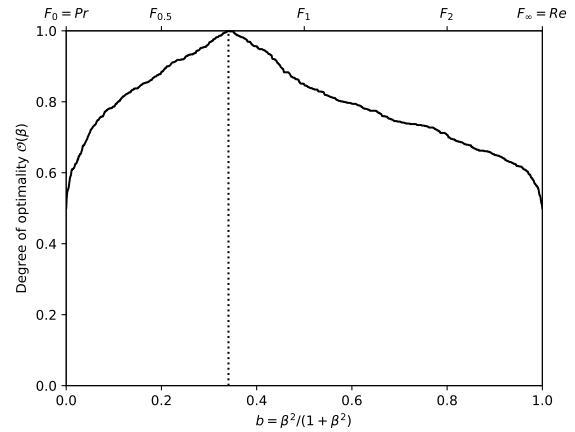
(c) The ranks of each classifier w.r.t. β . The optimal value (or range of optimal values) for β , shown here by the vertical line, is such that the number of swaps on its left is equal to the number of swaps on its right.



(d) The Fréchet variance $\sigma^2(\beta) = d_\tau^2(Pr; F_\beta) + d_\tau^2(F_\beta; Re)$ w.r.t. β . The optimal value (or range of optimal values) for β is where the curve has its minimum.

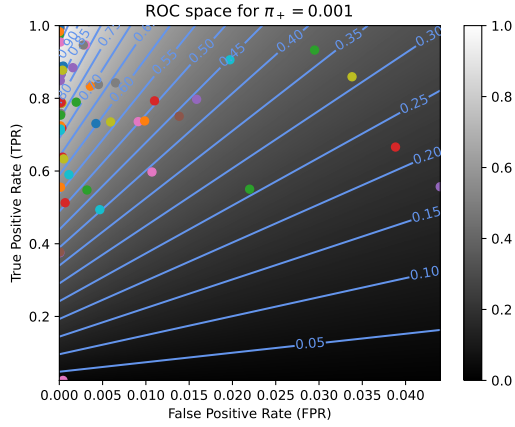


(e) Linear projection (PCA) of the manifold of the rankings induced by the F_β scores. The color points indicate the precision, the recall, F_1 , $SIVF$, as well as the optimal tradeoff. The optimal tradeoff is at the same distance of the two extremities when the distance is measured along the manifold, with Kendall's distance d_+ .

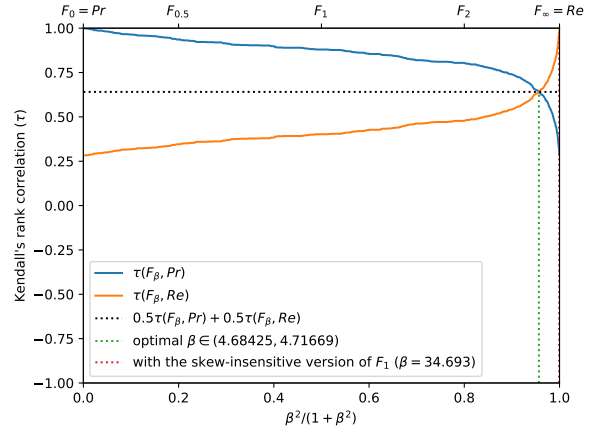


(f) The degree of optimality $\mathcal{O}(\beta)$ w.r.t. β . It is the probability to optimally ordering a pair of classifiers (BGS methods) given that it is not trivial (*i.e.*, that Pr and Re are in contradiction). The optimal value (or range of optimal values) for β is where the curve reaches 100%.

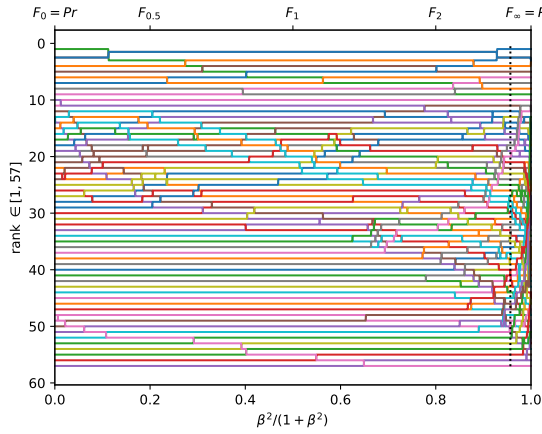
Figure A.3.15. Ranking of 57 BGS methods evaluated on the video "canoe" ($\pi_+ = 0.0354$).



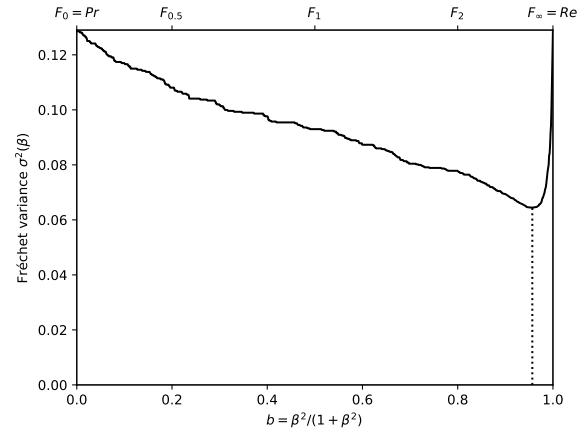
(a) The performances of 57 classifiers (BGS methods) depicted as points in the ROC space, with the isometrics of the optimal tradeoff score, from the ranking point of view, between precision and recall. See Eq. (12).



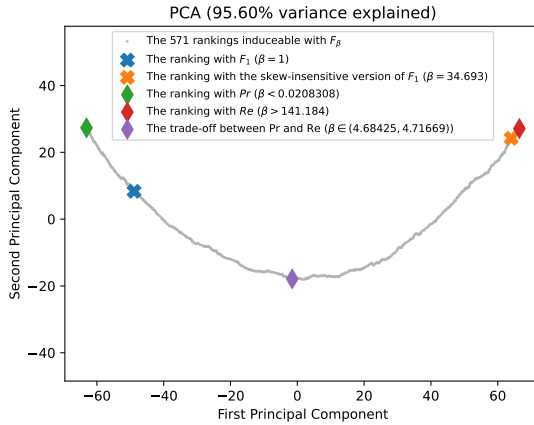
(b) The rank correlations $\tau(F_\beta; Pr)$ and $\tau(F_\beta; Re)$ w.r.t. β . The optimal value (or range of optimal values) for β is where the two curves intersect.



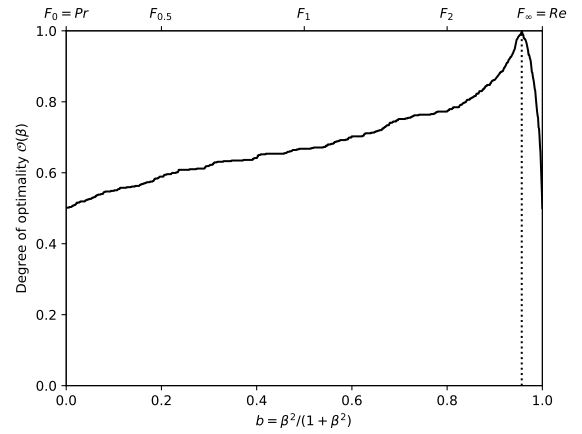
(c) The ranks of each classifier w.r.t. β . The optimal value (or range of optimal values) for β , shown here by the vertical line, is such that the number of swaps on its left is equal to the number of swaps on its right.



(d) The Fréchet variance $\sigma^2(\beta) = d_\tau^2(Pr; F_\beta) + d_\tau^2(F_\beta; Re)$ w.r.t. β . The optimal value (or range of optimal values) for β is where the curve has its minimum.

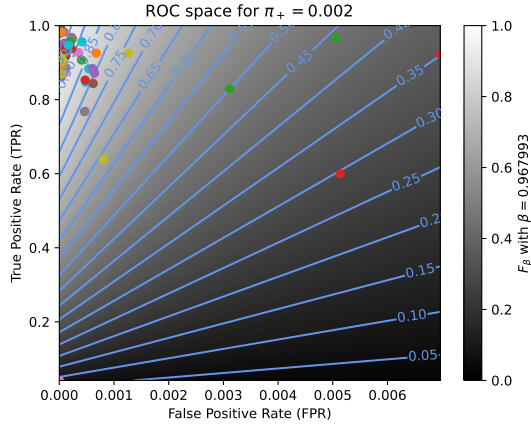


(e) Linear projection (PCA) of the manifold of the rankings induced by the F_β scores. The color points indicate the precision, the recall, F_1 , $SIVF$, as well as the optimal tradeoff. The optimal tradeoff is at the same distance of the two extremities when the distance is measured along the manifold, with Kendall's distance d_+ .

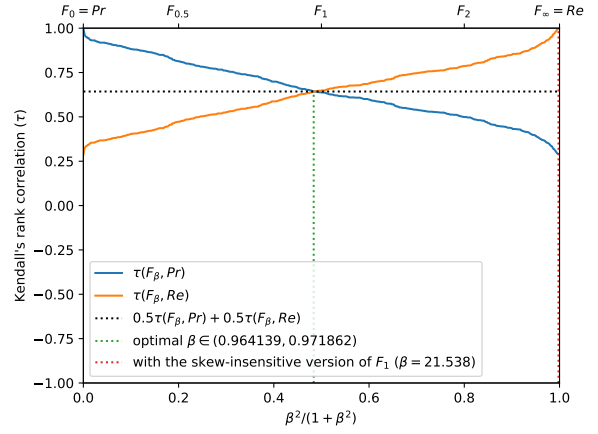


(f) The degree of optimality $\mathcal{O}(\beta)$ w.r.t. β . It is the probability to optimally ordering a pair of classifiers (BGS methods) given that it is not trivial (*i.e.*, that Pr and Re are in contradiction). The optimal value (or range of optimal values) for β is where the curve reaches 100%.

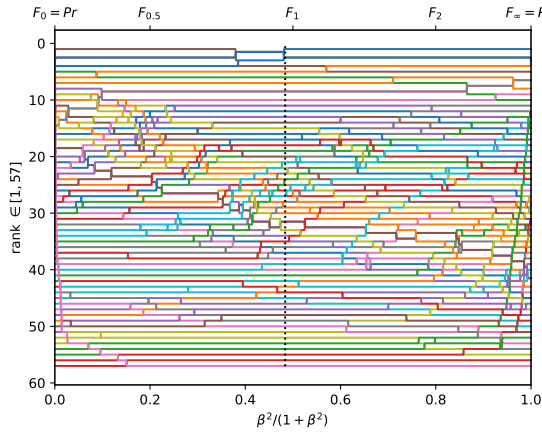
Figure A.3.16. Ranking of 57 BGS methods evaluated on the video "fountain01" ($\pi_+ = 0.0008$).



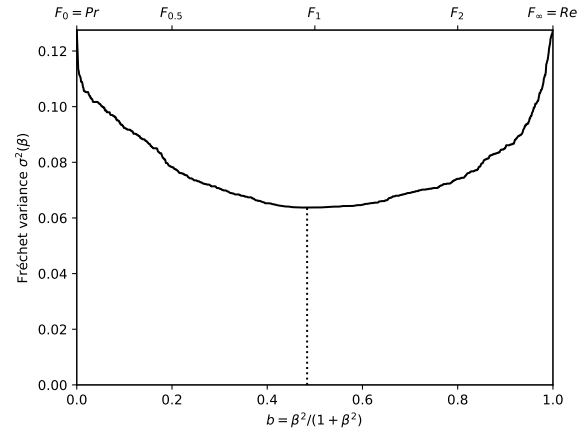
(a) The performances of 57 classifiers (BGS methods) depicted as points in the ROC space, with the isometrics of the optimal tradeoff score, from the ranking point of view, between precision and recall. See Eq. (12).



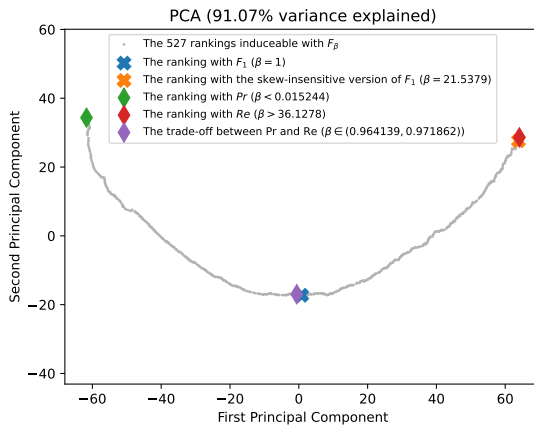
(b) The rank correlations $\tau(F_\beta; Pr)$ and $\tau(F_\beta; Re)$ w.r.t. β . The optimal value (or range of optimal values) for β is where the two curves intersect.



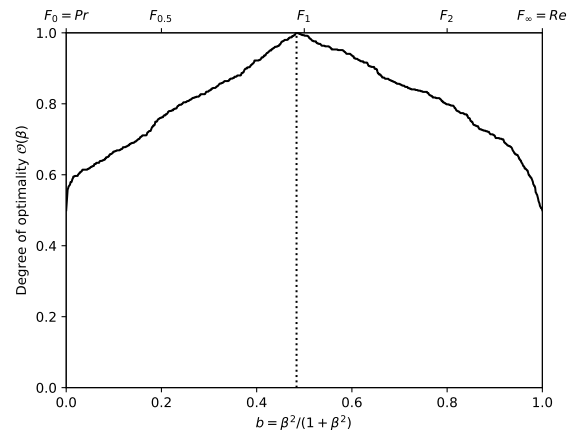
(c) The ranks of each classifier w.r.t. β . The optimal value (or range of optimal values) for β , shown here by the vertical line, is such that the number of swaps on its left is equal to the number of swaps on its right.



(d) The Fréchet variance $\sigma^2(\beta) = d_\tau^2(Pr; F_\beta) + d_\tau^2(F_\beta; Re)$ w.r.t. β . The optimal value (or range of optimal values) for β is where the curve has its minimum.

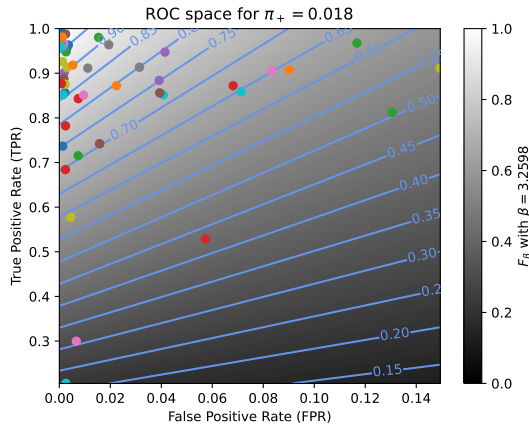


(e) Linear projection (PCA) of the manifold of the rankings induced by the F_β scores. The color points indicate the precision, the recall, F_1 , $SIVF$, as well as the optimal tradeoff. The optimal tradeoff is at the same distance of the two extremities when the distance is measured along the manifold, with Kendall's distance d_+ .

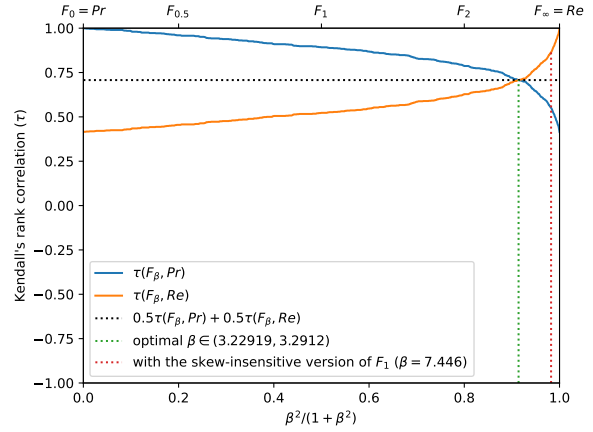


(f) The degree of optimality $\mathcal{O}(\beta)$ w.r.t. β . It is the probability to optimally ordering a pair of classifiers (BGS methods) given that it is not trivial (*i.e.*, that Pr and Re are in contradiction). The optimal value (or range of optimal values) for β is where the curve reaches 100%.

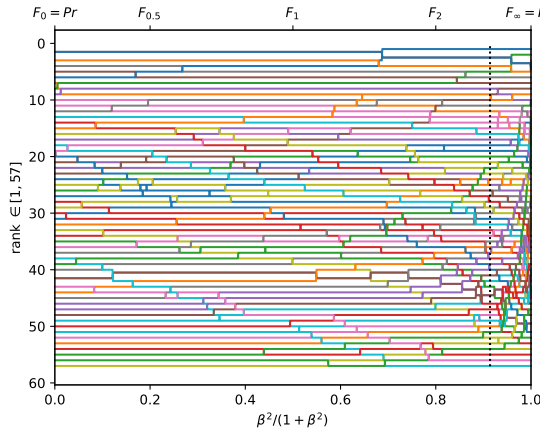
Figure A.3.17. Ranking of 57 BGS methods evaluated on the video "fountain02" ($\pi_+ = 0.0022$).



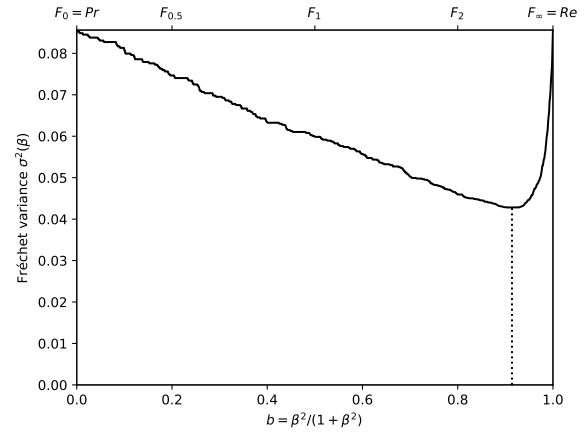
(a) The performances of 57 classifiers (BGS methods) depicted as points in the ROC space, with the isometrics of the optimal tradeoff score, from the ranking point of view, between precision and recall. See Eq. (12).



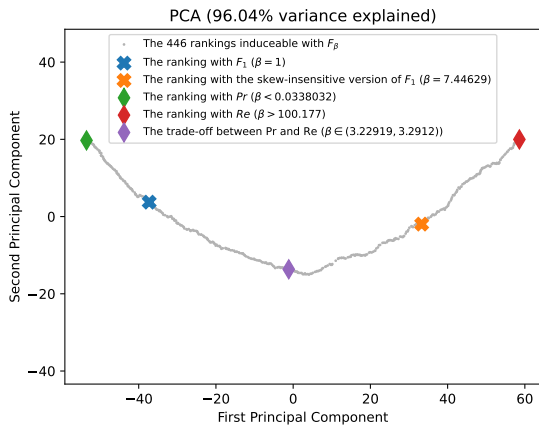
(b) The rank correlations $\tau(F_\beta; Pr)$ and $\tau(F_\beta; Re)$ w.r.t. β . The optimal value (or range of optimal values) for β is where the two curves intersect.



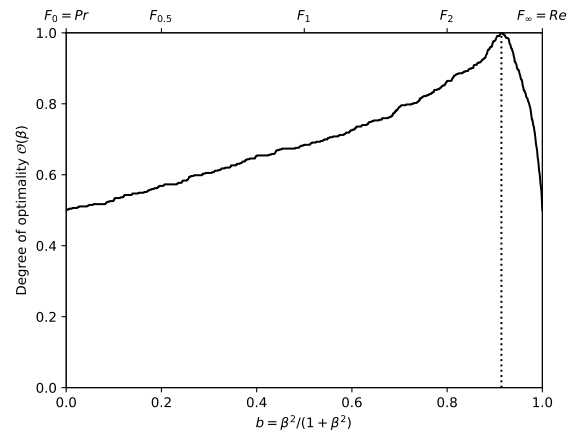
(c) The ranks of each classifier w.r.t. β . The optimal value (or range of optimal values) for β , shown here by the vertical line, is such that the number of swaps on its left is equal to the number of swaps on its right.



(d) The Fréchet variance $\sigma^2(\beta) = d_\tau^2(Pr; F_\beta) + d_\tau^2(F_\beta; Re)$ w.r.t. β . The optimal value (or range of optimal values) for β is where the curve has its minimum.

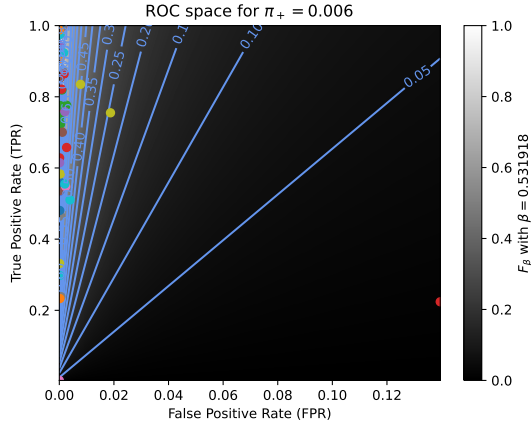


(e) Linear projection (PCA) of the manifold of the rankings induced by the F_β scores. The color points indicate the precision, the recall, F_1 , $SIVF$, as well as the optimal tradeoff. The optimal tradeoff is at the same distance of the two extremities when the distance is measured along the manifold, with Kendall's distance d_τ .

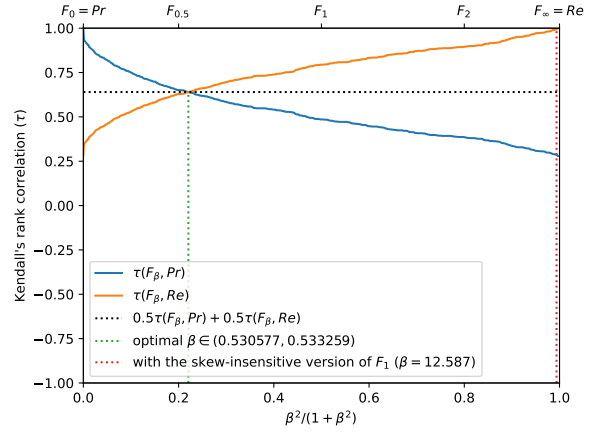


(f) The degree of optimality $\mathcal{O}(\beta)$ w.r.t. β . It is the probability to optimally ordering a pair of classifiers (BGS methods) given that it is not trivial (*i.e.*, that Pr and Re are in contradiction). The optimal value (or range of optimal values) for β is where the curve reaches 100%.

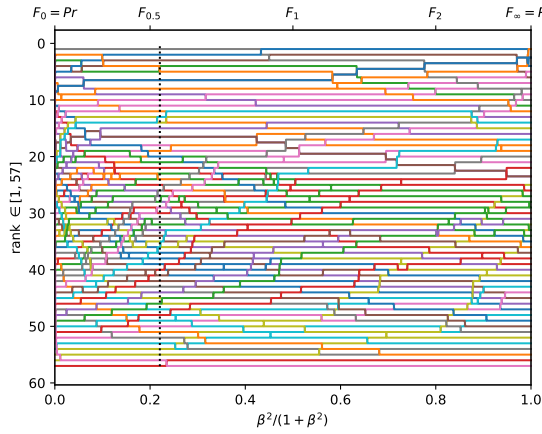
Figure A.3.18. Ranking of 57 BGS methods evaluated on the video "fall" ($\pi_+ = 0.0177$).



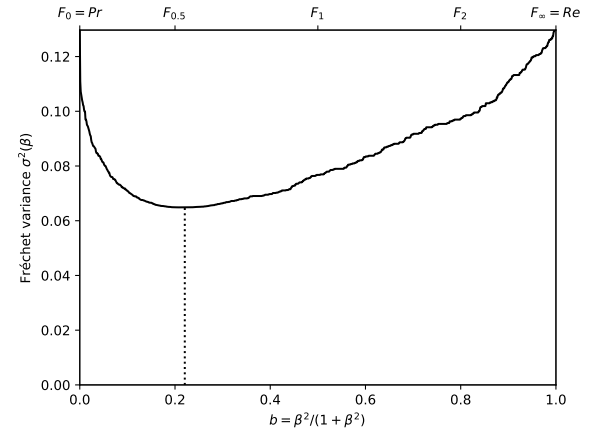
(a) The performances of 57 classifiers (BGS methods) depicted as points in the ROC space, with the isometrics of the optimal tradeoff score, from the ranking point of view, between precision and recall. See Eq. (12).



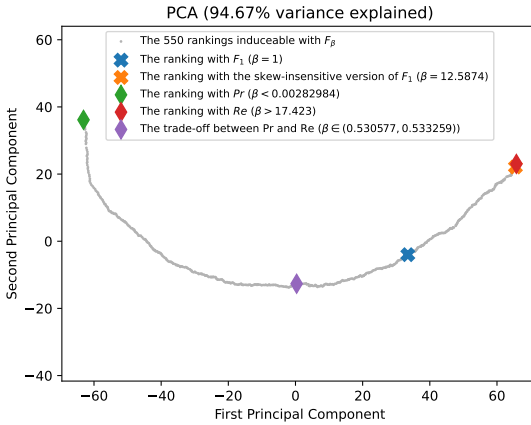
(b) The rank correlations $\tau(F_\beta; Pr)$ and $\tau(F_\beta; Re)$ w.r.t. β . The optimal value (or range of optimal values) for β is where the two curves intersect.



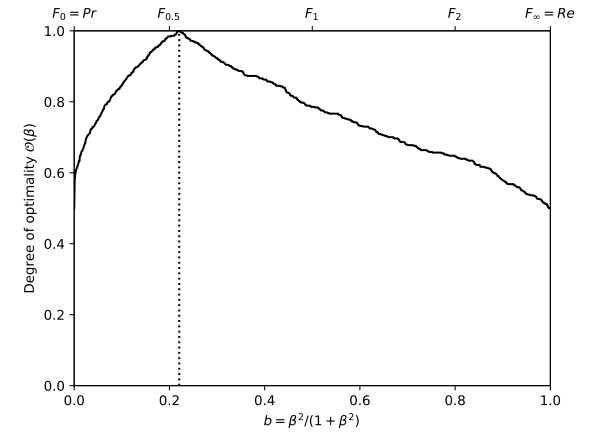
(c) The ranks of each classifier w.r.t. β . The optimal value (or range of optimal values) for β , shown here by the vertical line, is such that the number of swaps on its left is equal to the number of swaps on its right.



(d) The Fréchet variance $\sigma^2(\beta) = d_\tau^2(Pr; F_\beta) + d_\tau^2(F_\beta; Re)$ w.r.t. β . The optimal value (or range of optimal values) for β is where the curve has its minimum.

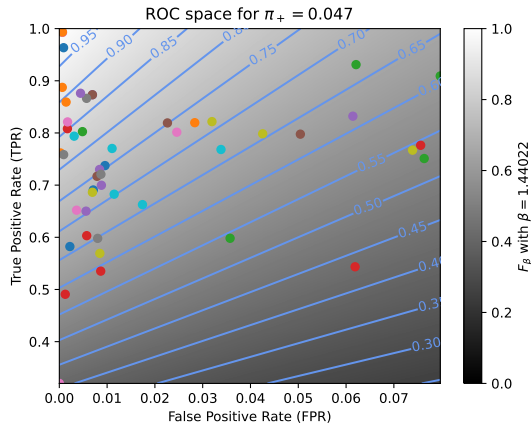


(e) Linear projection (PCA) of the manifold of the rankings induced by the F_β scores. The color points indicate the precision, the recall, F_1 , $SIVF$, as well as the optimal tradeoff. The optimal tradeoff is at the same distance of the two extremities when the distance is measured along the manifold, with Kendall's distance d_τ .

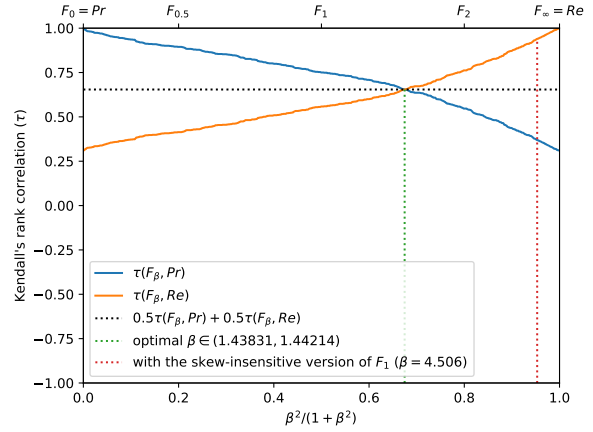


(f) The degree of optimality $\mathcal{O}(\beta)$ w.r.t. β . It is the probability to optimally ordering a pair of classifiers (BGS methods) given that it is not trivial (*i.e.*, that Pr and Re are in contradiction). The optimal value (or range of optimal values) for β is where the curve reaches 100%.

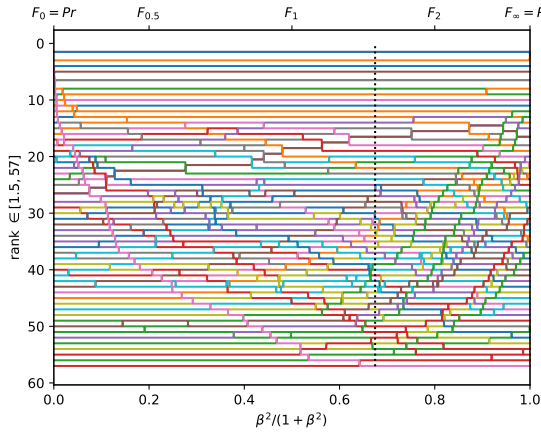
Figure A.3.19. Ranking of 57 BGS methods evaluated on the video "boats" ($\pi_+ = 0.0063$).



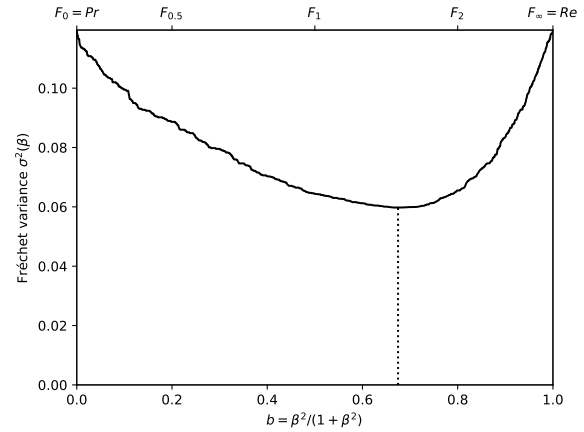
(a) The performances of 57 classifiers (BGS methods) depicted as points in the ROC space, with the isometrics of the optimal tradeoff score, from the ranking point of view, between precision and recall. See Eq. (12).



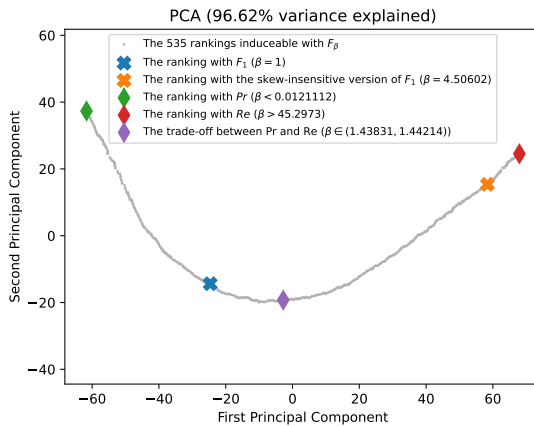
(b) The rank correlations $\tau(F_\beta; Pr)$ and $\tau(F_\beta; Re)$ w.r.t. β . The optimal value (or range of optimal values) for β is where the two curves intersect.



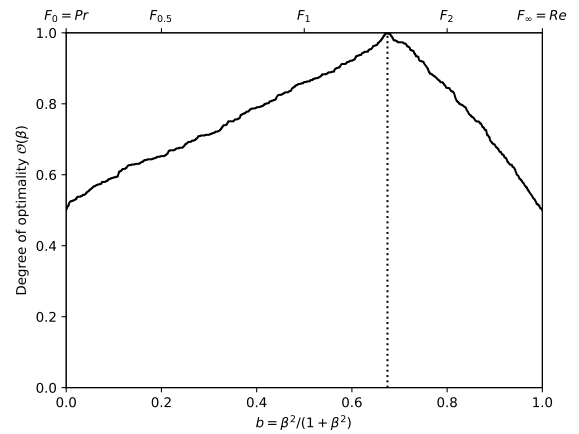
(c) The ranks of each classifier w.r.t. β . The optimal value (or range of optimal values) for β , shown here by the vertical line, is such that the number of swaps on its left is equal to the number of swaps on its right.



(d) The Fréchet variance $\sigma^2(\beta) = d_\tau^2(Pr; F_\beta) + d_\tau^2(F_\beta; Re)$ w.r.t. β . The optimal value (or range of optimal values) for β is where the curve has its minimum.

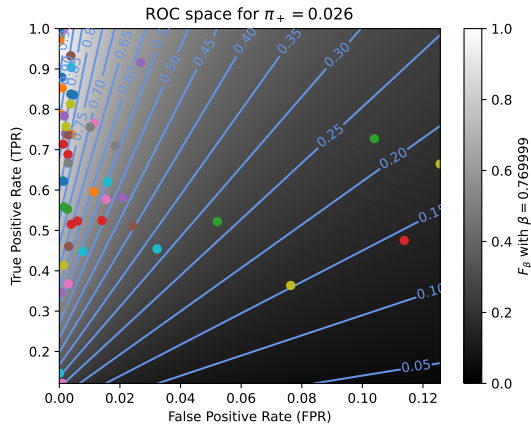


(e) Linear projection (PCA) of the manifold of the rankings induced by the F_β scores. The color points indicate the precision, the recall, F_1 , $SIVF$, as well as the optimal tradeoff. The optimal tradeoff is at the same distance of the two extremities when the distance is measured along the manifold, with Kendall's distance d_+ .

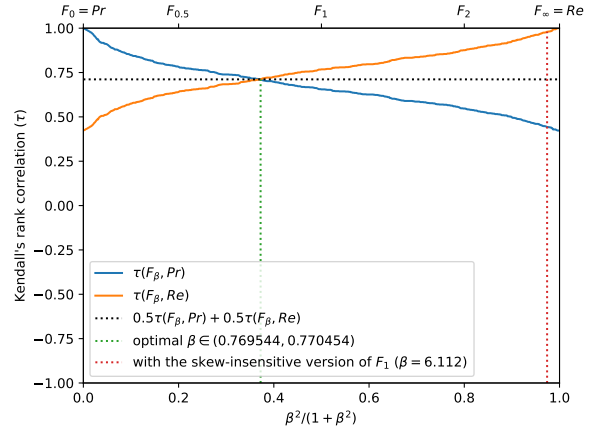


(f) The degree of optimality $\mathcal{O}(\beta)$ w.r.t. β . It is the probability to optimally ordering a pair of classifiers (BGS methods) given that it is not trivial (*i.e.*, that Pr and Re are in contradiction). The optimal value (or range of optimal values) for β is where the curve reaches 100%.

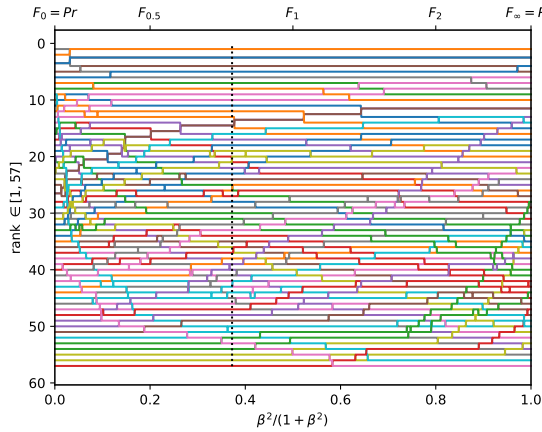
Figure A.3.20. Ranking of 57 BGS methods evaluated on the video "boulevard" ($\pi_+ = 0.0469$).



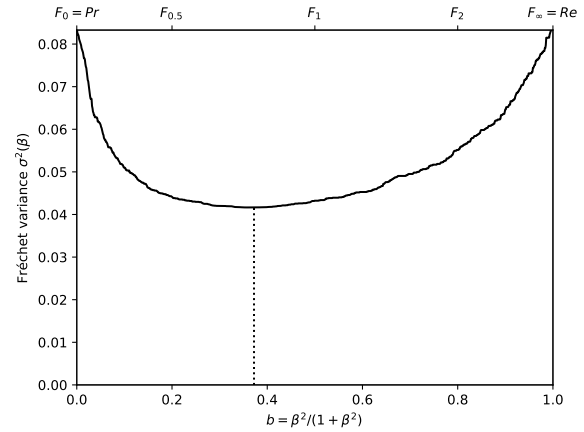
(a) The performances of 57 classifiers (BGS methods) depicted as points in the ROC space, with the isometrics of the optimal tradeoff score, from the ranking point of view, between precision and recall. See Eq. (12).



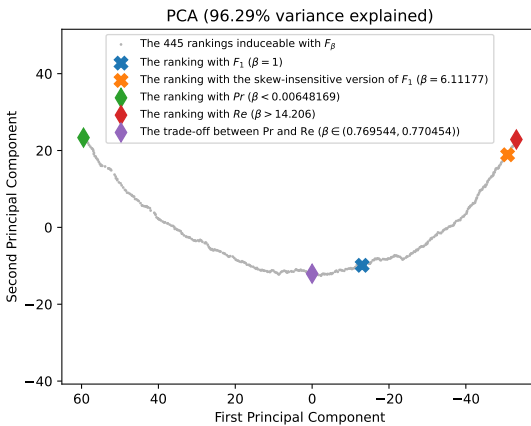
(b) The rank correlations $\tau(F_\beta; Pr)$ and $\tau(F_\beta; Re)$ w.r.t. β . The optimal value (or range of optimal values) for β is where the two curves intersect.



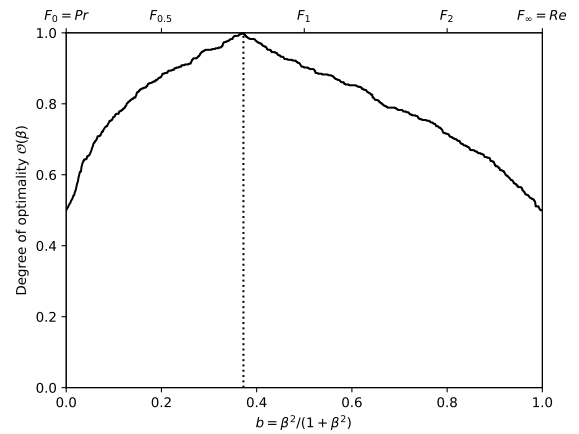
(c) The ranks of each classifier w.r.t. β . The optimal value (or range of optimal values) for β , shown here by the vertical line, is such that the number of swaps on its left is equal to the number of swaps on its right.



(d) The Fréchet variance $\sigma^2(\beta) = d_\tau^2(Pr; F_\beta) + d_\tau^2(F_\beta; Re)$ w.r.t. β . The optimal value (or range of optimal values) for β is where the curve has its minimum.

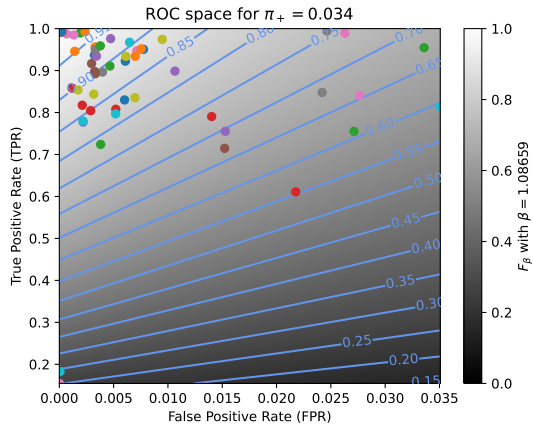


(e) Linear projection (PCA) of the manifold of the rankings induced by the F_β scores. The color points indicate the precision, the recall, F_1 , $SIVF$, as well as the optimal tradeoff. The optimal tradeoff is at the same distance of the two extremities when the distance is measured along the manifold, with Kendall's distance d_τ .

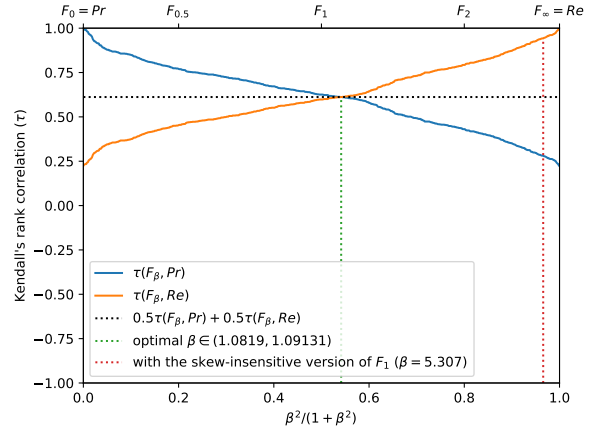


(f) The degree of optimality $\mathcal{O}(\beta)$ w.r.t. β . It is the probability to optimally ordering a pair of classifiers (BGS methods) given that it is not trivial (*i.e.*, that Pr and Re are in contradiction). The optimal value (or range of optimal values) for β is where the curve reaches 100%.

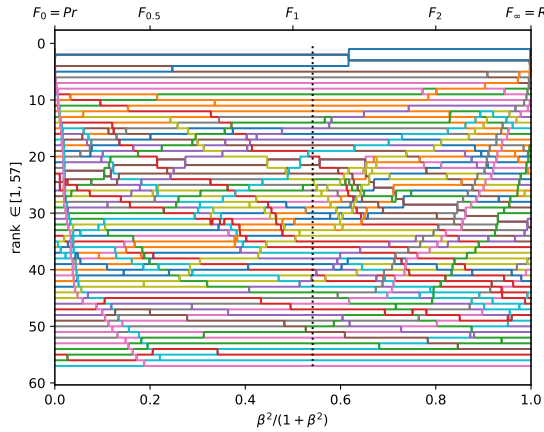
Figure A.3.21. Ranking of 57 BGS methods evaluated on the video "sidewalk" ($\pi_+ = 0.0261$).



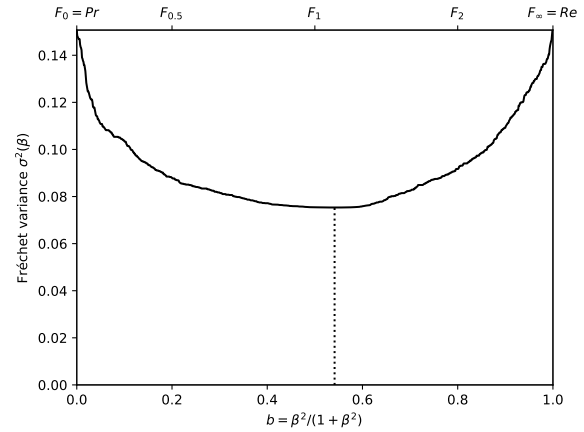
(a) The performances of 57 classifiers (BGS methods) depicted as points in the ROC space, with the isometrics of the optimal tradeoff score, from the ranking point of view, between precision and recall. See Eq. (12).



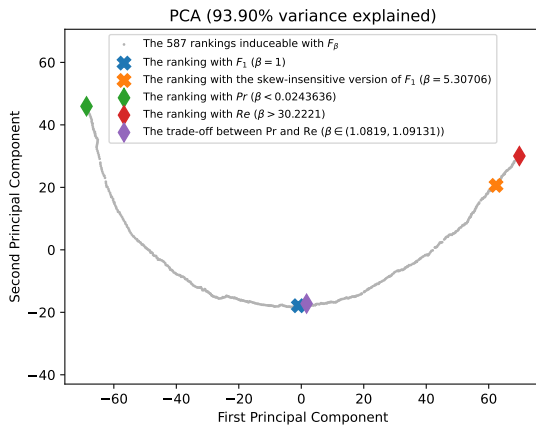
(b) The rank correlations $\tau(F_\beta; Pr)$ and $\tau(F_\beta; Re)$ w.r.t. β . The optimal value (or range of optimal values) for β is where the two curves intersect.



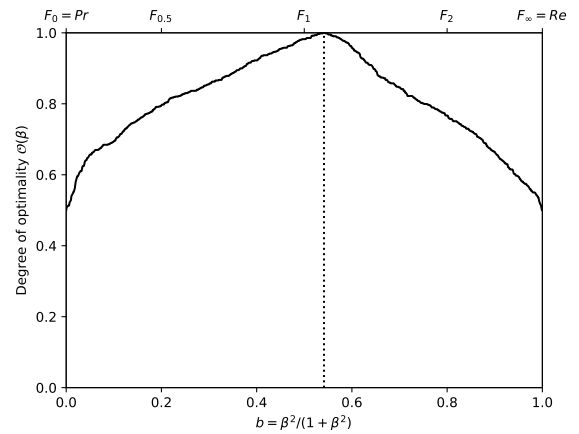
(c) The ranks of each classifier w.r.t. β . The optimal value (or range of optimal values) for β , shown here by the vertical line, is such that the number of swaps on its left is equal to the number of swaps on its right.



(d) The Fréchet variance $\sigma^2(\beta) = d_\tau^2(Pr; F_\beta) + d_\tau^2(F_\beta; Re)$ w.r.t. β . The optimal value (or range of optimal values) for β is where the curve has its minimum.

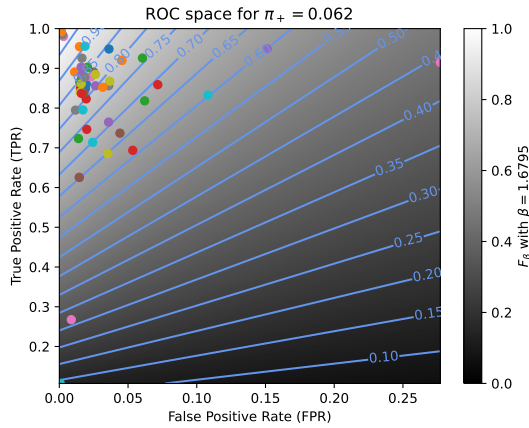


(e) Linear projection (PCA) of the manifold of the rankings induced by the F_β scores. The color points indicate the precision, the recall, F_1 , $SIVF$, as well as the optimal tradeoff. The optimal tradeoff is at the same distance of the two extremities when the distance is measured along the manifold, with Kendall's distance d_+ .

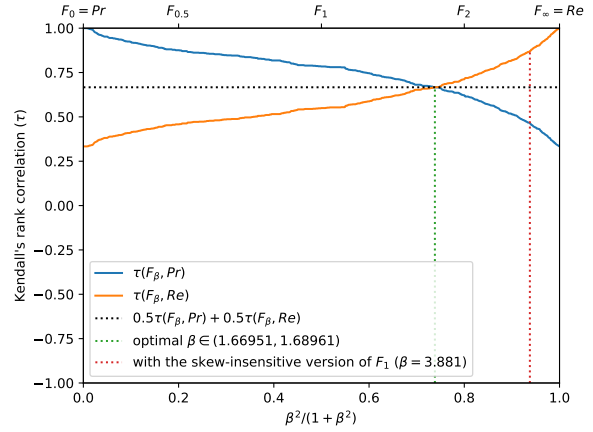


(f) The degree of optimality $\mathcal{O}(\beta)$ w.r.t. β . It is the probability to optimally ordering a pair of classifiers (BGS methods) given that it is not trivial (*i.e.*, that Pr and Re are in contradiction). The optimal value (or range of optimal values) for β is where the curve reaches 100%.

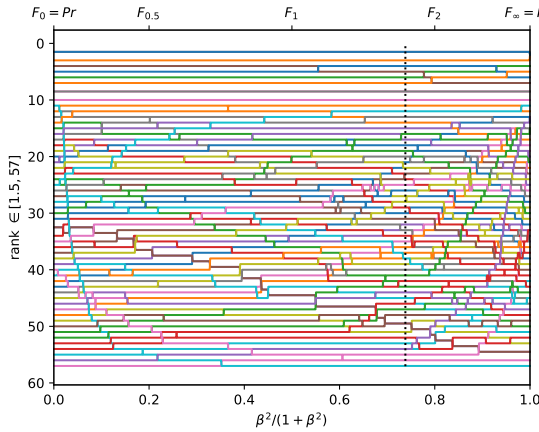
Figure A.3.22. Ranking of 57 BGS methods evaluated on the video "badminton" ($\pi_+ = 0.0343$).



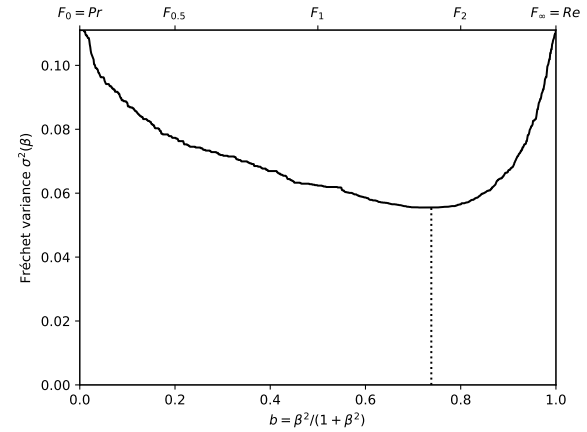
(a) The performances of 57 classifiers (BGS methods) depicted as points in the ROC space, with the isometrics of the optimal tradeoff score, from the ranking point of view, between precision and recall. See Eq. (12).



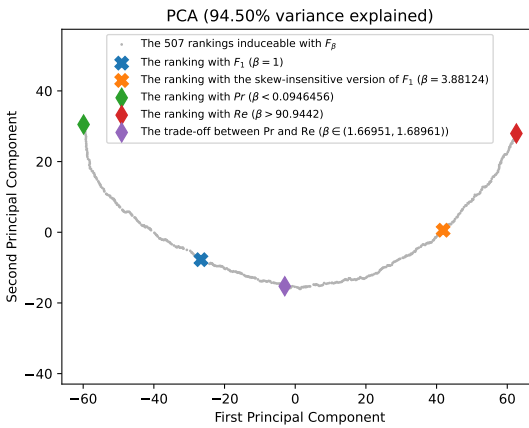
(b) The rank correlations $\tau(F_\beta; Pr)$ and $\tau(F_\beta; Re)$ w.r.t. β . The optimal value (or range of optimal values) for β is where the two curves intersect.



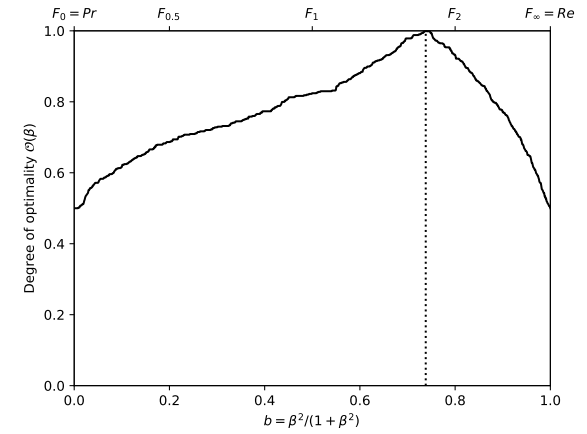
(c) The ranks of each classifier w.r.t. β . The optimal value (or range of optimal values) for β , shown here by the vertical line, is such that the number of swaps on its left is equal to the number of swaps on its right.



(d) The Fréchet variance $\sigma^2(\beta) = d_\tau^2(Pr; F_\beta) + d_\tau^2(F_\beta; Re)$ w.r.t. β . The optimal value (or range of optimal values) for β is where the curve has its minimum.

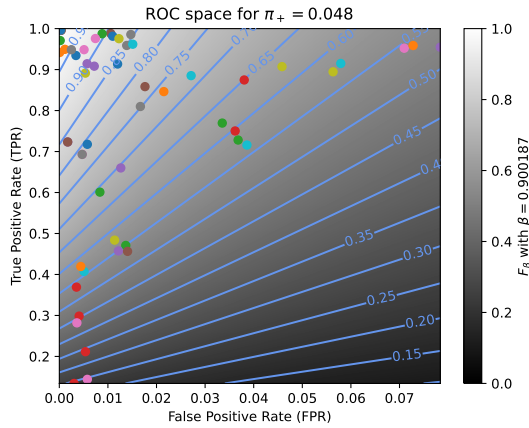


(e) Linear projection (PCA) of the manifold of the rankings induced by the F_β scores. The color points indicate the precision, the recall, F_1 , $SIVF$, as well as the optimal tradeoff. The optimal tradeoff is at the same distance of the two extremities when the distance is measured along the manifold, with Kendall's distance d_* .

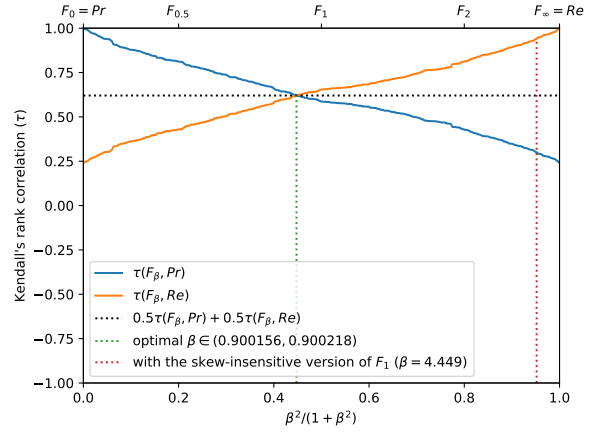


(f) The degree of optimality $\mathcal{O}(\beta)$ w.r.t. β . It is the probability to optimally ordering a pair of classifiers (BGS methods) given that it is not trivial (*i.e.*, that Pr and Re are in contradiction). The optimal value (or range of optimal values) for β is where the curve reaches 100%.

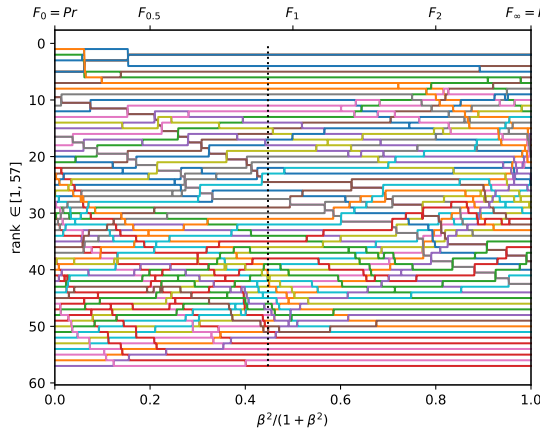
Figure A.3.23. Ranking of 57 BGS methods evaluated on the video "traffic" ($\pi_+ = 0.0623$).



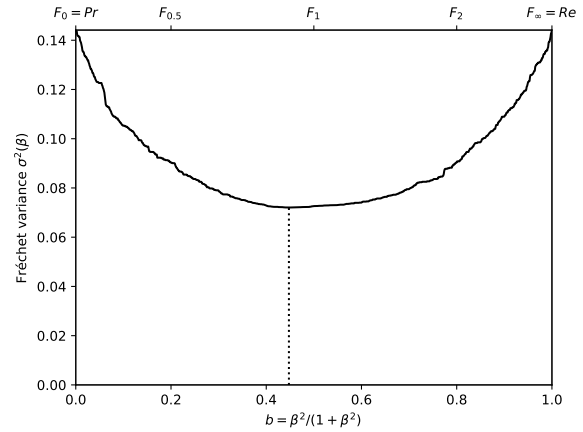
(a) The performances of 57 classifiers (BGS methods) depicted as points in the ROC space, with the isometrics of the optimal tradeoff score, from the ranking point of view, between precision and recall. See Eq. (12).



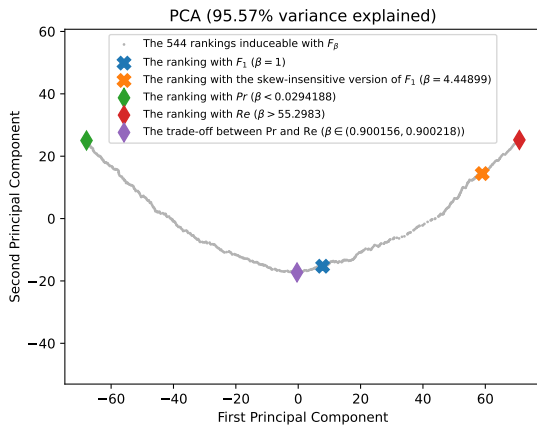
(b) The rank correlations $\tau(F_\beta; Pr)$ and $\tau(F_\beta; Re)$ w.r.t. β . The optimal value (or range of optimal values) for β is where the two curves intersect.



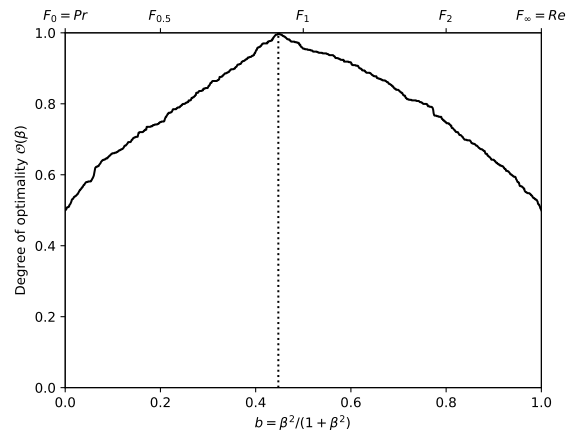
(c) The ranks of each classifier w.r.t. β . The optimal value (or range of optimal values) for β , shown here by the vertical line, is such that the number of swaps on its left is equal to the number of swaps on its right.



(d) The Fréchet variance $\sigma^2(\beta) = d_\tau^2(Pr; F_\beta) + d_\tau^2(F_\beta; Re)$ w.r.t. β . The optimal value (or range of optimal values) for β is where the curve has its minimum.

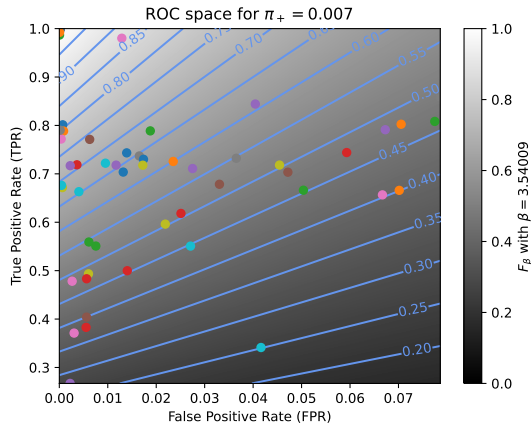


(e) Linear projection (PCA) of the manifold of the rankings induced by the F_β scores. The color points indicate the precision, the recall, F_1 , $SIVF$, as well as the optimal tradeoff. The optimal tradeoff is at the same distance of the two extremities when the distance is measured along the manifold, with Kendall's distance d_* .

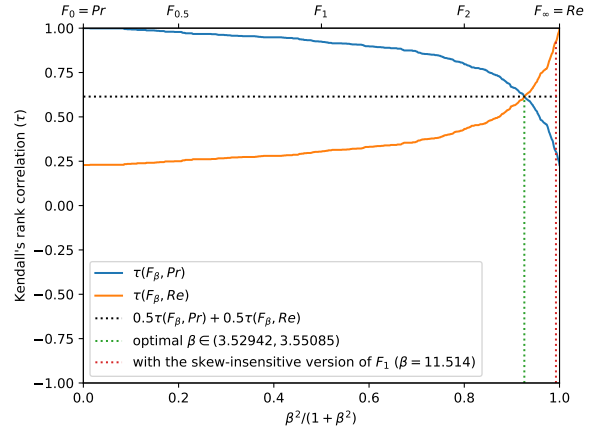


(f) The degree of optimality $\mathcal{O}(\beta)$ w.r.t. β . It is the probability to optimally ordering a pair of classifiers (BGS methods) given that it is not trivial (*i.e.*, that Pr and Re are in contradiction). The optimal value (or range of optimal values) for β is where the curve reaches 100%.

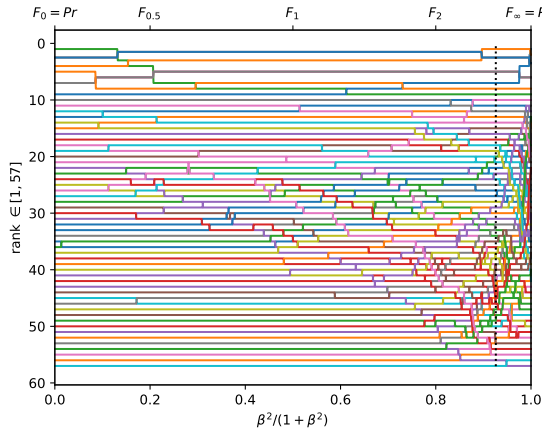
Figure A.3.24. Ranking of 57 BGS methods evaluated on the video "abandonedBox" ($\pi_+ = 0.0481$).



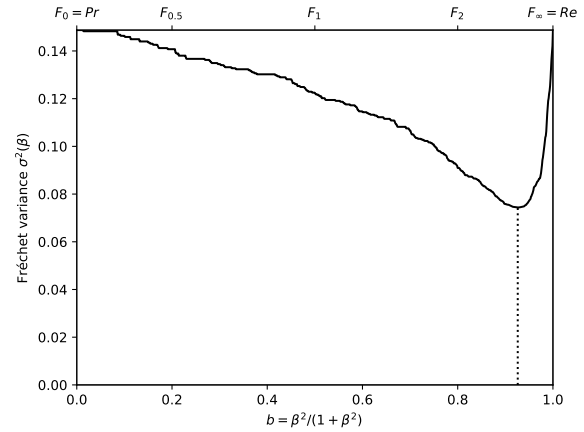
(a) The performances of 57 classifiers (BGS methods) depicted as points in the ROC space, with the isometrics of the optimal tradeoff score, from the ranking point of view, between precision and recall. See Eq. (12).



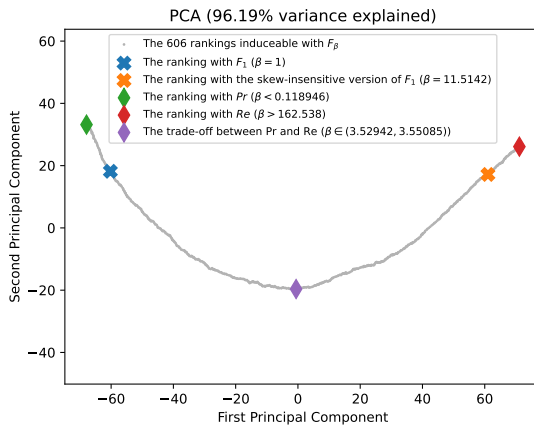
(b) The rank correlations $\tau(F_\beta; Pr)$ and $\tau(F_\beta; Re)$ w.r.t. β . The optimal value (or range of optimal values) for β is where the two curves intersect.



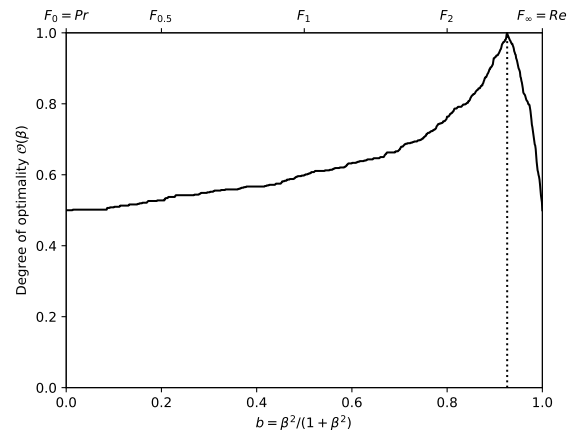
(c) The ranks of each classifier w.r.t. β . The optimal value (or range of optimal values) for β , shown here by the vertical line, is such that the number of swaps on its left is equal to the number of swaps on its right.



(d) The Fréchet variance $\sigma^2(\beta) = d_\tau^2(Pr; F_\beta) + d_\tau^2(F_\beta; Re)$ w.r.t. β . The optimal value (or range of optimal values) for β is where the curve has its minimum.

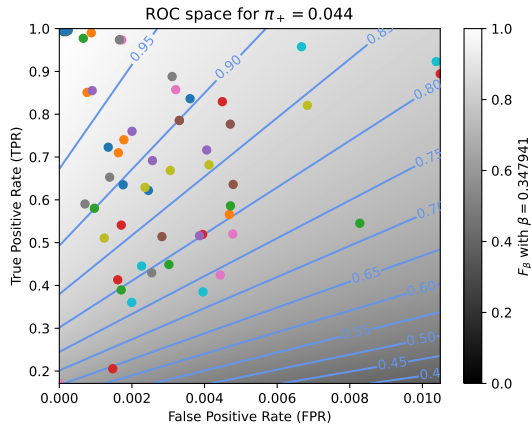


(e) Linear projection (PCA) of the manifold of the rankings induced by the F_β scores. The color points indicate the precision, the recall, F_1 , $SIVF$, as well as the optimal tradeoff. The optimal tradeoff is at the same distance of the two extremities when the distance is measured along the manifold, with Kendall's distance d_+ .

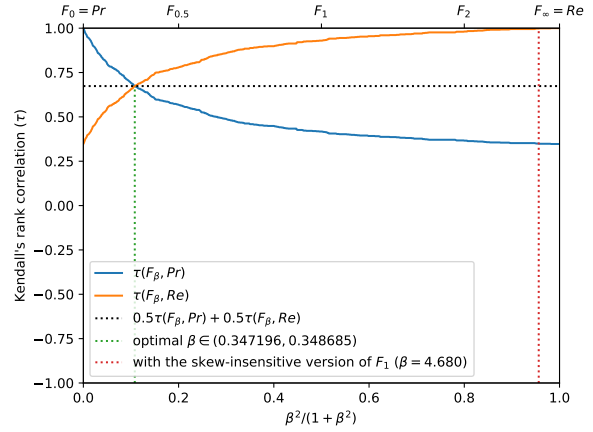


(f) The degree of optimality $\mathcal{O}(\beta)$ w.r.t. β . It is the probability to optimally ordering a pair of classifiers (BGS methods) given that it is not trivial (*i.e.*, that Pr and Re are in contradiction). The optimal value (or range of optimal values) for β is where the curve reaches 100%.

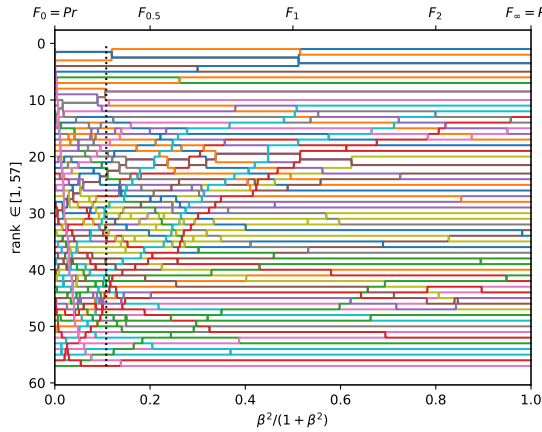
Figure A.3.25. Ranking of 57 BGS methods evaluated on the video "winterDriveway" ($\pi_+ = 0.0075$).



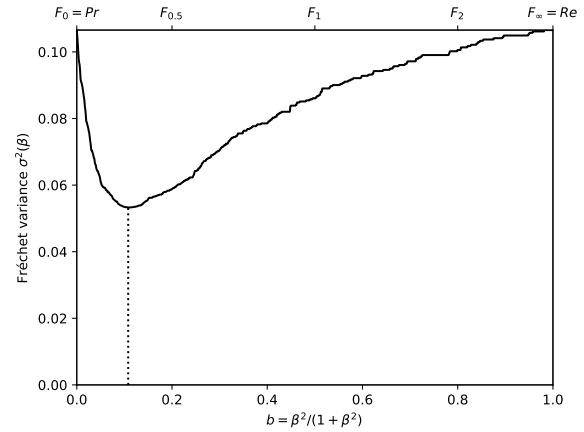
(a) The performances of 57 classifiers (BGS methods) depicted as points in the ROC space, with the isometrics of the optimal tradeoff score, from the ranking point of view, between precision and recall. See Eq. (12).



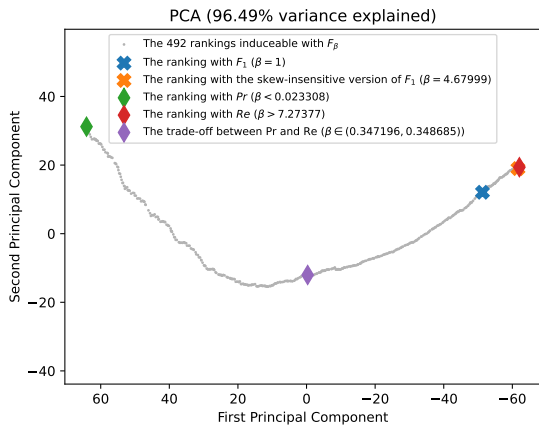
(b) The rank correlations $\tau(F_\beta; Pr)$ and $\tau(F_\beta; Re)$ w.r.t. β . The optimal value (or range of optimal values) for β is where the two curves intersect.



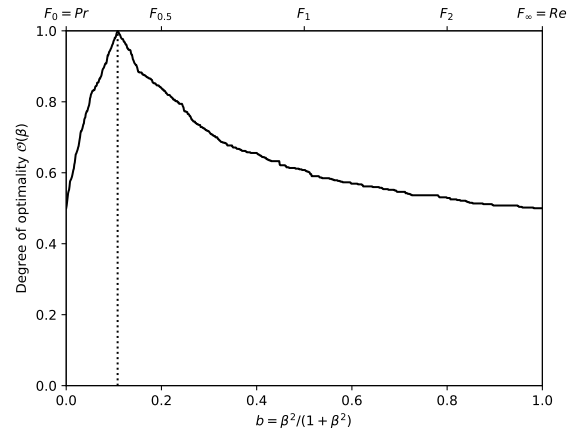
(c) The ranks of each classifier w.r.t. β . The optimal value (or range of optimal values) for β , shown here by the vertical line, is such that the number of swaps on its left is equal to the number of swaps on its right.



(d) The Fréchet variance $\sigma^2(\beta) = d_\tau^2(Pr; F_\beta) + d_\tau^2(F_\beta; Re)$ w.r.t. β . The optimal value (or range of optimal values) for β is where the curve has its minimum.

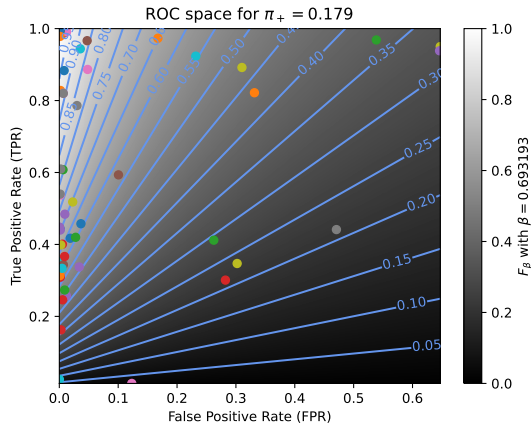


(e) Linear projection (PCA) of the manifold of the rankings induced by the F_β scores. The color points indicate the precision, the recall, F_1 , $SIVF$, as well as the optimal tradeoff. The optimal tradeoff is at the same distance of the two extremities when the distance is measured along the manifold, with Kendall's distance d_* .

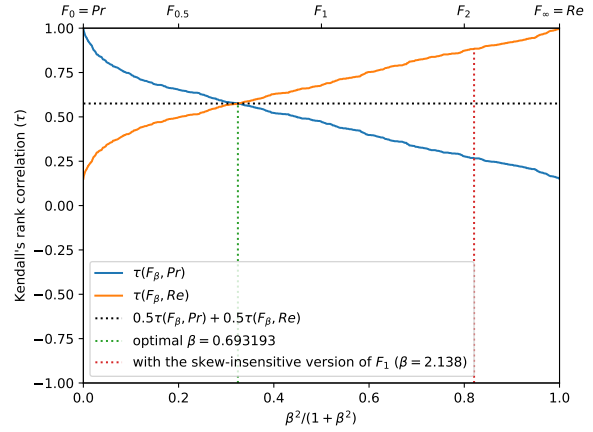


(f) The degree of optimality $\mathcal{O}(\beta)$ w.r.t. β . It is the probability to optimally ordering a pair of classifiers (BGS methods) given that it is not trivial (*i.e.*, that Pr and Re are in contradiction). The optimal value (or range of optimal values) for β is where the curve reaches 100%.

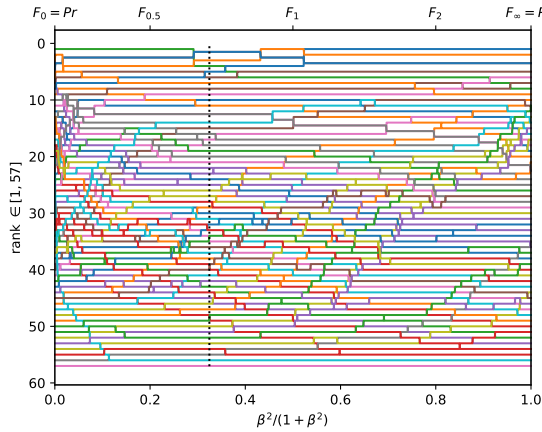
Figure A.3.26. Ranking of 57 BGS methods evaluated on the video "sofa" ($\pi_+ = 0.0437$).



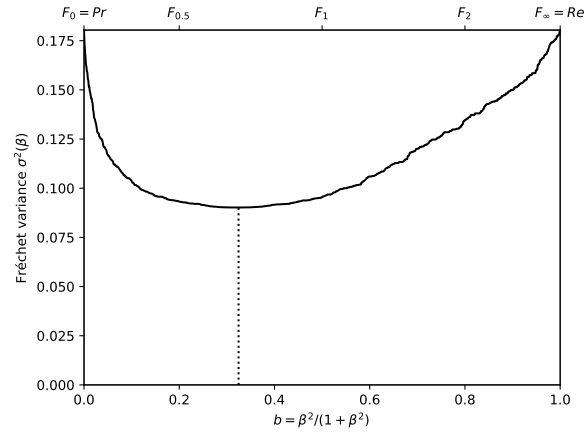
(a) The performances of 57 classifiers (BGS methods) depicted as points in the ROC space, with the isometrics of the optimal tradeoff score, from the ranking point of view, between precision and recall. See Eq. (12).



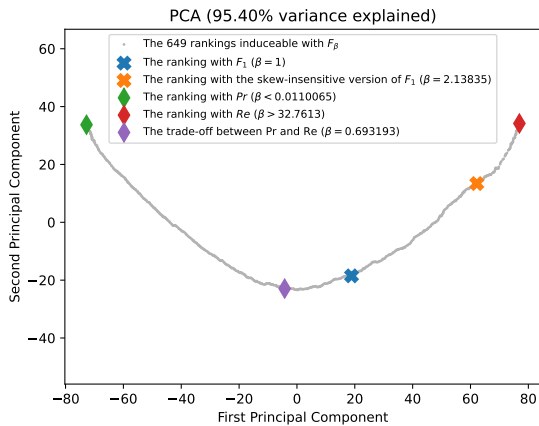
(b) The rank correlations $\tau(F_\beta; Pr)$ and $\tau(F_\beta; Re)$ w.r.t. β . The optimal value (or range of optimal values) for β is where the two curves intersect.



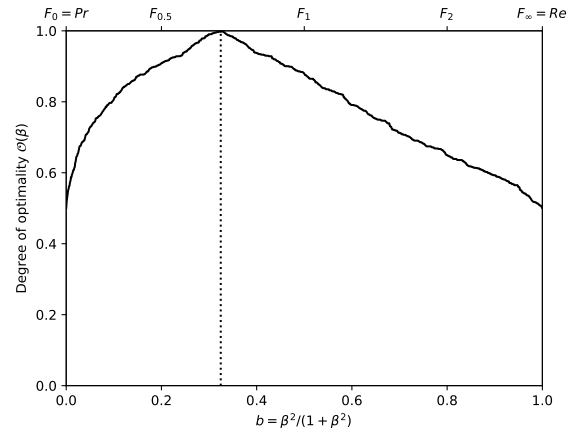
(c) The ranks of each classifier w.r.t. β . The optimal value (or range of optimal values) for β , shown here by the vertical line, is such that the number of swaps on its left is equal to the number of swaps on its right.



(d) The Fréchet variance $\sigma^2(\beta) = d_\tau^2(Pr; F_\beta) + d_\tau^2(F_\beta; Re)$ w.r.t. β . The optimal value (or range of optimal values) for β is where the curve has its minimum.

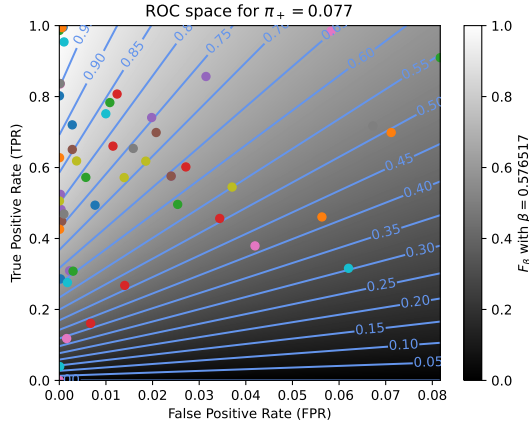


(e) Linear projection (PCA) of the manifold of the rankings induced by the F_β scores. The color points indicate the precision, the recall, F_1 , $SIVF$, as well as the optimal tradeoff. The optimal tradeoff is at the same distance of the two extremities when the distance is measured along the manifold, with Kendall's distance d_* .

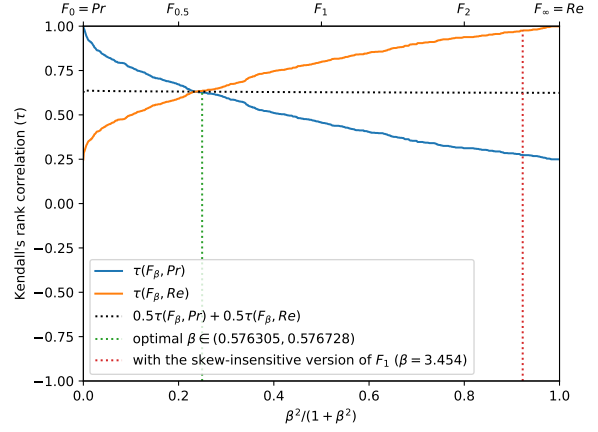


(f) The degree of optimality $\mathcal{O}(\beta)$ w.r.t. β . It is the probability to optimally ordering a pair of classifiers (BGS methods) given that it is not trivial (*i.e.*, that Pr and Re are in contradiction). The optimal value (or range of optimal values) for β is where the curve reaches 100%.

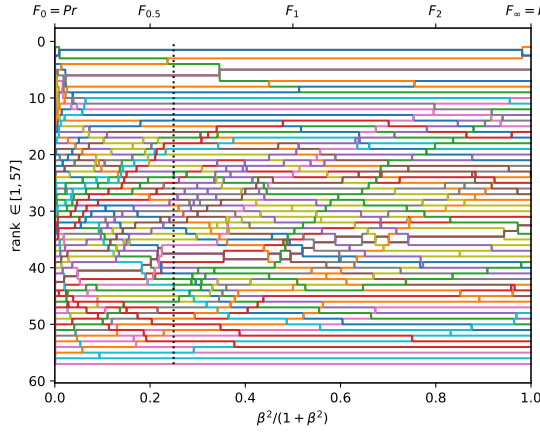
Figure A.3.27. Ranking of 57 BGS methods evaluated on the video "tramstop" ($\pi_+ = 0.1795$).



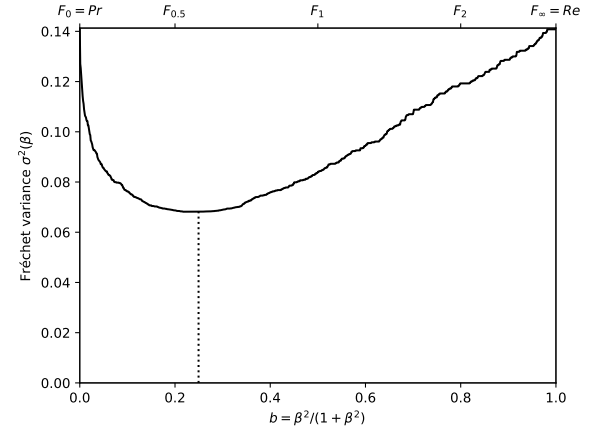
(a) The performances of 57 classifiers (BGS methods) depicted as points in the ROC space, with the isometrics of the optimal tradeoff score, from the ranking point of view, between precision and recall. See Eq. (12).



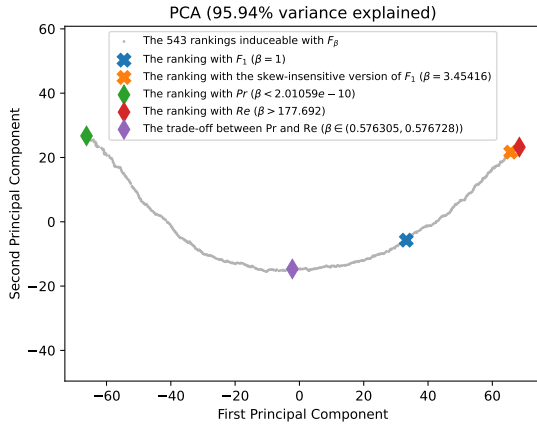
(b) The rank correlations $\tau(F_\beta; Pr)$ and $\tau(F_\beta; Re)$ w.r.t. β . The optimal value (or range of optimal values) for β is where the two curves intersect.



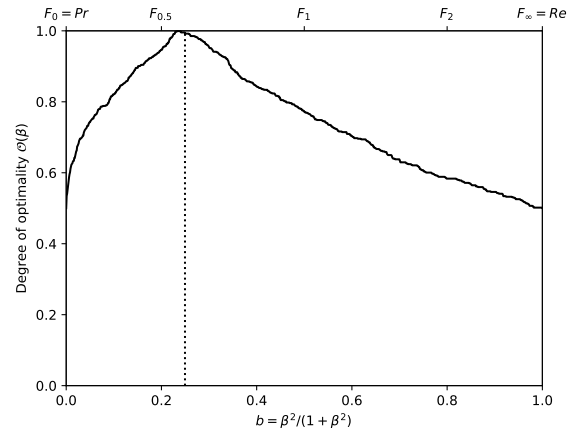
(c) The ranks of each classifier w.r.t. β . The optimal value (or range of optimal values) for β , shown here by the vertical line, is such that the number of swaps on its left is equal to the number of swaps on its right.



(d) The Fréchet variance $\sigma^2(\beta) = d_\tau^2(Pr; F_\beta) + d_\tau^2(F_\beta; Re)$ w.r.t. β . The optimal value (or range of optimal values) for β is where the curve has its minimum.

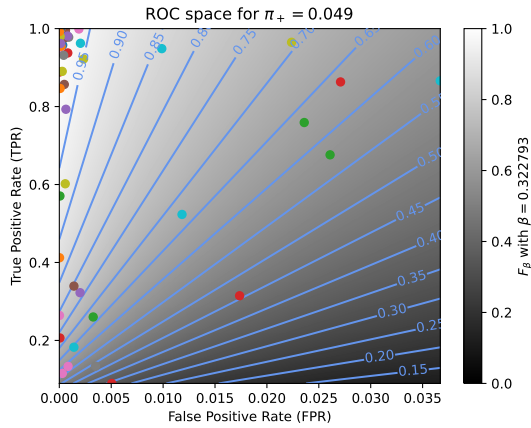


(e) Linear projection (PCA) of the manifold of the rankings induced by the F_β scores. The color points indicate the precision, the recall, F_1 , $SIVF$, as well as the optimal tradeoff. The optimal tradeoff is at the same distance of the two extremities when the distance is measured along the manifold, with Kendall's distance d_τ .

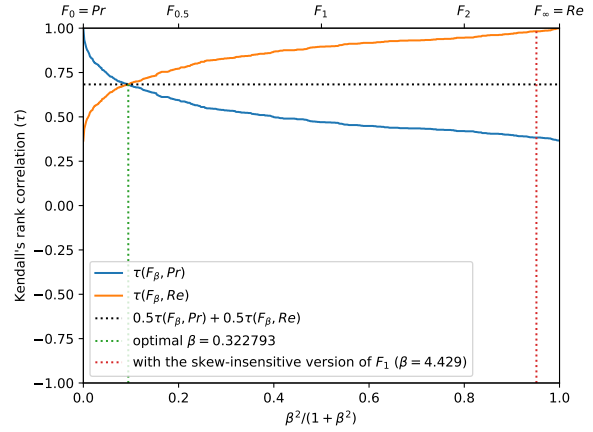


(f) The degree of optimality $\mathcal{O}(\beta)$ w.r.t. β . It is the probability to optimally ordering a pair of classifiers (BGS methods) given that it is not trivial (*i.e.*, that Pr and Re are in contradiction). The optimal value (or range of optimal values) for β is where the curve reaches 100%.

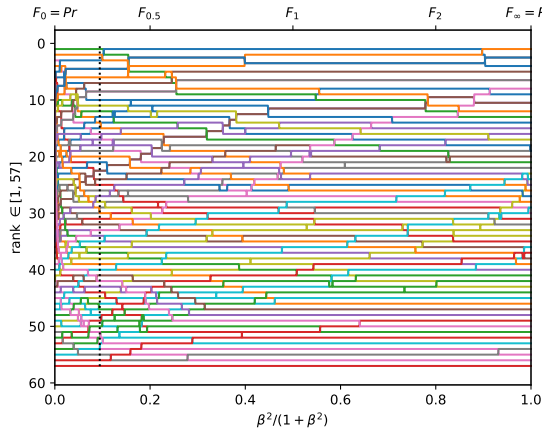
Figure A.3.28. Ranking of 57 BGS methods evaluated on the video "parking" ($\pi_+ = 0.0773$).



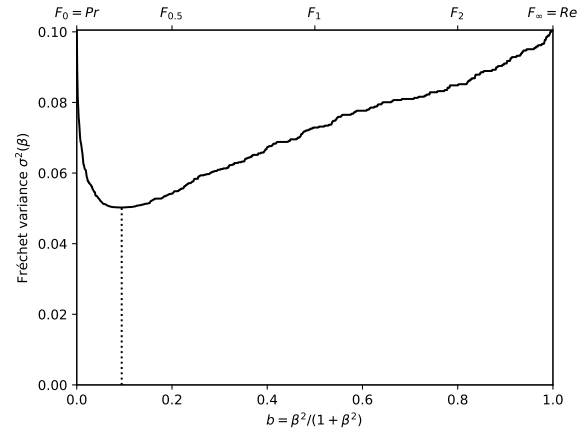
(a) The performances of 57 classifiers (BGS methods) depicted as points in the ROC space, with the isometrics of the optimal tradeoff score, from the ranking point of view, between precision and recall. See Eq. (12).



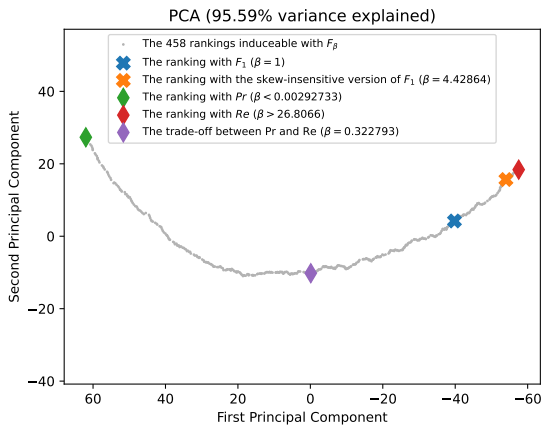
(b) The rank correlations $\tau(F_\beta; Pr)$ and $\tau(F_\beta; Re)$ w.r.t. β . The optimal value (or range of optimal values) for β is where the two curves intersect.



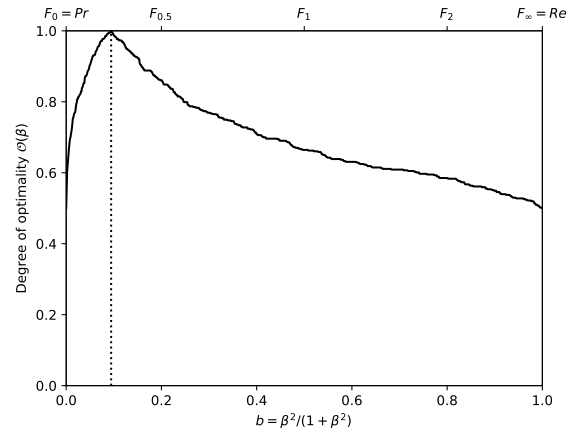
(c) The ranks of each classifier w.r.t. β . The optimal value (or range of optimal values) for β , shown here by the vertical line, is such that the number of swaps on its left is equal to the number of swaps on its right.



(d) The Fréchet variance $\sigma^2(\beta) = d_\tau^2(Pr; F_\beta) + d_\tau^2(F_\beta; Re)$ w.r.t. β . The optimal value (or range of optimal values) for β is where the curve has its minimum.

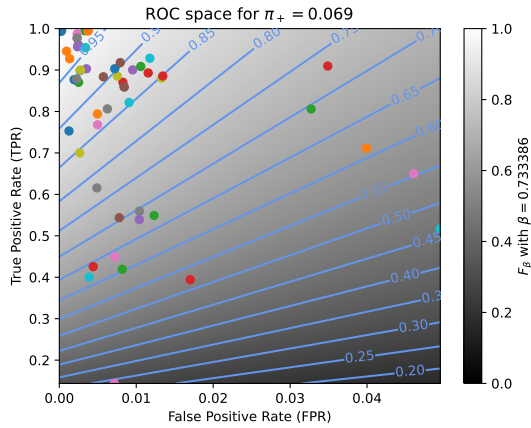


(e) Linear projection (PCA) of the manifold of the rankings induced by the F_β scores. The color points indicate the precision, the recall, F_1 , $SIVF$, as well as the optimal tradeoff. The optimal tradeoff is at the same distance of the two extremities when the distance is measured along the manifold, with Kendall's distance d_+ .

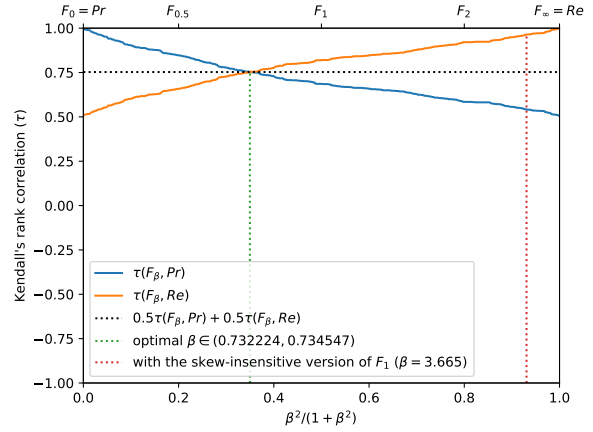


(f) The degree of optimality $\mathcal{O}(\beta)$ w.r.t. β . It is the probability to optimally ordering a pair of classifiers (BGS methods) given that it is not trivial (*i.e.*, that Pr and Re are in contradiction). The optimal value (or range of optimal values) for β is where the curve reaches 100%.

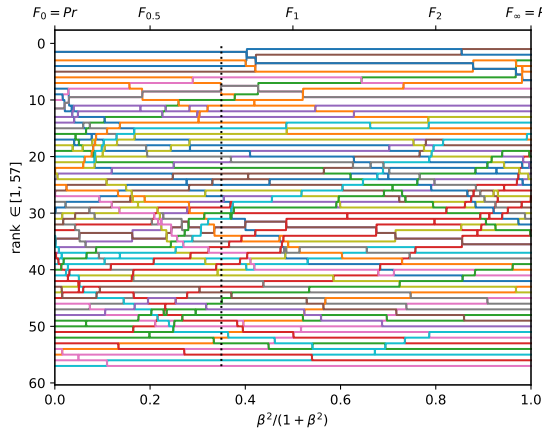
Figure A.3.29. Ranking of 57 BGS methods evaluated on the video "streetLight" ($\pi_+ = 0.0485$).



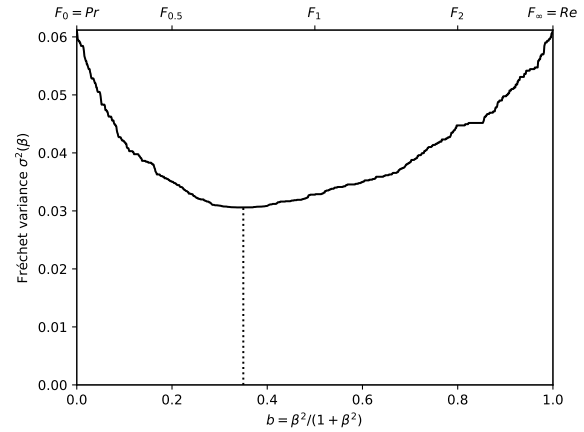
(a) The performances of 57 classifiers (BGS methods) depicted as points in the ROC space, with the isometrics of the optimal tradeoff score, from the ranking point of view, between precision and recall. See Eq. (12).



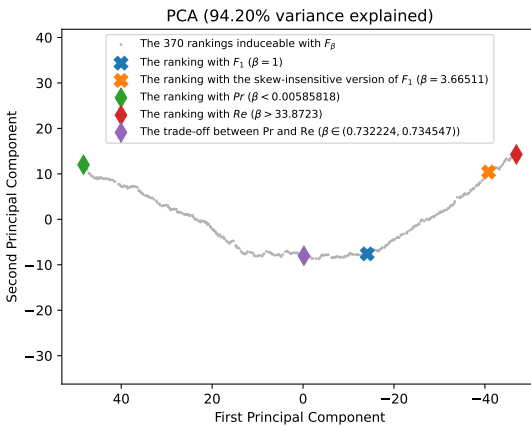
(b) The rank correlations $\tau(F_\beta; Pr)$ and $\tau(F_\beta; Re)$ w.r.t. β . The optimal value (or range of optimal values) for β is where the two curves intersect.



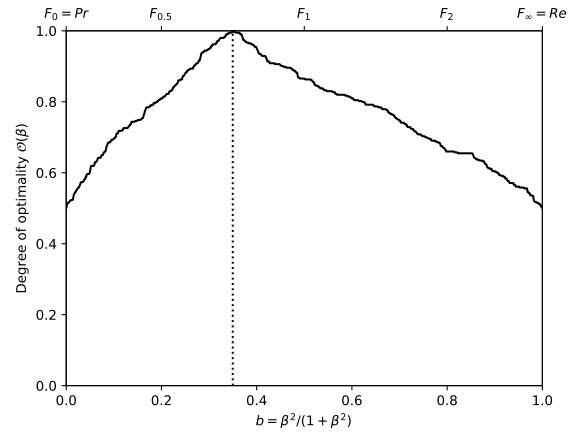
(c) The ranks of each classifier w.r.t. β . The optimal value (or range of optimal values) for β , shown here by the vertical line, is such that the number of swaps on its left is equal to the number of swaps on its right.



(d) The Fréchet variance $\sigma^2(\beta) = d_\tau^2(Pr; F_\beta) + d_\tau^2(F_\beta; Re)$ w.r.t. β . The optimal value (or range of optimal values) for β is where the curve has its minimum.

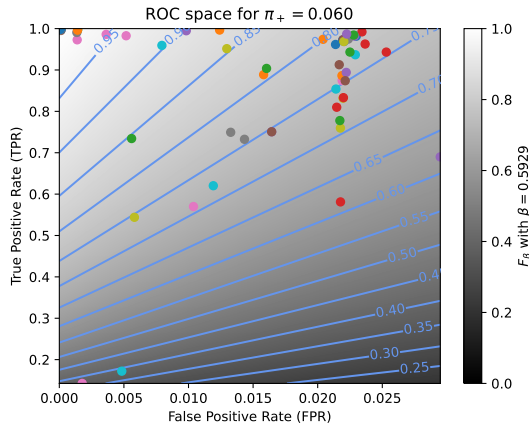


(e) Linear projection (PCA) of the manifold of the rankings induced by the F_β scores. The color points indicate the precision, the recall, F_1 , $SIVF$, as well as the optimal tradeoff. The optimal tradeoff is at the same distance of the two extremities when the distance is measured along the manifold, with Kendall's distance d_+ .

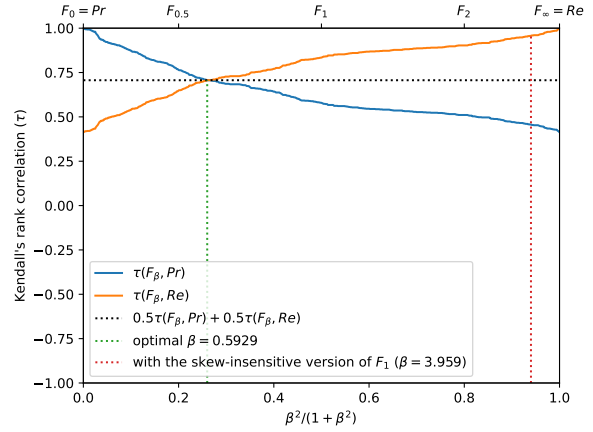


(f) The degree of optimality $\mathcal{O}(\beta)$ w.r.t. β . It is the probability to optimally ordering a pair of classifiers (BGS methods) given that it is not trivial (*i.e.*, that Pr and Re are in contradiction). The optimal value (or range of optimal values) for β is where the curve reaches 100%.

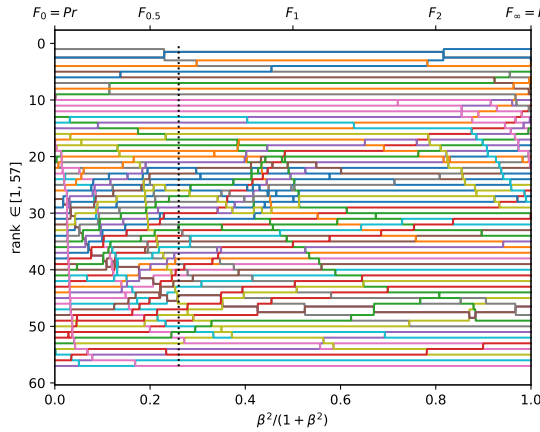
Figure A.3.30. Ranking of 57 BGS methods evaluated on the video "copyMachine" ($\pi_+ = 0.0693$).



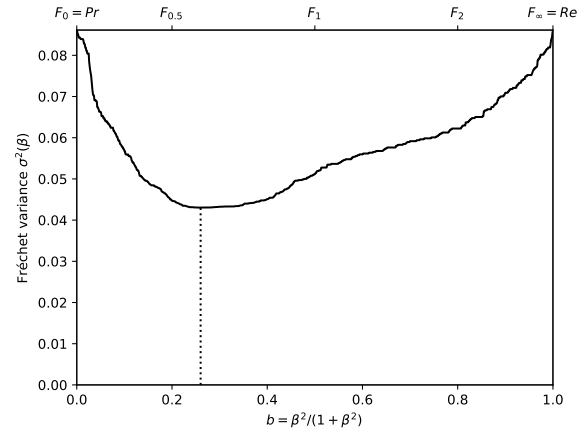
(a) The performances of 57 classifiers (BGS methods) depicted as points in the ROC space, with the isometrics of the optimal tradeoff score, from the ranking point of view, between precision and recall. See Eq. (12).



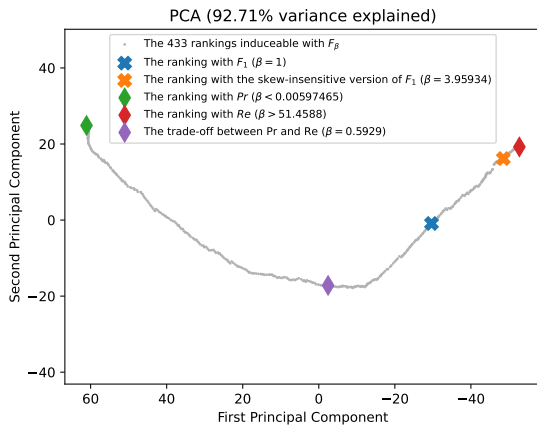
(b) The rank correlations $\tau(F_\beta; Pr)$ and $\tau(F_\beta; Re)$ w.r.t. β . The optimal value (or range of optimal values) for β is where the two curves intersect.



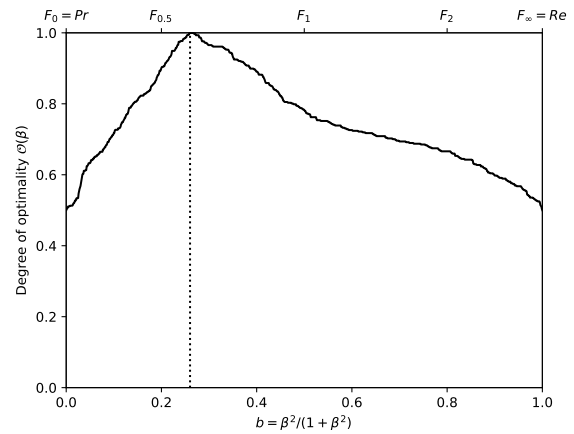
(c) The ranks of each classifier w.r.t. β . The optimal value (or range of optimal values) for β , shown here by the vertical line, is such that the number of swaps on its left is equal to the number of swaps on its right.



(d) The Fréchet variance $\sigma^2(\beta) = d_\tau^2(Pr; F_\beta) + d_\tau^2(F_\beta; Re)$ w.r.t. β . The optimal value (or range of optimal values) for β is where the curve has its minimum.

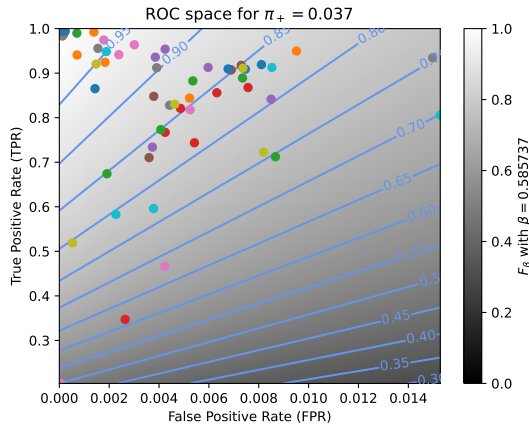


(e) Linear projection (PCA) of the manifold of the rankings induced by the F_β scores. The color points indicate the precision, the recall, F_1 , $SIVF$, as well as the optimal tradeoff. The optimal tradeoff is at the same distance of the two extremities when the distance is measured along the manifold, with Kendall's distance d_τ .

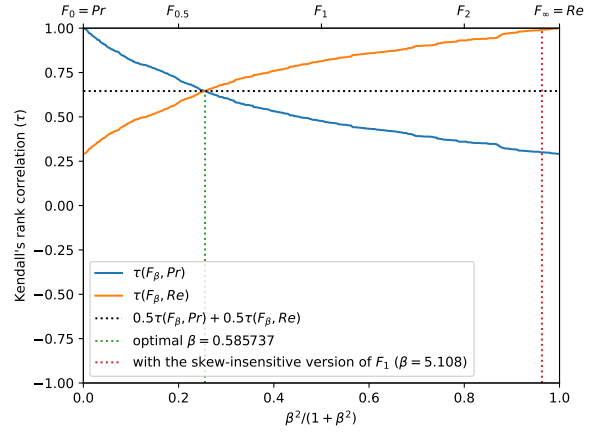


(f) The degree of optimality $\mathcal{O}(\beta)$ w.r.t. β . It is the probability to optimally ordering a pair of classifiers (BGS methods) given that it is not trivial (*i.e.*, that Pr and Re are in contradiction). The optimal value (or range of optimal values) for β is where the curve reaches 100%.

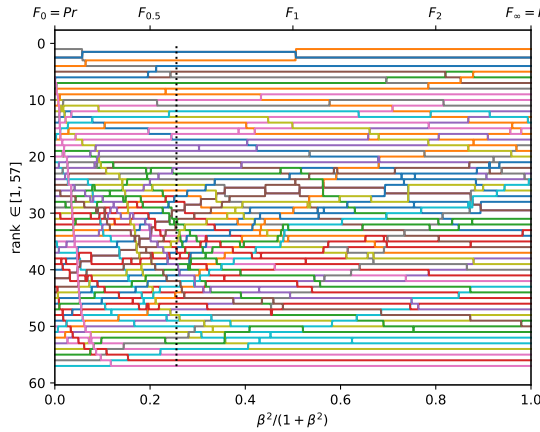
Figure A.3.31. Ranking of 57 BGS methods evaluated on the video "bungalows" ($\pi_+ = 0.0600$).



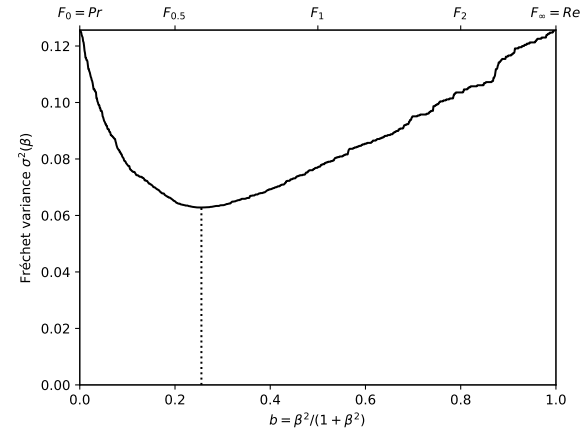
(a) The performances of 57 classifiers (BGS methods) depicted as points in the ROC space, with the isometrics of the optimal tradeoff score, from the ranking point of view, between precision and recall. See Eq. (12).



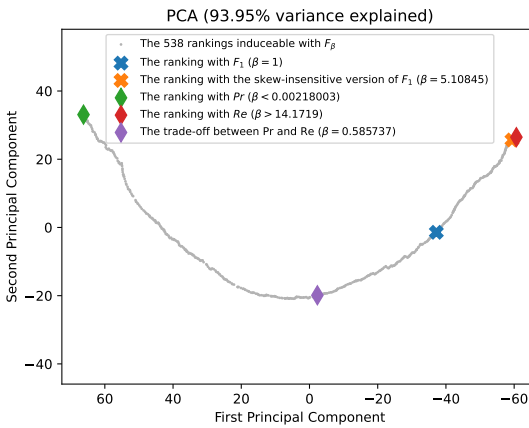
(b) The rank correlations $\tau(F_\beta; Pr)$ and $\tau(F_\beta; Re)$ w.r.t. β . The optimal value (or range of optimal values) for β is where the two curves intersect.



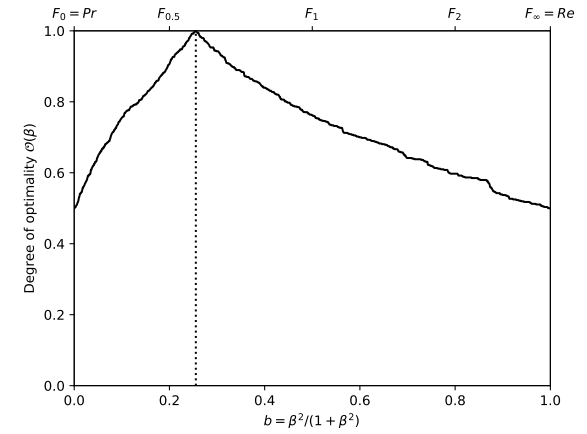
(c) The ranks of each classifier w.r.t. β . The optimal value (or range of optimal values) for β , shown here by the vertical line, is such that the number of swaps on its left is equal to the number of swaps on its right.



(d) The Fréchet variance $\sigma^2(\beta) = d_\tau^2(Pr; F_\beta) + d_\tau^2(F_\beta; Re)$ w.r.t. β . The optimal value (or range of optimal values) for β is where the curve has its minimum.

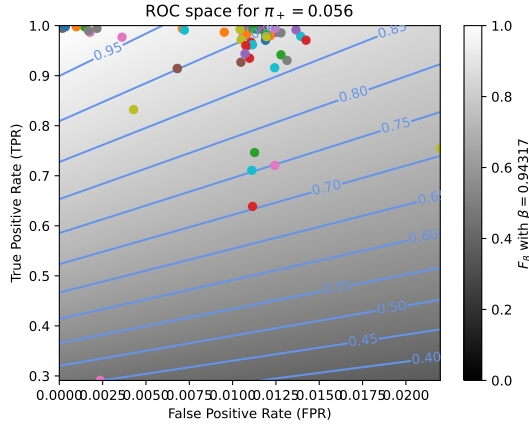


(e) Linear projection (PCA) of the manifold of the rankings induced by the F_β scores. The color points indicate the precision, the recall, F_1 , $SIVF$, as well as the optimal tradeoff. The optimal tradeoff is at the same distance of the two extremities when the distance is measured along the manifold, with Kendall's distance d_+ .

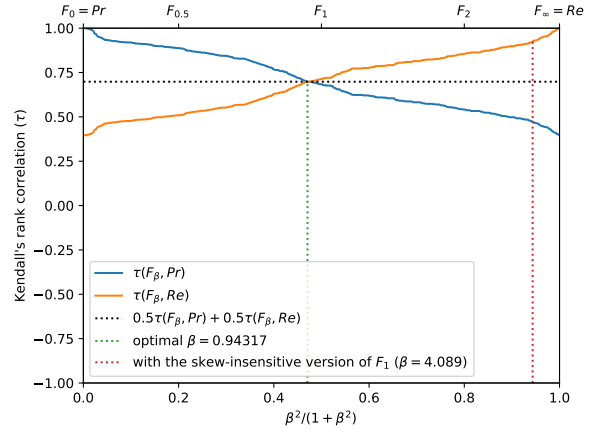


(f) The degree of optimality $\mathcal{O}(\beta)$ w.r.t. β . It is the probability to optimally ordering a pair of classifiers (BGS methods) given that it is not trivial (*i.e.*, that Pr and Re are in contradiction). The optimal value (or range of optimal values) for β is where the curve reaches 100%.

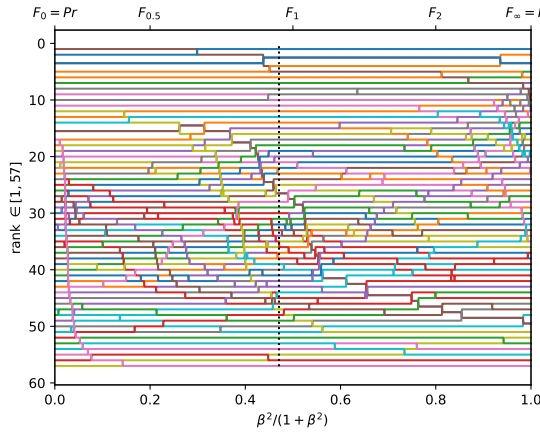
Figure A.3.32. Ranking of 57 BGS methods evaluated on the video "busStation" ($\pi_+ = 0.0369$).



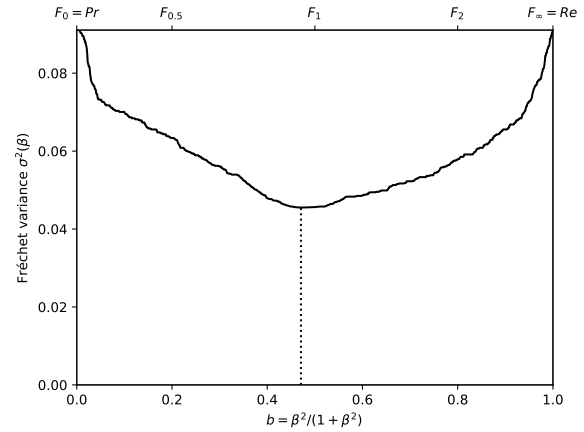
(a) The performances of 57 classifiers (BGS methods) depicted as points in the ROC space, with the isometrics of the optimal tradeoff score, from the ranking point of view, between precision and recall. See Eq. (12).



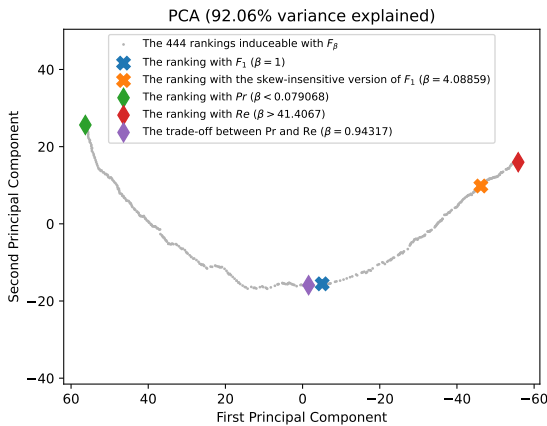
(b) The rank correlations $\tau(F_\beta; Pr)$ and $\tau(F_\beta; Re)$ w.r.t. β . The optimal value (or range of optimal values) for β is where the two curves intersect.



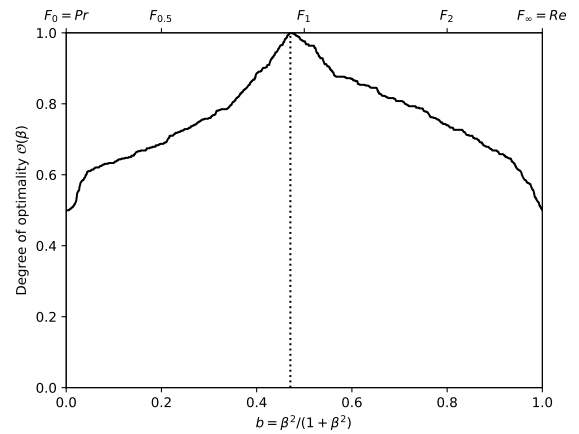
(c) The ranks of each classifier w.r.t. β . The optimal value (or range of optimal values) for β , shown here by the vertical line, is such that the number of swaps on its left is equal to the number of swaps on its right.



(d) The Fréchet variance $\sigma^2(\beta) = d_\tau^2(Pr; F_\beta) + d_\tau^2(F_\beta; Re)$ w.r.t. β . The optimal value (or range of optimal values) for β is where the curve has its minimum.

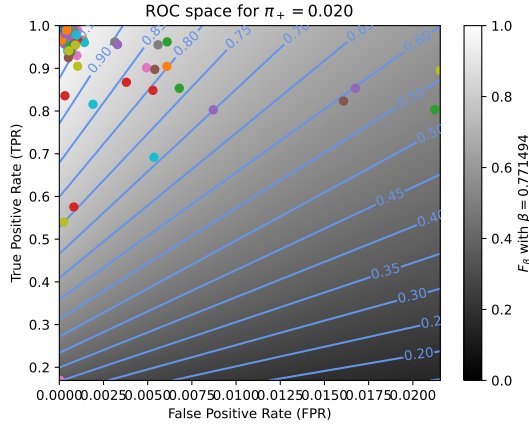


(e) Linear projection (PCA) of the manifold of the rankings induced by the F_β scores. The color points indicate the precision, the recall, F_1 , $SIVF$, as well as the optimal tradeoff. The optimal tradeoff is at the same distance of the two extremities when the distance is measured along the manifold, with Kendall's distance d_+ .

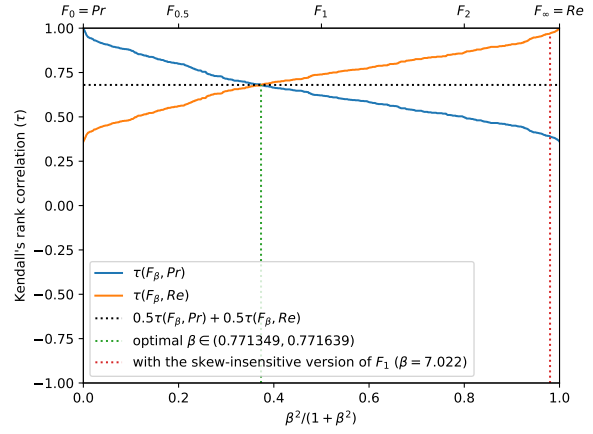


(f) The degree of optimality $\mathcal{O}(\beta)$ w.r.t. β . It is the probability to optimally ordering a pair of classifiers (BGS methods) given that it is not trivial (*i.e.*, that Pr and Re are in contradiction). The optimal value (or range of optimal values) for β is where the curve reaches 100%.

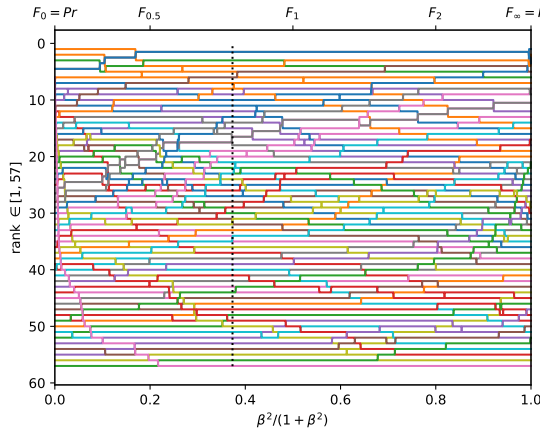
Figure A.3.33. Ranking of 57 BGS methods evaluated on the video "peopleInShade" ($\pi_+ = 0.0564$).



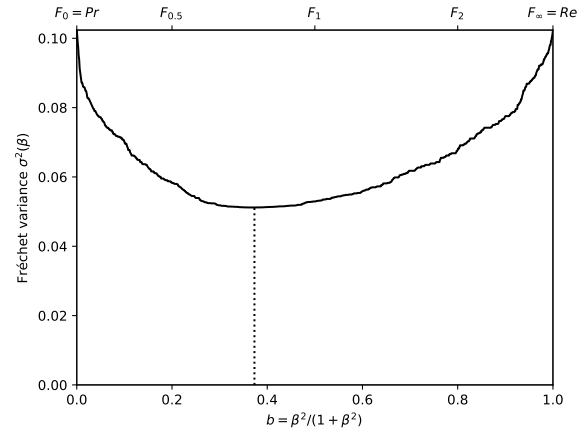
(a) The performances of 57 classifiers (BGS methods) depicted as points in the ROC space, with the isometrics of the optimal tradeoff score, from the ranking point of view, between precision and recall. See Eq. (12).



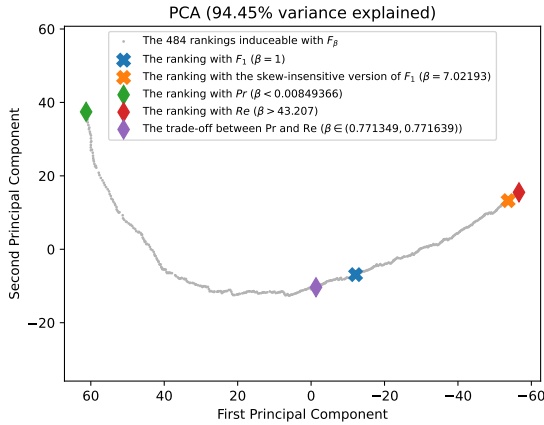
(b) The rank correlations $\tau(F_\beta; Pr)$ and $\tau(F_\beta; Re)$ w.r.t. β . The optimal value (or range of optimal values) for β is where the two curves intersect.



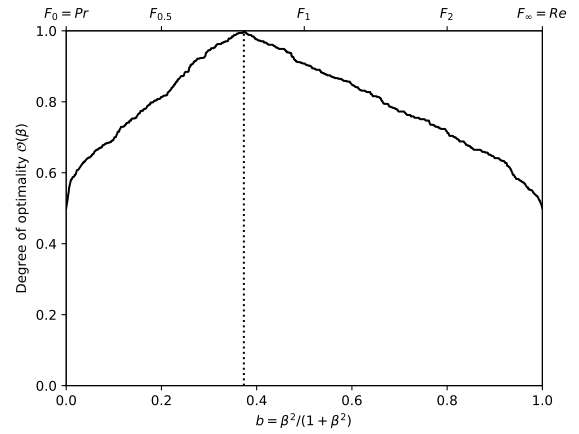
(c) The ranks of each classifier w.r.t. β . The optimal value (or range of optimal values) for β , shown here by the vertical line, is such that the number of swaps on its left is equal to the number of swaps on its right.



(d) The Fréchet variance $\sigma^2(\beta) = d_\tau^2(Pr; F_\beta) + d_\tau^2(F_\beta; Re)$ w.r.t. β . The optimal value (or range of optimal values) for β is where the curve has its minimum.

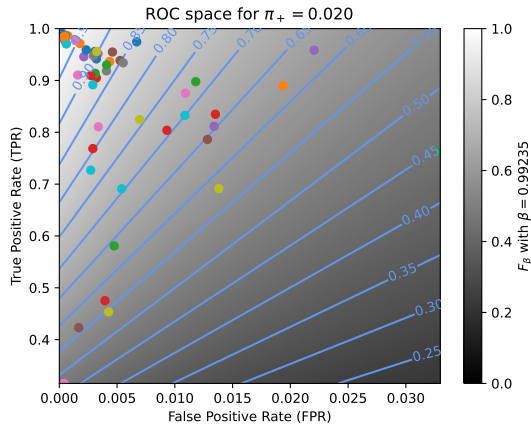


(e) Linear projection (PCA) of the manifold of the rankings induced by the F_β scores. The color points indicate the precision, the recall, F_1 , $SIVF$, as well as the optimal tradeoff. The optimal tradeoff is at the same distance of the two extremities when the distance is measured along the manifold, with Kendall's distance d_+ .

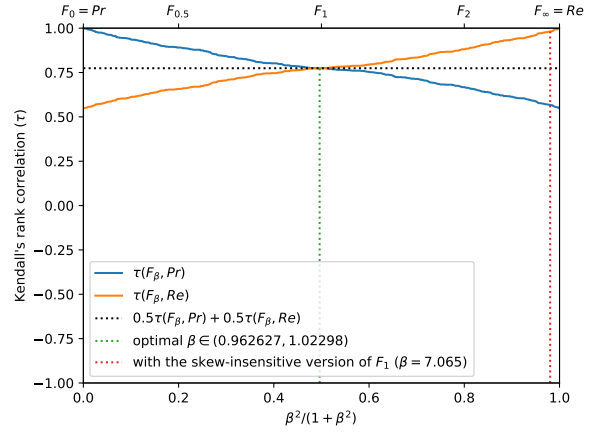


(f) The degree of optimality $\mathcal{O}(\beta)$ w.r.t. β . It is the probability to optimally ordering a pair of classifiers (BGS methods) given that it is not trivial (*i.e.*, that Pr and Re are in contradiction). The optimal value (or range of optimal values) for β is where the curve reaches 100%.

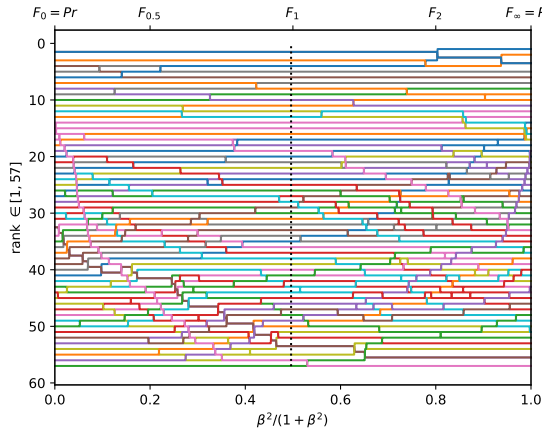
Figure A.3.34. Ranking of 57 BGS methods evaluated on the video "backdoor" ($\pi_+ = 0.0199$).



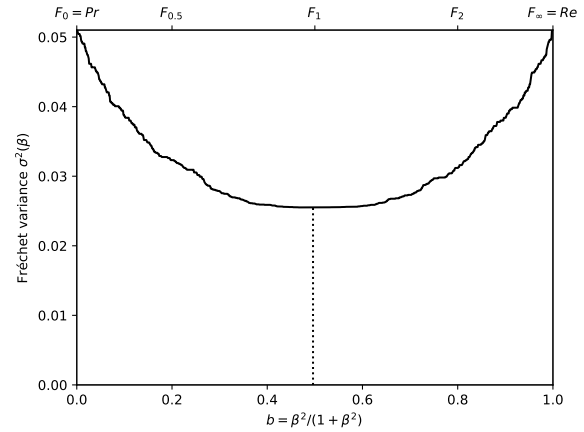
(a) The performances of 57 classifiers (BGS methods) depicted as points in the ROC space, with the isometrics of the optimal tradeoff score, from the ranking point of view, between precision and recall. See Eq. (12).



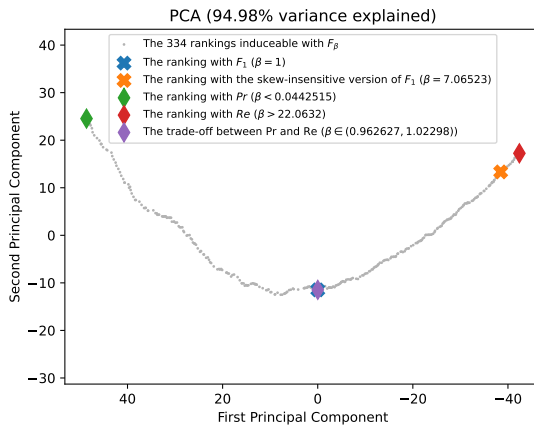
(b) The rank correlations $\tau(F_\beta; Pr)$ and $\tau(F_\beta; Re)$ w.r.t. β . The optimal value (or range of optimal values) for β is where the two curves intersect.



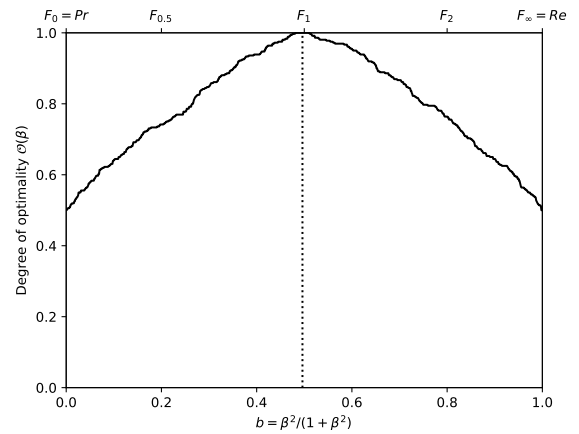
(c) The ranks of each classifier w.r.t. β . The optimal value (or range of optimal values) for β , shown here by the vertical line, is such that the number of swaps on its left is equal to the number of swaps on its right.



(d) The Fréchet variance $\sigma^2(\beta) = d_\tau^2(Pr; F_\beta) + d_\tau^2(F_\beta; Re)$ w.r.t. β . The optimal value (or range of optimal values) for β is where the curve has its minimum.

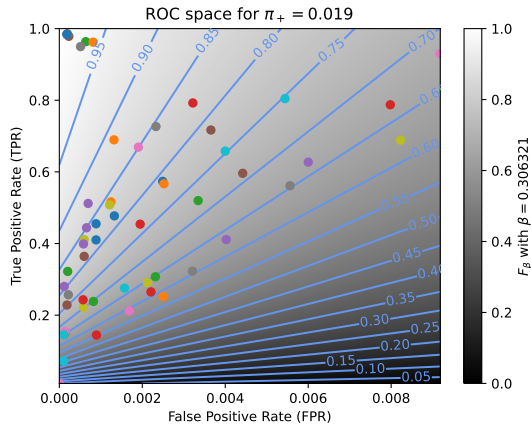


(e) Linear projection (PCA) of the manifold of the rankings induced by the F_β scores. The color points indicate the precision, the recall, F_1 , $SIVF$, as well as the optimal tradeoff. The optimal tradeoff is at the same distance of the two extremities when the distance is measured along the manifold, with Kendall's distance d_+ .

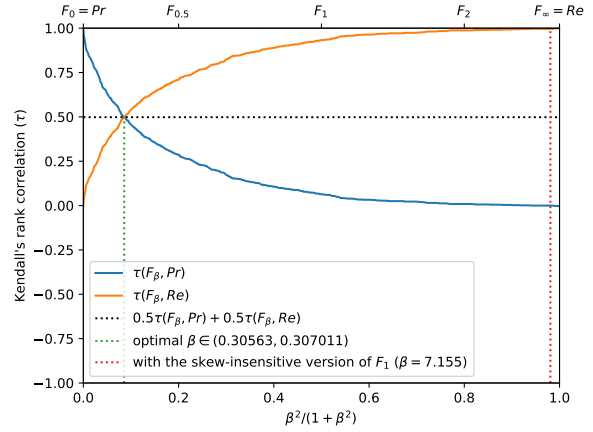


(f) The degree of optimality $\mathcal{O}(\beta)$ w.r.t. β . It is the probability to optimally ordering a pair of classifiers (BGS methods) given that it is not trivial (*i.e.*, that Pr and Re are in contradiction). The optimal value (or range of optimal values) for β is where the curve reaches 100%.

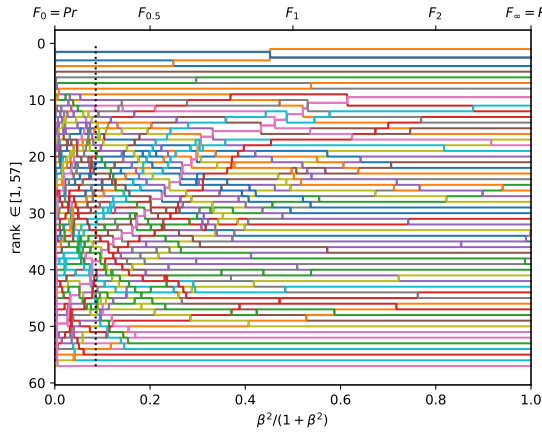
Figure A.3.35. Ranking of 57 BGS methods evaluated on the video "cubicle" ($\pi_+ = 0.0196$).



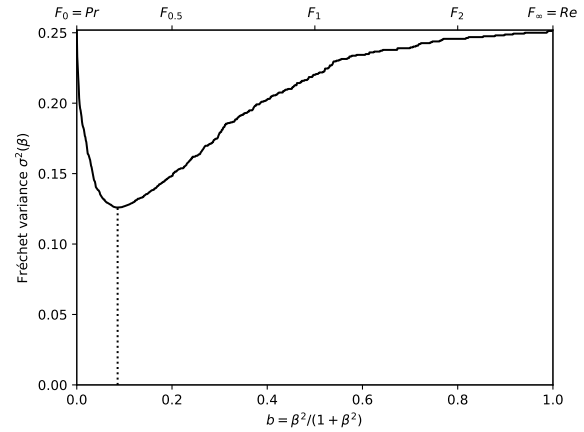
(a) The performances of 57 classifiers (BGS methods) depicted as points in the ROC space, with the isometrics of the optimal tradeoff score, from the ranking point of view, between precision and recall. See Eq. (12).



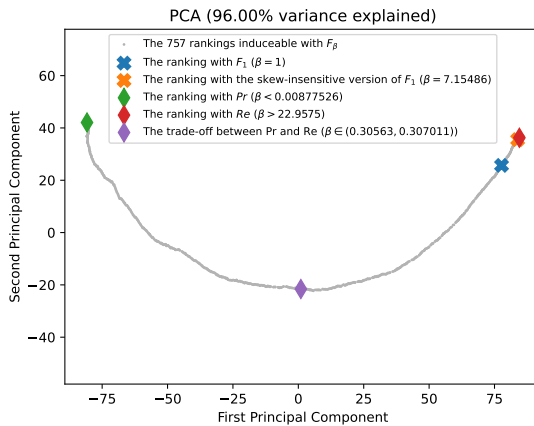
(b) The rank correlations $\tau(F_\beta; Pr)$ and $\tau(F_\beta; Re)$ w.r.t. β . The optimal value (or range of optimal values) for β is where the two curves intersect.



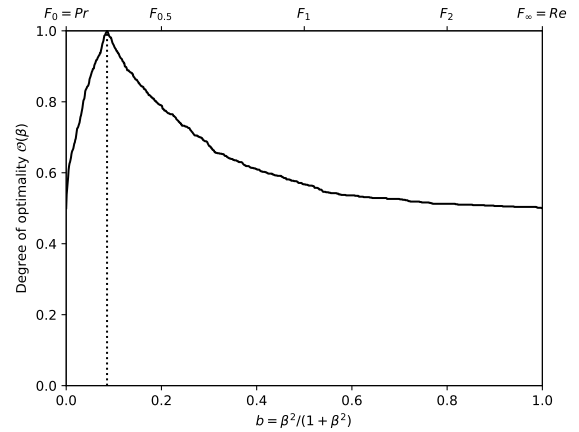
(c) The ranks of each classifier w.r.t. β . The optimal value (or range of optimal values) for β , shown here by the vertical line, is such that the number of swaps on its left is equal to the number of swaps on its right.



(d) The Fréchet variance $\sigma^2(\beta) = d_\tau^2(Pr; F_\beta) + d_\tau^2(F_\beta; Re)$ w.r.t. β . The optimal value (or range of optimal values) for β is where the curve has its minimum.

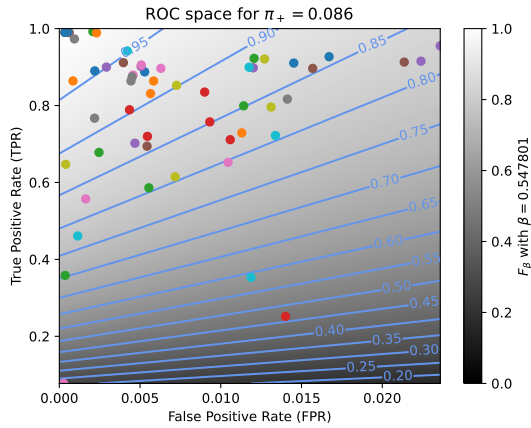


(e) Linear projection (PCA) of the manifold of the rankings induced by the F_β scores. The color points indicate the precision, the recall, F_1 , $SIVF$, as well as the optimal tradeoff. The optimal tradeoff is at the same distance of the two extremities when the distance is measured along the manifold, with Kendall's distance d_+ .

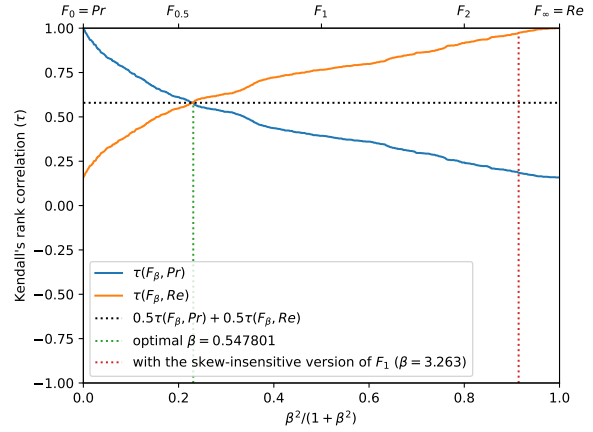


(f) The degree of optimality $\mathcal{O}(\beta)$ w.r.t. β . It is the probability to optimally ordering a pair of classifiers (BGS methods) given that it is not trivial (*i.e.*, that Pr and Re are in contradiction). The optimal value (or range of optimal values) for β is where the curve reaches 100%.

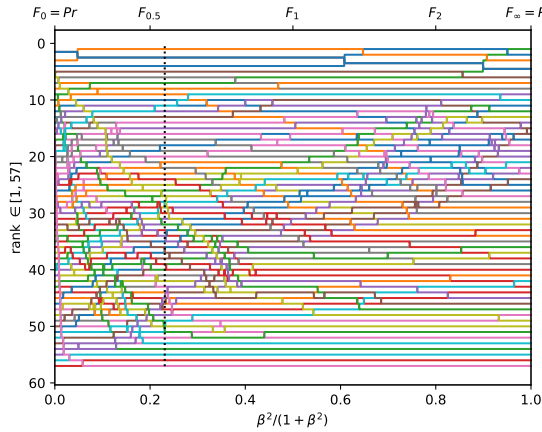
Figure A.3.36. Ranking of 57 BGS methods evaluated on the video "lakeSide" ($\pi_+ = 0.0192$).



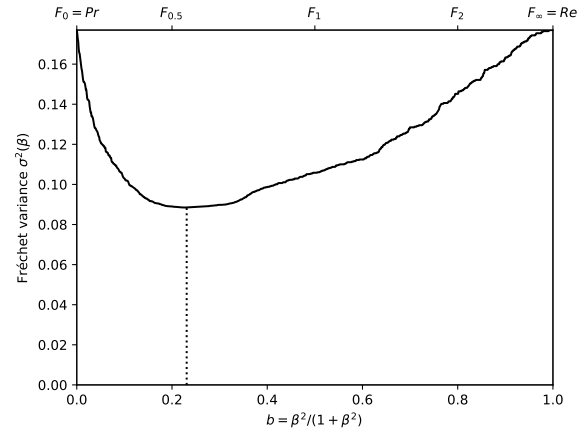
(a) The performances of 57 classifiers (BGS methods) depicted as points in the ROC space, with the isometrics of the optimal tradeoff score, from the ranking point of view, between precision and recall. See Eq. (12).



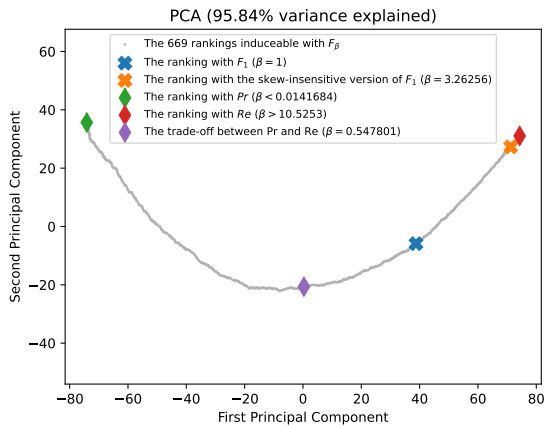
(b) The rank correlations $\tau(F_\beta; Pr)$ and $\tau(F_\beta; Re)$ w.r.t. β . The optimal value (or range of optimal values) for β is where the two curves intersect.



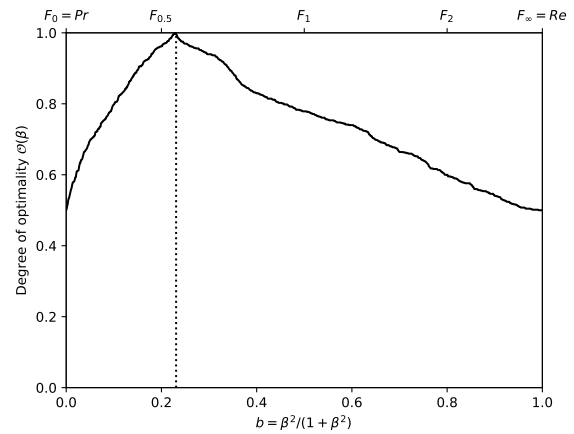
(c) The ranks of each classifier w.r.t. β . The optimal value (or range of optimal values) for β , shown here by the vertical line, is such that the number of swaps on its left is equal to the number of swaps on its right.



(d) The Fréchet variance $\sigma^2(\beta) = d_\tau^2(Pr; F_\beta) + d_\tau^2(F_\beta; Re)$ w.r.t. β . The optimal value (or range of optimal values) for β is where the curve has its minimum.

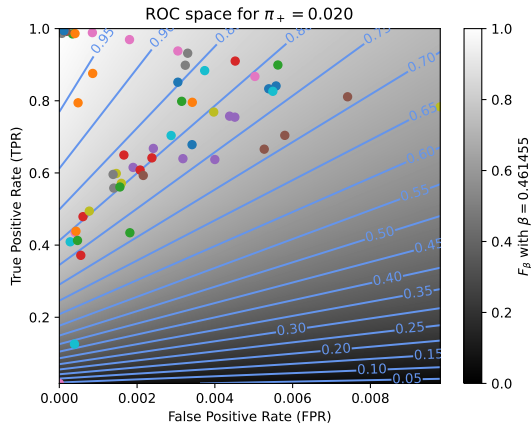


(e) Linear projection (PCA) of the manifold of the rankings induced by the F_β scores. The color points indicate the precision, the recall, F_1 , $SIVF$, as well as the optimal tradeoff. The optimal tradeoff is at the same distance of the two extremities when the distance is measured along the manifold, with Kendall's distance d_+ .

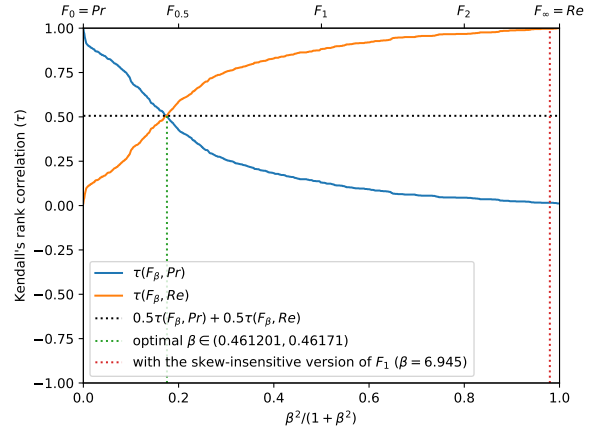


(f) The degree of optimality $\mathcal{O}(\beta)$ w.r.t. β . It is the probability to optimally ordering a pair of classifiers (BGS methods) given that it is not trivial (*i.e.*, that Pr and Re are in contradiction). The optimal value (or range of optimal values) for β is where the curve reaches 100%.

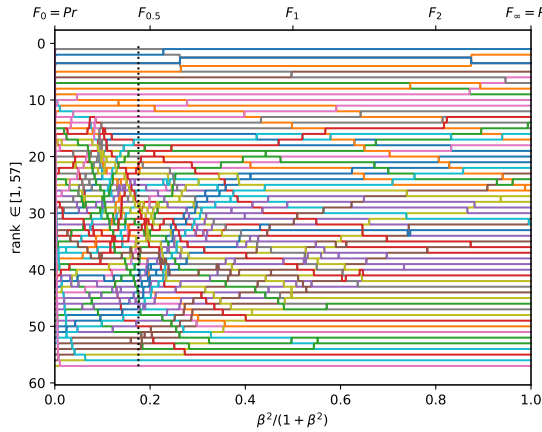
Figure A.3.37. Ranking of 57 BGS methods evaluated on the video "diningRoom" ($\pi_+ = 0.0859$).



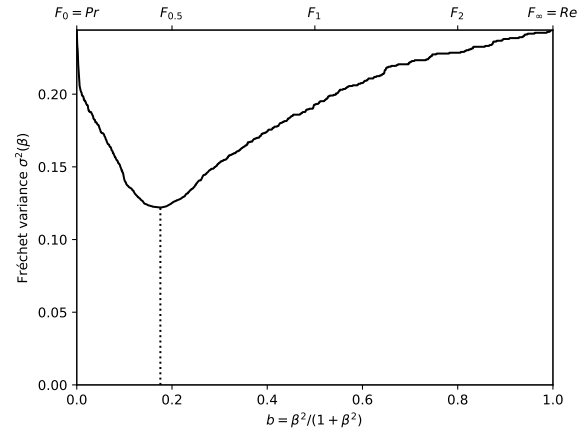
(a) The performances of 57 classifiers (BGS methods) depicted as points in the ROC space, with the isometrics of the optimal tradeoff score, from the ranking point of view, between precision and recall. See Eq. (12).



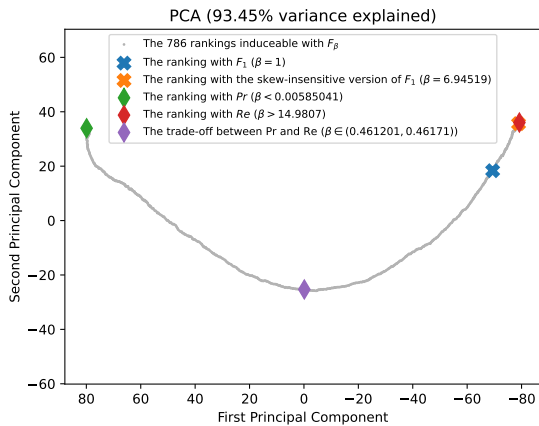
(b) The rank correlations $\tau(F_\beta; Pr)$ and $\tau(F_\beta; Re)$ w.r.t. β . The optimal value (or range of optimal values) for β is where the two curves intersect.



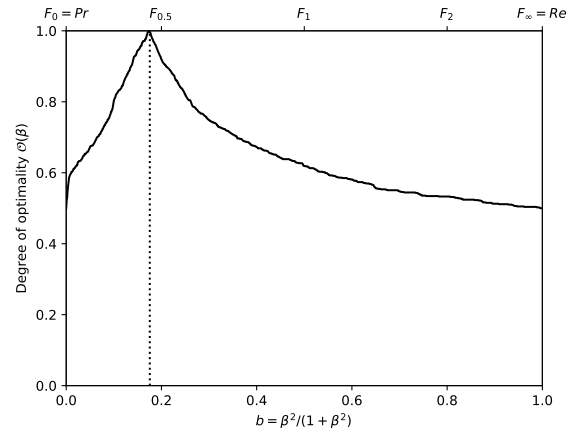
(c) The ranks of each classifier w.r.t. β . The optimal value (or range of optimal values) for β , shown here by the vertical line, is such that the number of swaps on its left is equal to the number of swaps on its right.



(d) The Fréchet variance $\sigma^2(\beta) = d_\tau^2(Pr; F_\beta) + d_\tau^2(F_\beta; Re)$ w.r.t. β . The optimal value (or range of optimal values) for β is where the curve has its minimum.

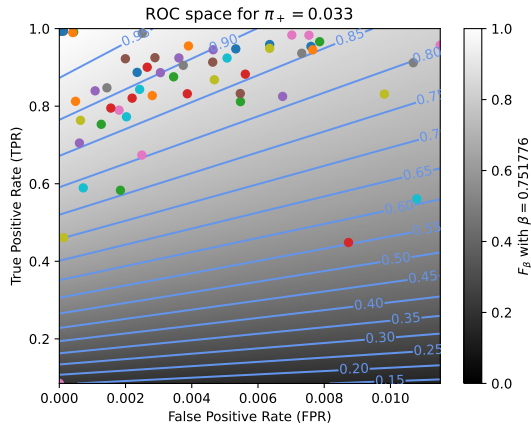


(e) Linear projection (PCA) of the manifold of the rankings induced by the F_β scores. The color points indicate the precision, the recall, F_1 , $SIVF$, as well as the optimal tradeoff. The optimal tradeoff is at the same distance of the two extremities when the distance is measured along the manifold, with Kendall's distance d_* .

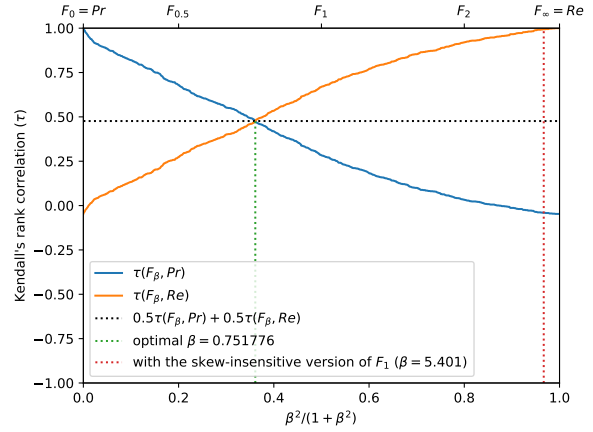


(f) The degree of optimality $\mathcal{O}(\beta)$ w.r.t. β . It is the probability to optimally ordering a pair of classifiers (BGS methods) given that it is not trivial (*i.e.*, that Pr and Re are in contradiction). The optimal value (or range of optimal values) for β is where the curve reaches 100%.

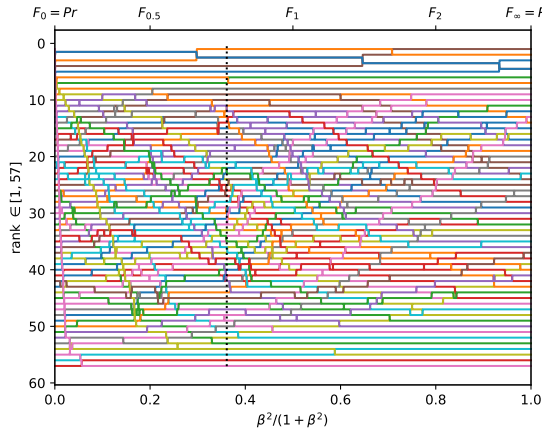
Figure A.3.38. Ranking of 57 BGS methods evaluated on the video "park" ($\pi_+ = 0.0203$).



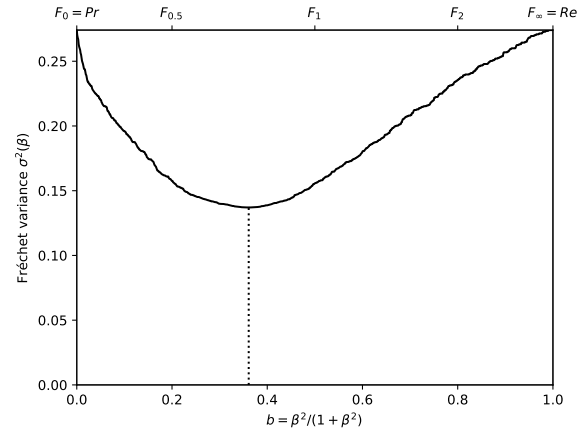
(a) The performances of 57 classifiers (BGS methods) depicted as points in the ROC space, with the isometrics of the optimal tradeoff score, from the ranking point of view, between precision and recall. See Eq. (12).



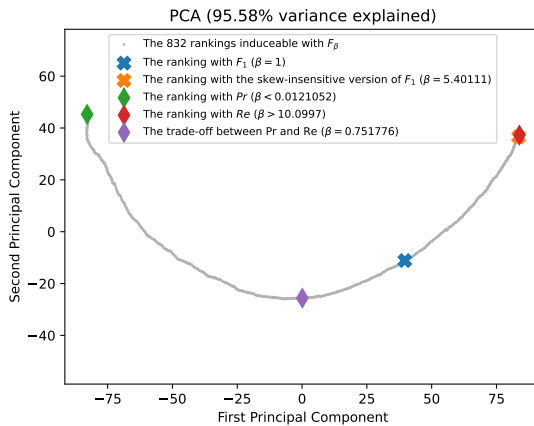
(b) The rank correlations $\tau(F_\beta; Pr)$ and $\tau(F_\beta; Re)$ w.r.t. β . The optimal value (or range of optimal values) for β is where the two curves intersect.



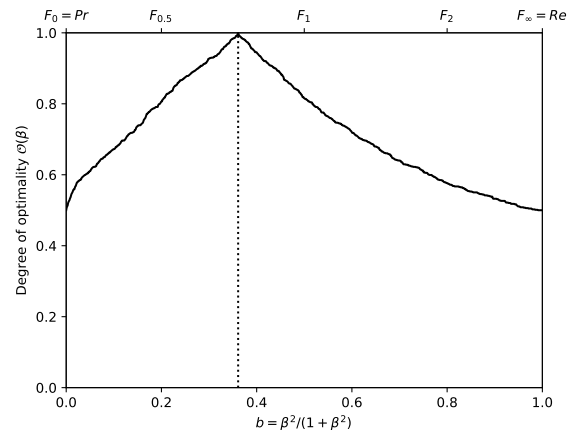
(c) The ranks of each classifier w.r.t. β . The optimal value (or range of optimal values) for β , shown here by the vertical line, is such that the number of swaps on its left is equal to the number of swaps on its right.



(d) The Fréchet variance $\sigma^2(\beta) = d_\tau^2(Pr; F_\beta) + d_\tau^2(F_\beta; Re)$ w.r.t. β . The optimal value (or range of optimal values) for β is where the curve has its minimum.

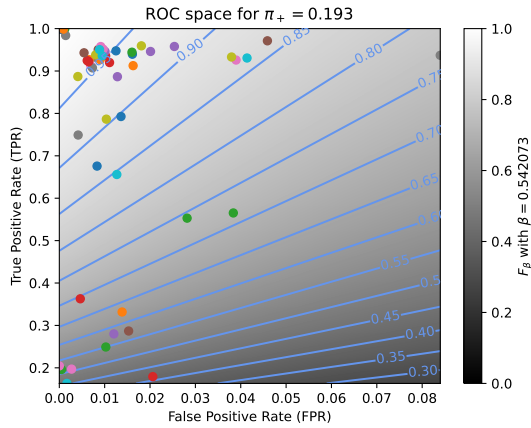


(e) Linear projection (PCA) of the manifold of the rankings induced by the F_β scores. The color points indicate the precision, the recall, F_1 , $SIVF$, as well as the optimal tradeoff. The optimal tradeoff is at the same distance of the two extremities when the distance is measured along the manifold, with Kendall's distance d_* .

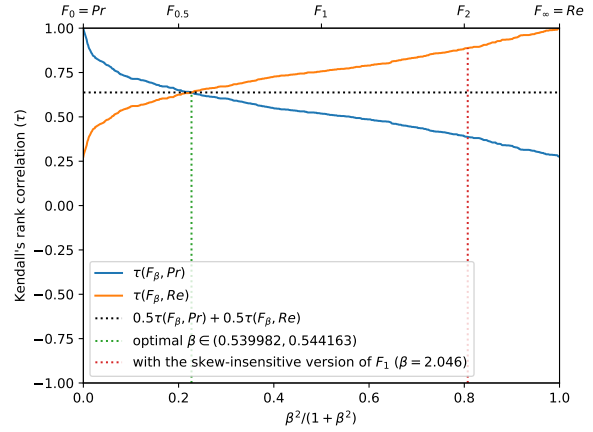


(f) The degree of optimality $\mathcal{O}(\beta)$ w.r.t. β . It is the probability to optimally ordering a pair of classifiers (BGS methods) given that it is not trivial (*i.e.*, that Pr and Re are in contradiction). The optimal value (or range of optimal values) for β is where the curve reaches 100%.

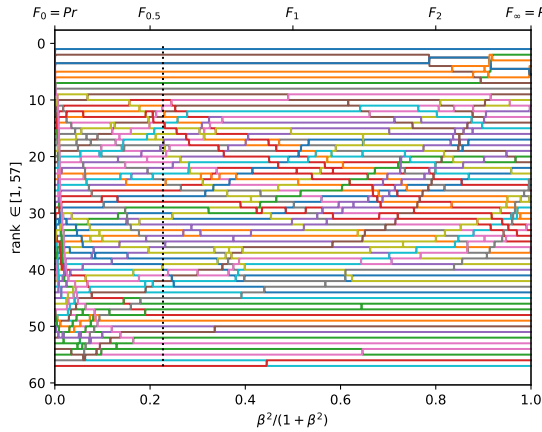
Figure A.3.39. Ranking of 57 BGS methods evaluated on the video "corridor" ($\pi_+ = 0.0331$).



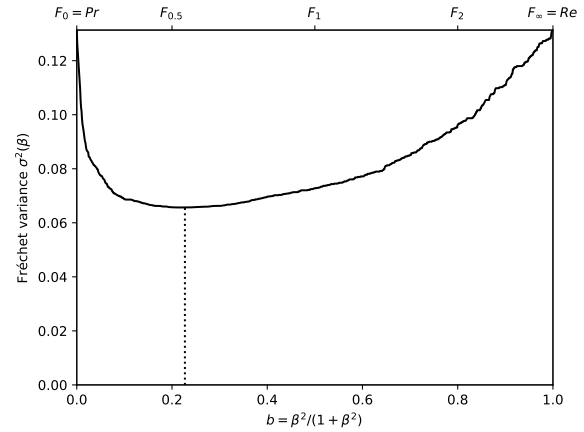
(a) The performances of 57 classifiers (BGS methods) depicted as points in the ROC space, with the isometrics of the optimal tradeoff score, from the ranking point of view, between precision and recall. See Eq. (12).



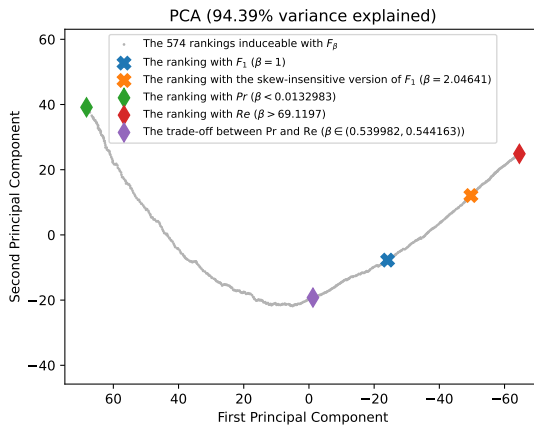
(b) The rank correlations $\tau(F_\beta; Pr)$ and $\tau(F_\beta; Re)$ w.r.t. β . The optimal value (or range of optimal values) for β is where the two curves intersect.



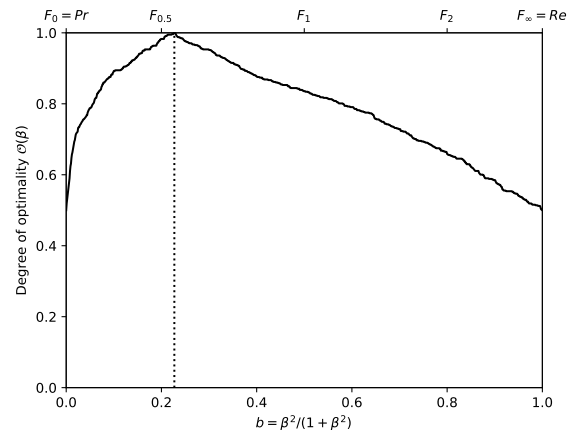
(c) The ranks of each classifier w.r.t. β . The optimal value (or range of optimal values) for β , shown here by the vertical line, is such that the number of swaps on its left is equal to the number of swaps on its right.



(d) The Fréchet variance $\sigma^2(\beta) = d_\tau^2(Pr; F_\beta) + d_\tau^2(F_\beta; Re)$ w.r.t. β . The optimal value (or range of optimal values) for β is where the curve has its minimum.

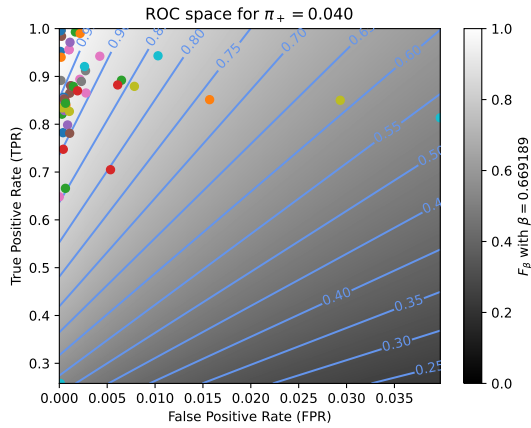


(e) Linear projection (PCA) of the manifold of the rankings induced by the F_β scores. The color points indicate the precision, the recall, F_1 , $SIVF$, as well as the optimal tradeoff. The optimal tradeoff is at the same distance of the two extremities when the distance is measured along the manifold, with Kendall's distance d_+ .

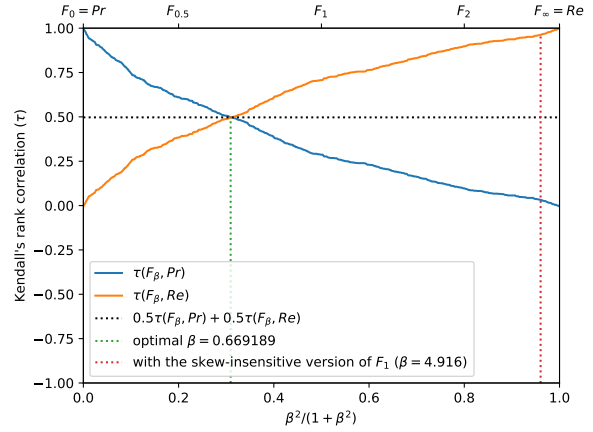


(f) The degree of optimality $\mathcal{O}(\beta)$ w.r.t. β . It is the probability to optimally ordering a pair of classifiers (BGS methods) given that it is not trivial (*i.e.*, that Pr and Re are in contradiction). The optimal value (or range of optimal values) for β is where the curve reaches 100%.

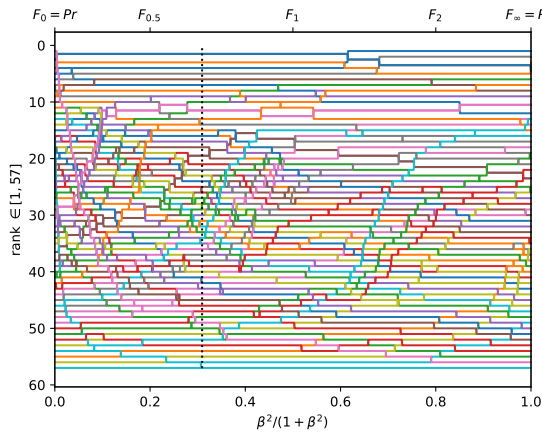
Figure A.3.40. Ranking of 57 BGS methods evaluated on the video "library" ($\pi_+ = 0.1928$).



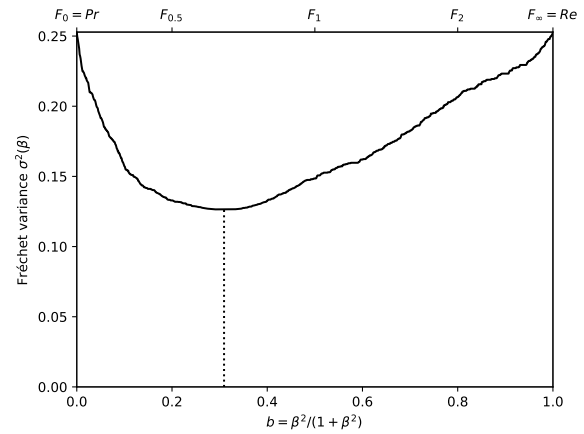
(a) The performances of 57 classifiers (BGS methods) depicted as points in the ROC space, with the isometrics of the optimal tradeoff score, from the ranking point of view, between precision and recall. See Eq. (12).



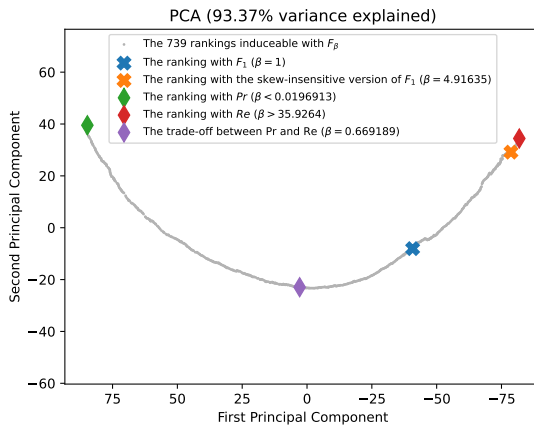
(b) The rank correlations $\tau(F_\beta; Pr)$ and $\tau(F_\beta; Re)$ w.r.t. β . The optimal value (or range of optimal values) for β is where the two curves intersect.



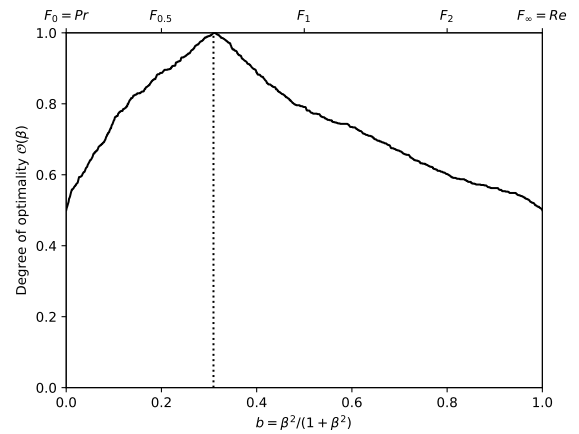
(c) The ranks of each classifier w.r.t. β . The optimal value (or range of optimal values) for β , shown here by the vertical line, is such that the number of swaps on its left is equal to the number of swaps on its right.



(d) The Fréchet variance $\sigma^2(\beta) = d_\tau^2(Pr; F_\beta) + d_\tau^2(F_\beta; Re)$ w.r.t. β . The optimal value (or range of optimal values) for β is where the curve has its minimum.

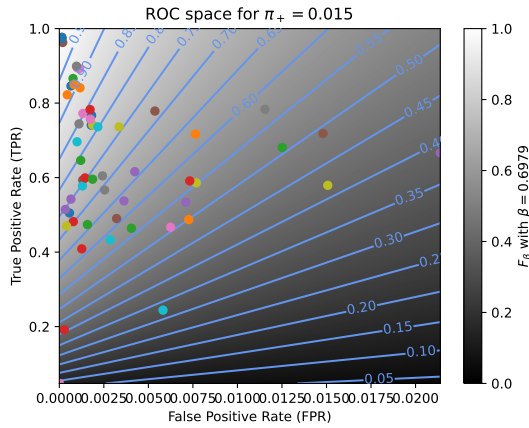


(e) Linear projection (PCA) of the manifold of the rankings induced by the F_β scores. The color points indicate the precision, the recall, F_1 , $SIVF$, as well as the optimal tradeoff. The optimal tradeoff is at the same distance of the two extremities when the distance is measured along the manifold, with Kendall's distance d_+ .

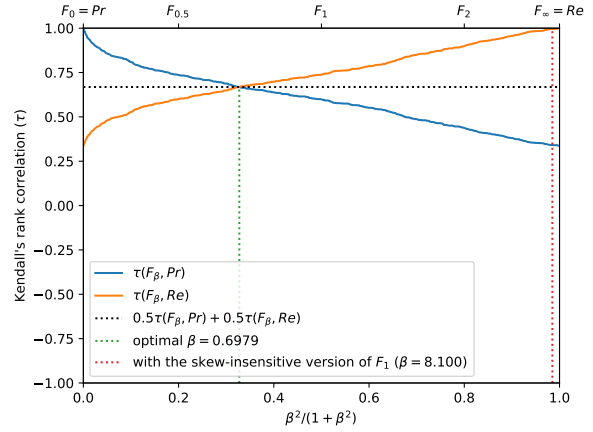


(f) The degree of optimality $\mathcal{O}(\beta)$ w.r.t. β . It is the probability to optimally ordering a pair of classifiers (BGS methods) given that it is not trivial (*i.e.*, that Pr and Re are in contradiction). The optimal value (or range of optimal values) for β is where the curve reaches 100%.

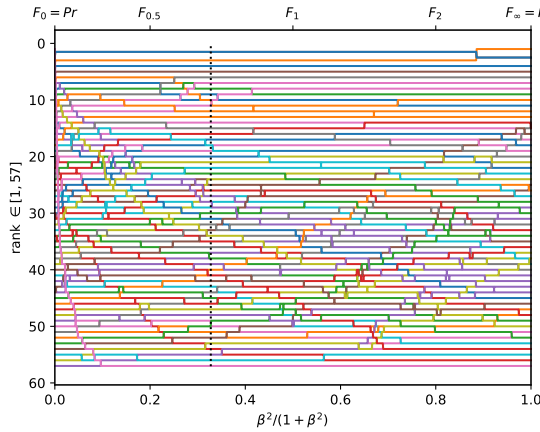
Figure A.3.41. Ranking of 57 BGS methods evaluated on the video "skating" ($\pi_+ = 0.0397$).



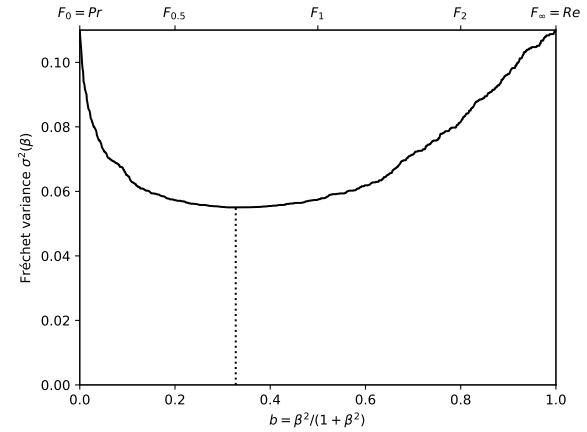
(a) The performances of 57 classifiers (BGS methods) depicted as points in the ROC space, with the isometrics of the optimal tradeoff score, from the ranking point of view, between precision and recall. See Eq. (12).



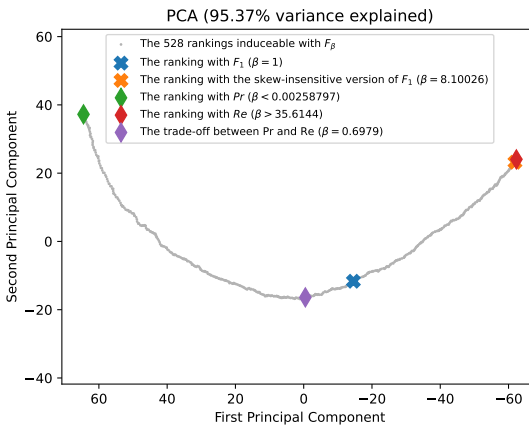
(b) The rank correlations $\tau(F_\beta; Pr)$ and $\tau(F_\beta; Re)$ w.r.t. β . The optimal value (or range of optimal values) for β is where the two curves intersect.



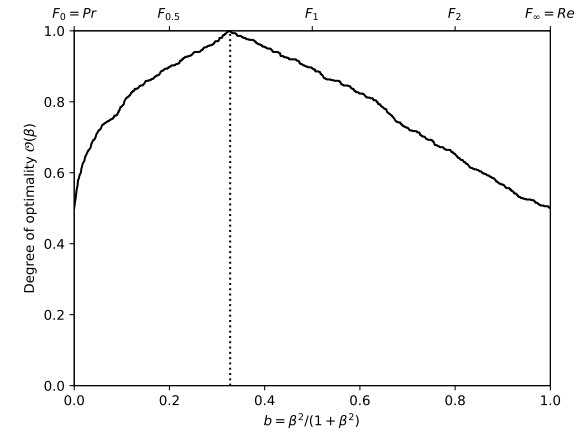
(c) The ranks of each classifier w.r.t. β . The optimal value (or range of optimal values) for β , shown here by the vertical line, is such that the number of swaps on its left is equal to the number of swaps on its right.



(d) The Fréchet variance $\sigma^2(\beta) = d_\tau^2(Pr; F_\beta) + d_\tau^2(F_\beta; Re)$ w.r.t. β . The optimal value (or range of optimal values) for β is where the curve has its minimum.

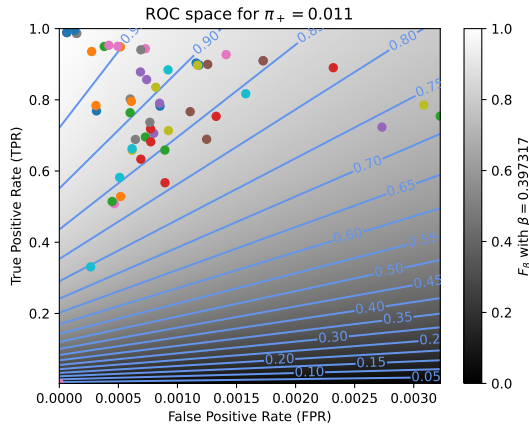


(e) Linear projection (PCA) of the manifold of the rankings induced by the F_β scores. The color points indicate the precision, the recall, F_1 , $SIVF$, as well as the optimal tradeoff. The optimal tradeoff is at the same distance of the two extremities when the distance is measured along the manifold, with Kendall's distance d_* .

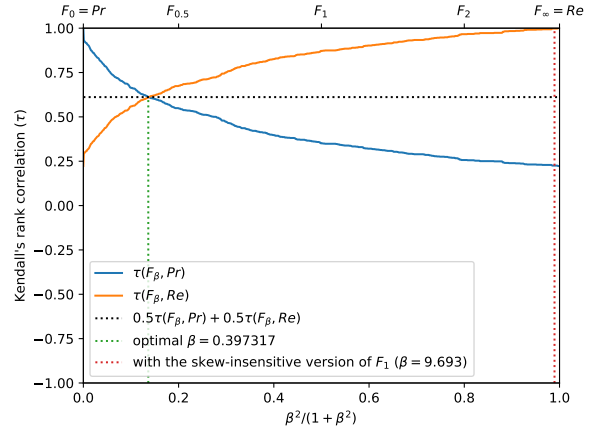


(f) The degree of optimality $\mathcal{O}(\beta)$ w.r.t. β . It is the probability to optimally ordering a pair of classifiers (BGS methods) given that it is not trivial (*i.e.*, that Pr and Re are in contradiction). The optimal value (or range of optimal values) for β is where the curve reaches 100%.

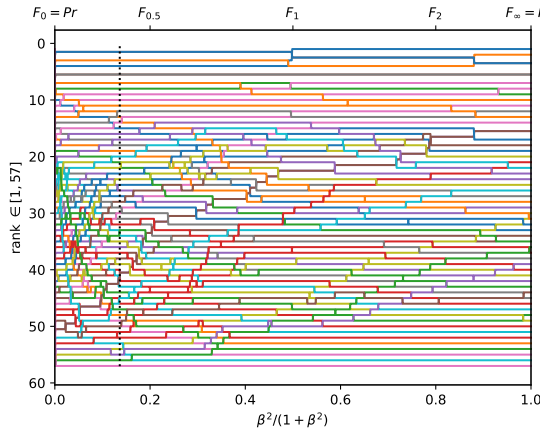
Figure A.3.42. Ranking of 57 BGS methods evaluated on the video "wetSnow" ($\pi_+ = 0.0150$).



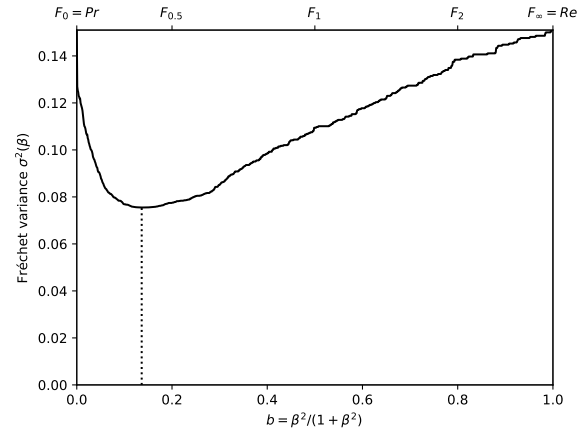
(a) The performances of 57 classifiers (BGS methods) depicted as points in the ROC space, with the isometrics of the optimal tradeoff score, from the ranking point of view, between precision and recall. See Eq. (12).



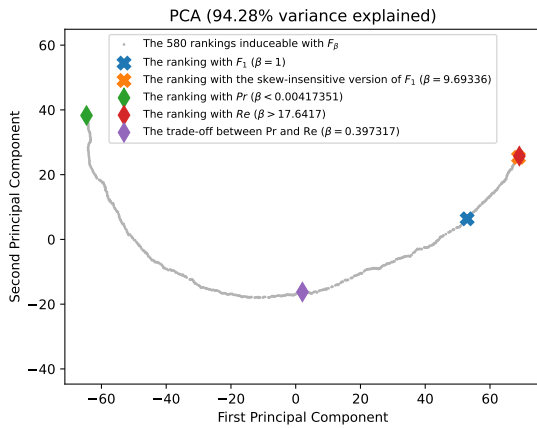
(b) The rank correlations $\tau(F_\beta; Pr)$ and $\tau(F_\beta; Re)$ w.r.t. β . The optimal value (or range of optimal values) for β is where the two curves intersect.



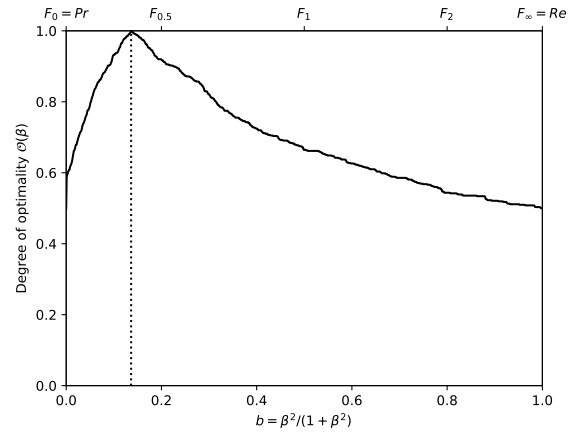
(c) The ranks of each classifier w.r.t. β . The optimal value (or range of optimal values) for β , shown here by the vertical line, is such that the number of swaps on its left is equal to the number of swaps on its right.



(d) The Fréchet variance $\sigma^2(\beta) = d_\tau^2(Pr; F_\beta) + d_\tau^2(F_\beta; Re)$ w.r.t. β . The optimal value (or range of optimal values) for β is where the curve has its minimum.

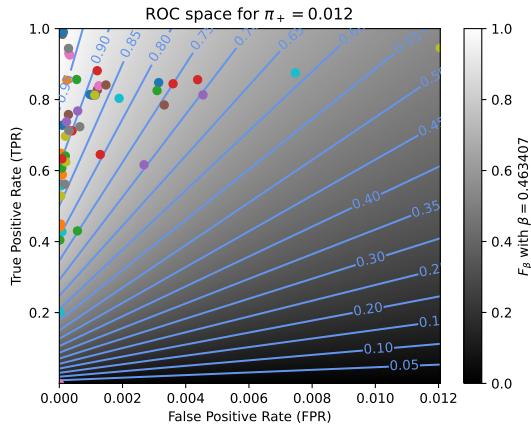


(e) Linear projection (PCA) of the manifold of the rankings induced by the F_β scores. The color points indicate the precision, the recall, F_1 , $SIVF$, as well as the optimal tradeoff. The optimal tradeoff is at the same distance of the two extremities when the distance is measured along the manifold, with Kendall's distance d_* .

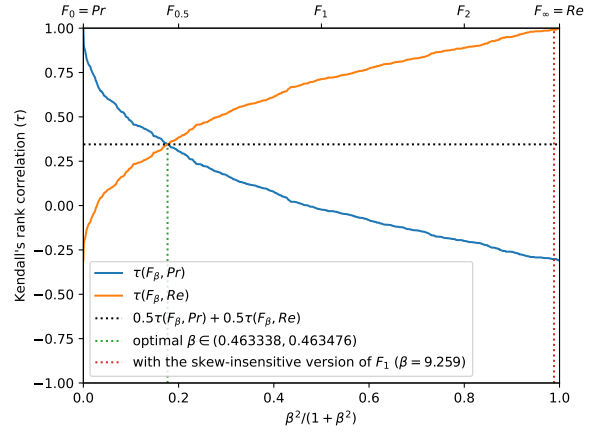


(f) The degree of optimality $\mathcal{O}(\beta)$ w.r.t. β . It is the probability to optimally ordering a pair of classifiers (BGS methods) given that it is not trivial (*i.e.*, that Pr and Re are in contradiction). The optimal value (or range of optimal values) for β is where the curve reaches 100%.

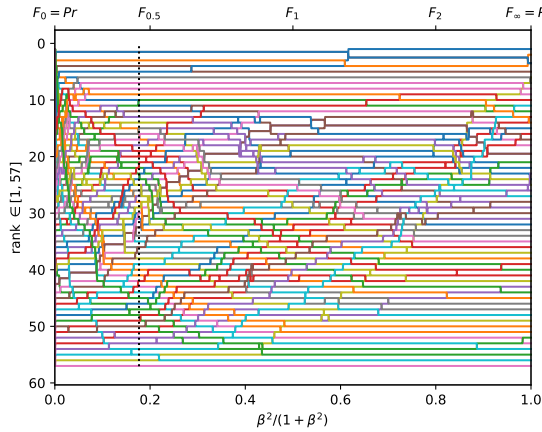
Figure A.3.43. Ranking of 57 BGS methods evaluated on the video "snowFall" ($\pi_+ = 0.0105$).



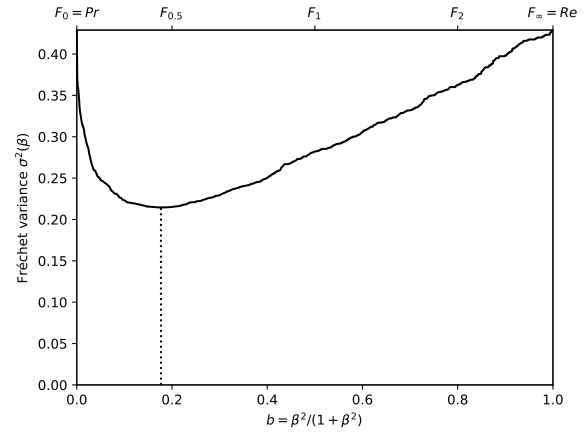
(a) The performances of 57 classifiers (BGS methods) depicted as points in the ROC space, with the isometrics of the optimal tradeoff score, from the ranking point of view, between precision and recall. See Eq. (12).



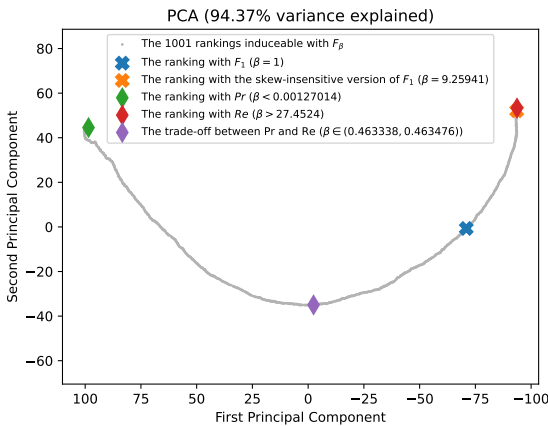
(b) The rank correlations $\tau(F_\beta; Pr)$ and $\tau(F_\beta; Re)$ w.r.t. β . The optimal value (or range of optimal values) for β is where the two curves intersect.



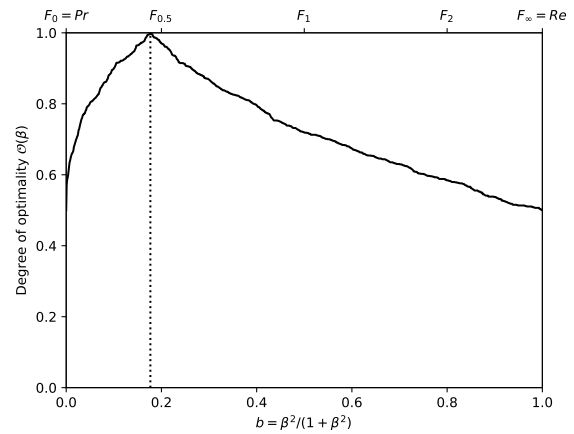
(c) The ranks of each classifier w.r.t. β . The optimal value (or range of optimal values) for β , shown here by the vertical line, is such that the number of swaps on its left is equal to the number of swaps on its right.



(d) The Fréchet variance $\sigma^2(\beta) = d_\tau^2(Pr; F_\beta) + d_\tau^2(F_\beta; Re)$ w.r.t. β . The optimal value (or range of optimal values) for β is where the curve has its minimum.

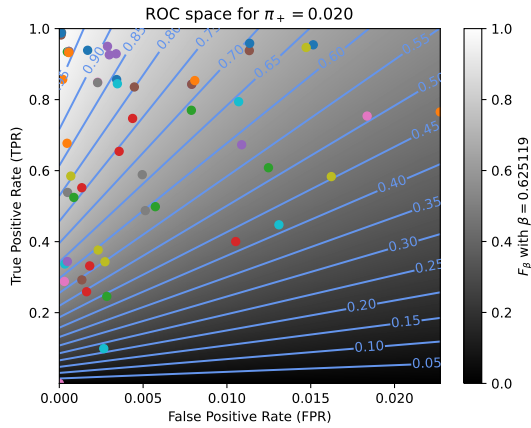


(e) Linear projection (PCA) of the manifold of the rankings induced by the F_β scores. The color points indicate the precision, the recall, F_1 , $SIVF$, as well as the optimal tradeoff. The optimal tradeoff is at the same distance of the two extremities when the distance is measured along the manifold, with Kendall's distance d_+ .

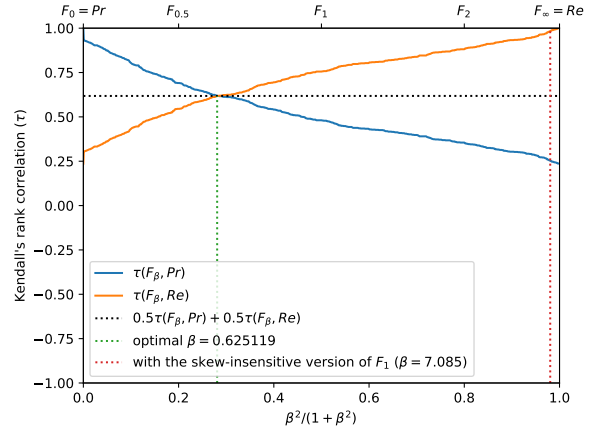


(f) The degree of optimality $\mathcal{O}(\beta)$ w.r.t. β . It is the probability to optimally ordering a pair of classifiers (BGS methods) given that it is not trivial (*i.e.*, that Pr and Re are in contradiction). The optimal value (or range of optimal values) for β is where the curve reaches 100%.

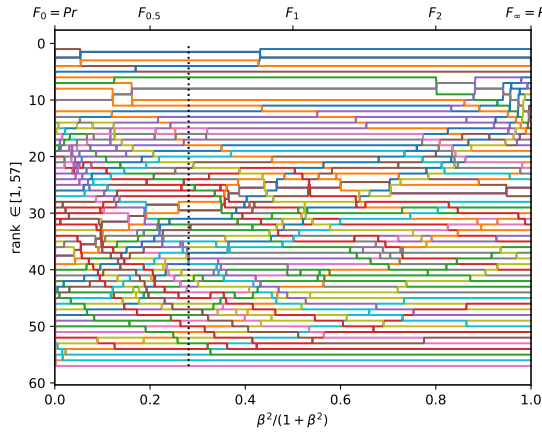
Figure A.3.44. Ranking of 57 BGS methods evaluated on the video "blizzard" ($\pi_+ = 0.0115$).



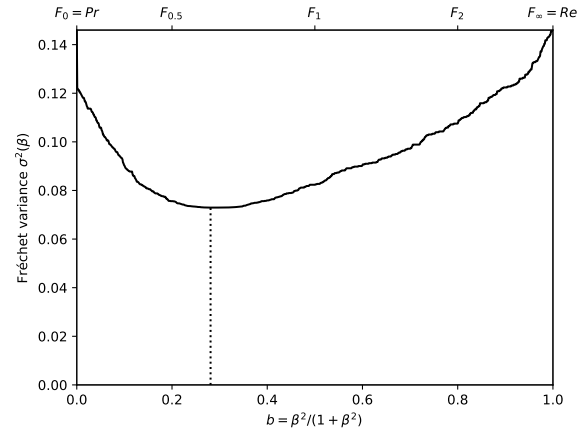
(a) The performances of 57 classifiers (BGS methods) depicted as points in the ROC space, with the isometrics of the optimal tradeoff score, from the ranking point of view, between precision and recall. See Eq. (12).



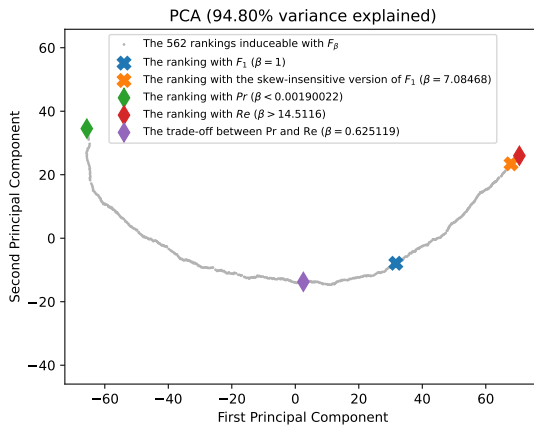
(b) The rank correlations $\tau(F_\beta; Pr)$ and $\tau(F_\beta; Re)$ w.r.t. β . The optimal value (or range of optimal values) for β is where the two curves intersect.



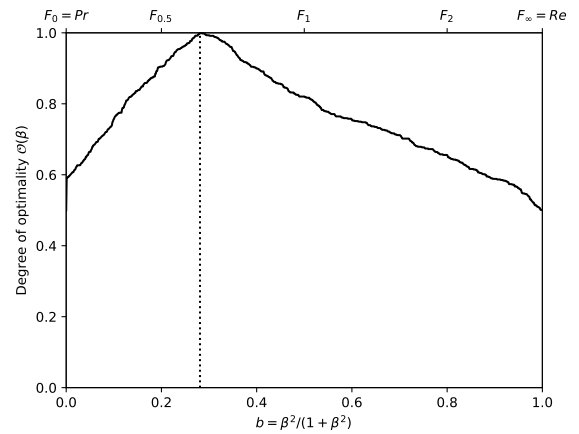
(c) The ranks of each classifier w.r.t. β . The optimal value (or range of optimal values) for β , shown here by the vertical line, is such that the number of swaps on its left is equal to the number of swaps on its right.



(d) The Fréchet variance $\sigma^2(\beta) = d_\tau^2(Pr; F_\beta) + d_\tau^2(F_\beta; Re)$ w.r.t. β . The optimal value (or range of optimal values) for β is where the curve has its minimum.

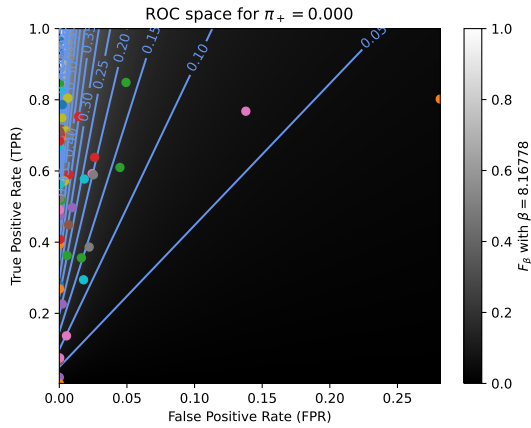


(e) Linear projection (PCA) of the manifold of the rankings induced by the F_β scores. The color points indicate the precision, the recall, F_1 , $SIVF$, as well as the optimal tradeoff. The optimal tradeoff is at the same distance of the two extremities when the distance is measured along the manifold, with Kendall's distance d_* .

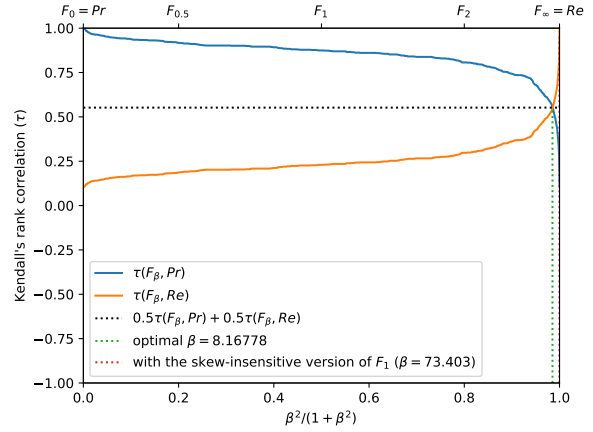


(f) The degree of optimality $\mathcal{O}(\beta)$ w.r.t. β . It is the probability to optimally ordering a pair of classifiers (BGS methods) given that it is not trivial (*i.e.*, that Pr and Re are in contradiction). The optimal value (or range of optimal values) for β is where the curve reaches 100%.

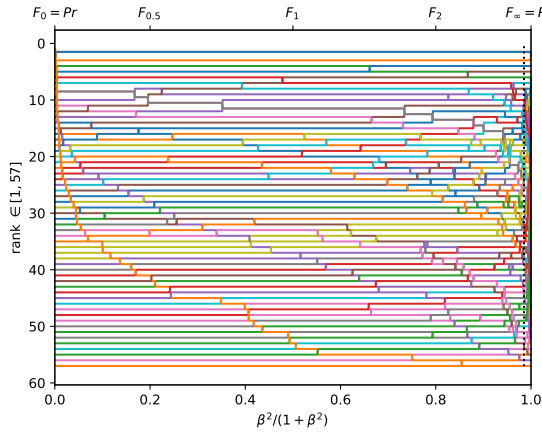
Figure A.3.45. Ranking of 57 BGS methods evaluated on the video "tunnelExit_0_35fps" ($\pi_+ = 0.0195$).



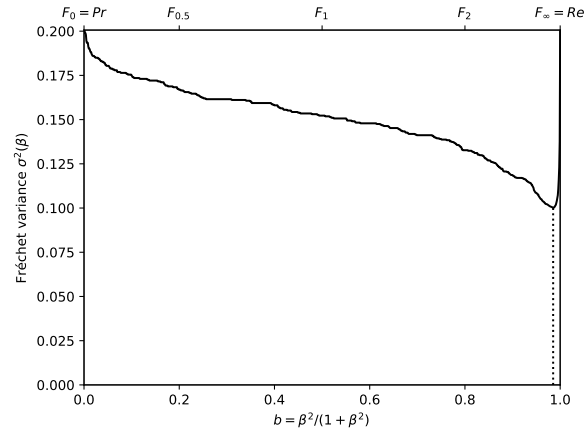
(a) The performances of 57 classifiers (BGS methods) depicted as points in the ROC space, with the isometrics of the optimal tradeoff score, from the ranking point of view, between precision and recall. See Eq. (12).



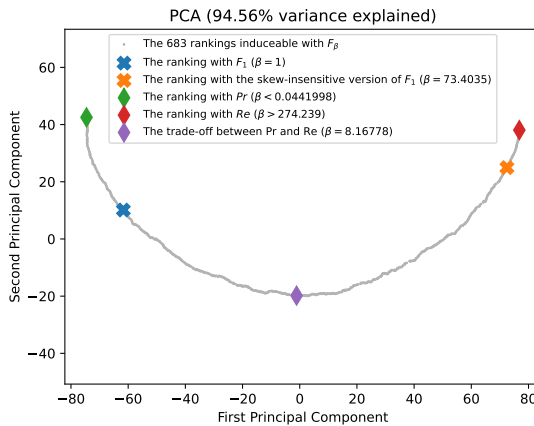
(b) The rank correlations $\tau(F_\beta; Pr)$ and $\tau(F_\beta; Re)$ w.r.t. β . The optimal value (or range of optimal values) for β is where the two curves intersect.



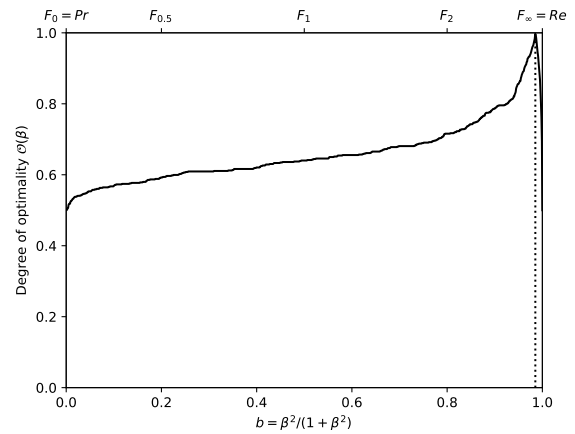
(c) The ranks of each classifier w.r.t. β . The optimal value (or range of optimal values) for β , shown here by the vertical line, is such that the number of swaps on its left is equal to the number of swaps on its right.



(d) The Fréchet variance $\sigma^2(\beta) = d_\tau^2(Pr; F_\beta) + d_\tau^2(F_\beta; Re)$ w.r.t. β . The optimal value (or range of optimal values) for β is where the curve has its minimum.

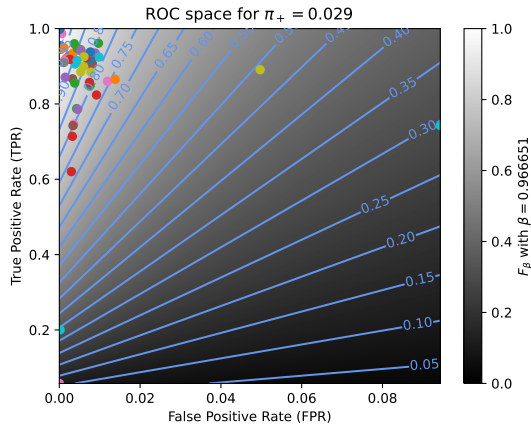


(e) Linear projection (PCA) of the manifold of the rankings induced by the F_β scores. The color points indicate the precision, the recall, F_1 , $SIVF$, as well as the optimal tradeoff. The optimal tradeoff is at the same distance of the two extremities when the distance is measured along the manifold, with Kendall's distance d_+ .

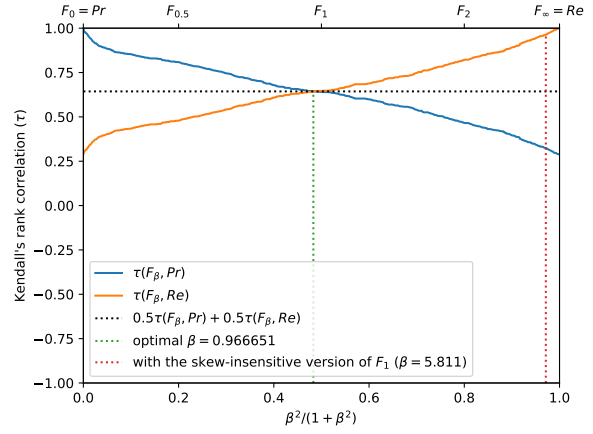


(f) The degree of optimality $\mathcal{O}(\beta)$ w.r.t. β . It is the probability to optimally ordering a pair of classifiers (BGS methods) given that it is not trivial (*i.e.*, that Pr and Re are in contradiction). The optimal value (or range of optimal values) for β is where the curve reaches 100%.

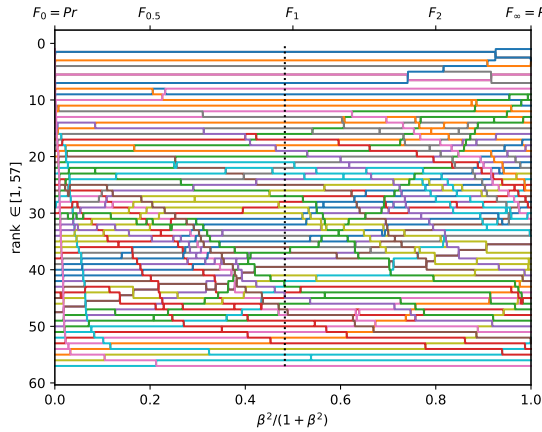
Figure A.3.46. Ranking of 57 BGS methods evaluated on the video "port_0_17fps" ($\pi_+ = 0.0002$).



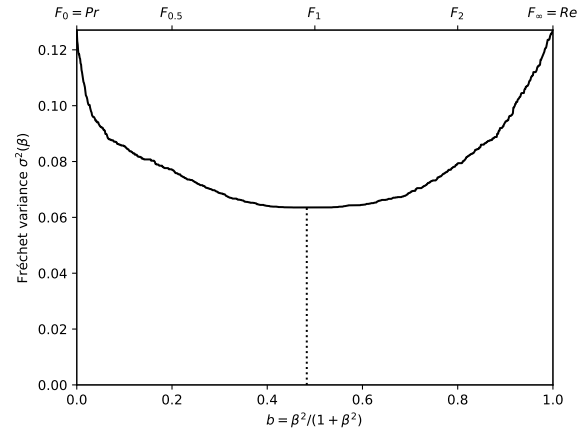
(a) The performances of 57 classifiers (BGS methods) depicted as points in the ROC space, with the isometrics of the optimal tradeoff score, from the ranking point of view, between precision and recall. See Eq. (12).



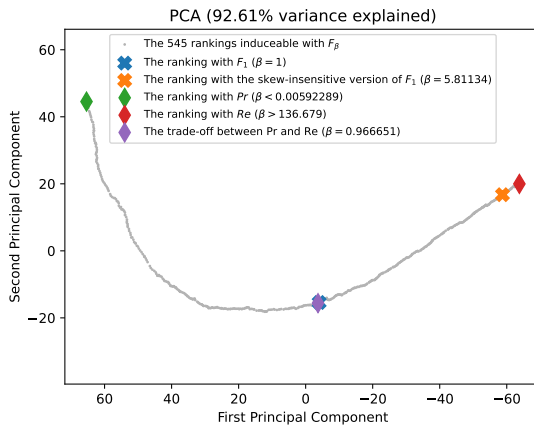
(b) The rank correlations $\tau(F_\beta; Pr)$ and $\tau(F_\beta; Re)$ w.r.t. β . The optimal value (or range of optimal values) for β is where the two curves intersect.



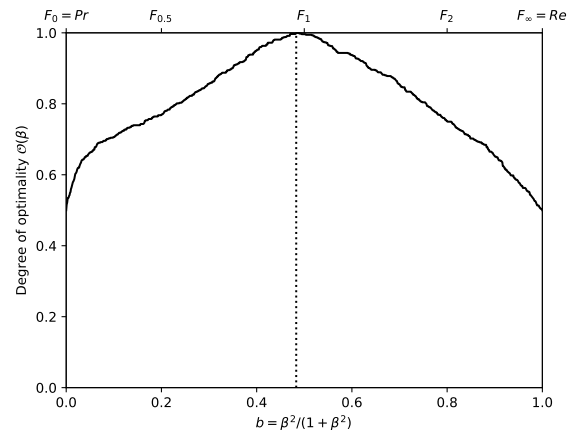
(c) The ranks of each classifier w.r.t. β . The optimal value (or range of optimal values) for β , shown here by the vertical line, is such that the number of swaps on its left is equal to the number of swaps on its right.



(d) The Fréchet variance $\sigma^2(\beta) = d_\tau^2(Pr; F_\beta) + d_\tau^2(F_\beta; Re)$ w.r.t. β . The optimal value (or range of optimal values) for β is where the curve has its minimum.

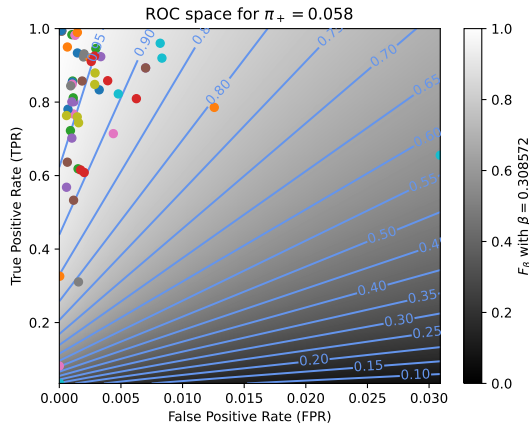


(e) Linear projection (PCA) of the manifold of the rankings induced by the F_β scores. The color points indicate the precision, the recall, F_1 , $SIVF$, as well as the optimal tradeoff. The optimal tradeoff is at the same distance of the two extremities when the distance is measured along the manifold, with Kendall's distance d_* .

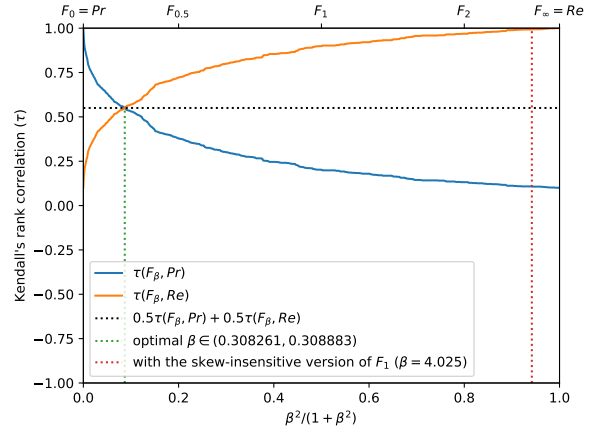


(f) The degree of optimality $\mathcal{O}(\beta)$ w.r.t. β . It is the probability to optimally ordering a pair of classifiers (BGS methods) given that it is not trivial (*i.e.*, that Pr and Re are in contradiction). The optimal value (or range of optimal values) for β is where the curve reaches 100%.

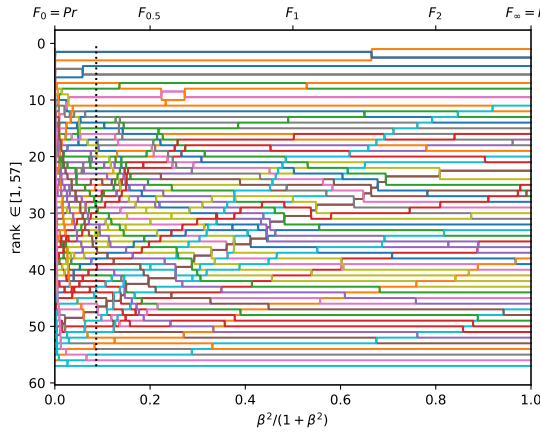
Figure A.3.47. Ranking of 57 BGS methods evaluated on the video "tramCrossroad_1fps" ($\pi_+ = 0.0288$).



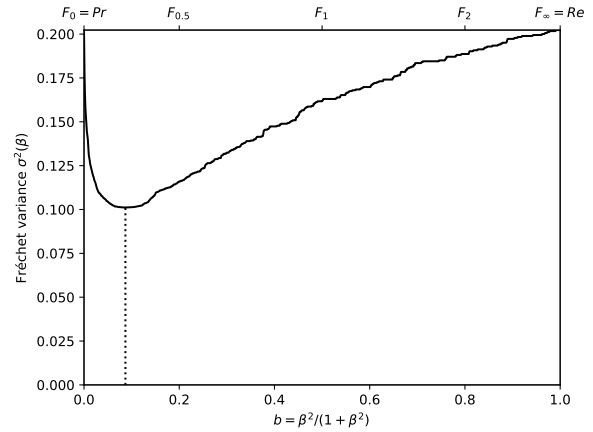
(a) The performances of 57 classifiers (BGS methods) depicted as points in the ROC space, with the isometrics of the optimal tradeoff score, from the ranking point of view, between precision and recall. See Eq. (12).



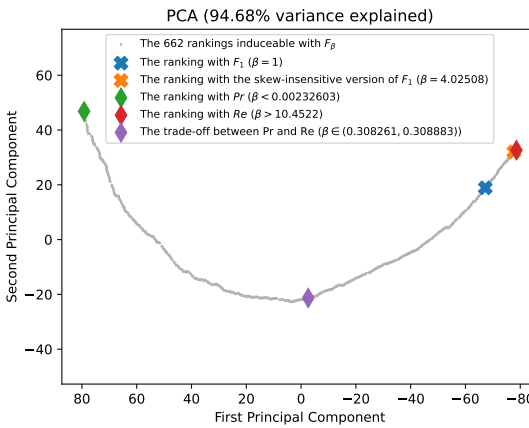
(b) The rank correlations $\tau(F_\beta; Pr)$ and $\tau(F_\beta; Re)$ w.r.t. β . The optimal value (or range of optimal values) for β is where the two curves intersect.



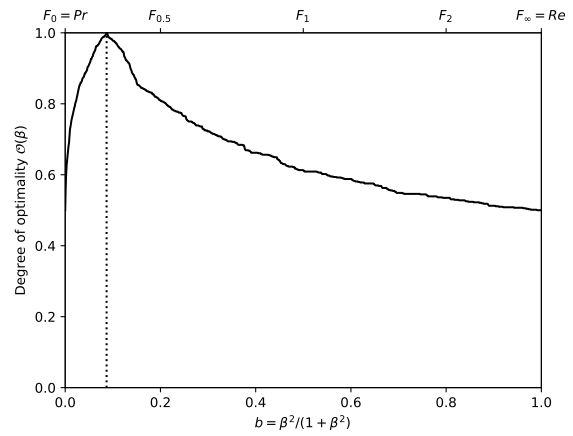
(c) The ranks of each classifier w.r.t. β . The optimal value (or range of optimal values) for β , shown here by the vertical line, is such that the number of swaps on its left is equal to the number of swaps on its right.



(d) The Fréchet variance $\sigma^2(\beta) = d_\tau^2(Pr; F_\beta) + d_\tau^2(F_\beta; Re)$ w.r.t. β . The optimal value (or range of optimal values) for β is where the curve has its minimum.

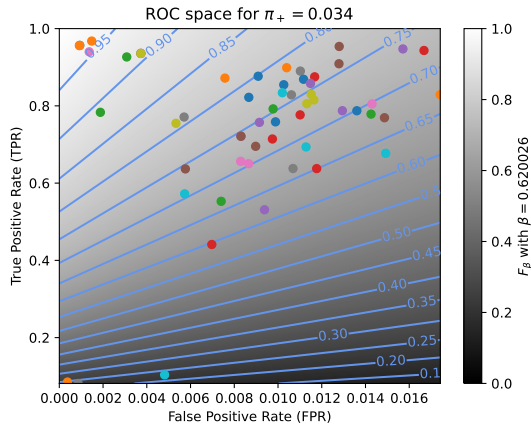


(e) Linear projection (PCA) of the manifold of the rankings induced by the F_β scores. The color points indicate the precision, the recall, F_1 , $SIVF$, as well as the optimal tradeoff. The optimal tradeoff is at the same distance of the two extremities when the distance is measured along the manifold, with Kendall's distance d_* .

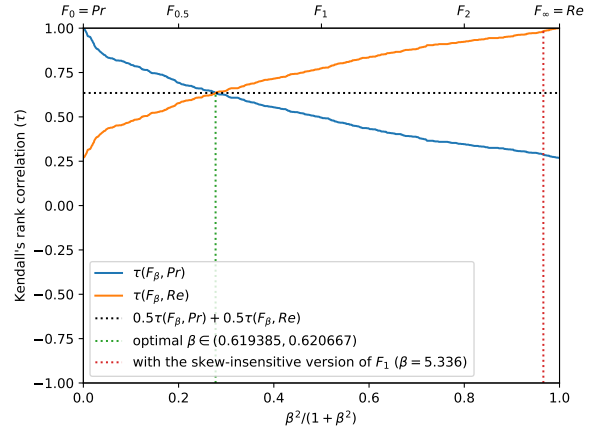


(f) The degree of optimality $\mathcal{O}(\beta)$ w.r.t. β . It is the probability to optimally ordering a pair of classifiers (BGS methods) given that it is not trivial (*i.e.*, that Pr and Re are in contradiction). The optimal value (or range of optimal values) for β is where the curve reaches 100%.

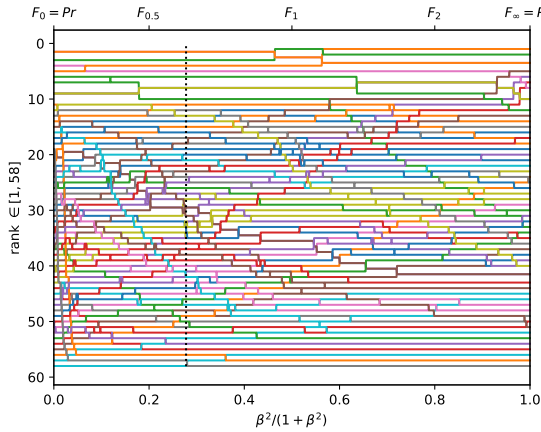
Figure A.3.48. Ranking of 57 BGS methods evaluated on the video "turnpike_0_5fps" ($\pi_+ = 0.0581$).



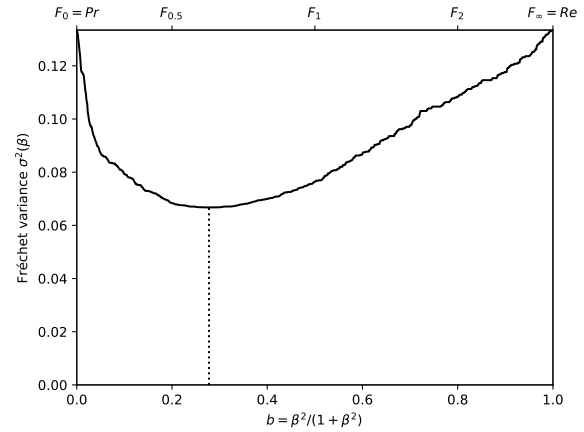
(a) The performances of 58 classifiers (BGS methods) depicted as points in the ROC space, with the isometrics of the optimal tradeoff score, from the ranking point of view, between precision and recall. See Eq. (12).



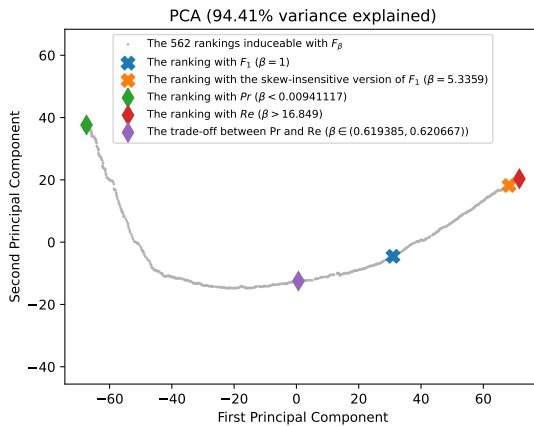
(b) The rank correlations $\tau(F_\beta; Pr)$ and $\tau(F_\beta; Re)$ w.r.t. β . The optimal value (or range of optimal values) for β is where the two curves intersect.



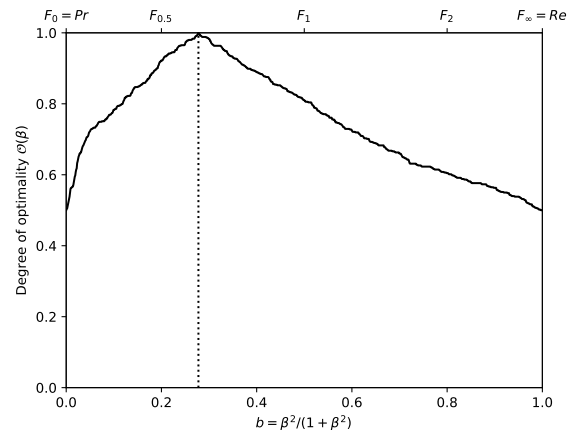
(c) The ranks of each classifier w.r.t. β . The optimal value (or range of optimal values) for β , shown here by the vertical line, is such that the number of swaps on its left is equal to the number of swaps on its right.



(d) The Fréchet variance $\sigma^2(\beta) = d_\tau^2(Pr; F_\beta) + d_\tau^2(F_\beta; Re)$ w.r.t. β . The optimal value (or range of optimal values) for β is where the curve has its minimum.

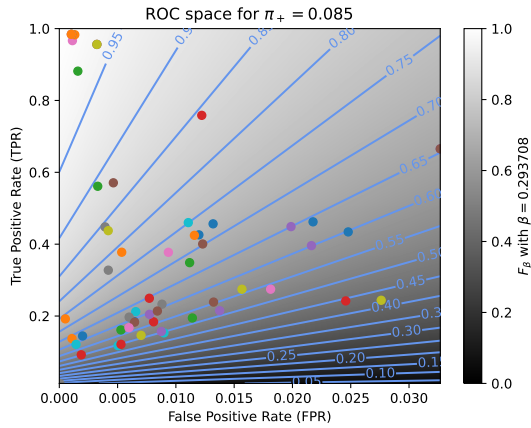


(e) Linear projection (PCA) of the manifold of the rankings induced by the F_β scores. The color points indicate the precision, the recall, F_1 , $SIVF$, as well as the optimal tradeoff. The optimal tradeoff is at the same distance of the two extremities when the distance is measured along the manifold, with Kendall's distance d_+ .

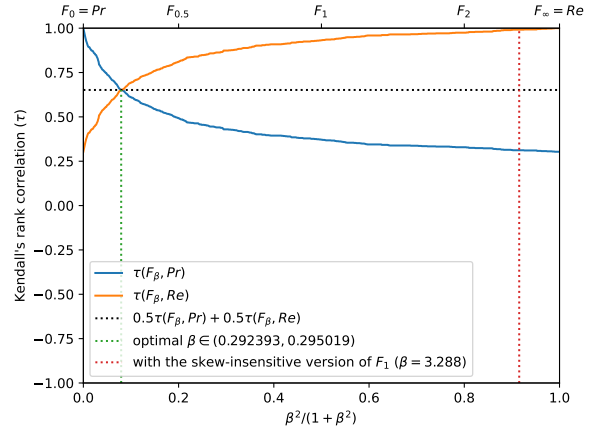


(f) The degree of optimality $\mathcal{O}(\beta)$ w.r.t. β . It is the probability to optimally ordering a pair of classifiers (BGS methods) given that it is not trivial (*i.e.*, that Pr and Re are in contradiction). The optimal value (or range of optimal values) for β is where the curve reaches 100%.

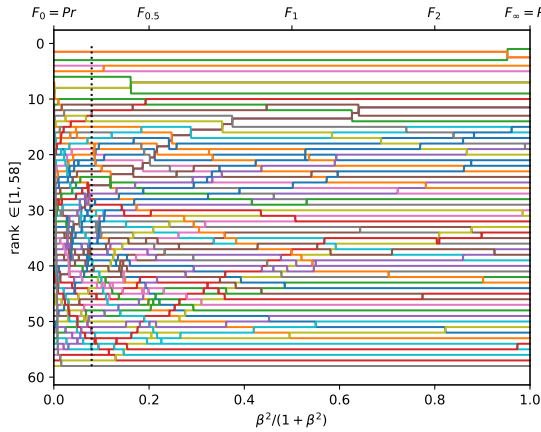
Figure A.3.49. Ranking of 58 BGS methods evaluated on the video "tramStation" ($\pi_+ = 0.0339$).



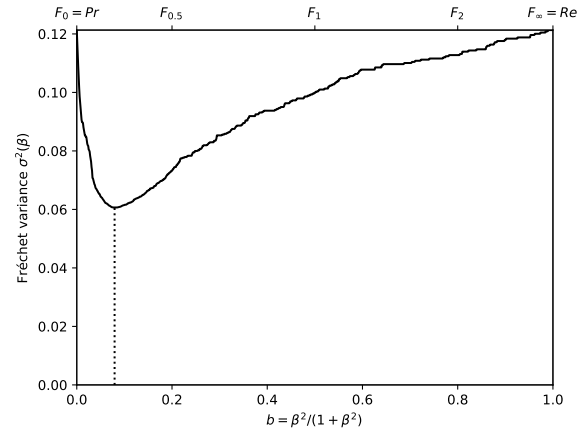
(a) The performances of 58 classifiers (BGS methods) depicted as points in the ROC space, with the isometrics of the optimal tradeoff score, from the ranking point of view, between precision and recall. See Eq. (12).



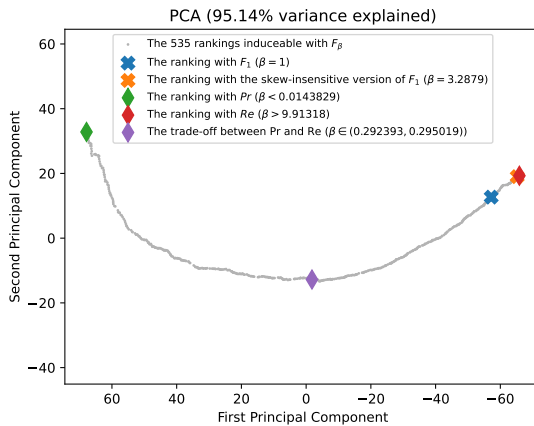
(b) The rank correlations $\tau(F_\beta; Pr)$ and $\tau(F_\beta; Re)$ w.r.t. β . The optimal value (or range of optimal values) for β is where the two curves intersect.



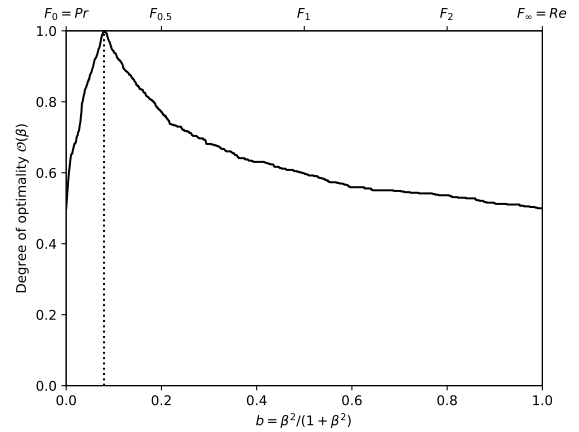
(c) The ranks of each classifier w.r.t. β . The optimal value (or range of optimal values) for β , shown here by the vertical line, is such that the number of swaps on its left is equal to the number of swaps on its right.



(d) The Fréchet variance $\sigma^2(\beta) = d_\tau^2(Pr; F_\beta) + d_\tau^2(F_\beta; Re)$ w.r.t. β . The optimal value (or range of optimal values) for β is where the curve has its minimum.

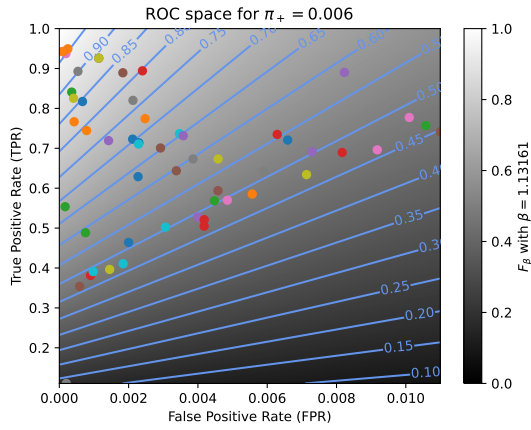


(e) Linear projection (PCA) of the manifold of the rankings induced by the F_β scores. The color points indicate the precision, the recall, F_1 , $SIVF$, as well as the optimal tradeoff. The optimal tradeoff is at the same distance of the two extremities when the distance is measured along the manifold, with Kendall's distance d_+ .

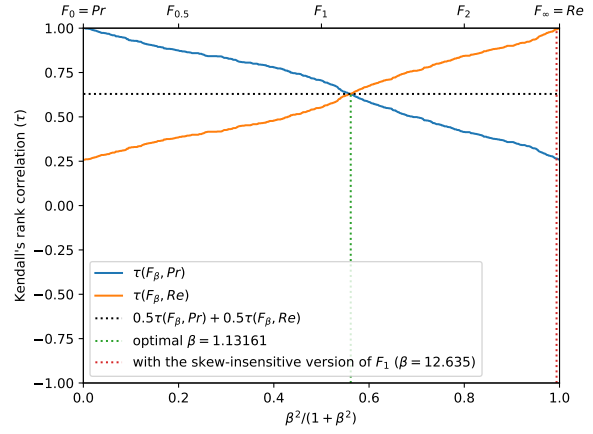


(f) The degree of optimality $\mathcal{O}(\beta)$ w.r.t. β . It is the probability to optimally ordering a pair of classifiers (BGS methods) given that it is not trivial (*i.e.*, that Pr and Re are in contradiction). The optimal value (or range of optimal values) for β is where the curve reaches 100%.

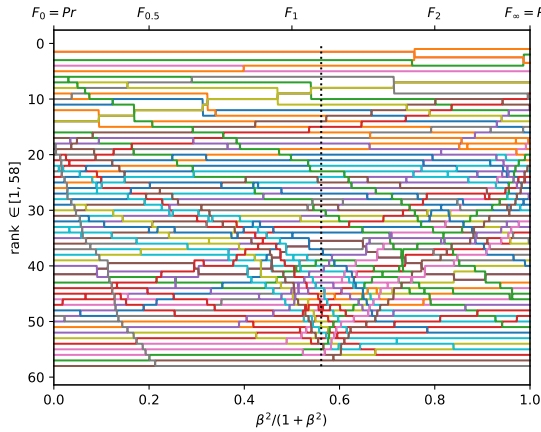
Figure A.3.50. Ranking of 58 BGS methods evaluated on the video "busyBoulevard" ($\pi_+ = 0.0847$).



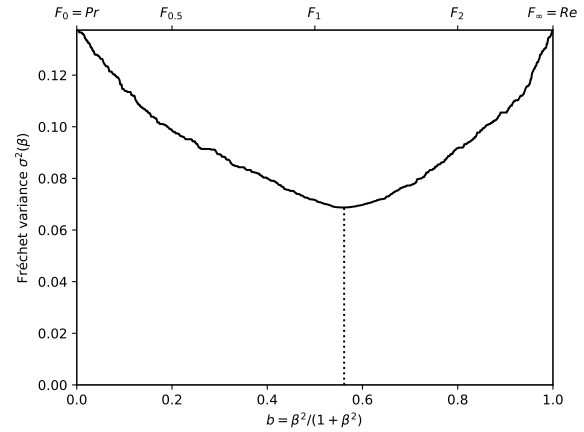
(a) The performances of 58 classifiers (BGS methods) depicted as points in the ROC space, with the isometrics of the optimal tradeoff score, from the ranking point of view, between precision and recall. See Eq. (12).



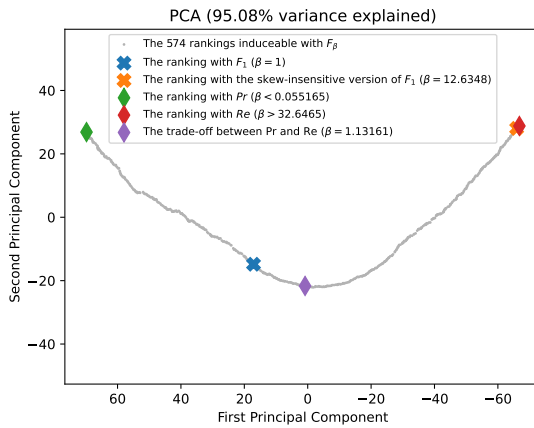
(b) The rank correlations $\tau(F_\beta; Pr)$ and $\tau(F_\beta; Re)$ w.r.t. β . The optimal value (or range of optimal values) for β is where the two curves intersect.



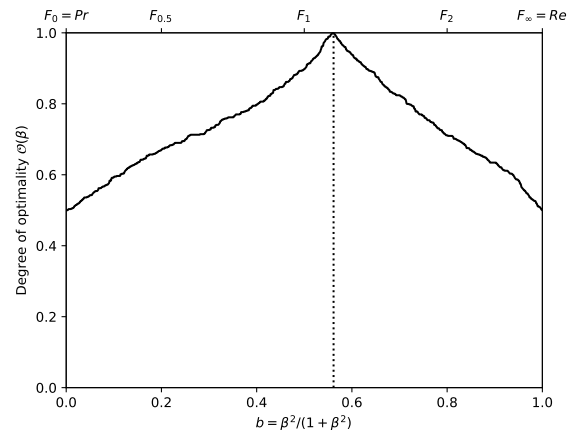
(c) The ranks of each classifier w.r.t. β . The optimal value (or range of optimal values) for β , shown here by the vertical line, is such that the number of swaps on its left is equal to the number of swaps on its right.



(d) The Fréchet variance $\sigma^2(\beta) = d_\tau^2(Pr; F_\beta) + d_\tau^2(F_\beta; Re)$ w.r.t. β . The optimal value (or range of optimal values) for β is where the curve has its minimum.

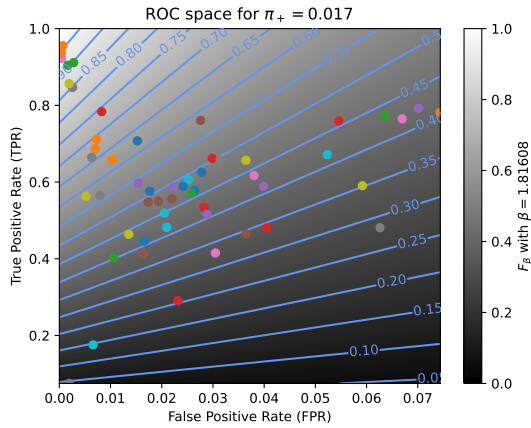


(e) Linear projection (PCA) of the manifold of the rankings induced by the F_β scores. The color points indicate the precision, the recall, F_1 , $SIVF$, as well as the optimal tradeoff. The optimal tradeoff is at the same distance of the two extremities when the distance is measured along the manifold, with Kendall's distance d_τ .

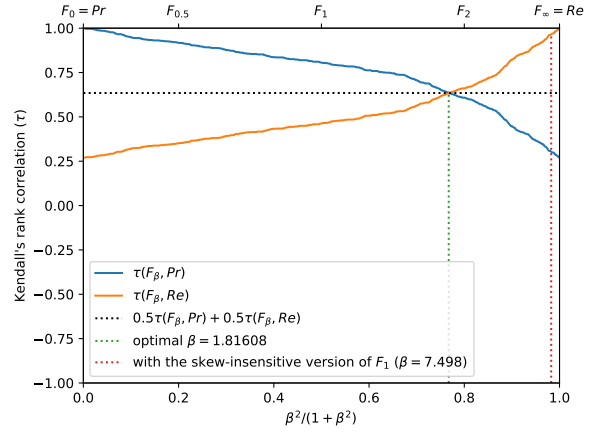


(f) The degree of optimality $\mathcal{O}(\beta)$ w.r.t. β . It is the probability to optimally ordering a pair of classifiers (BGS methods) given that it is not trivial (*i.e.*, that Pr and Re are in contradiction). The optimal value (or range of optimal values) for β is where the curve reaches 100%.

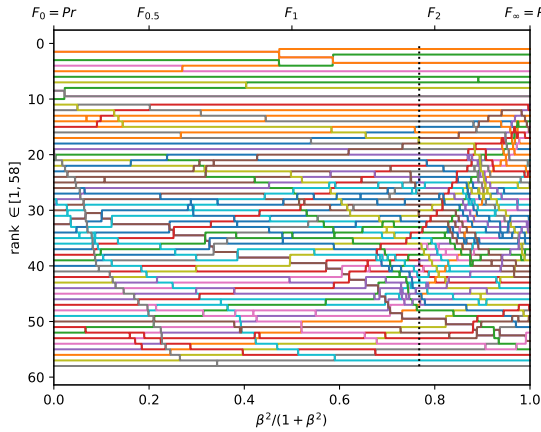
Figure A.3.51. Ranking of 58 BGS methods evaluated on the video "streetCornerAtNight" ($\pi_+ = 0.0062$).



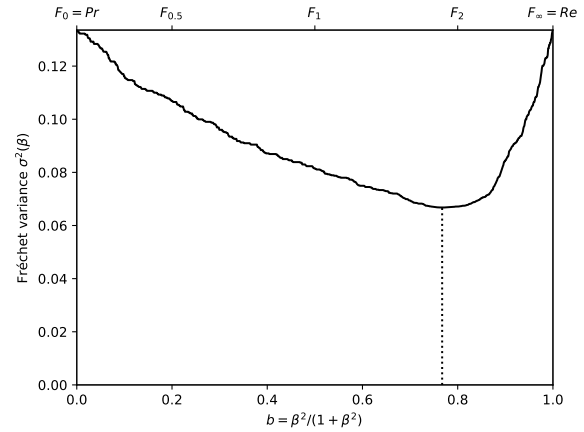
(a) The performances of 58 classifiers (BGS methods) depicted as points in the ROC space, with the isometrics of the optimal tradeoff score, from the ranking point of view, between precision and recall. See Eq. (12).



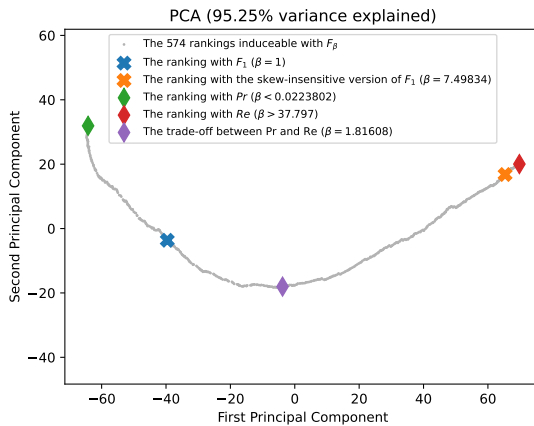
(b) The rank correlations $\tau(F_\beta; Pr)$ and $\tau(F_\beta; Re)$ w.r.t. β . The optimal value (or range of optimal values) for β is where the two curves intersect.



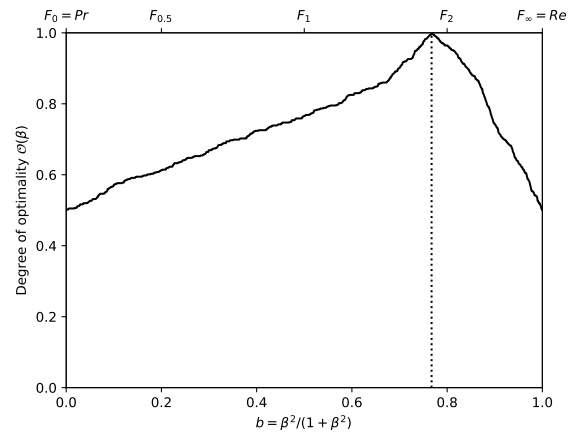
(c) The ranks of each classifier w.r.t. β . The optimal value (or range of optimal values) for β , shown here by the vertical line, is such that the number of swaps on its left is equal to the number of swaps on its right.



(d) The Fréchet variance $\sigma^2(\beta) = d_\tau^2(Pr; F_\beta) + d_\tau^2(F_\beta; Re)$ w.r.t. β . The optimal value (or range of optimal values) for β is where the curve has its minimum.

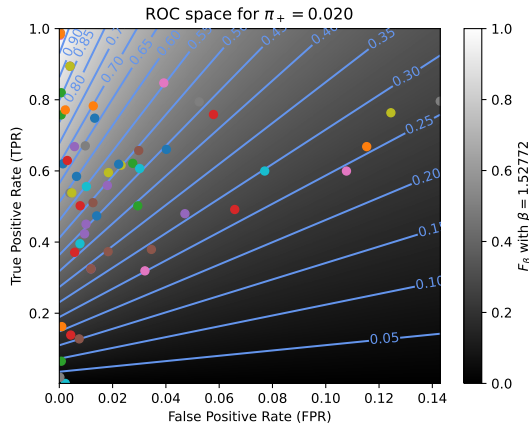


(e) Linear projection (PCA) of the manifold of the rankings induced by the F_β scores. The color points indicate the precision, the recall, F_1 , $SIVF$, as well as the optimal tradeoff. The optimal tradeoff is at the same distance of the two extremities when the distance is measured along the manifold, with Kendall's distance d_+ .

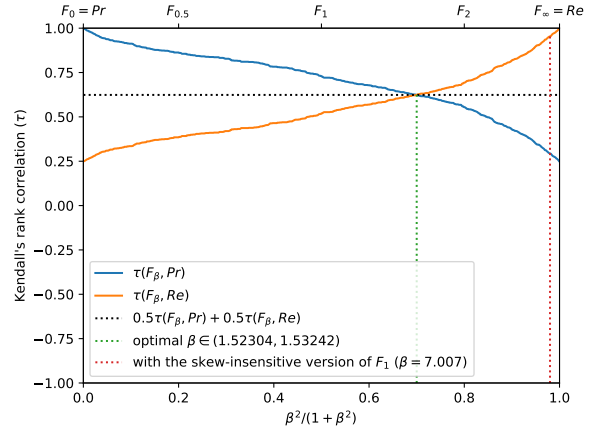


(f) The degree of optimality $\mathcal{O}(\beta)$ w.r.t. β . It is the probability to optimally ordering a pair of classifiers (BGS methods) given that it is not trivial (*i.e.*, that Pr and Re are in contradiction). The optimal value (or range of optimal values) for β is where the curve reaches 100%.

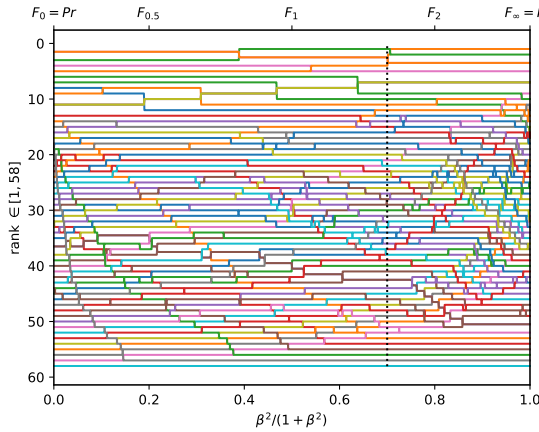
Figure A.3.52. Ranking of 58 BGS methods evaluated on the video "fluidHighway" ($\pi_+ = 0.0175$).



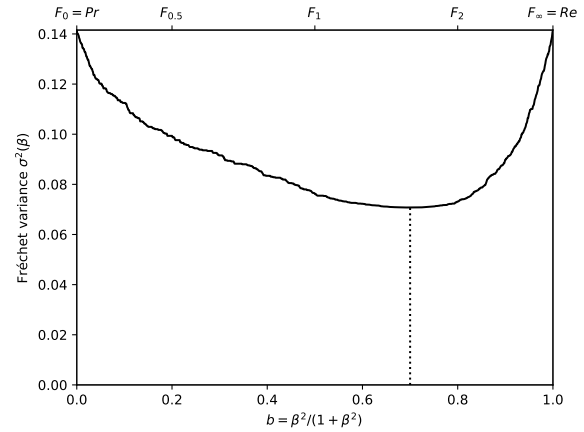
(a) The performances of 58 classifiers (BGS methods) depicted as points in the ROC space, with the isometrics of the optimal tradeoff score, from the ranking point of view, between precision and recall. See Eq. (12).



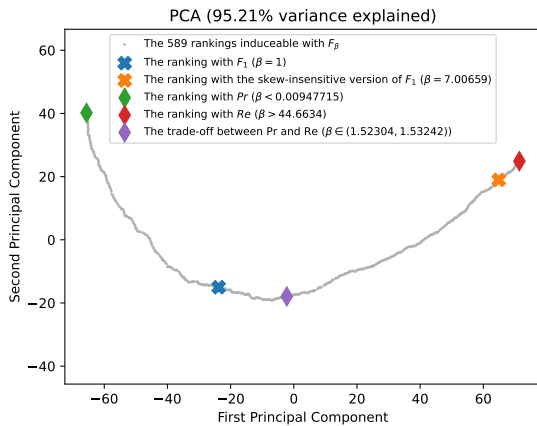
(b) The rank correlations $\tau(F_\beta; Pr)$ and $\tau(F_\beta; Re)$ w.r.t. β . The optimal value (or range of optimal values) for β is where the two curves intersect.



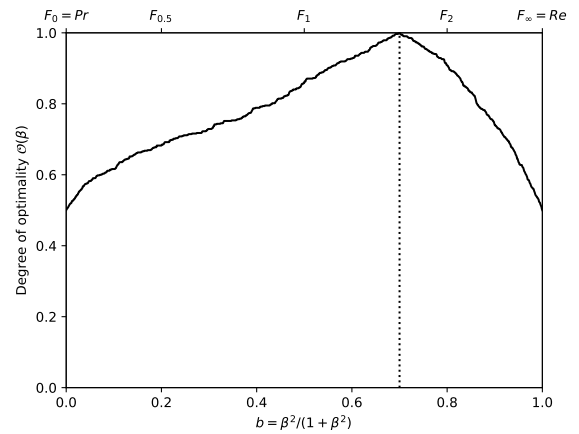
(c) The ranks of each classifier w.r.t. β . The optimal value (or range of optimal values) for β , shown here by the vertical line, is such that the number of swaps on its left is equal to the number of swaps on its right.



(d) The Fréchet variance $\sigma^2(\beta) = d_\tau^2(Pr; F_\beta) + d_\tau^2(F_\beta; Re)$ w.r.t. β . The optimal value (or range of optimal values) for β is where the curve has its minimum.

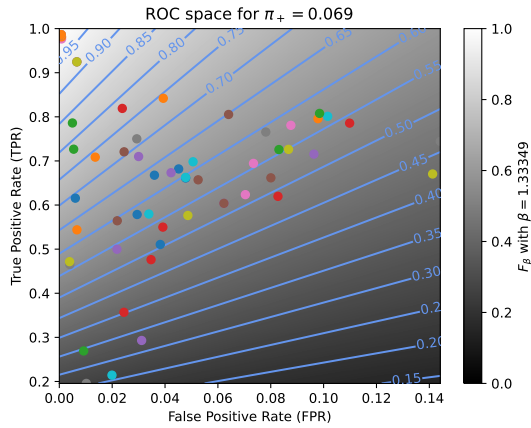


(e) Linear projection (PCA) of the manifold of the rankings induced by the F_β scores. The color points indicate the precision, the recall, F_1 , $SIVF$, as well as the optimal tradeoff. The optimal tradeoff is at the same distance of the two extremities when the distance is measured along the manifold, with Kendall's distance d_+ .

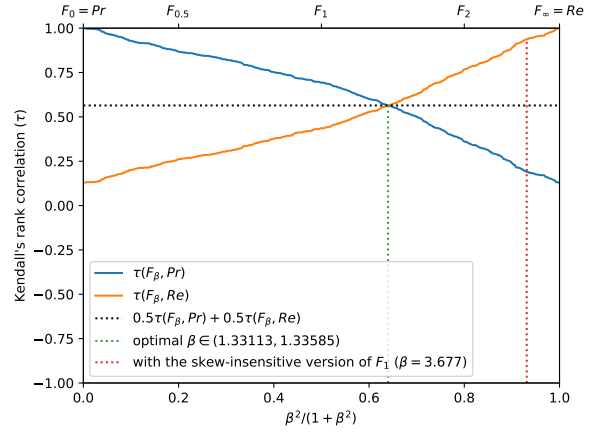


(f) The degree of optimality $\mathcal{O}(\beta)$ w.r.t. β . It is the probability to optimally ordering a pair of classifiers (BGS methods) given that it is not trivial (*i.e.*, that Pr and Re are in contradiction). The optimal value (or range of optimal values) for β is where the curve reaches 100%.

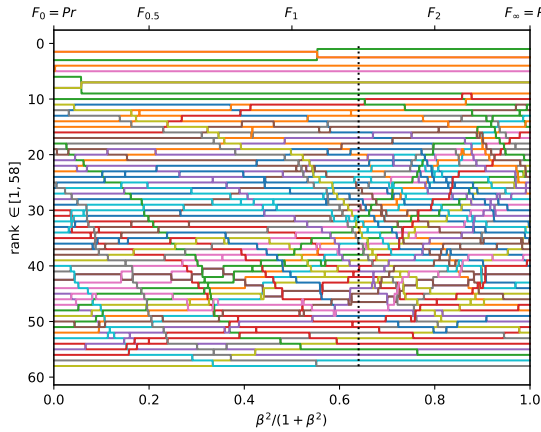
Figure A.3.53. Ranking of 58 BGS methods evaluated on the video "bridgeEntry" ($\pi_+ = 0.0200$).



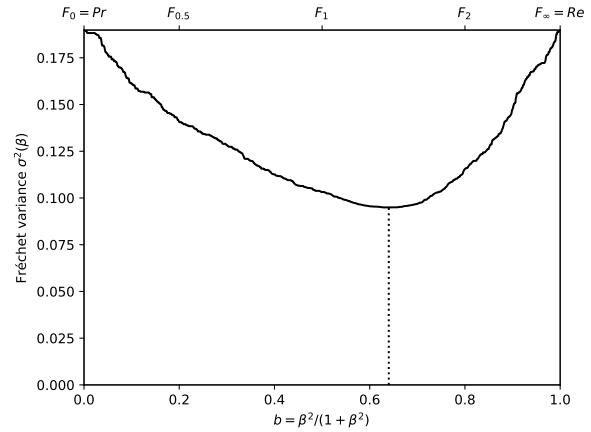
(a) The performances of 58 classifiers (BGS methods) depicted as points in the ROC space, with the isometrics of the optimal tradeoff score, from the ranking point of view, between precision and recall. See Eq. (12).



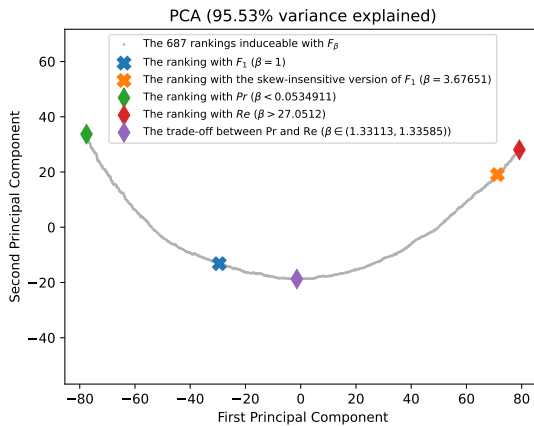
(b) The rank correlations $\tau(F_\beta; Pr)$ and $\tau(F_\beta; Re)$ w.r.t. β . The optimal value (or range of optimal values) for β is where the two curves intersect.



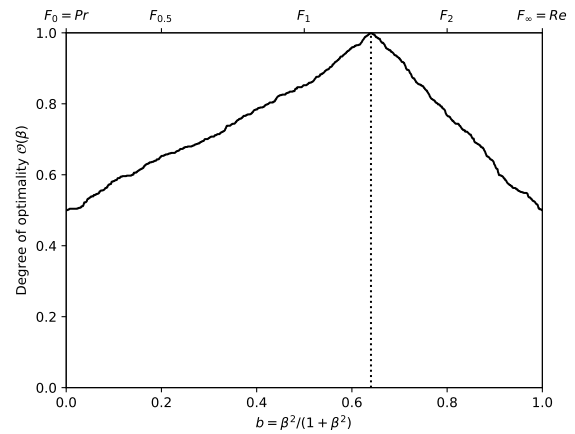
(c) The ranks of each classifier w.r.t. β . The optimal value (or range of optimal values) for β , shown here by the vertical line, is such that the number of swaps on its left is equal to the number of swaps on its right.



(d) The Fréchet variance $\sigma^2(\beta) = d_\tau^2(Pr; F_\beta) + d_\tau^2(F_\beta; Re)$ w.r.t. β . The optimal value (or range of optimal values) for β is where the curve has its minimum.

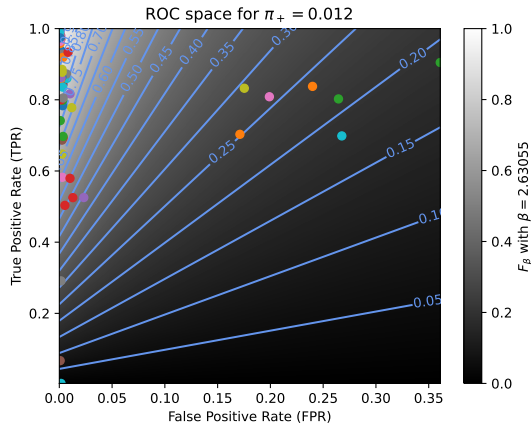


(e) Linear projection (PCA) of the manifold of the rankings induced by the F_β scores. The color points indicate the precision, the recall, F_1 , $SIVF$, as well as the optimal tradeoff. The optimal tradeoff is at the same distance of the two extremities when the distance is measured along the manifold, with Kendall's distance d_τ .

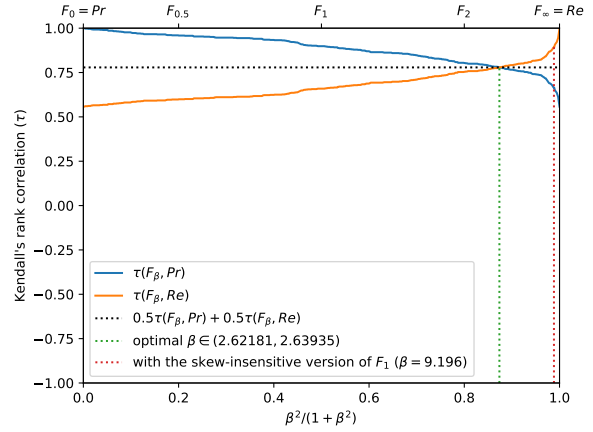


(f) The degree of optimality $\mathcal{O}(\beta)$ w.r.t. β . It is the probability to optimally ordering a pair of classifiers (BGS methods) given that it is not trivial (*i.e.*, that Pr and Re are in contradiction). The optimal value (or range of optimal values) for β is where the curve reaches 100%.

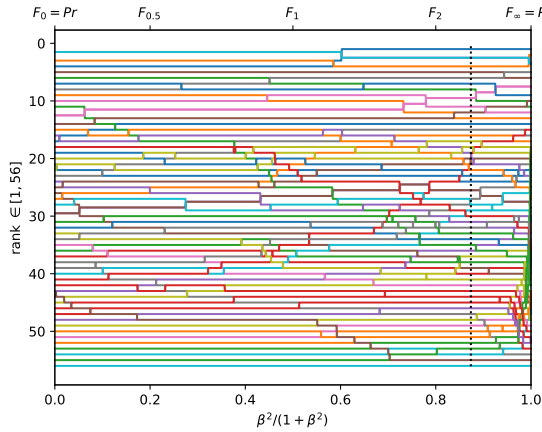
Figure A.3.54. Ranking of 58 BGS methods evaluated on the video "winterStreet" ($\pi_+ = 0.0689$).



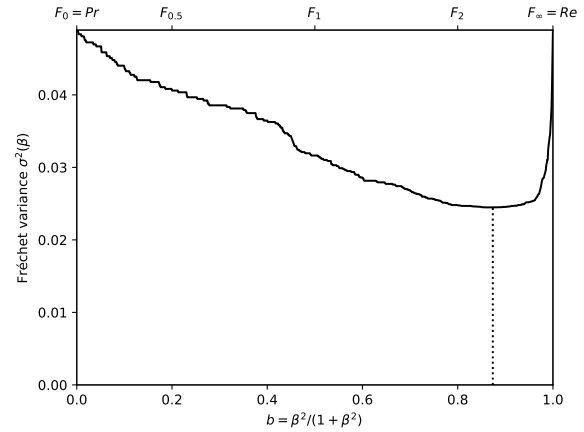
(a) The performances of 56 classifiers (BGS methods) depicted as points in the ROC space, with the isometrics of the optimal tradeoff score, from the ranking point of view, between precision and recall. See Eq. (12).



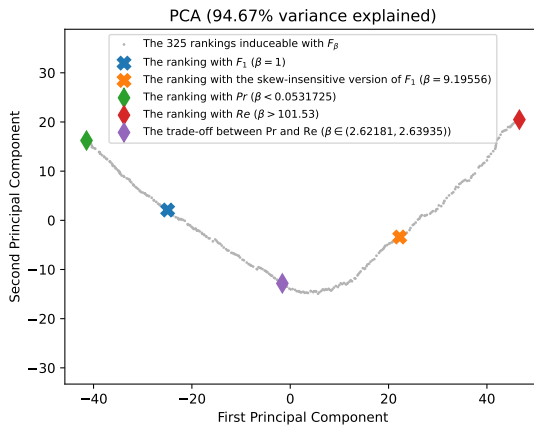
(b) The rank correlations $\tau(F_\beta; Pr)$ and $\tau(F_\beta; Re)$ w.r.t. β . The optimal value (or range of optimal values) for β is where the two curves intersect.



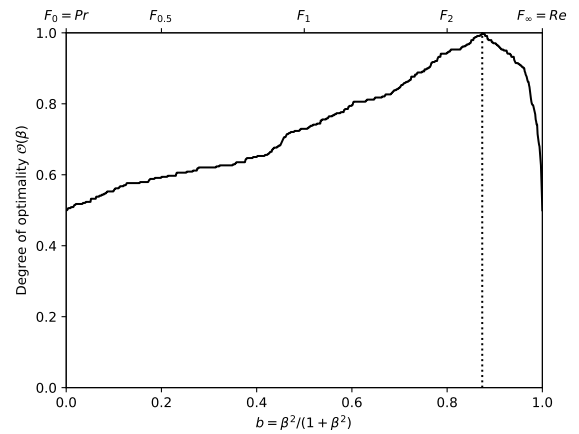
(c) The ranks of each classifier w.r.t. β . The optimal value (or range of optimal values) for β , shown here by the vertical line, is such that the number of swaps on its left is equal to the number of swaps on its right.



(d) The Fréchet variance $\sigma^2(\beta) = d_\tau^2(Pr; F_\beta) + d_\tau^2(F_\beta; Re)$ w.r.t. β . The optimal value (or range of optimal values) for β is where the curve has its minimum.

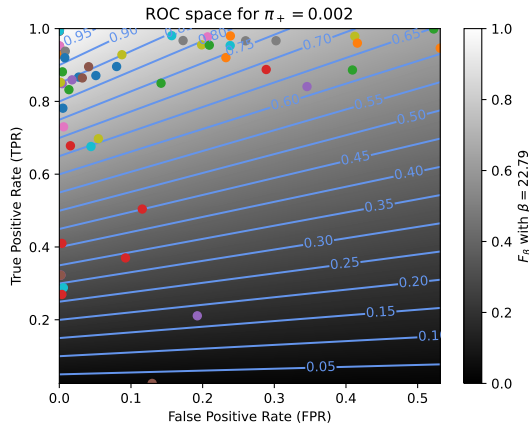


(e) Linear projection (PCA) of the manifold of the rankings induced by the F_β scores. The color points indicate the precision, the recall, F_1 , $SIVF$, as well as the optimal tradeoff. The optimal tradeoff is at the same distance of the two extremities when the distance is measured along the manifold, with Kendall's distance d_+ .

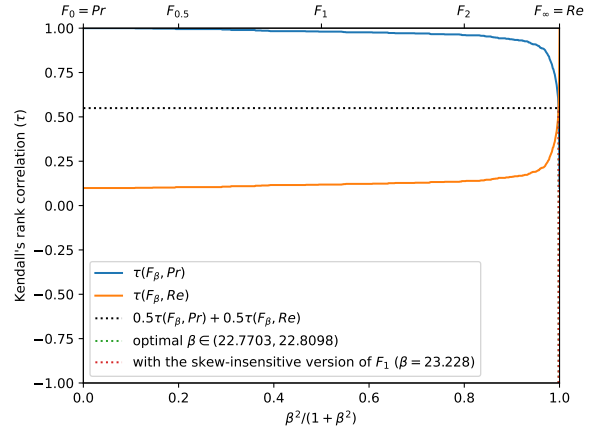


(f) The degree of optimality $\mathcal{O}(\beta)$ w.r.t. β . It is the probability to optimally ordering a pair of classifiers (BGS methods) given that it is not trivial (*i.e.*, that Pr and Re are in contradiction). The optimal value (or range of optimal values) for β is where the curve reaches 100%.

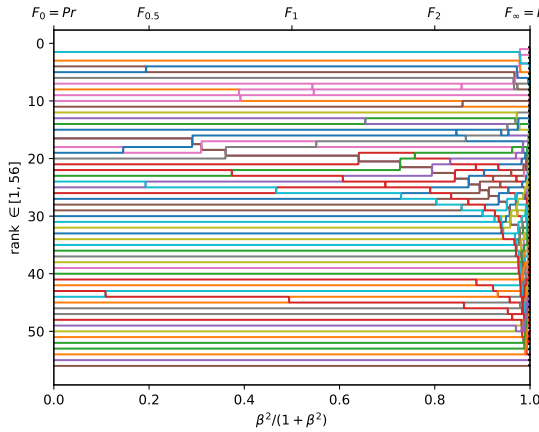
Figure A.3.55. Ranking of 56 BGS methods evaluated on the video "twoPositionPTZCam" ($\pi_+ = 0.0117$).



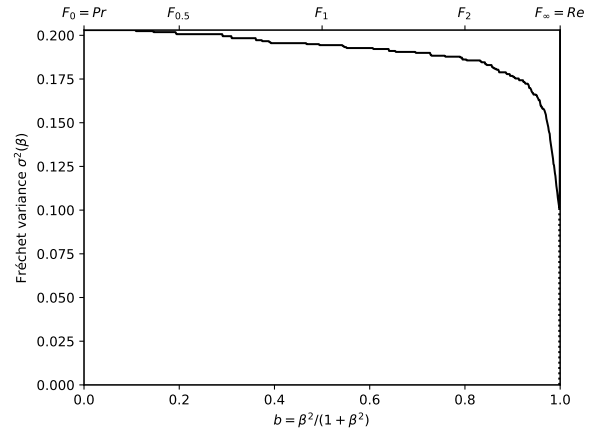
(a) The performances of 56 classifiers (BGS methods) depicted as points in the ROC space, with the isometrics of the optimal tradeoff score, from the ranking point of view, between precision and recall. See Eq. (12).



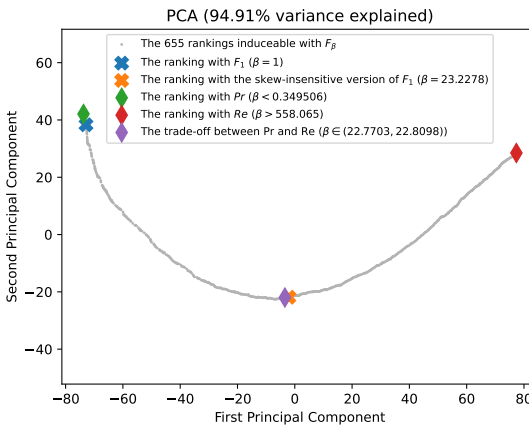
(b) The rank correlations $\tau(Pr; F_\beta)$ and $\tau(F_\beta; Re)$ w.r.t. β . The optimal value (or range of optimal values) for β is where the two curves intersect.



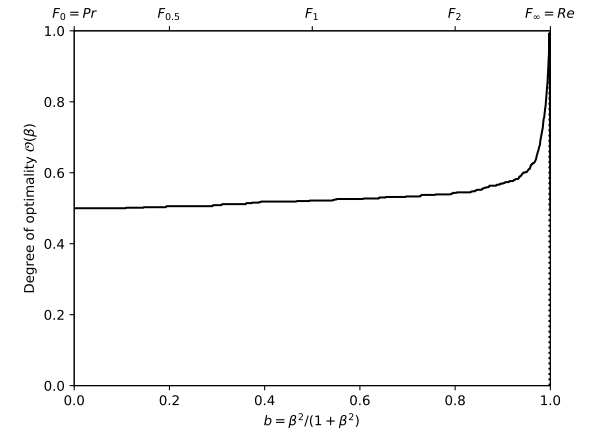
(c) The ranks of each classifier w.r.t. β . The optimal value (or range of optimal values) for β , shown here by the vertical line, is such that the number of swaps on its left is equal to the number of swaps on its right.



(d) The Fréchet variance $\sigma^2(\beta) = d_\tau^2(Pr; F_\beta) + d_\tau^2(F_\beta; Re)$ w.r.t. β . The optimal value (or range of optimal values) for β is where the curve has its minimum.

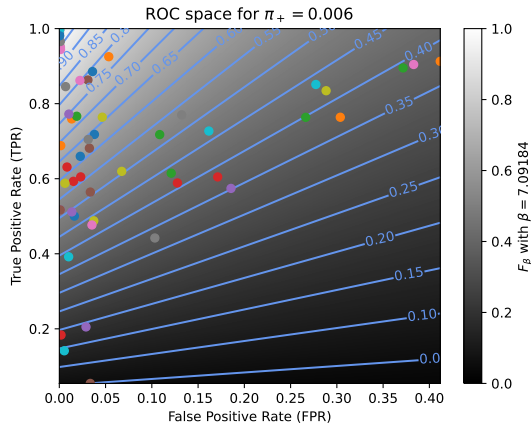


(e) Linear projection (PCA) of the manifold of the rankings induced by the F_β scores. The color points indicate the precision, the recall, F_1 , $SIVF$, as well as the optimal tradeoff. The optimal tradeoff is at the same distance of the two extremities when the distance is measured along the manifold, with Kendall's distance d_+ .

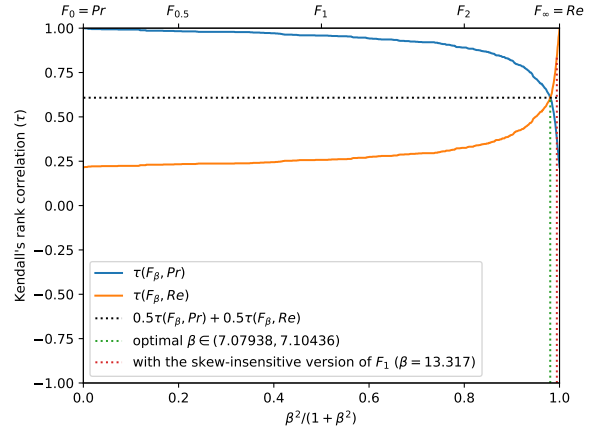


(f) The degree of optimality $\mathcal{O}(\beta)$ w.r.t. β . It is the probability to optimally ordering a pair of classifiers (BGS methods) given that it is not trivial (*i.e.*, that Pr and Re are in contradiction). The optimal value (or range of optimal values) for β is where the curve reaches 100%.

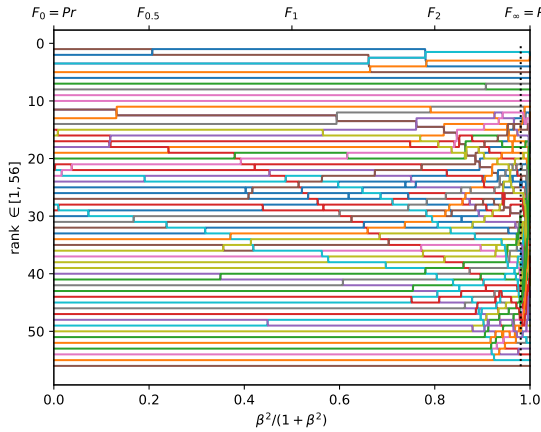
Figure A.3.56. Ranking of 56 BGS methods evaluated on the video "zoomInZoomOut" ($\pi_+ = 0.0019$).



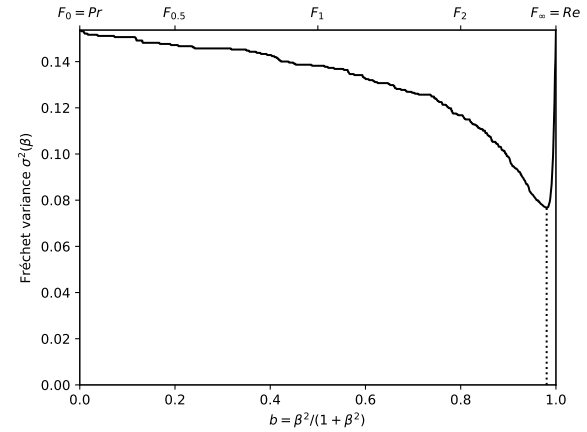
(a) The performances of 56 classifiers (BGS methods) depicted as points in the ROC space, with the isometrics of the optimal tradeoff score, from the ranking point of view, between precision and recall. See Eq. (12).



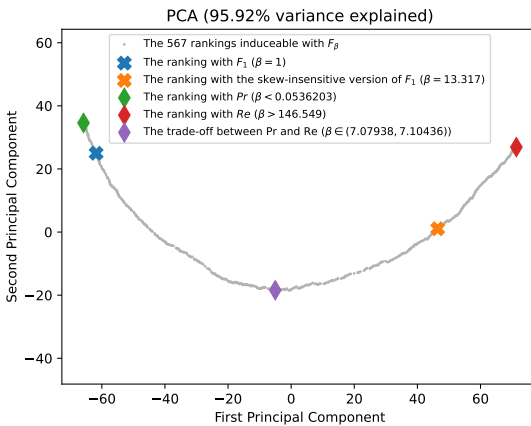
(b) The rank correlations $\tau(F_\beta; Pr)$ and $\tau(F_\beta; Re)$ w.r.t. β . The optimal value (or range of optimal values) for β is where the two curves intersect.



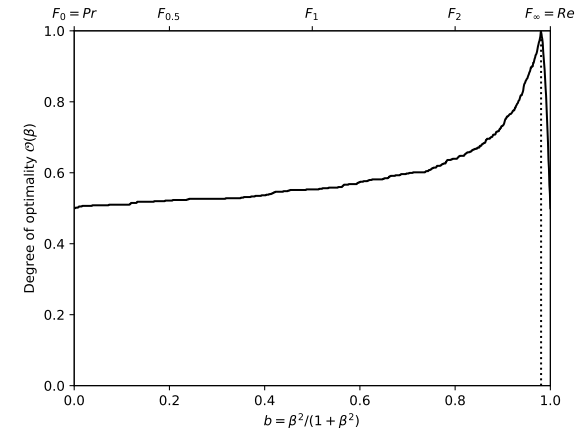
(c) The ranks of each classifier w.r.t. β . The optimal value (or range of optimal values) for β , shown here by the vertical line, is such that the number of swaps on its left is equal to the number of swaps on its right.



(d) The Fréchet variance $\sigma^2(\beta) = d_\tau^2(Pr; F_\beta) + d_\tau^2(F_\beta; Re)$ w.r.t. β . The optimal value (or range of optimal values) for β is where the curve has its minimum.

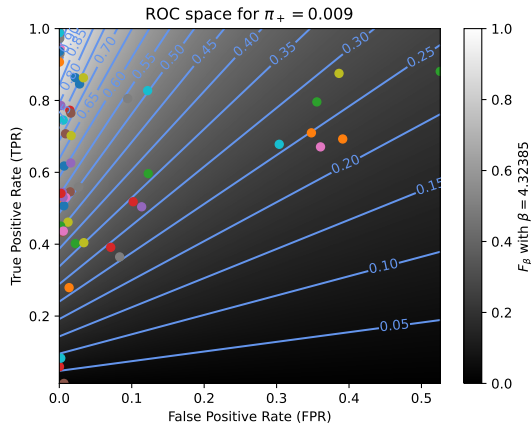


(e) Linear projection (PCA) of the manifold of the rankings induced by the F_β scores. The color points indicate the precision, the recall, F_1 , $SIVF$, as well as the optimal tradeoff. The optimal tradeoff is at the same distance of the two extremities when the distance is measured along the manifold, with Kendall's distance d_+ .

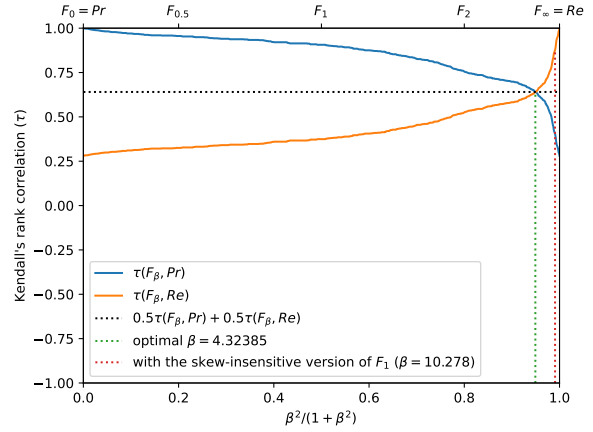


(f) The degree of optimality $\mathcal{O}(\beta)$ w.r.t. β . It is the probability to optimally ordering a pair of classifiers (BGS methods) given that it is not trivial (*i.e.*, that Pr and Re are in contradiction). The optimal value (or range of optimal values) for β is where the curve reaches 100%.

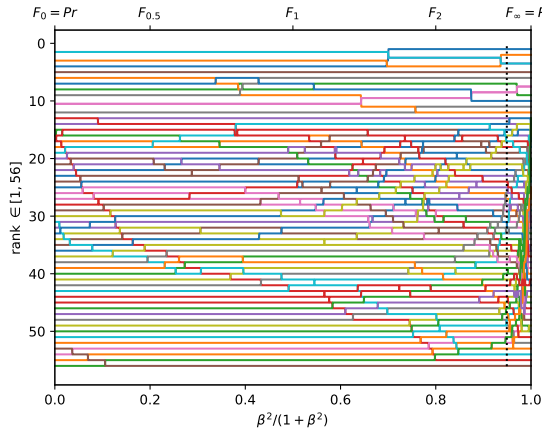
Figure A.3.57. Ranking of 56 BGS methods evaluated on the video "continuousPan" ($\pi_+ = 0.0056$).



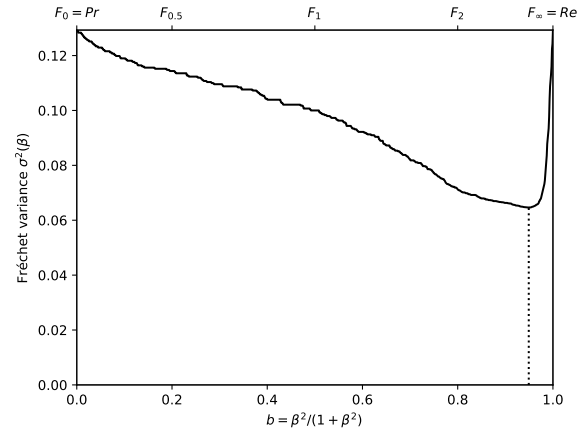
(a) The performances of 56 classifiers (BGS methods) depicted as points in the ROC space, with the isometrics of the optimal tradeoff score, from the ranking point of view, between precision and recall. See Eq. (12).



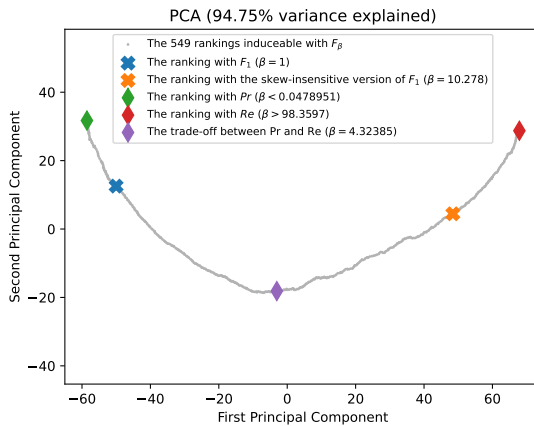
(b) The rank correlations $\tau(F_\beta; Pr)$ and $\tau(F_\beta; Re)$ w.r.t. β . The optimal value (or range of optimal values) for β is where the two curves intersect.



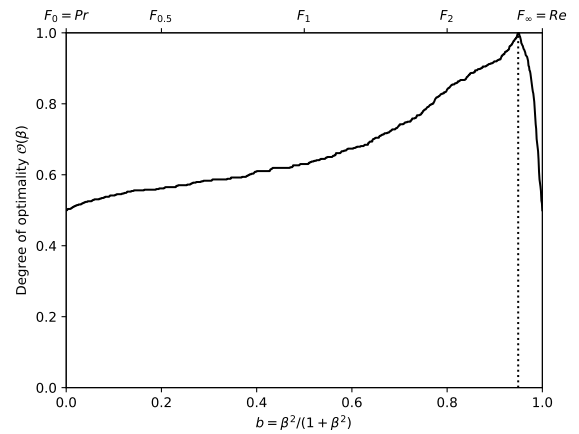
(c) The ranks of each classifier w.r.t. β . The optimal value (or range of optimal values) for β , shown here by the vertical line, is such that the number of swaps on its left is equal to the number of swaps on its right.



(d) The Fréchet variance $\sigma^2(\beta) = d_\tau^2(Pr; F_\beta) + d_\tau^2(F_\beta; Re)$ w.r.t. β . The optimal value (or range of optimal values) for β is where the curve has its minimum.

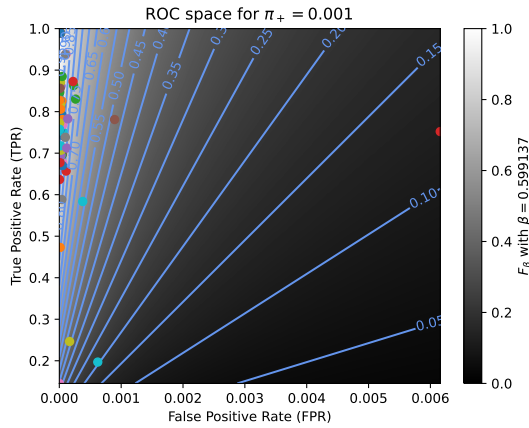


(e) Linear projection (PCA) of the manifold of the rankings induced by the F_β scores. The color points indicate the precision, the recall, F_1 , $SIVF$, as well as the optimal tradeoff. The optimal tradeoff is at the same distance of the two extremities when the distance is measured along the manifold, with Kendall's distance d_+ .

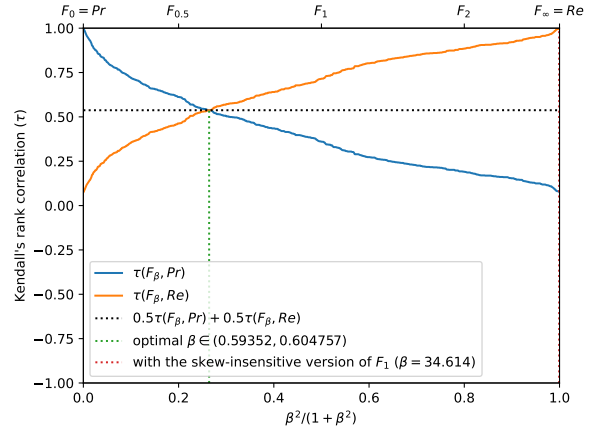


(f) The degree of optimality $\mathcal{O}(\beta)$ w.r.t. β . It is the probability to optimally ordering a pair of classifiers (BGS methods) given that it is not trivial (*i.e.*, that Pr and Re are in contradiction). The optimal value (or range of optimal values) for β is where the curve reaches 100%.

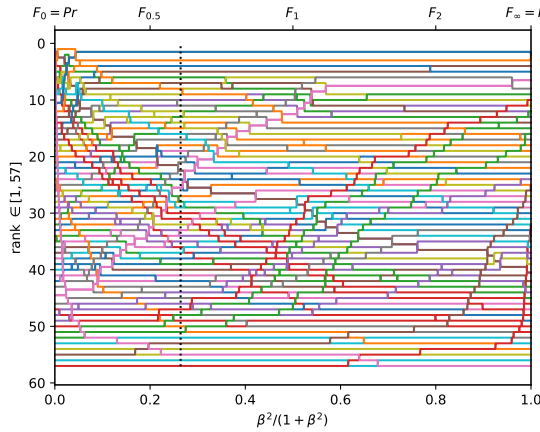
Figure A.3.58. Ranking of 56 BGS methods evaluated on the video "intermittentPan" ($\pi_+ = 0.0094$).



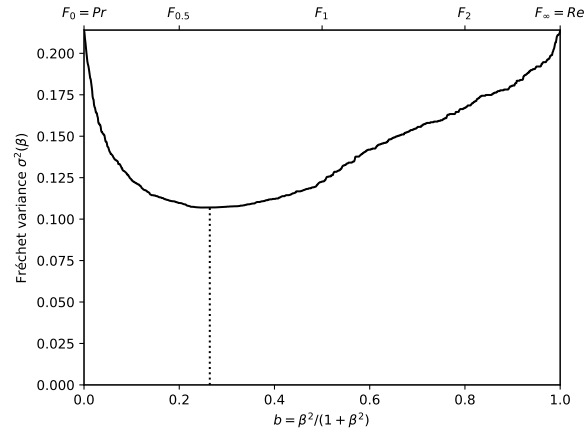
(a) The performances of 57 classifiers (BGS methods) depicted as points in the ROC space, with the isometrics of the optimal tradeoff score, from the ranking point of view, between precision and recall. See Eq. (12).



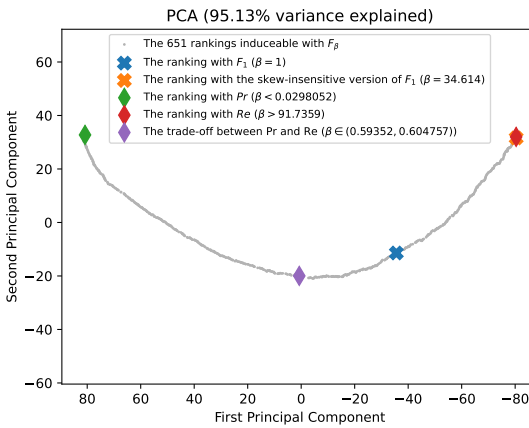
(b) The rank correlations $\tau(F_\beta; Pr)$ and $\tau(F_\beta; Re)$ w.r.t. β . The optimal value (or range of optimal values) for β is where the two curves intersect.



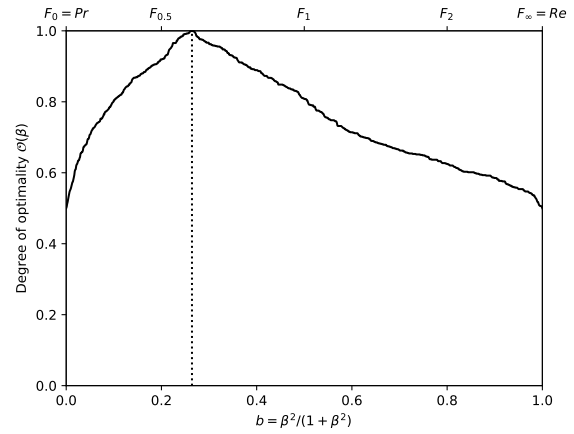
(c) The ranks of each classifier w.r.t. β . The optimal value (or range of optimal values) for β , shown here by the vertical line, is such that the number of swaps on its left is equal to the number of swaps on its right.



(d) The Fréchet variance $\sigma^2(\beta) = d_\tau^2(Pr; F_\beta) + d_\tau^2(F_\beta; Re)$ w.r.t. β . The optimal value (or range of optimal values) for β is where the curve has its minimum.

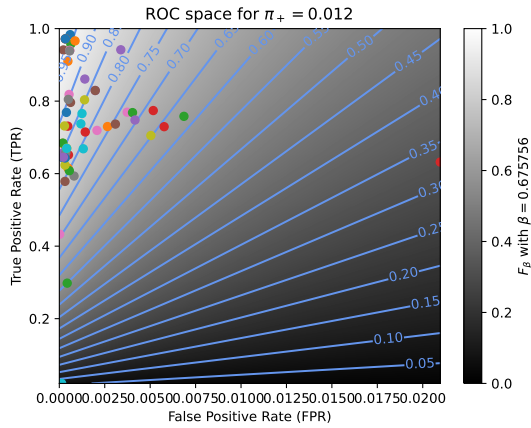


(e) Linear projection (PCA) of the manifold of the rankings induced by the F_β scores. The color points indicate the precision, the recall, F_1 , $SIVF$, as well as the optimal tradeoff. The optimal tradeoff is at the same distance of the two extremities when the distance is measured along the manifold, with Kendall's distance d_+ .

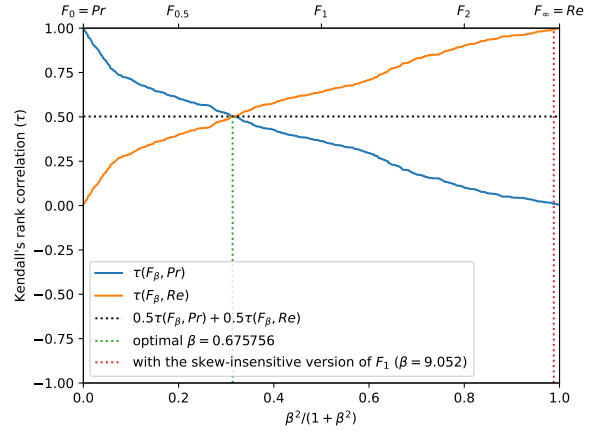


(f) The degree of optimality $\mathcal{O}(\beta)$ w.r.t. β . It is the probability to optimally ordering a pair of classifiers (BGS methods) given that it is not trivial (*i.e.*, that Pr and Re are in contradiction). The optimal value (or range of optimal values) for β is where the curve reaches 100%.

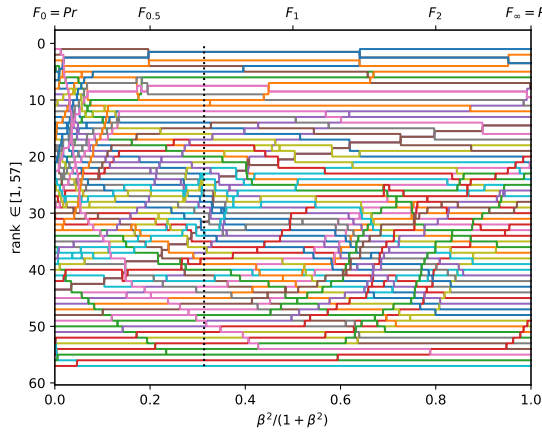
Figure A.3.59. Ranking of 57 BGS methods evaluated on the video "turbulence2" ($\pi_+ = 0.0008$).



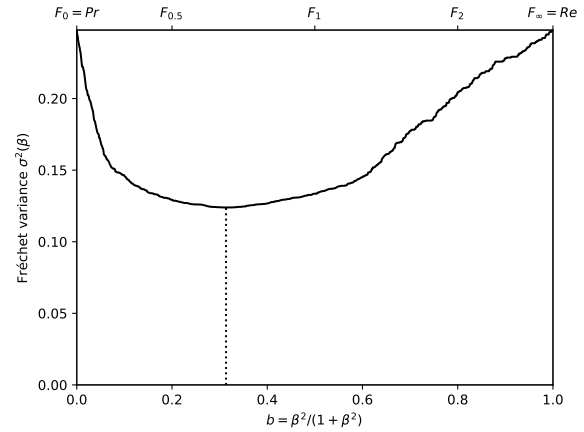
(a) The performances of 57 classifiers (BGS methods) depicted as points in the ROC space, with the isometrics of the optimal tradeoff score, from the ranking point of view, between precision and recall. See Eq. (12).



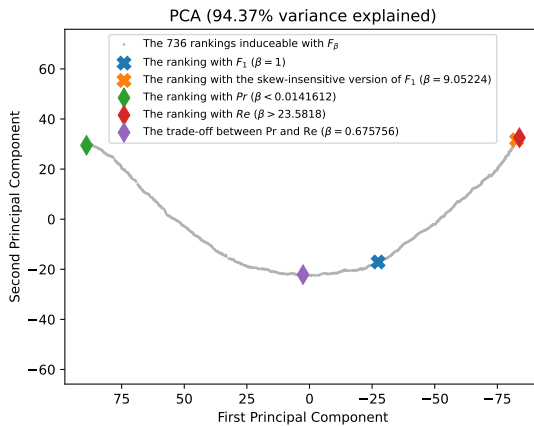
(b) The rank correlations $\tau(F_\beta; Pr)$ and $\tau(F_\beta; Re)$ w.r.t. β . The optimal value (or range of optimal values) for β is where the two curves intersect.



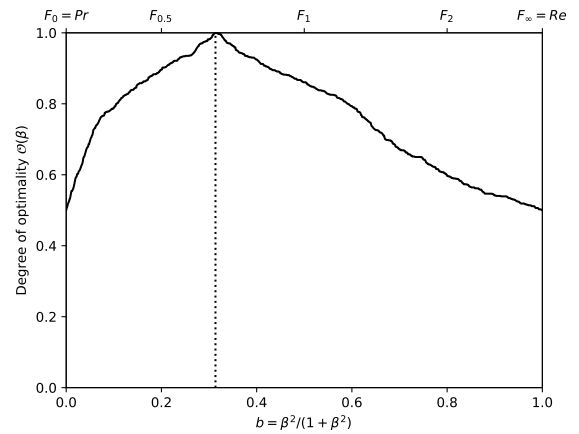
(c) The ranks of each classifier w.r.t. β . The optimal value (or range of optimal values) for β , shown here by the vertical line, is such that the number of swaps on its left is equal to the number of swaps on its right.



(d) The Fréchet variance $\sigma^2(\beta) = d_\tau^2(Pr; F_\beta) + d_\tau^2(F_\beta; Re)$ w.r.t. β . The optimal value (or range of optimal values) for β is where the curve has its minimum.

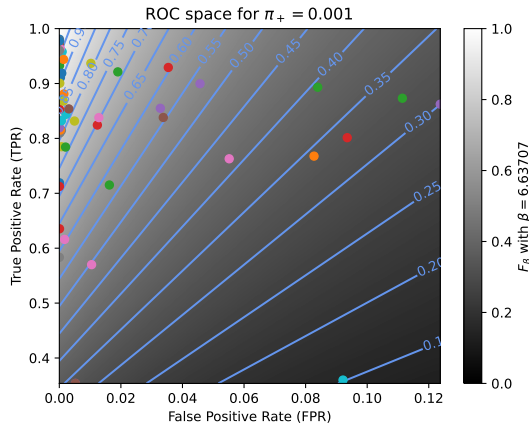


(e) Linear projection (PCA) of the manifold of the rankings induced by the F_β scores. The color points indicate the precision, the recall, F_1 , $SIVF$, as well as the optimal tradeoff. The optimal tradeoff is at the same distance of the two extremities when the distance is measured along the manifold, with Kendall's distance d_+ .

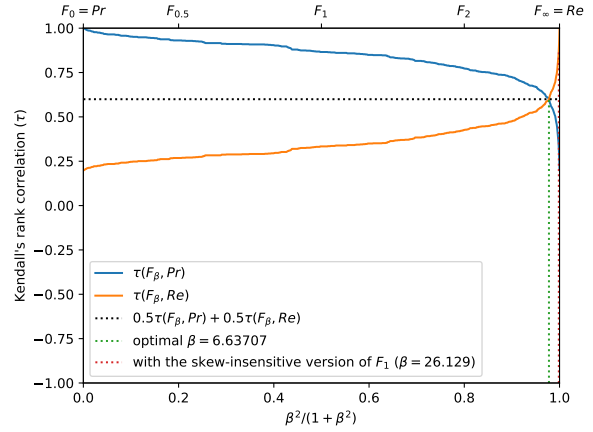


(f) The degree of optimality $\mathcal{O}(\beta)$ w.r.t. β . It is the probability to optimally ordering a pair of classifiers (BGS methods) given that it is not trivial (*i.e.*, that Pr and Re are in contradiction). The optimal value (or range of optimal values) for β is where the curve reaches 100%.

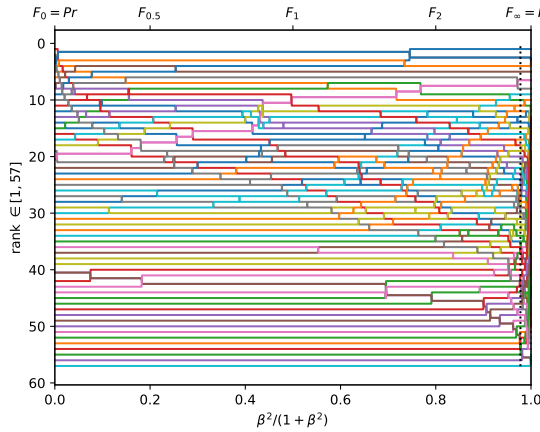
Figure A.3.60. Ranking of 57 BGS methods evaluated on the video "turbulence3" ($\pi_+ = 0.0121$).



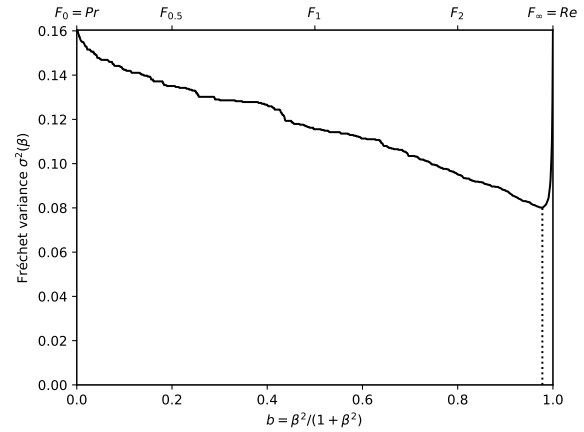
(a) The performances of 57 classifiers (BGS methods) depicted as points in the ROC space, with the isometrics of the optimal tradeoff score, from the ranking point of view, between precision and recall. See Eq. (12).



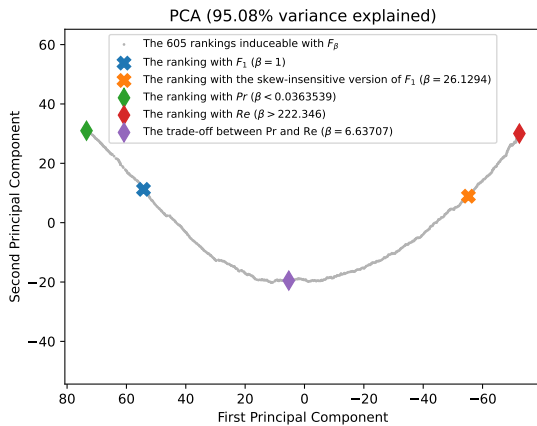
(b) The rank correlations $\tau(F_\beta; Pr)$ and $\tau(F_\beta; Re)$ w.r.t. β . The optimal value (or range of optimal values) for β is where the two curves intersect.



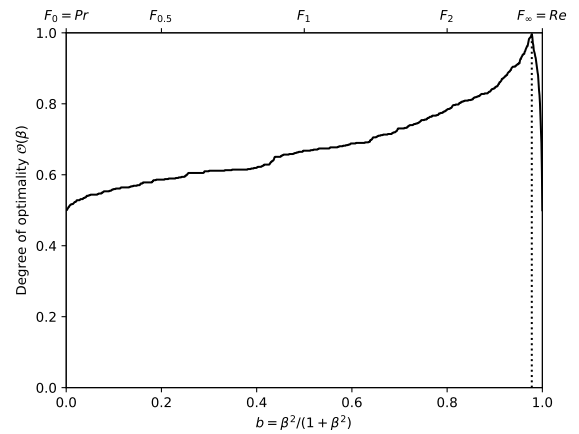
(c) The ranks of each classifier w.r.t. β . The optimal value (or range of optimal values) for β , shown here by the vertical line, is such that the number of swaps on its left is equal to the number of swaps on its right.



(d) The Fréchet variance $\sigma^2(\beta) = d_\tau^2(Pr; F_\beta) + d_\tau^2(F_\beta; Re)$ w.r.t. β . The optimal value (or range of optimal values) for β is where the curve has its minimum.

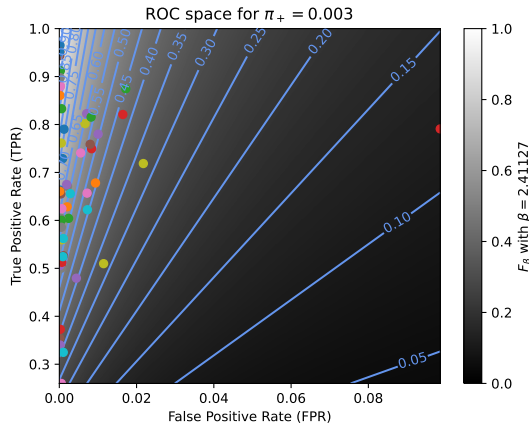


(e) Linear projection (PCA) of the manifold of the rankings induced by the F_β scores. The color points indicate the precision, the recall, F_1 , $SIVF$, as well as the optimal tradeoff. The optimal tradeoff is at the same distance of the two extremities when the distance is measured along the manifold, with Kendall's distance d_τ .

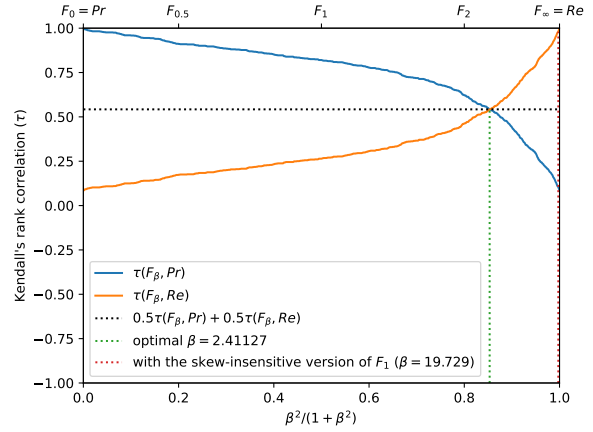


(f) The degree of optimality $\mathcal{O}(\beta)$ w.r.t. β . It is the probability to optimally ordering a pair of classifiers (BGS methods) given that it is not trivial (*i.e.*, that Pr and Re are in contradiction). The optimal value (or range of optimal values) for β is where the curve reaches 100%.

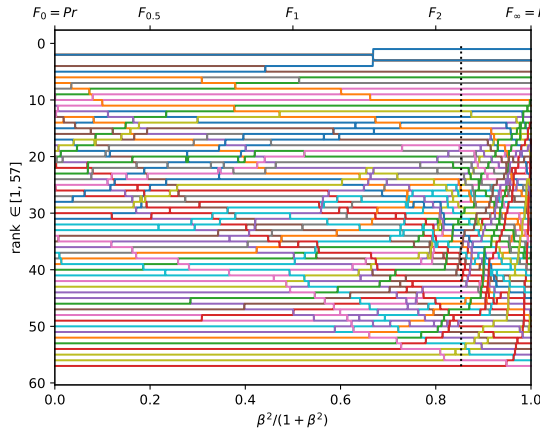
Figure A.3.61. Ranking of 57 BGS methods evaluated on the video "turbulence0" ($\pi_+ = 0.0015$).



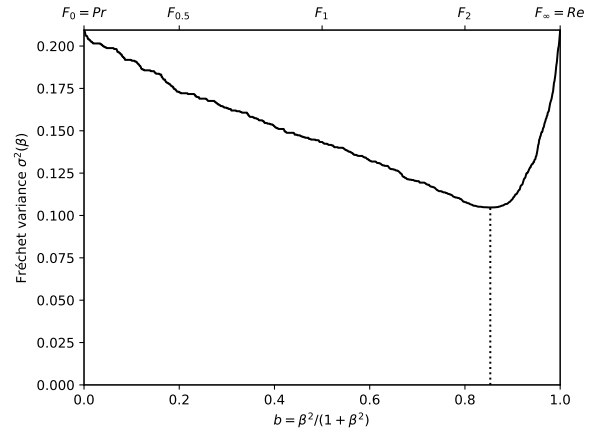
(a) The performances of 57 classifiers (BGS methods) depicted as points in the ROC space, with the isometrics of the optimal tradeoff score, from the ranking point of view, between precision and recall. See Eq. (12).



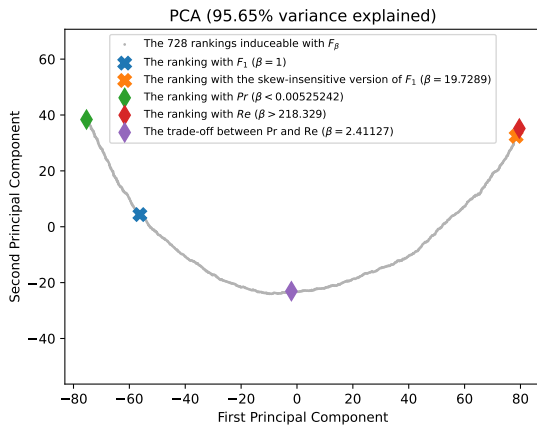
(b) The rank correlations $\tau(F_\beta; Pr)$ and $\tau(F_\beta; Re)$ w.r.t. β . The optimal value (or range of optimal values) for β is where the two curves intersect.



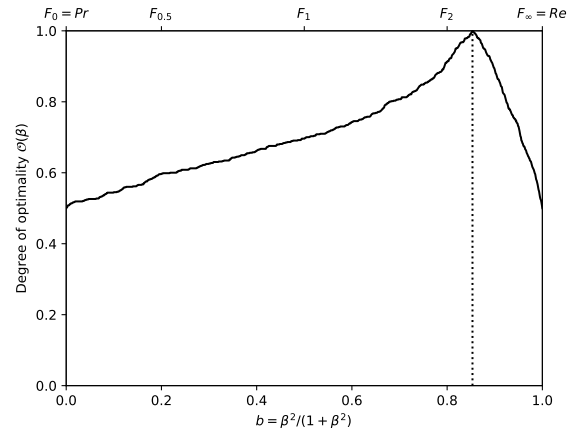
(c) The ranks of each classifier w.r.t. β . The optimal value (or range of optimal values) for β , shown here by the vertical line, is such that the number of swaps on its left is equal to the number of swaps on its right.



(d) The Fréchet variance $\sigma^2(\beta) = d_\tau^2(Pr; F_\beta) + d_\tau^2(F_\beta; Re)$ w.r.t. β . The optimal value (or range of optimal values) for β is where the curve has its minimum.



(e) Linear projection (PCA) of the manifold of the rankings induced by the F_β scores. The color points indicate the precision, the recall, F_1 , $SIVF$, as well as the optimal tradeoff. The optimal tradeoff is at the same distance of the two extremities when the distance is measured along the manifold, with Kendall's distance d_+ .



(f) The degree of optimality $\mathcal{O}(\beta)$ w.r.t. β . It is the probability to optimally ordering a pair of classifiers (BGS methods) given that it is not trivial (*i.e.*, that Pr and Re are in contradiction). The optimal value (or range of optimal values) for β is where the curve reaches 100%.

Figure A.3.62. Ranking of 57 BGS methods evaluated on the video "turbulence1" ($\pi_+ = 0.0026$).

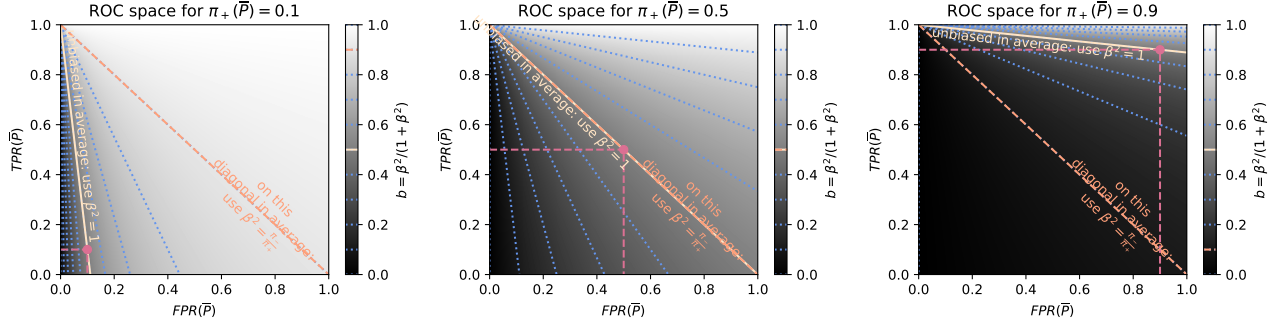


Figure A.3.63. Visualization of our heuristic in ROC space. The recommended value for $b = \frac{\beta^2}{1+\beta^2}$ is the value at the point $(\mathbf{E}[FPR], \mathbf{E}[TPR])$ when the priors are fixed, and the value at the point $(FPR(\bar{P}), TPR(\bar{P}))$ in the general case. This visualization is specific to certain priors: the common priors when the priors are fixed, and $(\pi_-(\bar{P}), \pi_+(\bar{P}))$ in the general case. The more the prior π_+ of the positive class increases, the more the recommended value for β decreases (compare with Fig. 2).

A.3.8. More information on our simple heuristic for ROC users

We provide here additional information about the simple heuristic introduced in Sec. 4.6.

$$\beta^2 = \frac{\mathbf{E}[PFP]}{\mathbf{E}[PFN]} \Leftrightarrow b = \frac{\mathbf{E}[PFP]}{\mathbf{E}[PFN] + \mathbf{E}[PFP]} \quad (70)$$

This heuristic was designed for the typical performances that researchers in the computer vision community (and more specifically those working on “change detection” and “background subtraction”) have found useful to report in public benchmarks. For this community, we are fortunate to have a large number of domains (videos) in which a wide range of methods have been evaluated and their performances reported in public rankings. There is however no guarantee that this heuristic performs well in all cases. Nevertheless, as shown in Tab. 1, our heuristic performs reasonably well for all the parametric distributions studied in this paper. It is therefore worth describing it in depth.

As shown in Fig. A.3.63, it is possible to depict the heuristic in the Receiver Operating Characteristic (ROC) space, which is by definition $ROC = (FPR, TPR)$. We start by discussing the particular case in which the class priors are fixed, and then discuss the general case.

- When the class priors (π_-, π_+) are fixed, as $PFP = \pi_- FPR$ and $PFN = \pi_+ FNR$, our heuristic can be rewritten as

$$\beta^2 = \frac{\pi_- \mathbf{E}[FPR]}{\pi_+ \mathbf{E}[FNR]} \Leftrightarrow b = \frac{\pi_- \mathbf{E}[FPR]}{\pi_+ \mathbf{E}[FNR] + \pi_- \mathbf{E}[FPR]} \quad (71)$$

Moreover, as $FNR = 1 - TPR$, we have

$$\beta^2 = \frac{\pi_- \mathbf{E}[FPR]}{\pi_+ (1 - \mathbf{E}[TPR])} \Leftrightarrow b = \frac{\pi_- \mathbf{E}[FPR]}{\pi_+ (1 - \mathbf{E}[TPR]) + \pi_- \mathbf{E}[FPR]} \quad (72)$$

This last form allows one to see the recommended b (or β) as a function of $\mathbf{E}[FPR]$ and $\mathbf{E}[TPR]$, or in other words as a function of the position of the centroid in ROC.

- In the general case, it is also possible to use the same visualization of the heuristic in ROC. However, instead of looking at the centroid of the performance points, one should look at where the *summarized performance* \bar{P} is projected. Let us remind that, when working with a finite set $\Pi \subset \mathbb{P}_{(\Omega, \Sigma)}$ of performances, the works [28, 30] proposed a consistent way of averaging the score values for all scores. The summarized value for a score X is $X(\bar{P})$, where $\bar{P} \in \mathbb{P}_{(\Omega, \Sigma)}$ is the performance given by $\frac{1}{|\Pi|} \sum_{P \in \Pi} P$. In other words, instead of arithmetically averaging score values, it has been proposed to average, or summarize, performances.

- For all unconditional probabilistic scores X (such as PFP and PFN), we have $\mathbf{E}[X] = \frac{1}{|\Pi|} \sum_{P \in \Pi} X(P) = X(\bar{P})$. The recommended β depends only on the average, summarized, performance \bar{P} .

$$\beta^2 = \frac{PFP(\bar{P})}{PFN(\bar{P})} \Leftrightarrow b = \frac{PFP(\bar{P})}{PFN(\bar{P}) + PFP(\bar{P})} \quad (73)$$

- In general, for the conditional probabilistic scores X , one does not have $X(\bar{P}) = \frac{1}{|\Pi|} \sum_{P \in \Pi} X(P)$. So, $X(\bar{P})$ is not necessarily equal to $\mathbf{E}[X]$. This is the case for TNR , FPR , FNR , and TPR . But as $PF\bar{P}(\bar{P}) = \pi_-(\bar{P}) F\bar{P}R(\bar{P})$ and $PF\bar{N}(\bar{P}) = \pi_+(\bar{P}) F\bar{N}R(\bar{P})$,

$$\beta^2 = \frac{\pi_-(\bar{P}) F\bar{P}R(\bar{P})}{\pi_+(\bar{P}) F\bar{N}R(\bar{P})} \Leftrightarrow b = \frac{\pi_-(\bar{P}) F\bar{P}R(\bar{P})}{\pi_+(\bar{P}) F\bar{N}R(\bar{P}) + \pi_-(\bar{P}) F\bar{P}R(\bar{P})}. \quad (74)$$

Moreover, as $F\bar{N}R(\bar{P}) = 1 - T\bar{P}R(\bar{P})$, we have

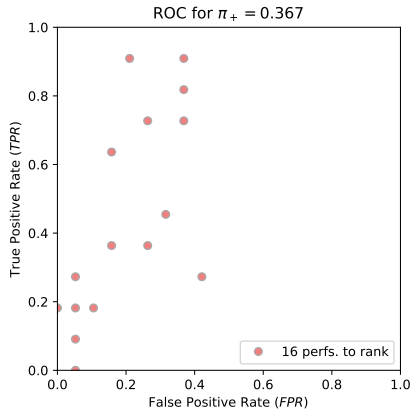
$$\beta^2 = \frac{\pi_-(\bar{P}) F\bar{P}R(\bar{P})}{\pi_+(\bar{P})(1 - T\bar{P}R(\bar{P}))} \Leftrightarrow b = \frac{\pi_-(\bar{P}) F\bar{P}R(\bar{P})}{\pi_+(\bar{P})(1 - T\bar{P}R(\bar{P})) + \pi_-(\bar{P}) F\bar{P}R(\bar{P})}. \quad (75)$$

It should be stressed that, when the priors differ from one performance to another, the point $(F\bar{P}R(\bar{P}), T\bar{P}R(\bar{P}))$ does not coincide with $(\mathbf{E}[F\bar{P}R], \mathbf{E}[T\bar{P}R])$. By comparing Eq. (72) with Eq. (75), we see that the same visualization can be used. However, instead of looking at $(\mathbf{E}[F\bar{P}R], \mathbf{E}[T\bar{P}R])$, one has to look at $(F\bar{P}R(\bar{P}), T\bar{P}R(\bar{P}))$.

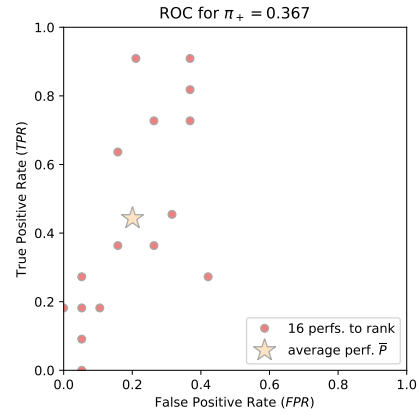
Our heuristic recommends to rank w.r.t. F_1 when the average performance is unbiased (i.e., $Pr = Re$). In the sense of Byrt *et al.* [3], a classifier is unbiased when the classifier predicts as much positive samples as there are in reality. The probability for the predicted class to be positive $P(\{fp, tp\})$ equals the probability for the ground-truth class to be positive $P(\{fn, tp\})$. Thus, $PF\bar{P} = PF\bar{N}$ and $Pr = Re$. In ROC, this corresponds to a line passing through $(F\bar{P}R, T\bar{P}R) = (0, 1)$ and $(F\bar{P}R, T\bar{P}R) = (\pi_+, \pi_+)$. When the performance is unbiased in average, the heuristic recommends $\beta^2 = 1$. This can be seen by taking $\mathbf{E}[PF\bar{P}] = \mathbf{E}[PF\bar{N}]$ in Eq. (70) or $PF\bar{P}(\bar{P}) = PF\bar{N}(\bar{P})$ in Eq. (73).

Our heuristic recommends to rank w.r.t. $SIVF$ when the priors are fixed, and w.r.t. F_β with $\beta^2 = \pi_-/\pi_+$ in the general case, when the average performance is on the descending diagonal of ROC. If the average performance is on the descending diagonal of ROC, we have $\mathbf{E}[F\bar{P}R] = 1 - \mathbf{E}[T\bar{P}R]$ when the priors are fixed, or $F\bar{P}R(\bar{P}) = 1 - T\bar{P}R(\bar{P})$ in the general case. Thus, by looking at Eqs. (72) and (75), we see that the recommended value for β^2 is π_-/π_+ . When the priors are fixed, the F-score corresponding to this value induces the same performance ordering as the skew-insensitive version of F_1 , $SIVF$, defined in [10] as $SIVF = \frac{2TPR}{TPR + F\bar{P}R + 1}$.

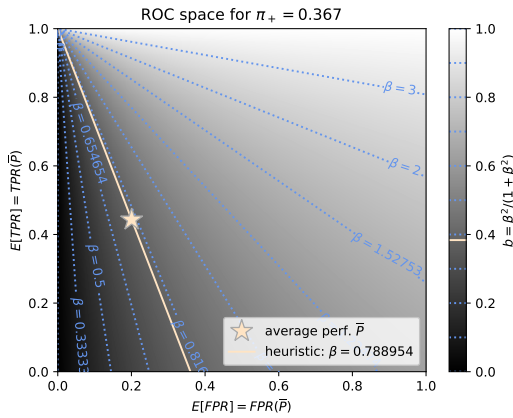
A detailed use of our heuristic on the CADA-RRE example is shown, step by step, in Fig. A.3.64.



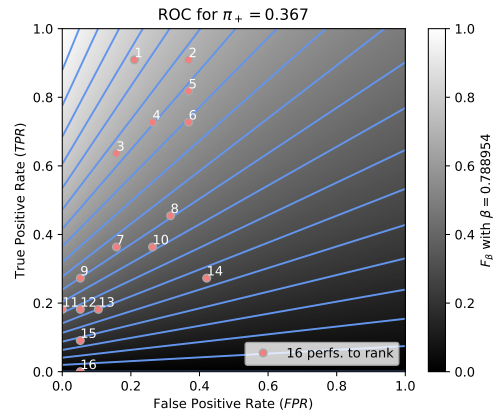
(a) Step 1. Point cloud in the ROC space showing the performances of the methods to rank. Note that all these performances correspond to fixed class priors.



(b) Step 2. Computation of the summarized performance \bar{P} [28]. As all performances correspond to fixed class priors, it is located at the centroid of the point cloud (bisque star).



(c) Step 3. Use of our heuristic. One reads the recommended value for $b = \frac{\beta^2}{1 + \beta^2}$ at $(FPR(\bar{P}), TPR(\bar{P}))$.



(d) Step 4. Drawing the score F_β for the recommended β in the background of ROC, with superimposed isometrics depicting the performance ordering induced by it.

Figure A.3.64. Example of use of our heuristic our CADA-RRE example (see Sec. A.2.4).